01 Apr 1968

Structural behavior of small-scale steel models

William A. Litle

David C. Foster

Duke Oakes

Philip A. Falcone

et. al. For a complete list of authors, see https://scholarsmine.mst.edu/ccfss-library/196

STEEL RESEARCH for construction

STRUCTURAL BEHAVIOR OF SMALL-SCALE STEEL MODELS

—*Massachusetts Institute of Technology*

I Fabrication Techniques for Small-Scale Steel Models

II Ultimate Strength Behavior of Small-Scale 8WF31 Beam-Columns

III Ultimate Strength Behavior of Small-Scale Steel Frameworks

Committee of Structural Steel Producers • Committee of Steel Plate Producers

american iron and steel institute

BULLETIN No. 10, APRIL, 1968

STRUCTURAL BEHAVIOR OF SMALL-SCALE STEEL MODELS

DEPARTMENT OF CIVIL ENGINEERING

SCHOOL OF ENGINEERING

MASSACHUSETTS INSTITUTE OF TECHNOLOGY

Committee of Structural Steel Producers • Committee of Steel Plate Producers

american iron and steel institute

PRINTED IN U.S.A. 3M 468

Fabrication Techniques for Small-Scale Steel Models

by

WILLIAM A. LITLE

DAVID CLARKE FOSTER

ACKNOWLEDGEMENT

This research project was carried out in the Structural Models Laboratory of the Department of Civil Engineering at the Massachusetts Institute of Technology. The project was sponsored by the Committee of Structural Steel Producers and the Committee of Steel Plate Producers of American Iron and Steel Institute, and the Structural Steel Fabricators of New England.

TABLE OF CONTENTS

Table of Contents (Continued)

ABSTRACT

This project was directed to the problem of fabricating small scale steel wide flange sections, small scale joints, and a small scale building frame. It was accomplished through the testing of 44 tensile coupons of which 18 were butt welded, the study of feasible fabrication techniques, the testing of four milled wide flanged beams and eight fabricated joints, and the construction of a 1/15-scale space framework.

The essential conclusions derived from the various experiments and experiences are as follows:

1. The chemical and mechanical properties of C1020 hot rolled steel are such that it may be used satisfactorily in the modeling of steel structures.
2. Milling wide flange sections from hot rolled bar stock is a reliable and accurate method for fabricating small scale sections with element thickness down to 25 thousandths of an inch.
3. Tension and joint tests demonstrated that the heliarc process with Industrial Stainless 410 filler rods provides more than adequate strength and ductility for joining C1020 model sections.
4. High ultimate values obtained in the non-annealed joint tests are a result of the heating effect of the welding process and/or a change in the chemical properties of the steel due to the filler rod.
   a. Pre-annealing of the sections before welding did not lower the ultimate moment values obtained to the post-annealed value.
   b. Non-annealed welded tension samples failed outside the one-inch gauge length or just inside adjacent to the gauge line.
   c. Beam tests demonstrated little difference between the annealed and non-annealed yield and ultimate moments.
5. Fabrication of a complete framework is possible, but it is necessary to fix elements during assembly and to follow a predetermined sequence of assembly to reduce shrinkage deformations. This sequence may vary with each structure.
6. Until more refinements are made in the welding process, it is necessary to anneal whole frameworks to obtain member behavior consistent with stress-strain characteristics of the material.

LIST OF TABLES

LIST OF FIGURES

List of Figures (Continued)

PART I

I. INTRODUCTION

1.1 Small Scale Model Studies

The analysis and design of steel frameworks has become increasingly sophisticated and efficient in the last decade through the use of improved design tables and computer techniques. For conventional structures, present methods of analysis can be employed with confidence with the proportioning of members based upon some prescribed criteria, such as building and bridge construction codes. When these methods can be employed, there can be no economic justification for the model study of a structure. One must keep in mind, however, that existing criteria are based upon member behavior which is sometimes complex and indeterminate. For unconventional structures, a rigorous mathematical analysis is sometimes insufficient for describing geometries and structural behavior. It is in these areas, increasing knowledge of member and whole structure behavior, and the study of a highly unconventional structure, where no mathematical analysis may be applied, that model studies can be useful.

The use of experimental methods has already been demonstrated in tests carried out on full scale sections at Lehigh University and other schools. These tests have brought about the incorporation of plastic design into the building code, given information on the distribution of residual stresses in sections due to welding and hot rolling, and increased knowledge on member behavior under axial load, flexure, etc.

Full scale tests have been quite valuable, but have a number of limitations. Because of member sizes, full scale tests have been restricted to simple members and simple one-, two-, or three-story structures. In addition, very few laboratories have the facilities for testing full size elements. A small scale model study would overcome the size problem and would be less time-consuming and less costly. Testing of whole structures to study their complex behavior would become possible and the great reduction in loads necessary to cause failure would enable more laboratories to undertake these studies without building expensive facilities.

1.2 Purpose of Present Research

This project was directed to the problem of fabricating small scale steel wide flange sections, small scale joints, and a small scale building frame. It was accomplished through testing of 44 tensile coupons of which 18 were butt welded, the study of feasible fabrication techniques, the testing of four milled wide flange beams and eight fabricated joints, and the construction of a 1/15-scale space framework.

1.3 Background

1.3.1 Material

Plastics, brasses, and steels are three materials which have been used for model studies of steel sections at the M.I.T. Civil Engineering Laboratory for Structural Models.

The advantages of the plastics and brasses are that only small loads are necessary to cause failure of these materials, and they are relatively easy to fabricate. Their big disadvantage is that they do not fulfill similitude requirements necessary to model plastic behavior of steel sections. The plastic possesses a much higher yield strain than the steels and the development of a yield plateau in the brasses is a highly indeterminate occurrence.

Steel as a model material overcomes matching stress-strain characteristics with structural steel, and because of this was used as the model material in the project.

1.3.2 Section Fabrication

In earlier work, two techniques had been used for the fabrication of small scale wide flange members. The first of these was the use of

electron beam welding to fuse flange and web plates of appropriate width and thickness to form the desired section. Although the process produces reliable welds, skips and slight deviations from the flange centerline caused separation of the flange and web during testing (Ref. 3). Such wide flange sections cost about forty dollars per foot.

The second process was the milling of sections from rectangular bar stock. This process was used on both brass and steel with tolerances generally kept within eight per cent of given dimensions. Results obtained on steel model sections produced a good correlation with similar simple beam tests conducted at Lehigh University. The milled sections cost from $10.00 to $40.00 per foot, depending on the company and material.

2. MODEL TECHNIQUES

2.1 Section Fabrication

Five techniques were considered for the section fabrication of the small scale beams for this project. These were hot rolling, die extruding, electron beam welding, resistance welding, and milling bar stock.

At the present time, the smallest sections commercially available hot rolled are tees, angles, and channels with a minimum thickness of one-eighth of an inch. At the one-eighth to one-fifteenth scales envisioned for the model work, minimum thicknesses down to about 0.025 inch would be required. Rolling facilities for such sections are not available and no economic justification can be presented for developing them. Regarding die extrusion, the obvious cost is the tooling cost for the die. If large quantities would be anticipated for each section, the high initial cost of dies could be amortized. However, experience indicates that the occasions demand small quantities of a number of different sections rather than large quantities of a few sections.

A new look at the latest developments in electron beam welding technology did not indicate that the earlier drawbacks (see Section 1.3.2) could be easily overcome. Accordingly, no new section fabrications were attempted using this procedure. In the opinion of Thompson Electric Co., Lynn, Mass. (a manufacturer of resistance welding equipment), the tooling costs for resistance welding of flange and web plates would be at least equal to current costs for milling the shapes from rectangular bars. In addition, the flange-web separation experienced in electron beam welded samples might still occur.

Although the cost of milling wide flange shapes is much higher than would be desirable, it seems at the present time to be the most appropriate procedure. As more experience with the technique is gained, it is felt that costs will decrease substantially. At the same time, other techniques will continue to be investigated.

2.2 Materials

Three types of steel were considered. These were SAE C1010, C1020, and B1113. The C1010 and C1020 steels were chosen for similarity of chemical and mechanical properties with structural low carbon steels. The B1113 steel was chosen for its good machinability characteristics, an important factor since the beams are to be milled from bar stock. A comparison of mechanical and chemical properties for these SAE steels and ASTM–A36 steel is shown in Table 1.

Tensile coupons were milled from C1010, C1020 and B1113 and tested to determine strength and ductility properties. Results from these tests are summarized in Figure 1 and are compared with the curve for A36 steel. Sixteen C1010 and C1020 tests were a part of this project, while the B1113 curves were taken from Reference 4.

The C1020 steel, having stress-strain curves similar to, but slightly higher than the minimum ASTM A36 values, was tentatively selected as the model material. However, the final selection was delayed until joining techniques had been investigated.

TABLE 1

Mechanical and Chemical Properties of ASTM
A36 (Ref. 2) and SAE B1113, C1010, and C1020 (Ref. 5)

	C	*Mn*	*P*	*S*	Minimum Yield Stress (ksi)	Minimum Tensile Strength (ksi)	%E 2-inch Gauge
A36	.25	.80–1.20	.040	.50	36**	58**	23**
B1113 (C.R.)	.13	.70–1.00	.07–.12	.24–.33	60*	78*	10*
C1010 (C.R.)	.08–.13	.30–.60	.040	.050	41*	48*	20*
C1020 (H.R.)	.18–.23	.30–.60	.040	.050	30*	55*	25*

** TYPICAL MINIMUM * SPECIMEN MINIMUM

2.3 Joining Techniques

2.3.1 Silver Solder

In sister projects (Ref. 3, 4) concerned with studies of model sections, silver solder has been used to join sections. It provides adequate strength when used with brass and bronze, but lacks sufficient plastic strength to join main steel elements. This was verified in tension tests of butt welded samples of C1010 steel, in which the silver soldered joints failed soon after yielding of the C1010 steel. Silver solder does seem adequate for joining secondary members such as web stiffeners.

2.3.2 Heliarc Welding (TIG)

Both MIG (metallic inert gas) and TIG (tungsten inert gas) welding processes were investigated. With 0.030-inch diameter consumable electrodes it was found that the MIG welds were extremely heavy, and with the thin material it was difficult to prevent burnthrough and spatter. The TIG process allowed for greater control at the small scales and smoother, cleaner welds were obtained. In the TIG process the tungsten electrode is not consumed, but rather a filler wire is fed into the arc, melted, and propelled toward the joint being formed. Shielding of the arc is obtained with inert gases which prevent oxidation of the weld. The gas atoms are ionized and carry the arc from the electrode to the work (Fig. 2). Argon and helium are the two inert gases most widely used, with the argon used alone or in combination with the helium. These gases are not expensive, provide a smooth arc, and hence cause little spatter. Argon operates at a lower arc voltage than most gases and therefore lessens the chance of burnthrough with thin material. The equipment, which includes generators, gas tanks, welding torch, safety equipment, etc., costs about $2000 and requires experience to produce good welds.

2.3.3 Tension Tests of Butt Welded Joints

Eighteen standard tension samples, milled from C1010, C1020 and B1113 steels, were cut across the center of their gauge length. Butt welding was accomplished using the TIG system, with Oxweld 65 filler wires for the C1010 and C1020 specimens and Industrial Stainless 410 filler wires for the B1113 specimens. Table 2 gives the chemical properties of these filler

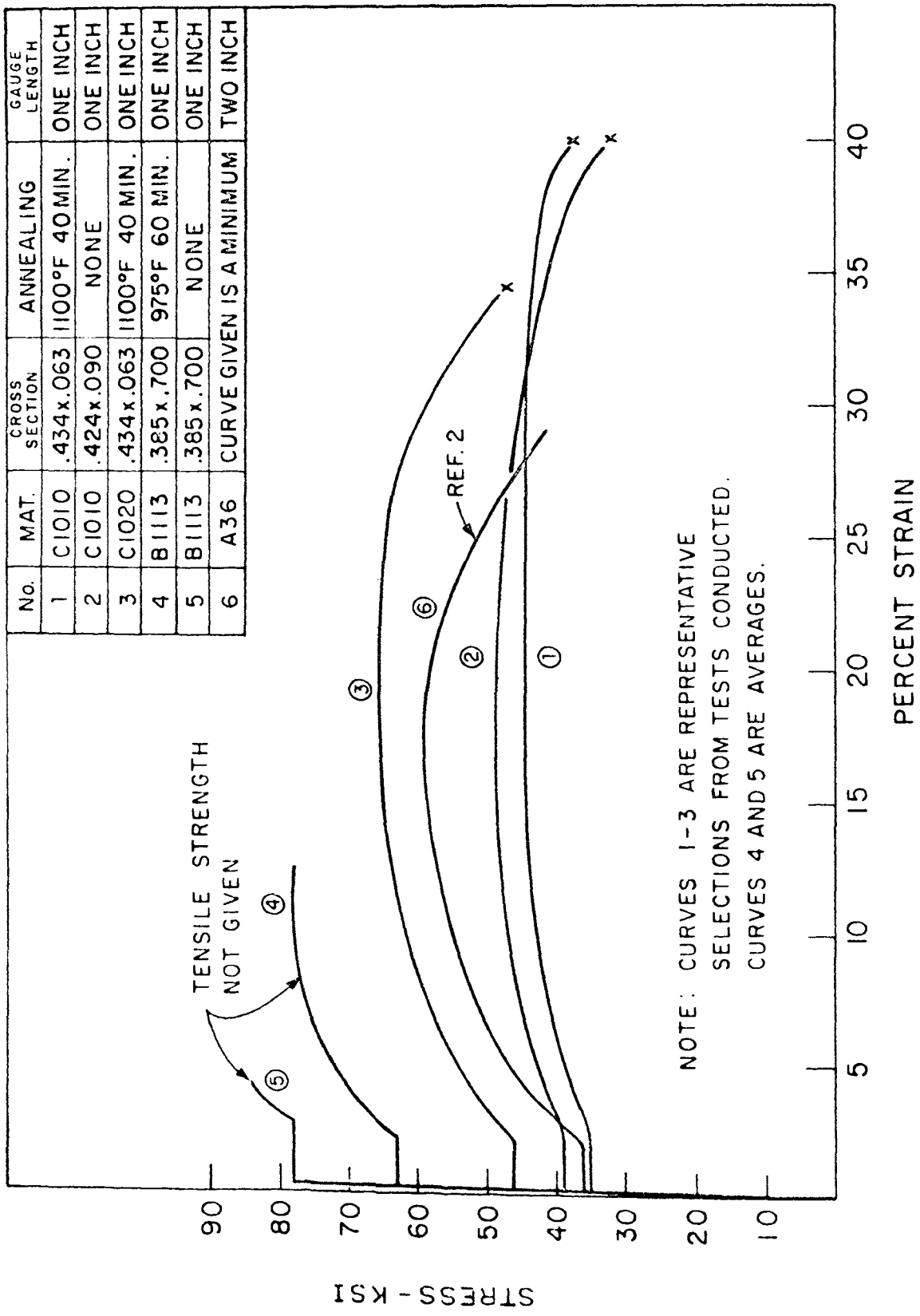

FIGURE 1–TYPICAL STRESS-STRAIN CURVES OF SAE C1010, C1020, B1113, ASTM-A36 STEELS

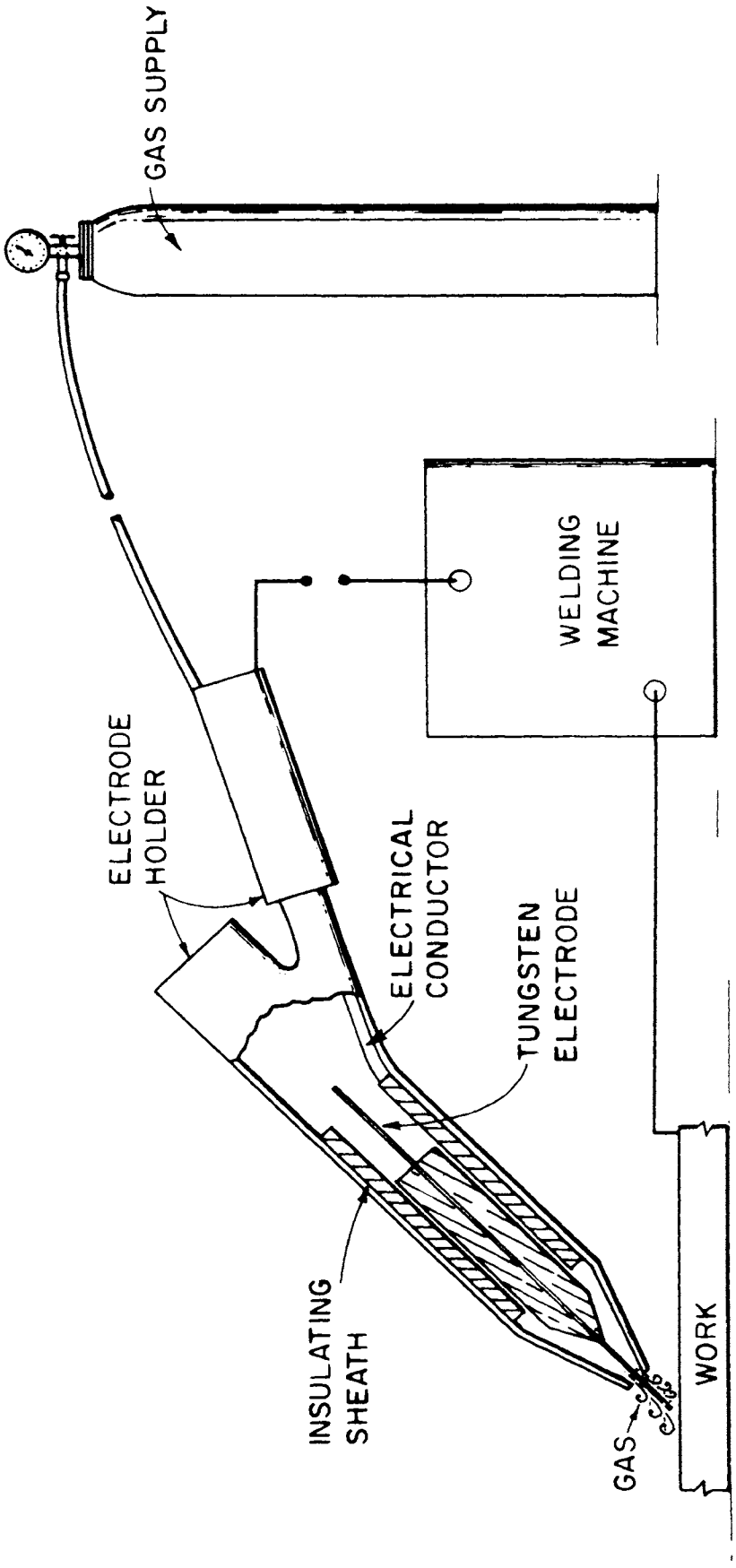

FIGURE 2–SCHEMATIC DIAGRAM OF HELIARC WELDING PROCESS (REF. 7)

materials. Typical test results are shown in Figure 3. In all of the tests, there was a material rather than a joint failure. Four of the annealed C1010 samples failed inside the one-inch gauge length with yield and tensile strengths similar to the plain tension tests, while the other two failed outside the gauge lengths. Three of the six unannealed C1010 samples failed outside of the one-inch gauge length, and for those failing inside, the one-inch extensometer indicated strains which were less than 50% of those occurring in the annealed state. The C1020 samples were annealed and failed adjacent to the weld with tensile strengths slightly higher than those found in the plain tension tests. SAE B1113 steel is extremely hard to weld due to its high sulfur and phosphor content. Successful welds were accomplished with chrome iron filler wire, but after annealing the specimens had a hard thick surface scale. As seen by comparing Figures 1 and 3, annealing significantly reduced the yield strengths.

2.4 Conclusions on Materials and Joining Techniques

On the basis of its mechanical properties and its weldability, SAE C1020 hot rolled steel was selected as the most appropriate material for ultimate strength model studies of A36 steel structures. Its availability in thin sections or sheet thicknesses lends to its use in models of a variety of structural forms. For the machining (milling) of wide flange shapes from rectangular bar stock, it is not as convenient as SAE B1113 steel. However, the B1113 steel exhibits certain strength and weldability characteristics that overbalance its desirable machining characterisitics.

Heliarc welding with Oxweld 65 and Industrial Stainless 410 filler wires produced joints of undetermined strength and ductility, since in every butt welded tension test a ductile failure occurred in the base material rather than in the joint. Specimens which were annealed after welding generally failed adjacent to the butt weld. On the other hand, the unannealed specimens seemed to exhibit a heat-affected zone adjacent to the weld such that most of these specimens failed outside the one-inch gauge length that was used.

2.5 Model Sections

One-fifteenth-scale 21WF62 and 14WF103 sections were milled from C1020 hot rolled steel bar stock by Precision Shapes Co. of Suffern, New York. Specified dimensions and as-delivered dimensions are shown in Table 3. Cost for the milled sections was about $27 per foot. The finished sections were delivered in six- to ten-foot lengths. The 14WF103 evidenced very little camber, but a sweep of up to ½ inch in one nine-foot section was present. This presented no problem, however, since the maximum required length was three feet. The 21WF62 sections were twisted about the longitudinal axis, with one having a 30-degree rotation from one end to the other. When these sections were cut and/or annealed, some of this twist was reduced, but not eliminated.

TABLE 2

Chemical and Physical Properties
of Heliarc Filler Rods

	C	*Mn*	*Si*	*S*	*P*	*Cr*	*Ph*	*Zn*	*Ti*	*T.S.* (ksi)
410 Stainless	.15	1.0	1.0	.030	.04	12	—	—		85–100
Oxweld 65	.04	1.20	.50	.020	.017	—	.10	.07	.10	75–95

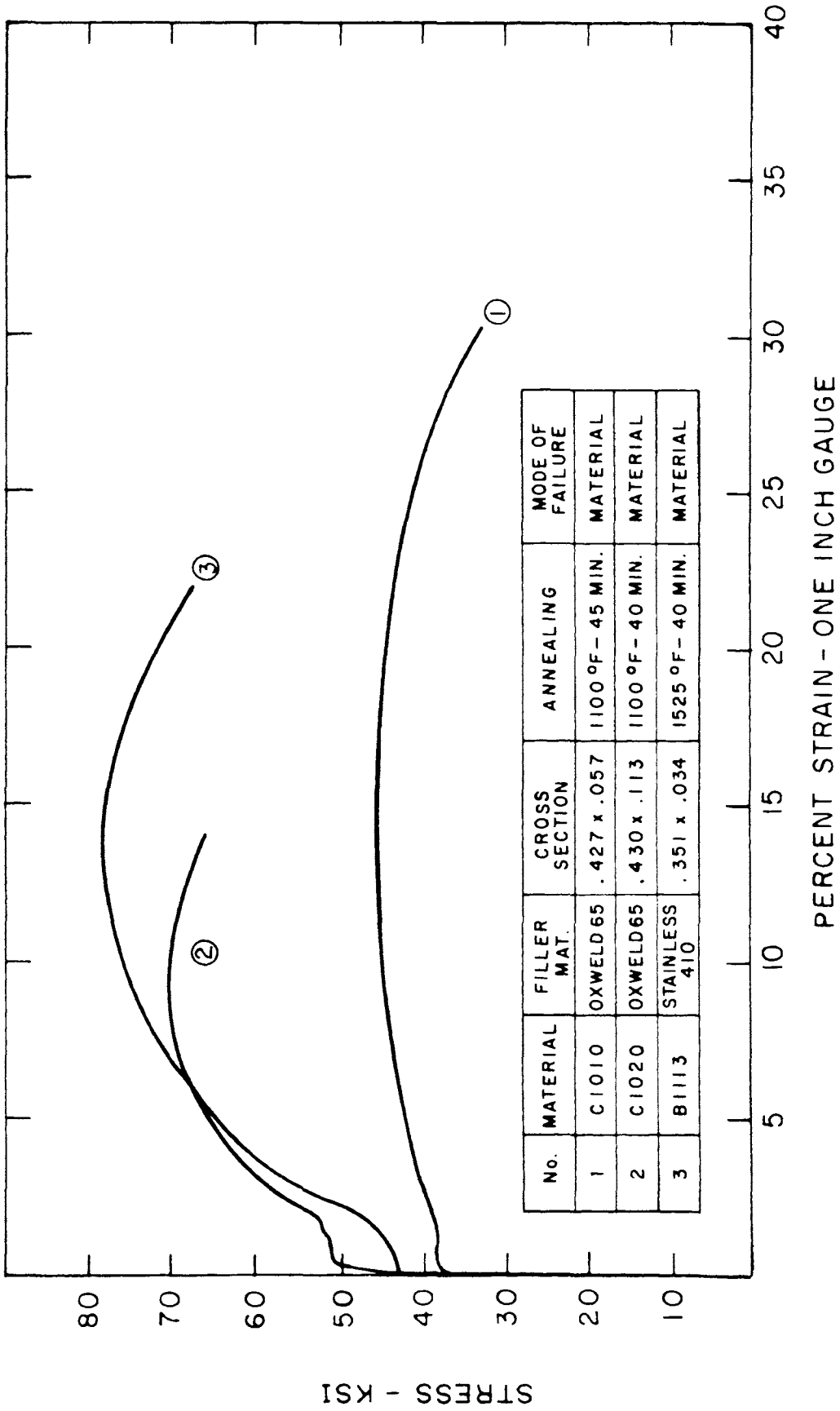

FIGURE 3–STRESS-STRAIN CURVES FOR C1010, C1020, B1113 WELDED TENSION SAMPLES

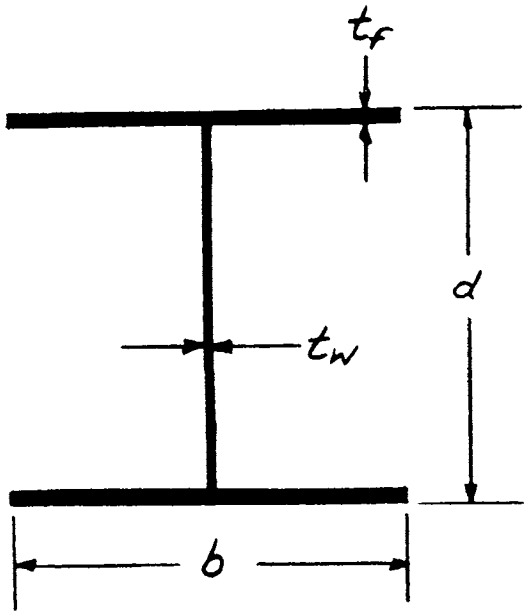

TABLE 3

Comparison of Specified and Actual Dimensions
for 14WF103 and 21WF62 Sections

SPECIFIED DIMENSIONS

Section	d (in)	b (in)	t_f (in)	t_w (in)	I (in^4)*
14WF103	.950	.972	.054	.036	.0230
21WF62	1.400	.548	.041	.027	.0262

ACTUAL AVERAGE DIMENSIONS

Section	d (in)	b (in)	t_f (in)	t_w (in)	I (in^4)*
14WF103	.950	.972	.052	.034	.0225
21WF62	1.402	.548	.041	.028	.0265

* CALCULATED FROM DIMENSIONS

3. JOINT AND BEAM TESTS

3.1 Joint Tests

3.1.1 Purpose

The joint tests had three purposes: 1) to determine the strength of the weld in a joint connection, 2) to determine the effect and necessity of annealing welded members, and 3) to test the members themselves and to compare actual yield and ultimate moments with calculated theoretical moments. Nine tests were planned: six knee-joint tests (three 14WF103–14WF103 connections and three 14WF103–21WF62 connections, Figs. 4 and 5), and three cantilever tests of 21WF62 sections welded to the flanges of 14WF103 columns (Fig. 6). For each type connection, there would be three conditions of heat treatment. One joint would have its members annealed at 1000 degrees F for one hour with an oven cool prior to welding. The second joint would be annealed in the same manner after welding. The third was not to be annealed.

3.1.2 Tension Tests on Flange and Web Samples

To determine stress-strain characteristics of the steel used in the fabrication of the sections, four tension specimens were machined from samples taken from the flange and web of a 14WF103 section and six from the web of a 21WF62 section. Three samples of the 21WF62 and two of the 14WF103 were annealed at 1000 degrees F for 45 minutes and oven cooled. The average yield values obtained from the annealed and non-annealed test specimens of both sections were used in calculations of yield and plastic moments for the annealed and non-annealed joint and beam tests. These values are shown in Table 4.

TABLE 4

Section Yield Strength
(0.2% Offset)

Section	Annealed	Non-Annealed
14WF103	37.6 ksi	35.1 ksi
21WF62	44.6 ksi	47.2 ksi

3.1.3 Joint Test Results

3.1.3.1 14WF103–14WF103 Connection

Figure 10 gives results for the 14WF103–14WF103 connection for combined bending and axial load. The bending moment for the corner joint tests was taken about the intersection of the neutral axes and is called the haunch moment. Theoretical moments were calculated at the face of the joints and then were extrapolated to the intersection of the member centerlines (See Fig. 9). The results for one test are not shown, that of the first post-annealed test. This specimen was discarded due to annealing irregularities. A second connection originally scheduled for pre-annealing was post-annealed and substituted for the above connection.

Predicted moments agree closely with the experimental values for the annealed case, but underestimate the strength for the unannealed joint. Computed M_y and M_p values were not modified to account for axial load since P/P_y max. was only about 0.13. Flange buckling was initiated in the plastic region and became quite pronounced before web buckling occurred. There was no evidence of failure in the welds. Rotation of the joint based on its horizontal deflection averaged .007 radians at yield and .06 radians at ultimate load.

3.1.3.2 14WF103–21WF62 Connection

The results of the 14WF103–21WF62 joint tests are given in Figure 11. The pre-annealed connection is included in this series and as can be seen, reached an ultimate moment 100 inch-pounds higher than that of the post-annealed sample. The non-annealed sample resisted the highest moment, about 140 inch-pounds higher than that of the post-annealed joint. The computed yield and plastic moments are based upon failure of the 21WF62 section. (Although the 21WF62 has a much lower section modulus than the 14WF103, it has a

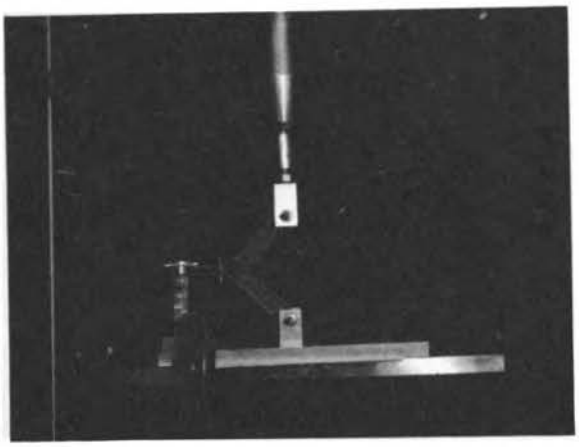

FIGURE 4a–14WF103–14WF103 TESTING SETUP

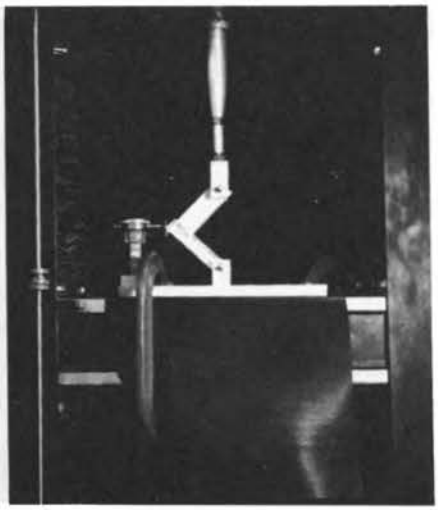

FIGURE 5a–14WF103–21WF62 TESTING SETUP

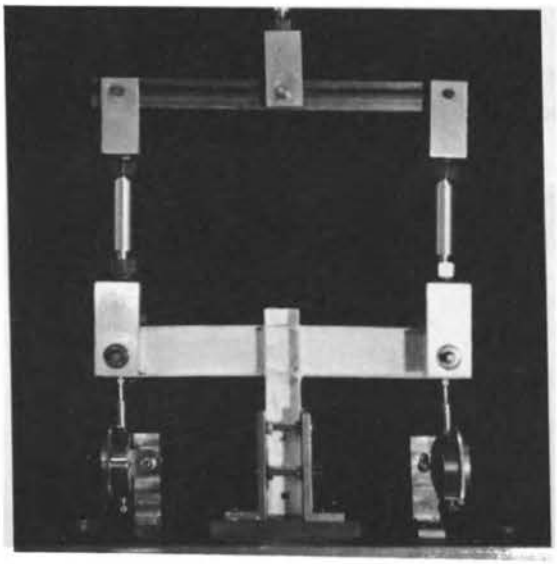

FIGURE 6a–CANTILEVER TESTING SETUP

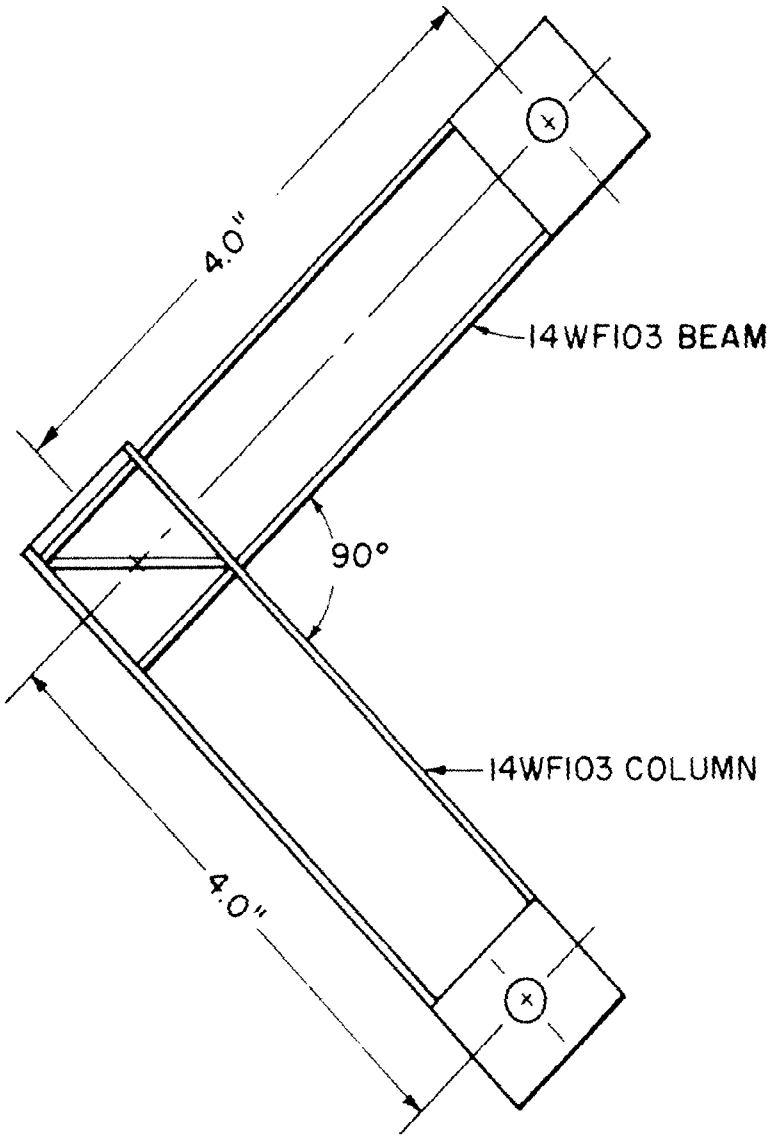

FIGURE 4b–DIMENSIONS FOR 14WF103–14WF103 CORNER JOINT

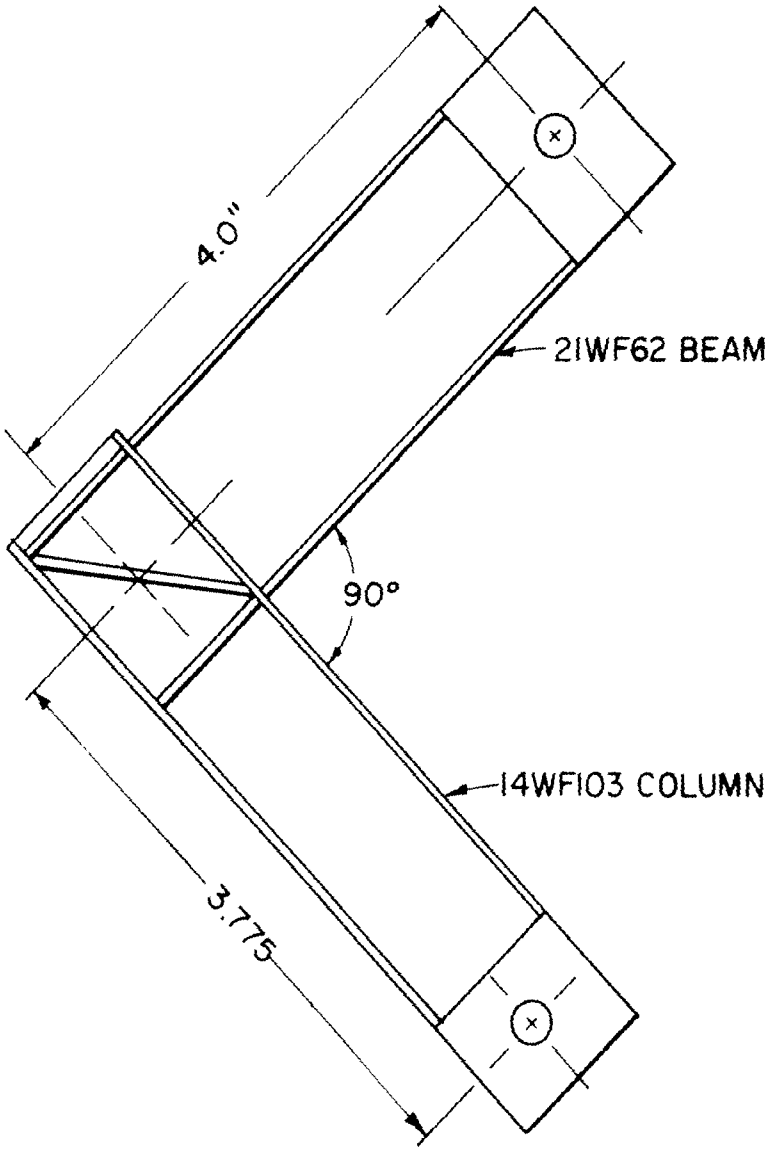

FIGURE 5b–DIMENSIONS FOR 14WF103–21WF62 CORNER JOINT

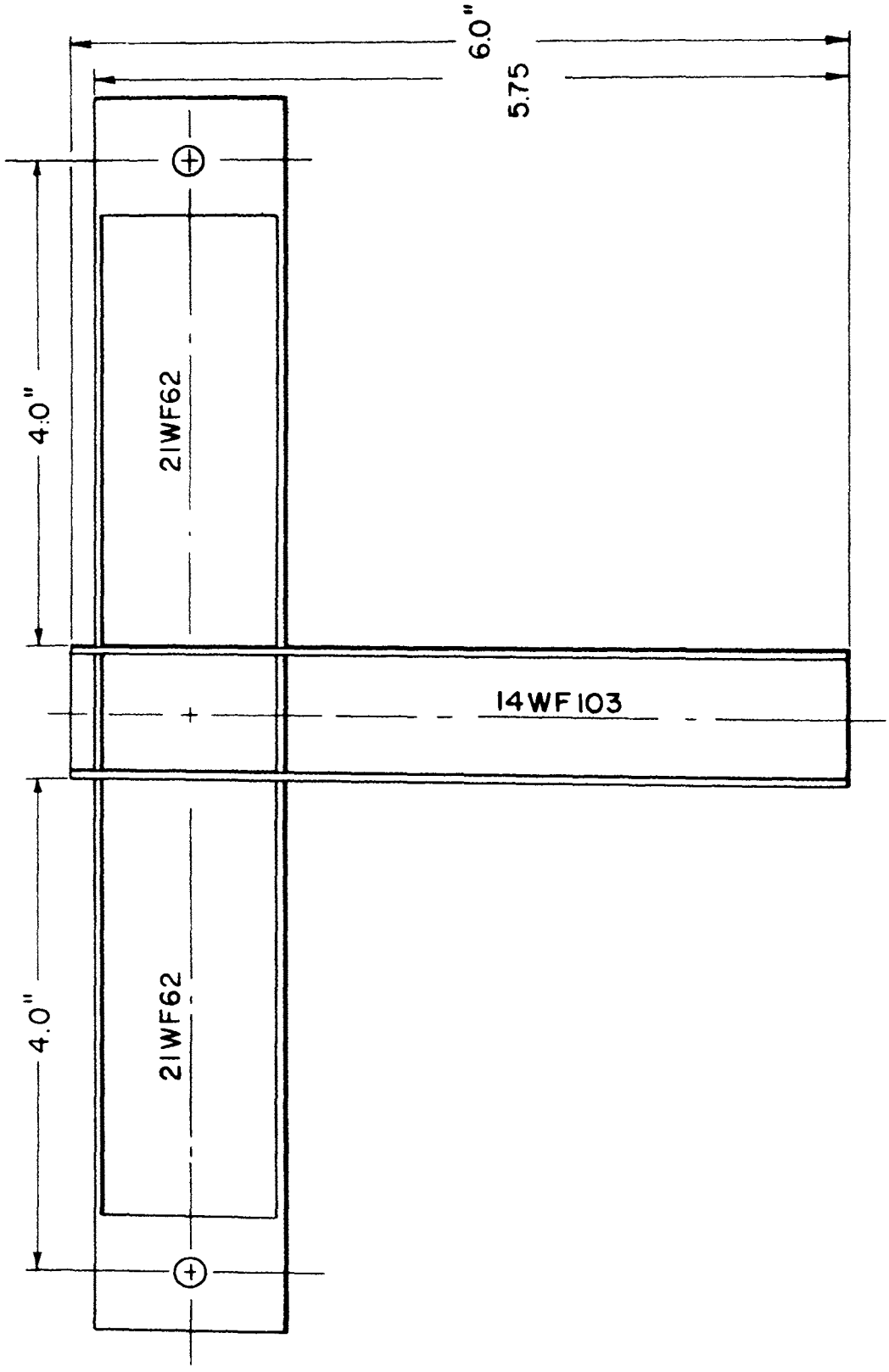

FIGURE 6b—DIMENSION FOR INTERIOR JOINT 14WF103 COLUMN-21WF62 BEAM

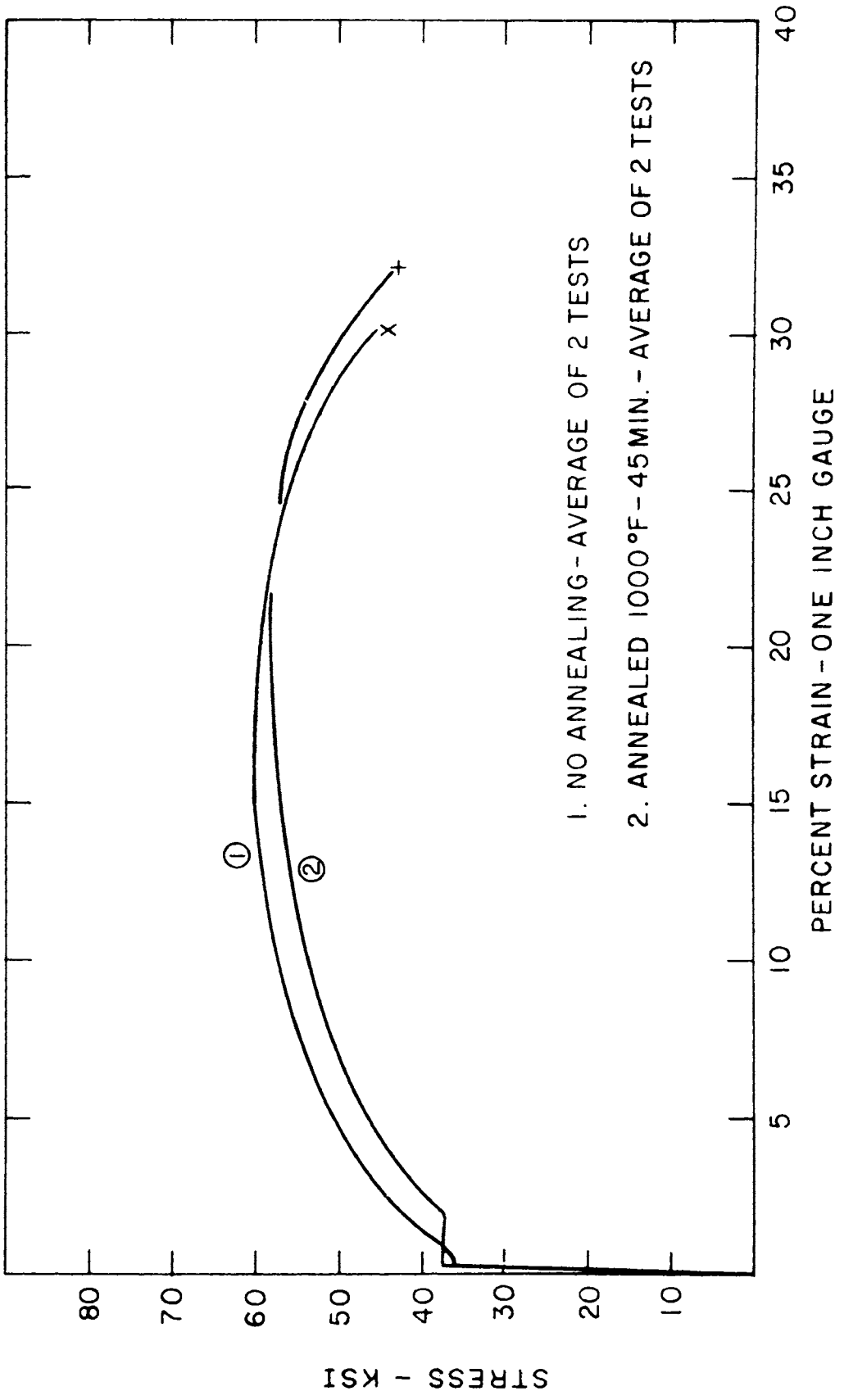

FIGURE 7—ANNEALING-EFFECT ON 14WF103 WEB AND FLANGE TENSION SAMPLES—C1020 H.R. STEEL

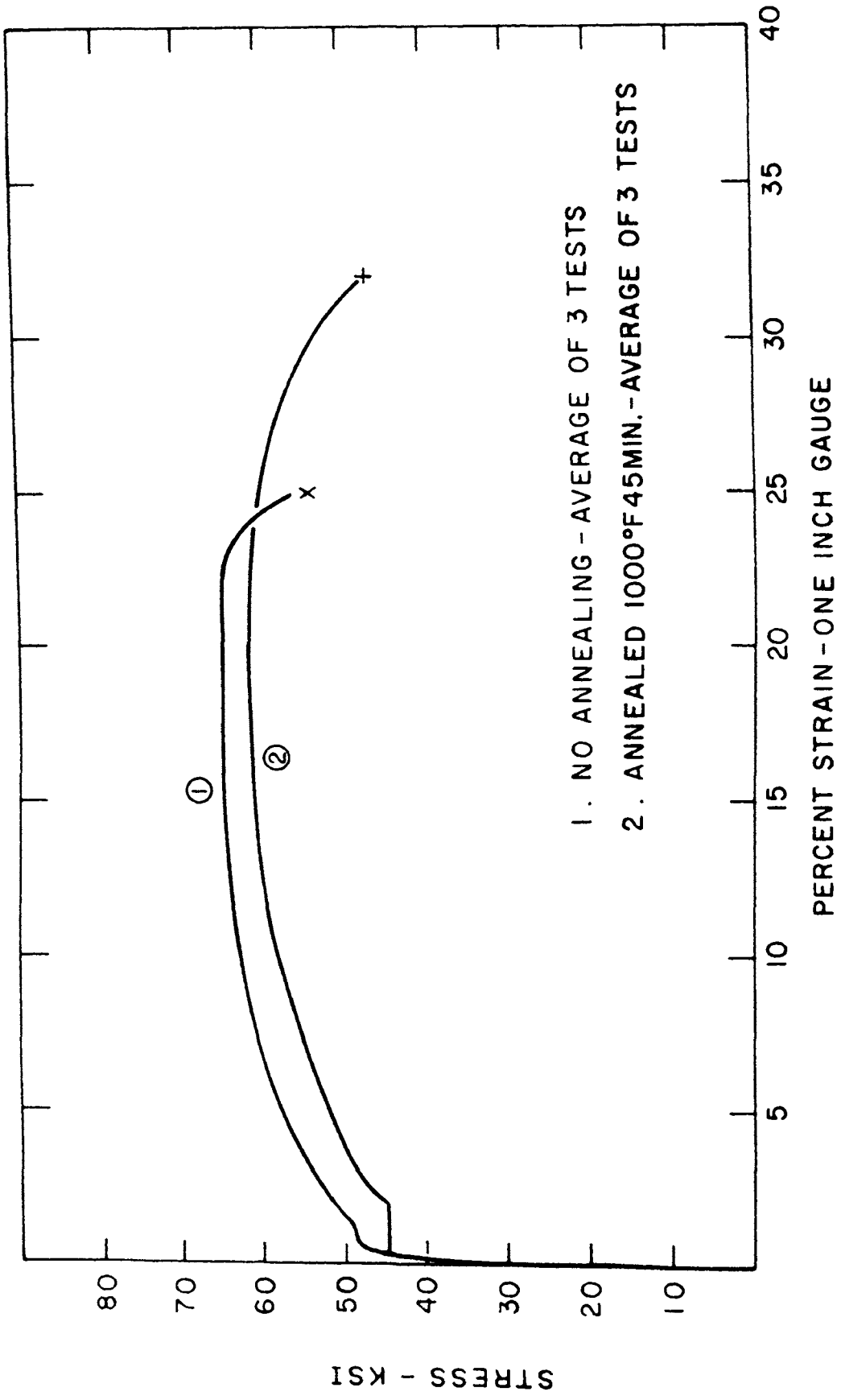

FIGURE 8—ANNEALING-EFFECT ON 21WF62 WEB TENSION SAMPLES—C1020 H.R. STEEL

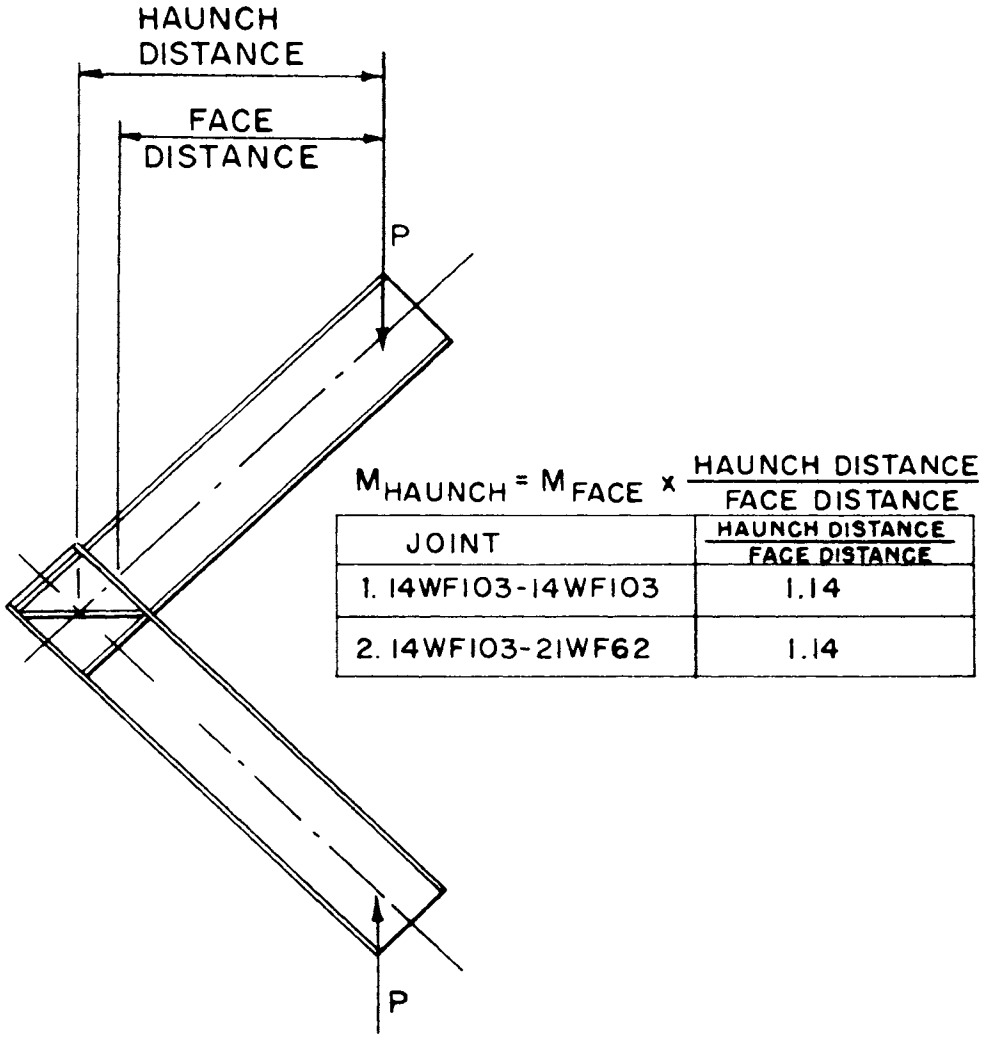

$$M_{HAUNCH} = M_{FACE} \times \frac{\text{HAUNCH DISTANCE}}{\text{FACE DISTANCE}}$$

JOINT	HAUNCH DISTANCE / FACE DISTANCE
1. 14WF103-14WF103	1.14
2. 14WF103-21WF62	1.14

FIGURE 9–EXTRAPOLATION OF YIELD AND PLASTIC MOMENTS FROM KNEE FACE TO KNEE HAUNCH

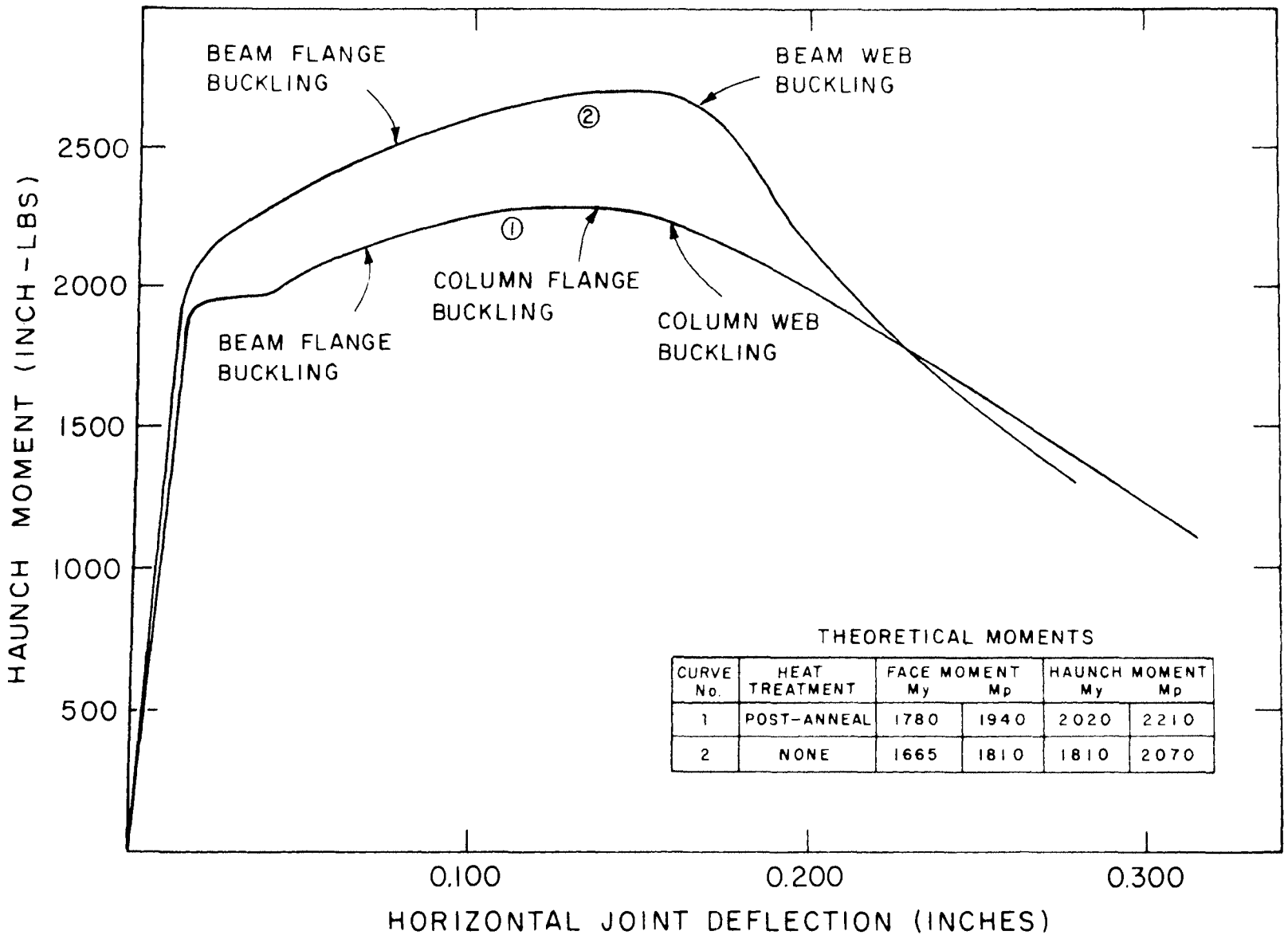

THEORETICAL MOMENTS

CURVE No.	HEAT TREATMENT	FACE MOMENT My	FACE MOMENT Mp	HAUNCH MOMENT My	HAUNCH MOMENT Mp
1	POST-ANNEAL	1780	1940	2020	2210
2	NONE	1665	1810	1810	2070

FIGURE 10–14WF103–14WF103 MOMENT DEFLECTION CURVES

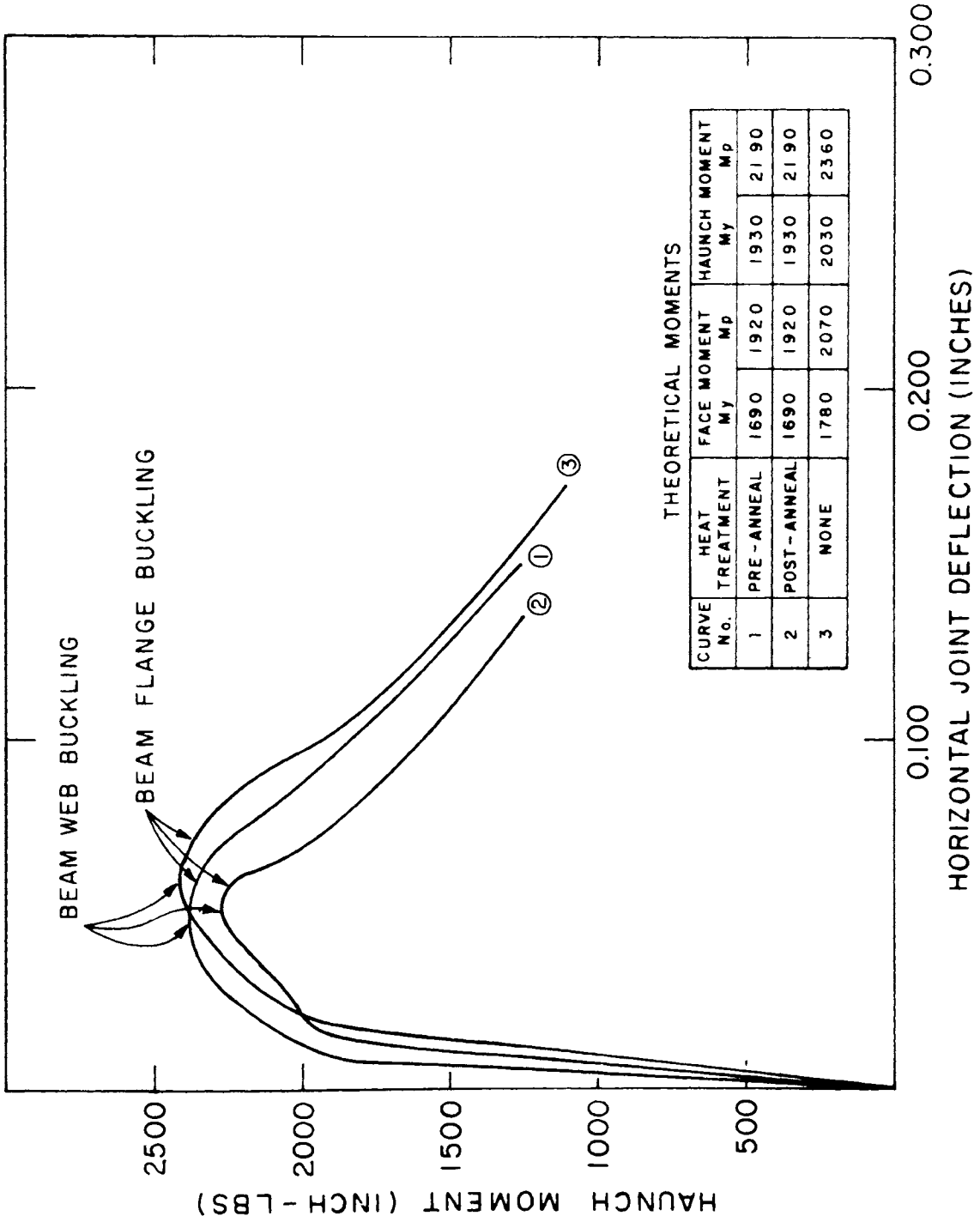

FIGURE 11—14WF103—21WF62 MOMENT DEFLECTION CURVES

higher yield stress and hence the value of M_p for the 21WF62 is only slightly less than that for the 14WF103.) Rotation for this connection averaged .01 radians at yield and .035 radians at ultimate load.

3.1.3.3 Cantilever Tests

Results for the cantilever tests are given in Figures 13 through 15. The theoretical bending-deflection curve includes shear deflections on the order of .005 inches at yield. The variation in Figure 13 of curve A from this theoretical curve is partly due to the fact that the 21WF62 members were slightly twisted. The twist in the flange increased readings on the dial gauge, which was originally centered under the web. Moment arms were taken from the center line of the column to the point of load, and calculated yield and plastic moments were adjusted from the face values by multiplication of the column center-line distance divided by the face distance (Fig. 12).

Yield and ultimate moments for the post-annealed test were in good agreement with computed moments. An "upper" and "lower" yield moment was found for both beams, but their significance is not known at the present time. The pre-annealed section supported 400 inch-pounds more than the computed ultimate moment. The non-annealed section supported the greatest ultimate moment, over 900 inch-pounds higher than its computed ultimate moment. Assuming the value reached was in fact the plastic moment for the section, it would correspond to a yield stress of 67 ksi at the flange. Unloading of all the sections was initiated shortly after flange and web buckling had taken place.

3.2 Beam Tests

3.2.1 Purpose

The third-point loaded 21WF62 and 14WF103 beams were intended to help in determining the influence of annealing on the behavior of milled wide flange sections. The joint tests had left somewhat open the question of which was more critical, the cold working and initial stresses induced by milling the wide flange shapes or the influences brought about by the heliarc welding.

3.2.2 Test Results

Figures 16a and 17a show the test setup, while figures 16b and 17b give results for two 14WF103 and two 21WF62 beams respectively.

The behavior of the unannealed 14WF103 beam was very similar to that of the annealed specimen, although both reached only about 93 per cent of the predicted plastic moment. These low values may have been due to the fact that the predicted plastic moment values were based on tension coupons taken from other lengths of material. In fact, five other annealed 14WF103 beams were tested by student groups in an M.I.T. graduate subject laboratory. Each beam behaved in a more predictable manner, with a typical response being indicated by curve 3 in Figure 16.

The 21WF62 beams buckled laterally shortly after reaching yield moments. Lateral bracing had been provided so that $\ell/r_y = 37$, a value slightly above the 35 specified for A36 steel in the 1963 AISC specifications. In actual fact, the 21WF62 material had a yield stress in excess of 40,000 psi, so that a bracing spacing corresponding to perhaps ℓ/r_y even less than 30 should have been used. While the tests were abruptly ended before any conclusive information regarding annealed vs. unannealed specimens could be obtained, it does not appear that any significant behavior difference would have occurred. In a somewhat negative way, it has indicated that models must be braced in the same way as prototype or, conversely, that models may be used to study such things as bracing requirements.

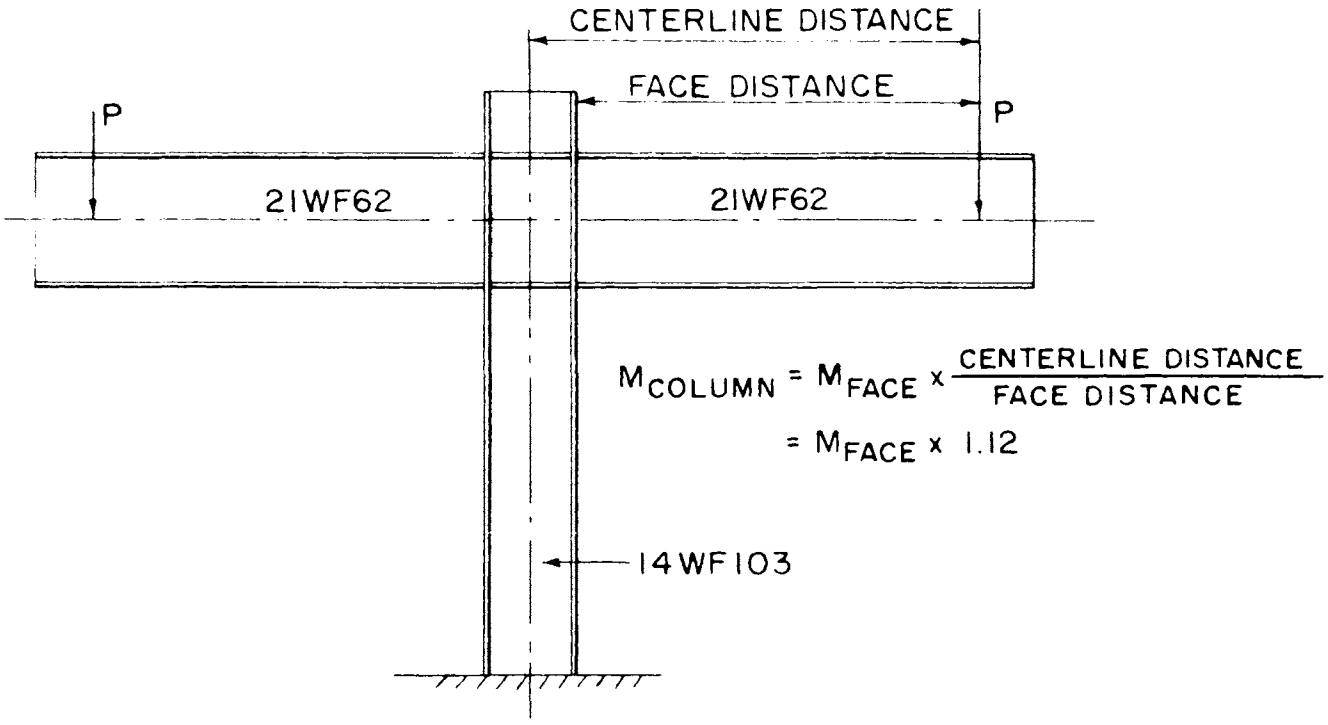

FIGURE 12—EXTRAPOLATION OF YIELD AND PLASTIC MOMENTS FROM FLANGE FACE TO COLUMN CENTERLINE

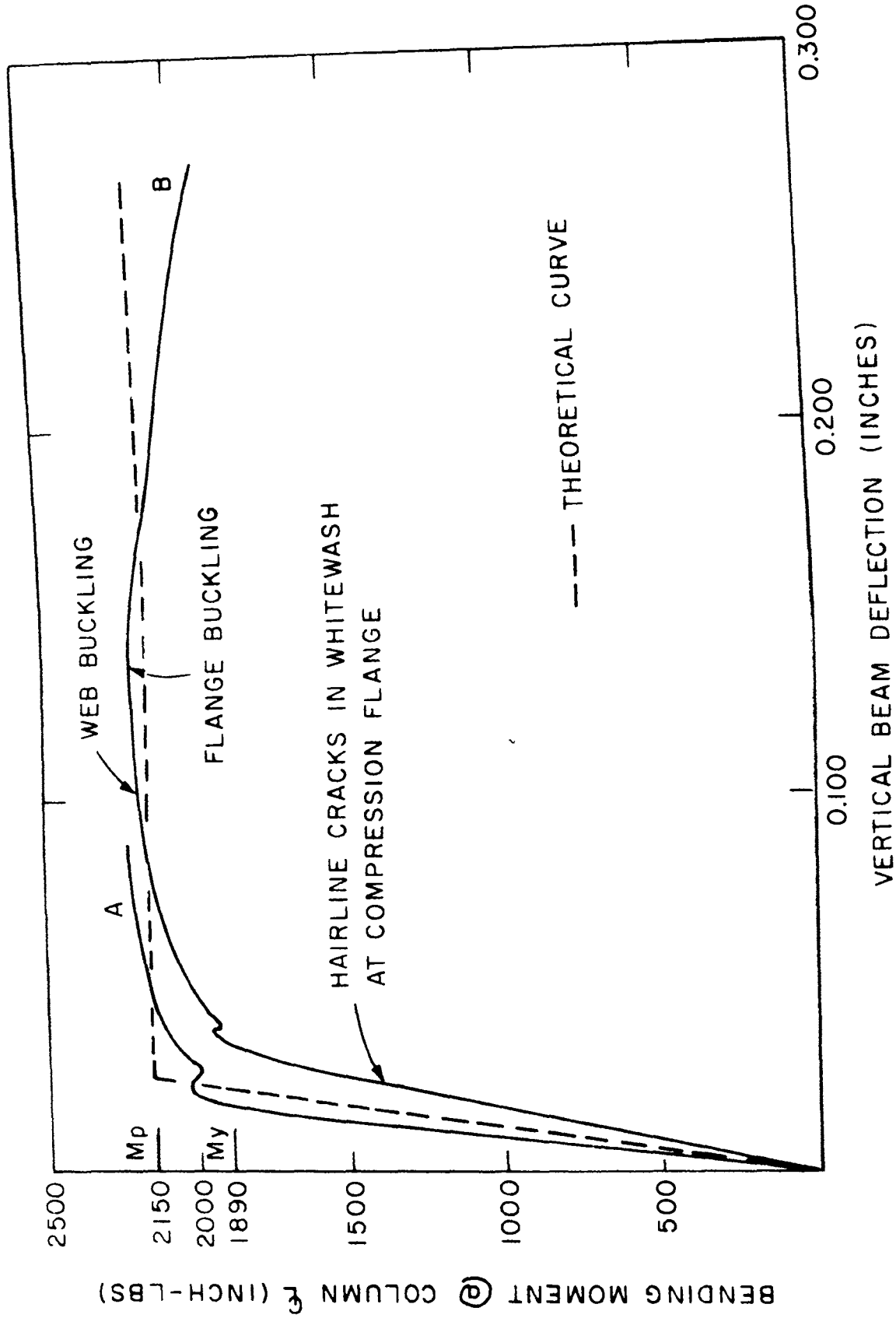

FIGURE 13–MOMENT-DEFLECTION CURVE FOR POST-ANNEALED CANTILEVER TEST

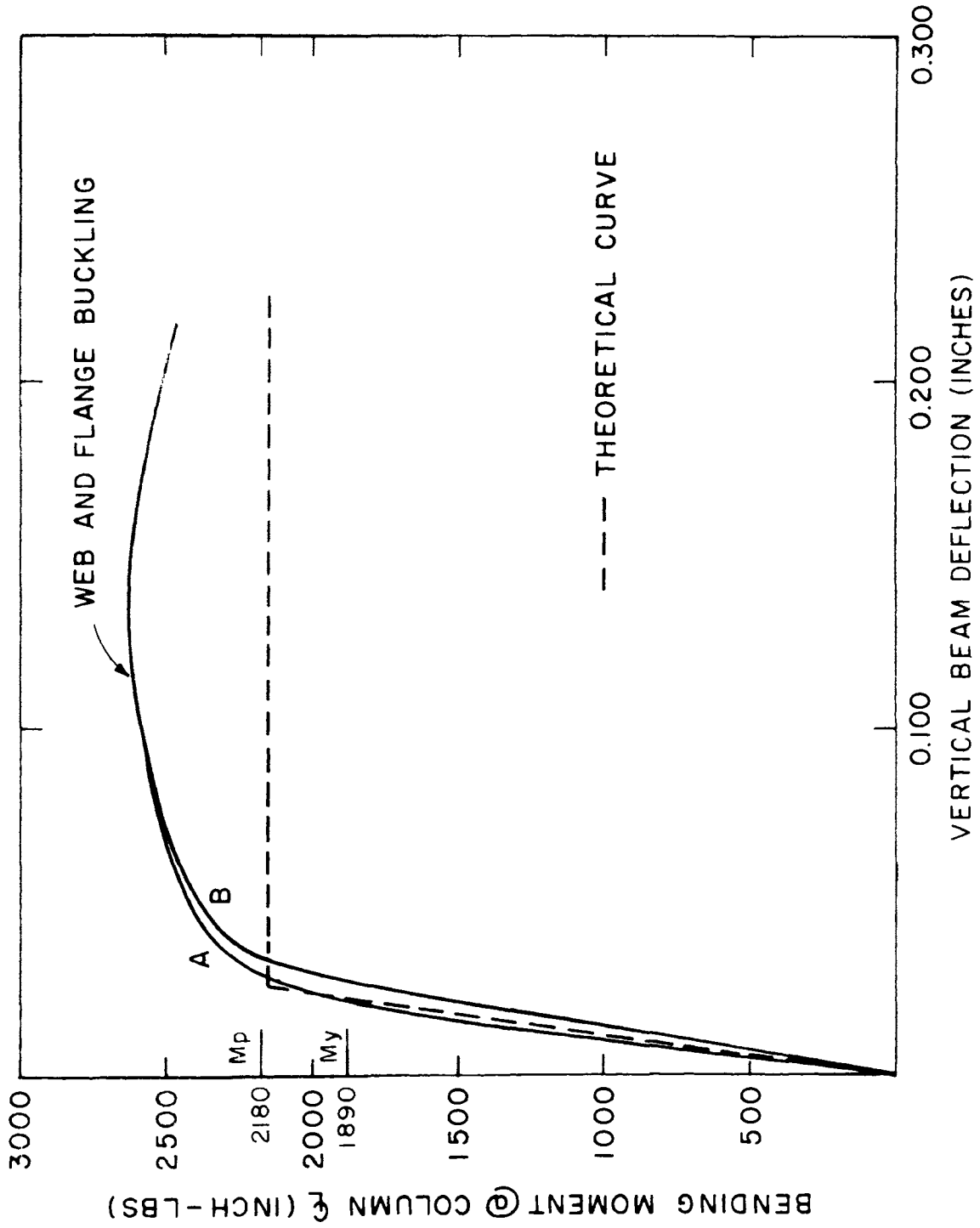

FIGURE 14—MOMENT DEFLECTION CURVE FOR PRE-ANNEALED CANTILEVER TEST

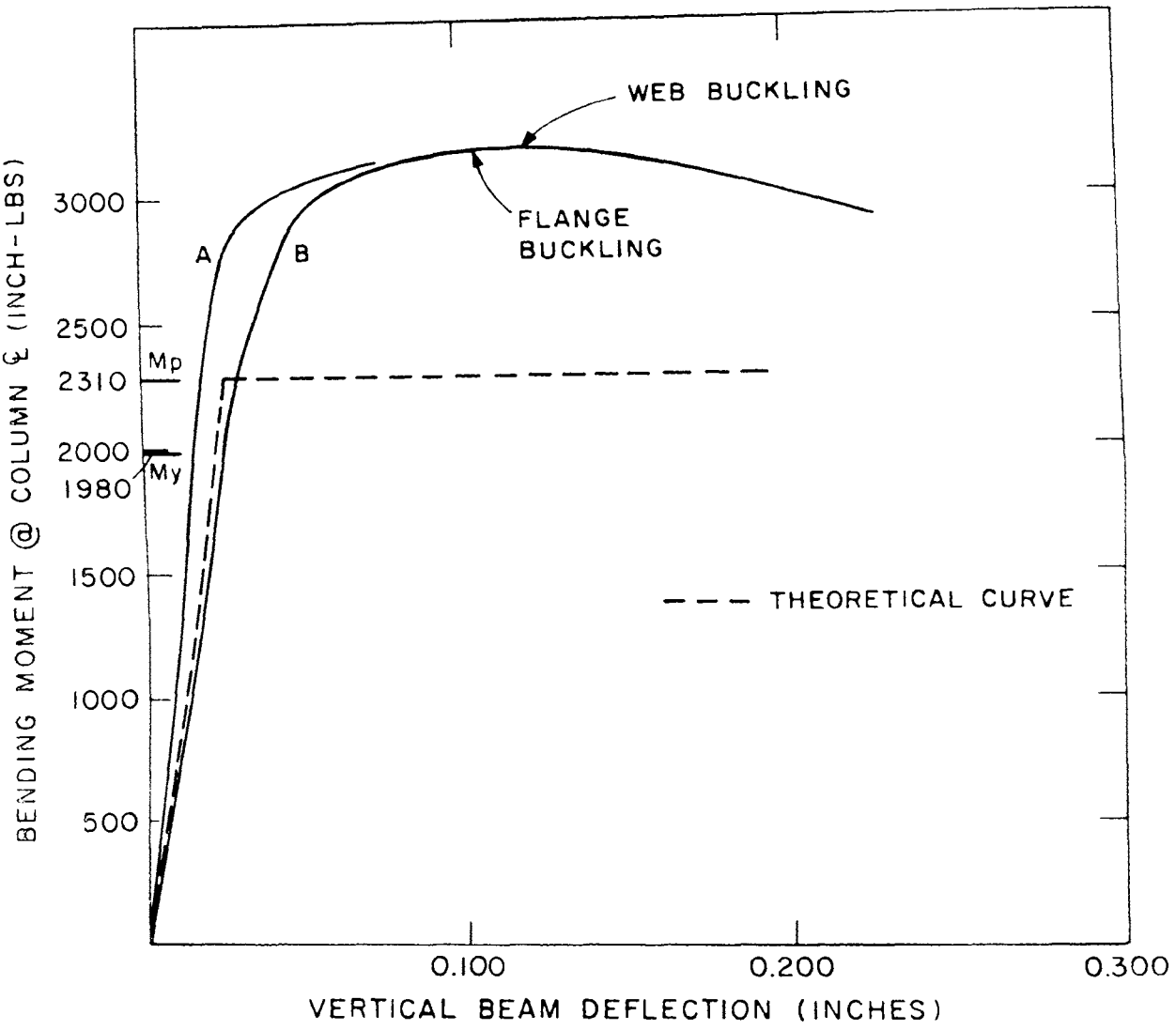

FIGURE 15–MOMENT DEFLECTION CURVE FOR NON-ANNEALED CANTILEVER TEST

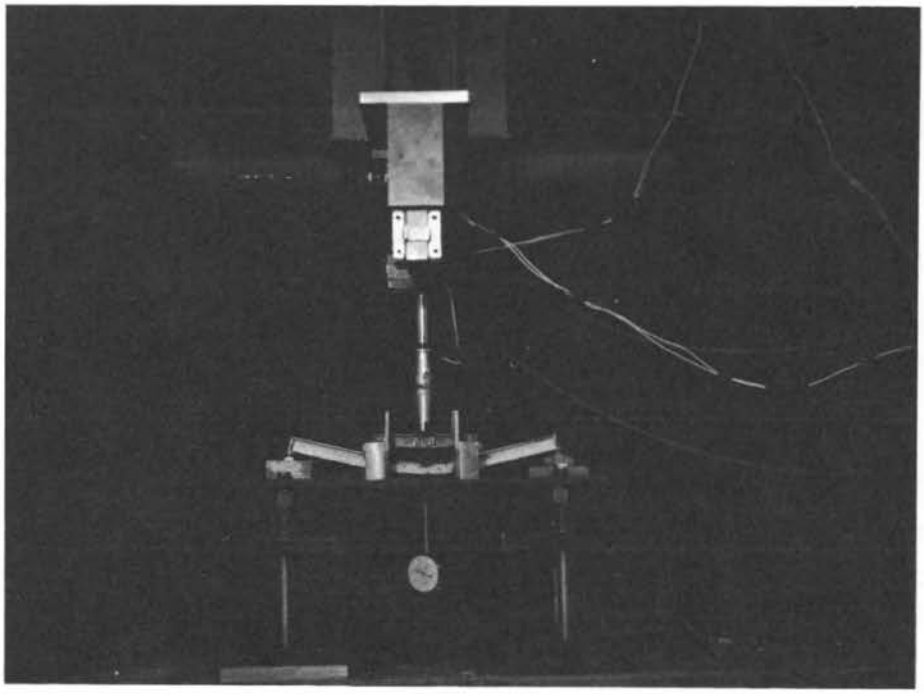

FIGURE 16a—14WF103 BEAM TEST SETUP

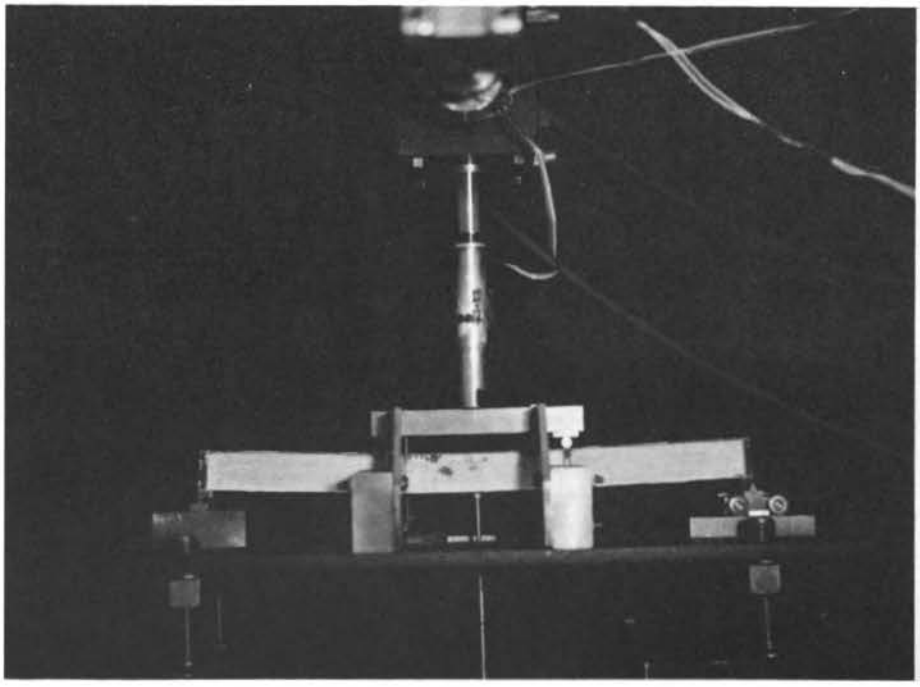

FIGURE 17a—21WF62 BEAM TEST SETUP

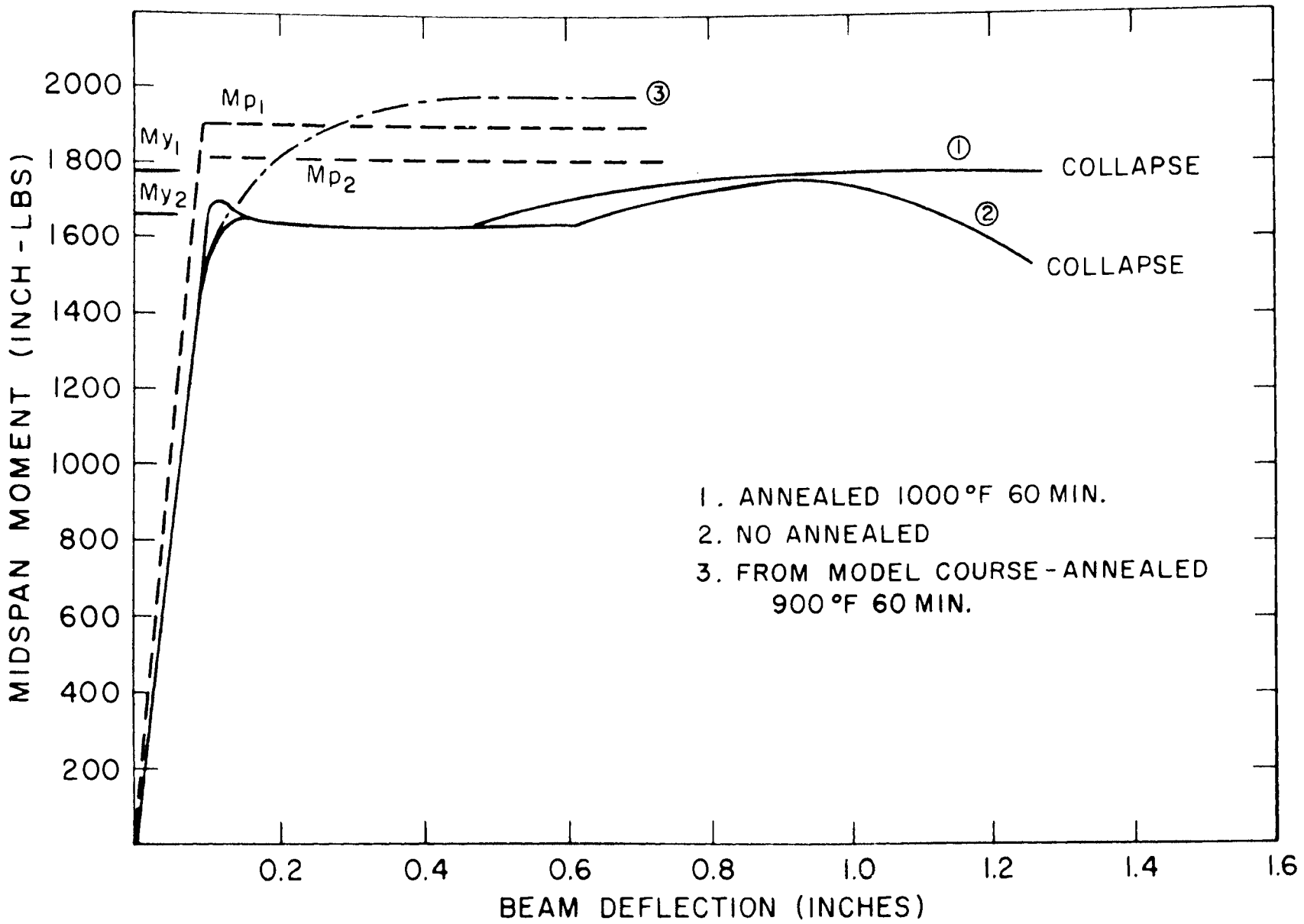

FIGURE 16b—MOMENT-DEFLECTION CURVES FOR 14WF103 BEAMS

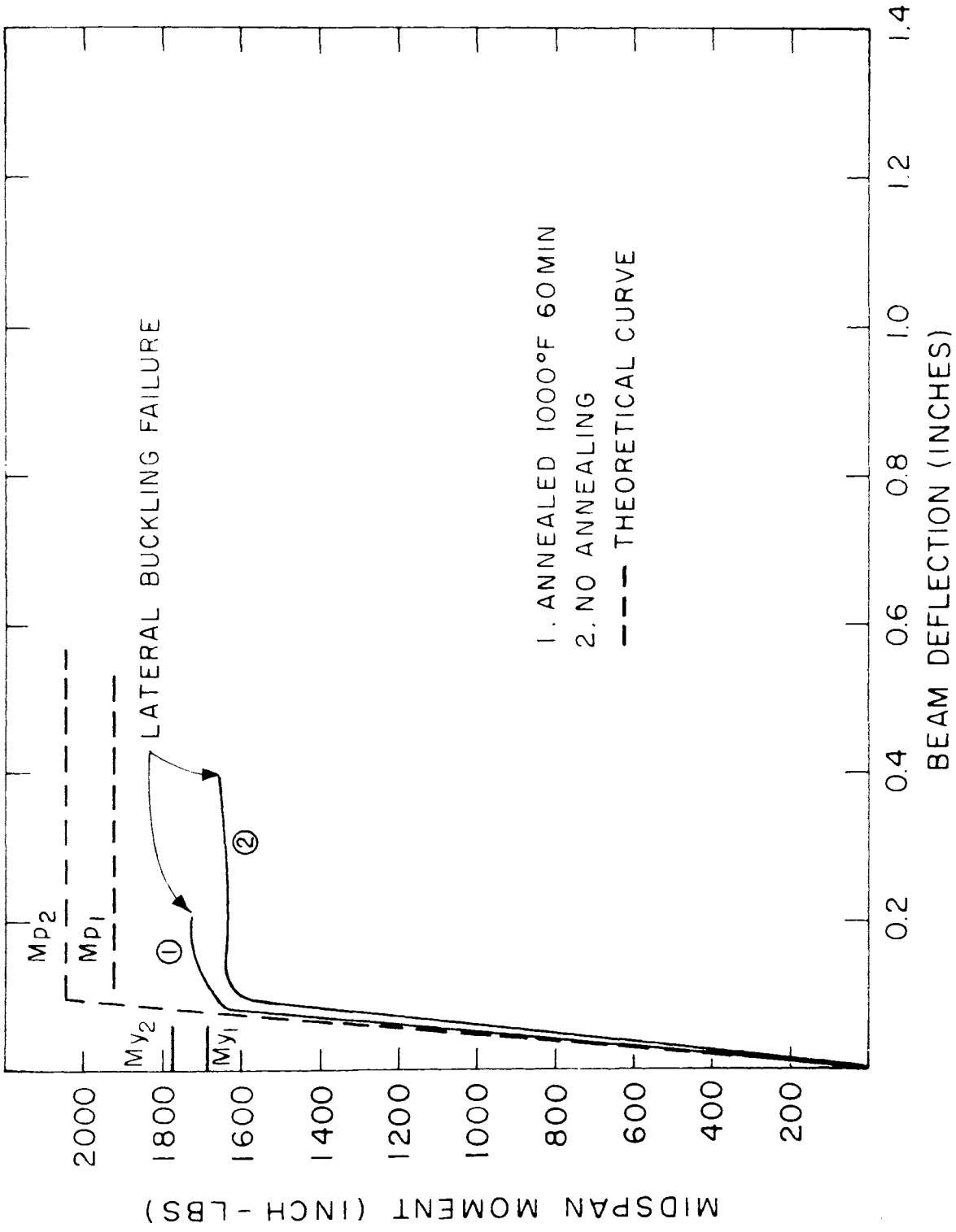

FIGURE 17b–MOMENT-DEFLECTION CURVES FOR 21WF62 MODEL BEAMS

4. FRAMEWORK FABRICATION

The purpose of fabricating a framework was to determine the problems that would arise in the fabricating, and the accuracy that could be obtained in the finished product. Testing of the framework was not scheduled in this project. The framework dimensions may be seen in Figure 18, with joint details in Figures 19 and 20.

The 14WF103 columns and 21WF62 beams were cut to proper lengths on a high speed band saw and the seats, stiffeners, and plates milled from mild steel. Before any welding could be done, all parts were cleaned to remove dust, oil, and oxides.

The first step in the actual welding was the securing of a 21WF62 beam in a jig, followed by the tacking of the beam seat and top plate onto the bottom and top flange of the beam (Figs. 22 and 23). During tacking, these secondary pieces were held in place with small clamps. These clamps were then removed and the seat and top plate welded all around (Figs. 22 and 23). The beam was then vapor-honed to remove an oxidation on the finished weld (Fig. 24). The vapor-hone is a mixture of compressed air, water, and a very fine grit of clay-like texture. In this same manner, all the beams were completed (Fig. 25).

The 14WF103 columns were marked off at the corresponding beam height and the web stiffeners were lightly hammered into position. The web stiffeners were milled slightly oversize to compensate for shrinkage during welding. The web stiffeners were tacked, welded all around, and the affected area vapor-honed (Figs. 26 to 28). Due to a slight shrinkage about the weak axis at the first floor level, a camber occurred at the foot of the column and was subsequently straightened with a rawhide hammer.

A special jig consisting of a flat steel plate with small right angles welded to its surface at corresponding floor levels was used in the fabrication of the three portal frames in the framework. The columns were clamped on either side of the plate, with one flange of each column flat against the plate. The beams were then clamped against the small angles, with the beam seats and top plates resting against the web of the column (Fig. 29). Seats and top plates were then tacked to the columns (Fig. 30). After all beams were tacked, the weld was completed around each seat and top plate with the frame still clamped (Fig. 31). The frames were not vapor-honed. Figure 32 shows one frame completed. Two portal frames were then clamped on either side and perpendicular to the above mentioned plate such that the webs of the columns and the plate were in parallel planes. These frames were spaced at a distance equal to the length of the longitudinal beams to be welded in place. The longitudinal beams were shimmed at the proper height above the plate so they would be centered on the flanges of the columns, and clamped to the angles (Fig. 33). These beams were then tacked to the flanges of the columns (Fig. 34). The assembly was turned over and beams tacked on the other side by the same process (Fig. 35). These welds were then completed with the frames and beams still clamped. The other side was then reclamped and the welds completed. The beam web-column flange weld facing outside the framework had to be done while the opposite side was clamped to the jig.

The remaining frame was added to the subassembly by the process just described (Fig. 36). Figures 37 and 38 show the completed steel framework.

During fabrication of the joint for testing, Part II, Section 2, it was discovered that the Oxweld 65 proved difficult to work with when a great deal of welding was to be done at one place. An oxidized slag formed on top of the molten pool during welding and inhibited penetration of the filler material. The use of 410 filler material relieved this difficulty, and since it showed an undetermined strength of greater than 80 ksi in tension tests, it was decided to use this throughout the remainder of the project on both joint and framework fabrication. Frame-

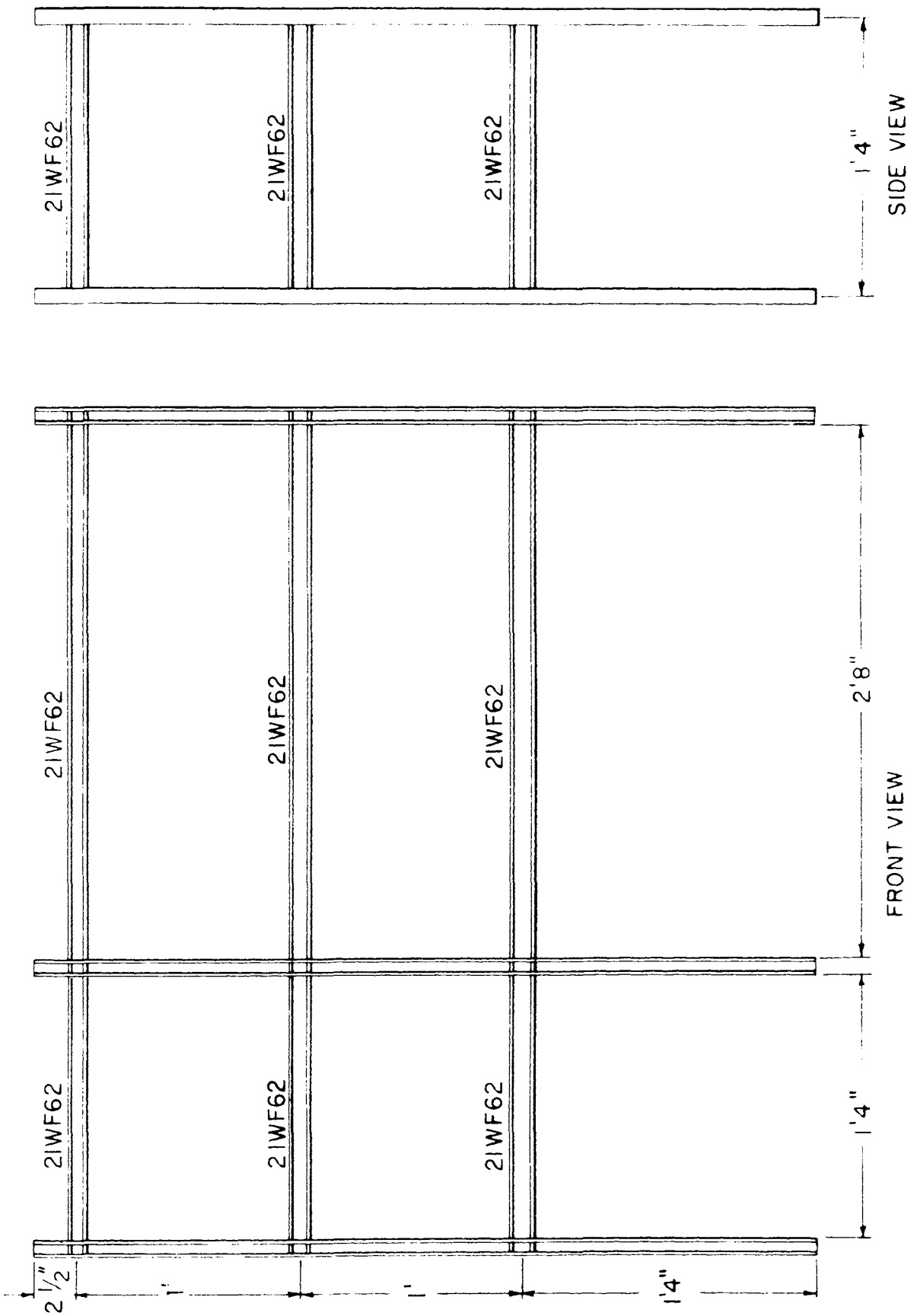

FIGURE 18–ASSEMBLY DRAWING

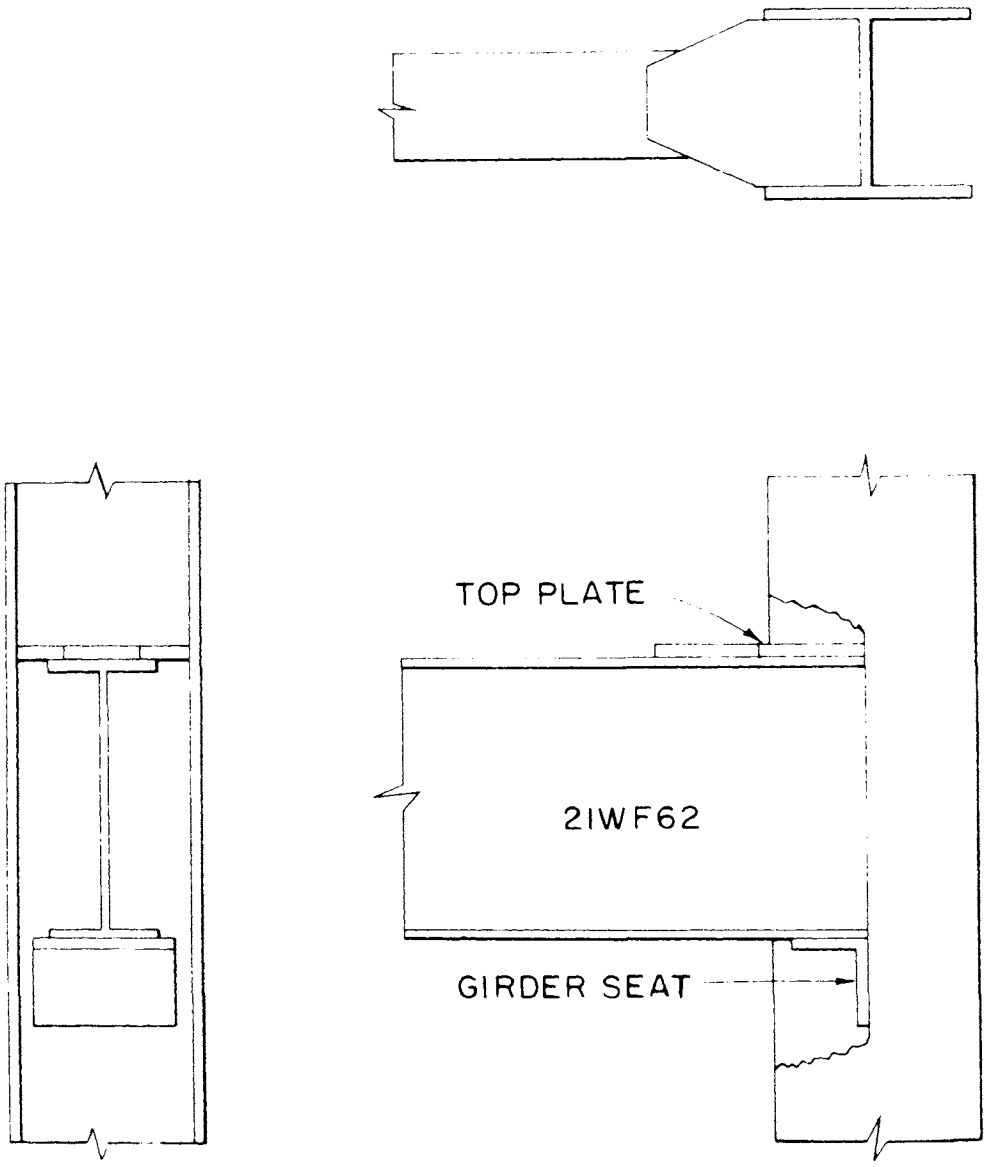

SCALE-FULL SIZE
GIRDER SEAT AND TOP PLATE 1/16" THICK

FIGURE 19–GIRDER TO COLUMN WEB JOINT DETAIL

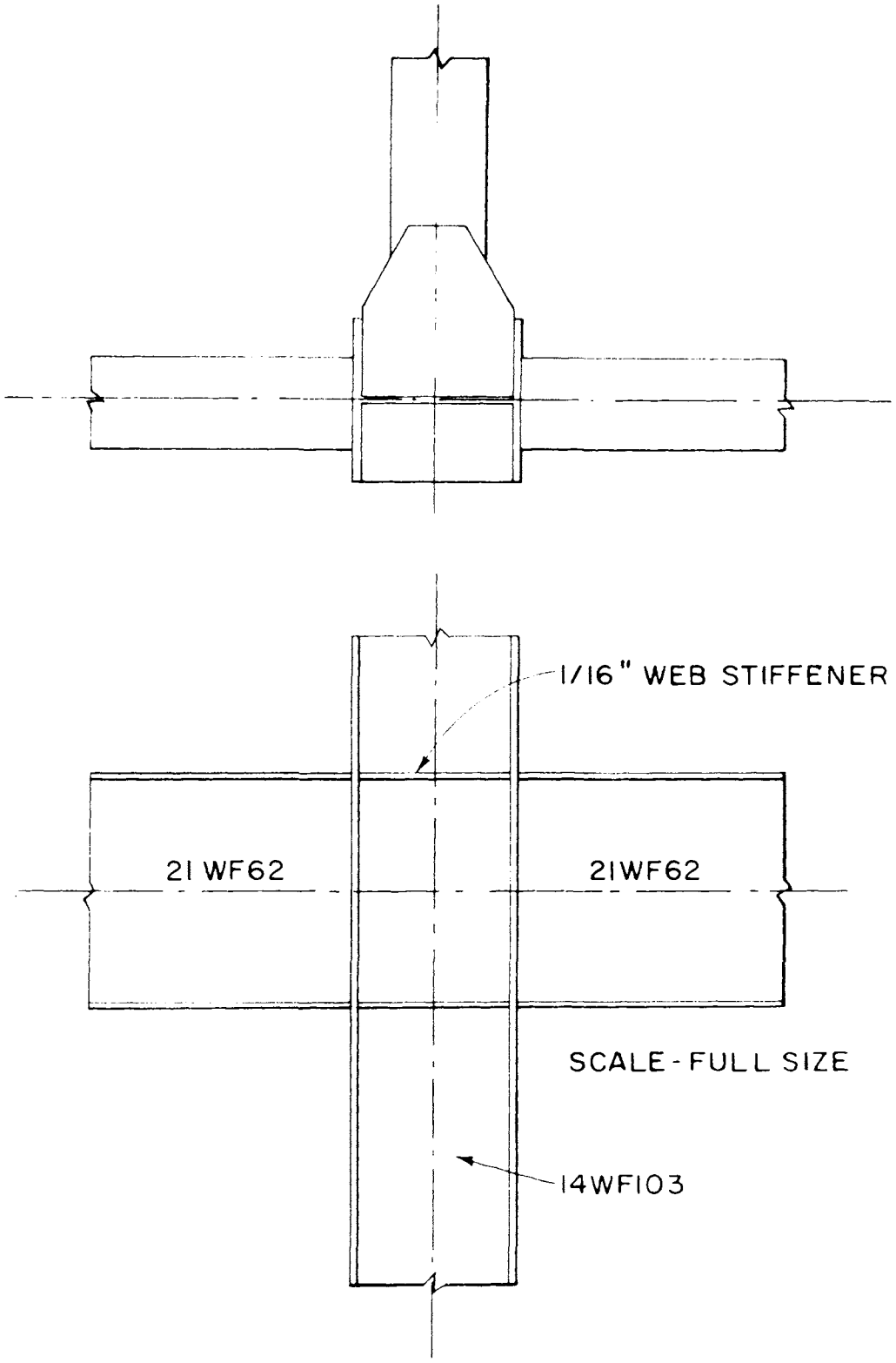

FIGURE 20—GIRDER TO COLUMN FLANGE CONNECTION

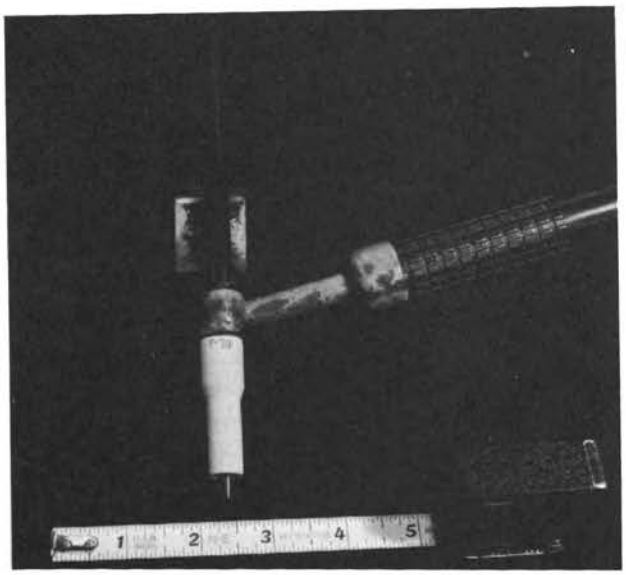

FIGURE 21–HELIARC WELDER

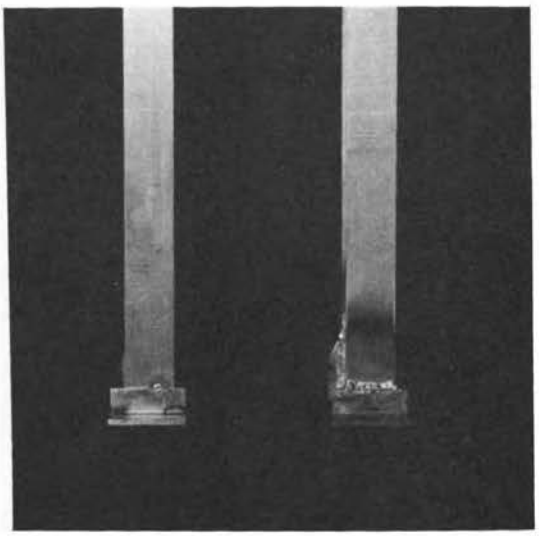

FIGURE 22–TACK AND FINISHED WELD ON BEAM SEAT

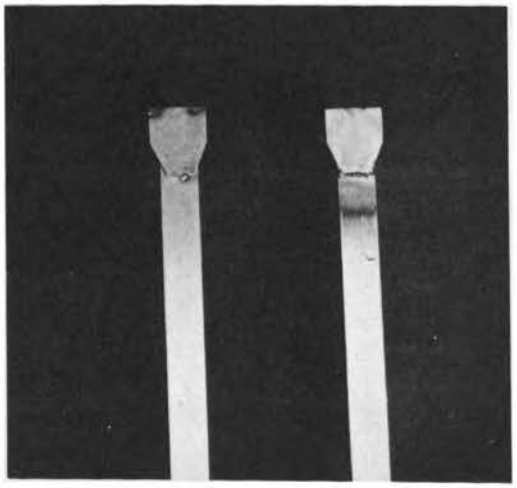

FIGURE 23–TACK AND FINISHED WELD ON TOP PLATE

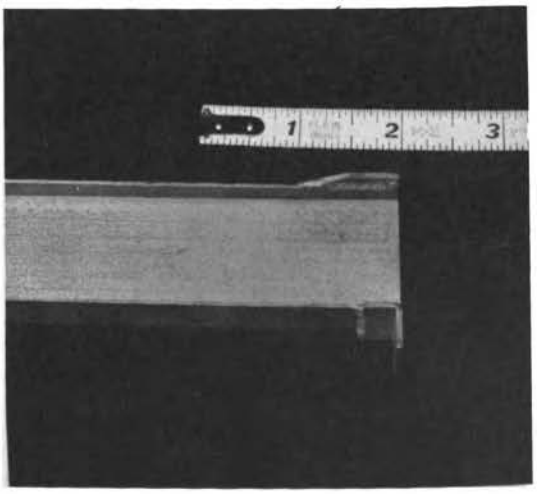

FIGURE 24–WELD VAPOR HONED

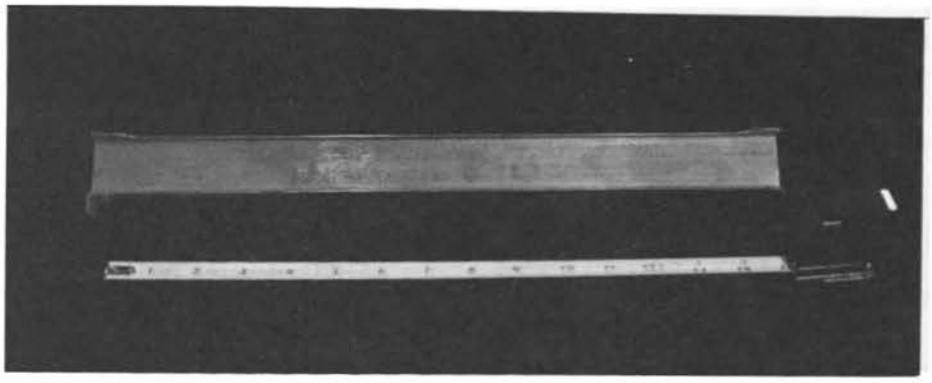

FIGURE 25–FINISHED BEAM

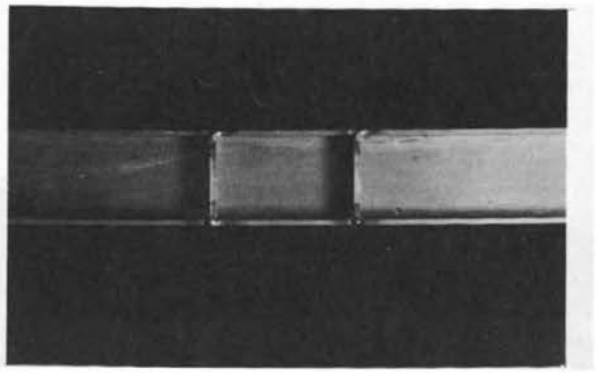

FIGURE 26–TACKED WEB STIFFENER

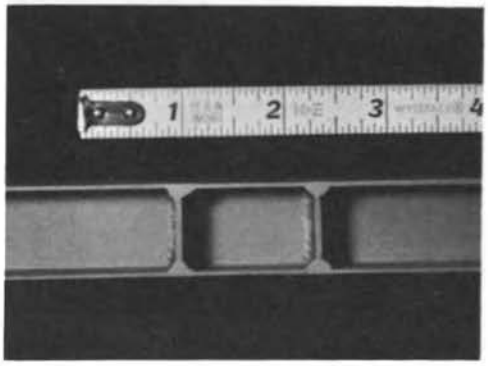

FIGURE 27–WEB STIFFENER WELDED AND VAPOR HONED

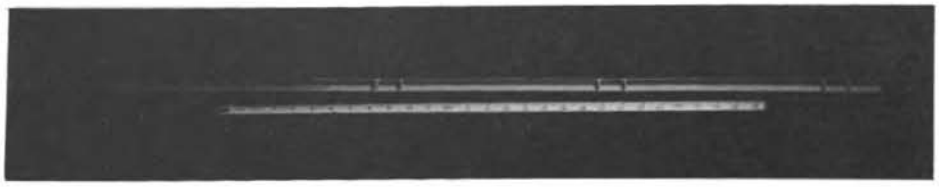

FIGURE 28–FINISHED COLUMN

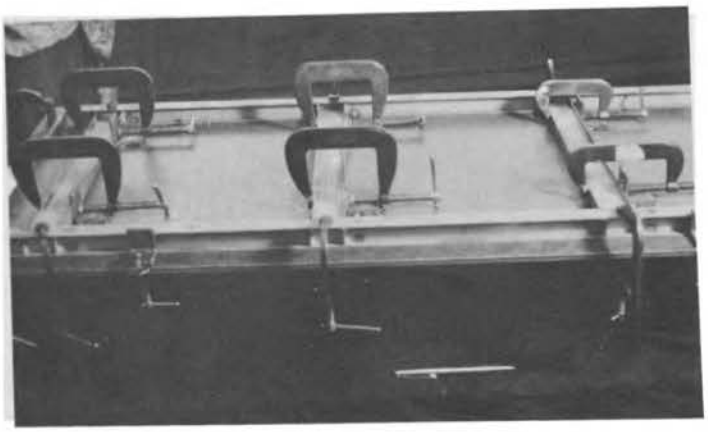

FIGURE 29–COLUMNS AND BEAMS CLAMPED IN PLACE FOR WELDING

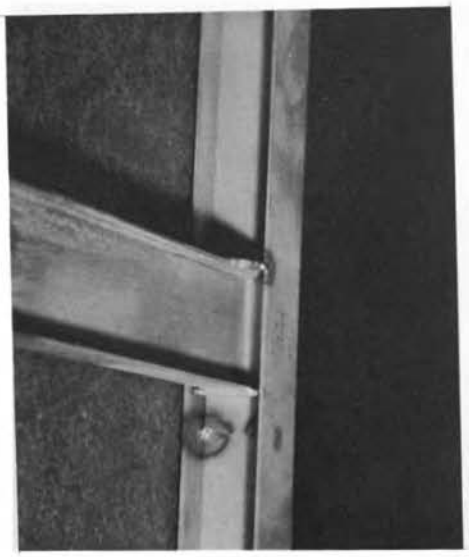

FIGURE 30–BEAM TACKED TO COLUMN WEB

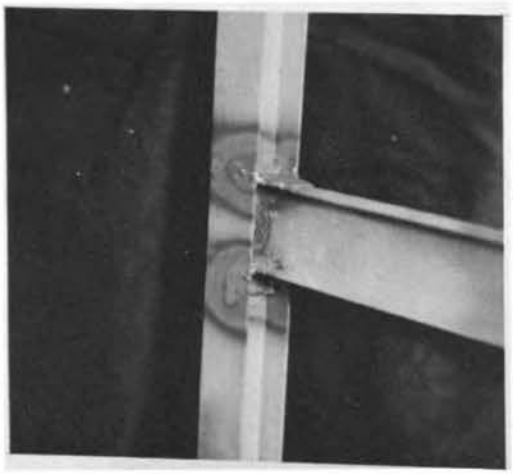

FIGURE 31–COMPLETED BEAM TO COLUMN WEB CONNECTION

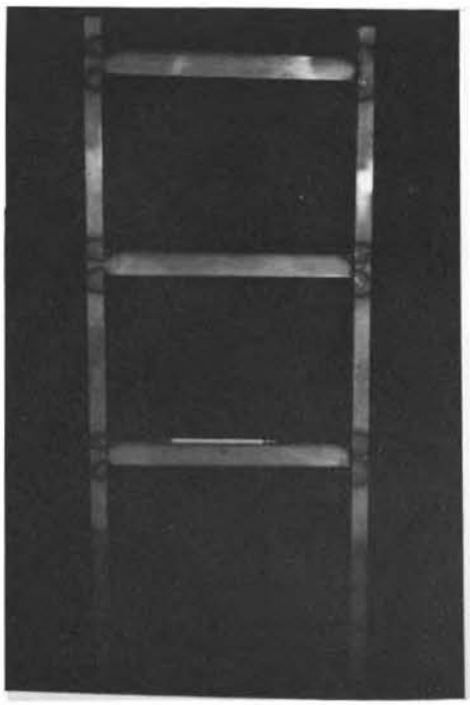

FIGURE 32–COMPLETED FRAME SUBASSEMBLY
(Note Heat Affected Zones)

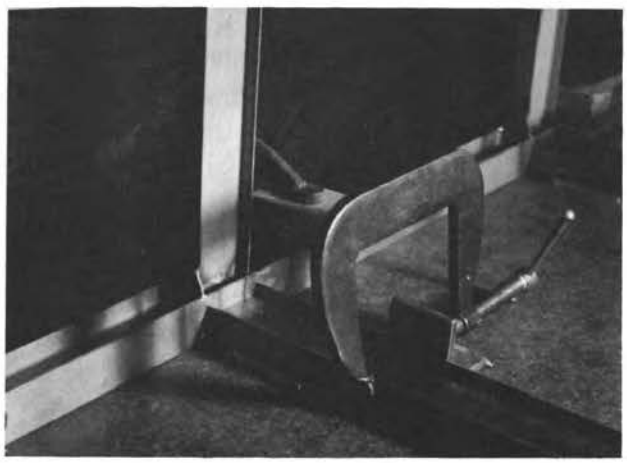

FIGURE 33–BEAM TO COLUMN-FLANGE CONNECTION CLAMPED IN PLACE FOR WELDING

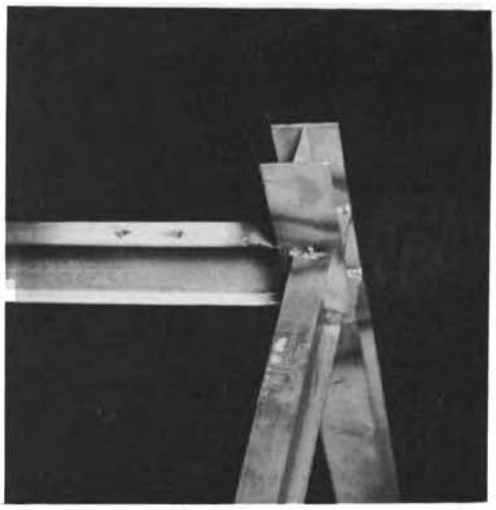

FIGURE 34–TACK WELD ON BEAM TO COLUMN FLANGE CONNECTION

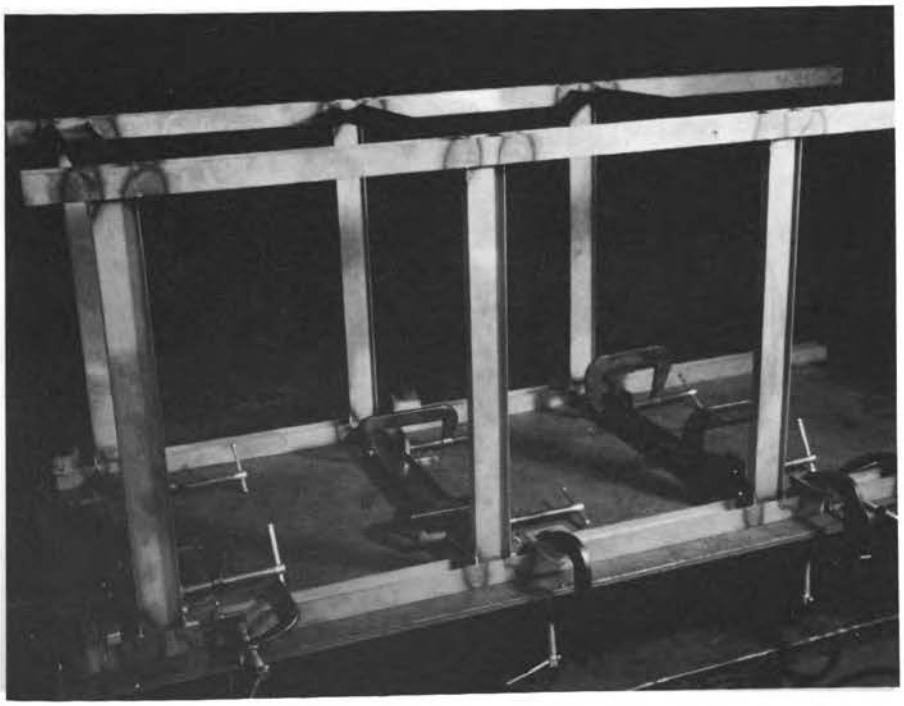

FIGURE 35–FORMATION OF FRAMEWORK SUBASSEMBLY

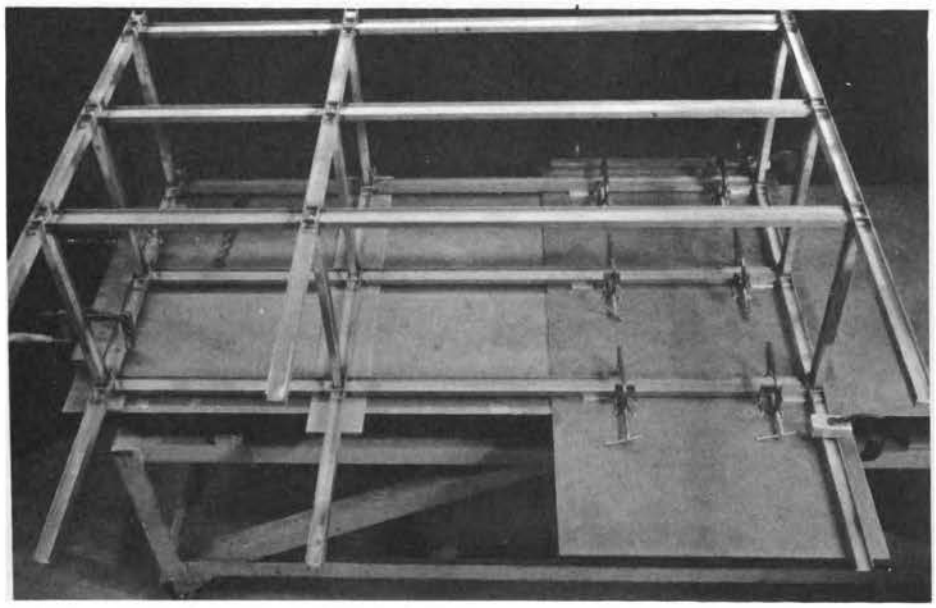

FIGURE 36–ADDITION OF LAST FRAME SUBASSEMBLY

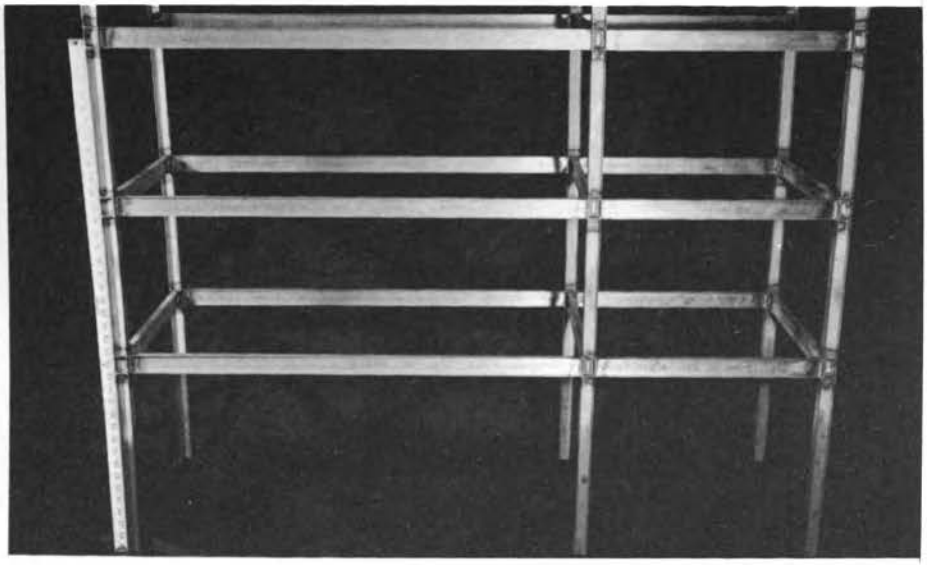

FIGURE 37–COMPLETED FRAMEWORK

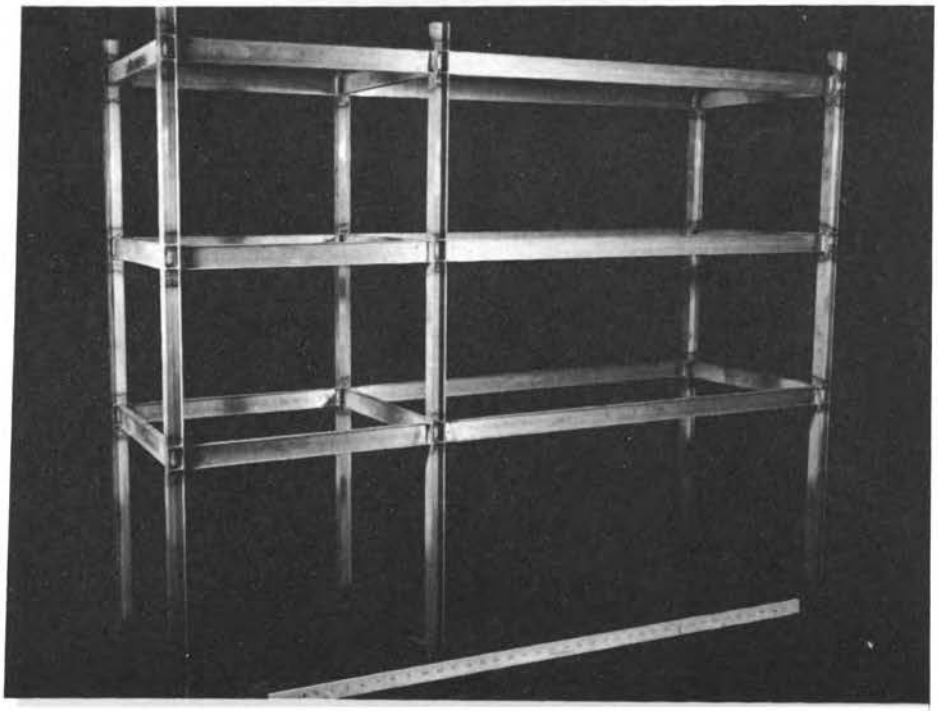

FIGURE 38–COMPLETED FRAMEWORK

work fabrication began with 1/16th-inch-diameter rods giving a weld thickness of approximately .14 inches, but these were replaced with .032-inch-diameter rods giving a much finer weld on the order of .08-inch thickness. Argon was used throughout fabrication as the shielding gas. Figure 21 pictures the heliarc torch used throughout the fabrication.

The geometry of the completed framework is given in Tables 5 and 6 (refer to Fig. 39). Maximum out-of-plane displacement is not reflected here, but was about one-quarter inch. It is felt the results are satisfactory for this initial attempt at framework fabrication.

5. CONCLUSIONS

1. The chemical and mechanical properties of C1020 hot rolled steel are such that it may be used satisfactorily in the modeling of steel structures.
2. Milling wide flange sections from hot rolled bar stock is a reliable and accurate method for fabricating small scale sections with element thicknesses down to 25 thousandths of an inch.
3. Tension and joint tests demonstrated that the heliarc process with Industrial Stainless 410 filler rods provides more than adequate strength and ductility for joining C1020 steel model sections.
4. The higher-than-predicted ultimate moments obtained in the non-annealed joint tests are primarily a result of the welding process.
   a. Sections which were annealed after welding had lower ultimate load capacity than those which were not annealed.
   b. Non-annealed welded tension samples failed away from the welded zone even though the minimum cross-section area occurred in the welds.
   c. The annealed and non-annealed beam tests showed the same yield and ultimate moments.
5. Fabrication of a complete framework is possible, but it is necessary to fix elements during assembly and to follow a predetermined sequence of assembly to reduce shrinkage deformations. This sequence may vary with each structure.
6. Until more refinements are made in the welding process, it is necessary to anneal whole frameworks to obtain member behavior consistent with stress-strain characteristics of the material.

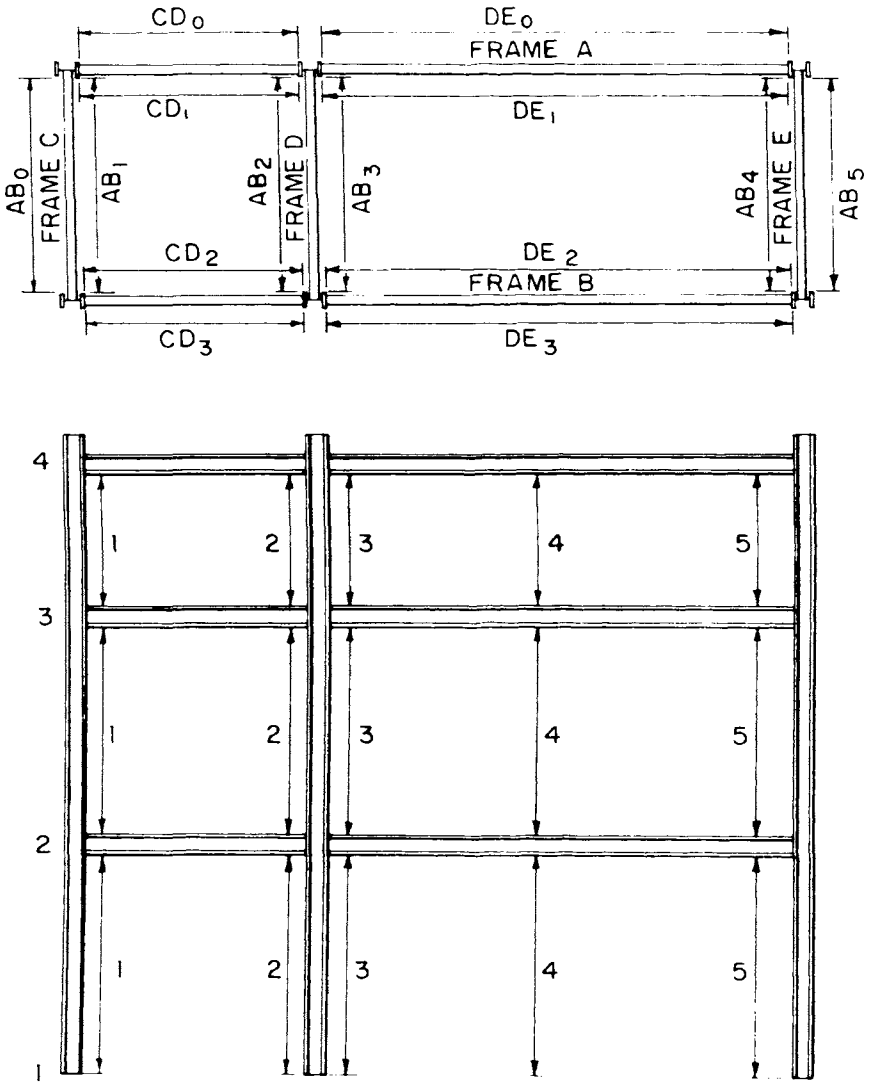

FIGURE 39–SECTIONS TAKEN FOR MEASURING FINISHED FRAMEWORK

TABLE 5

DISTANCE BETWEEN FLOORS–FLANGE TO FLANGE (in inches)

(Refer to Figure 39)

		Floor Distance			Specified Dimension		
Frame	Section	1-2	2-3	3-4	1-2	2-3	3-4
A	1	14.77	10.62	10.59	15.30	10.60	10.60
A	2	14.76	10.59	10.57		10.60	10.60
A	3	14.74	10.61	10.58		10.60	10.60
A	4	14.72	10.62	10.59		10.60	10.60
A	5	14.74	10.62	10.61		10.60	10.60
B	1	14.74	10.62	10.61		10.60	10.60
B	2	14.83	10.62	10.59		10.60	10.60
B	3	14.81	10.62	10.59		10.60	10.60
B	4	14.81	10.61	10.60		10.60	10.60
B	5	14.74	10.62	10.59		10.60	10.60
C	1	14.73	10.62	10.58		10.60	10.60
C	2	14.73	10.62	10.59		10.60	10.60
D	1	14.80	10.62	10.59		10.60	10.60
D	2	14.81	10.61	10.59		10.60	10.60
E	1	14.74	10.62	10.60		10.60	10.60
E	2	14.73	10.62	10.59		10.60	10.60

TABLE 6

COLUMN TO COLUMN DISTANCE

FLANGE EDGE TO FLANGE EDGE (in inches)

(Refer to Figure 39)

Distance	Floor Level 2	3	4	Specified Dimension
DE_0	32.02	32.02	32.03	32.00
DE_1	32.04	32.00	32.04	32.00
DE_2	32.00	32.01	32.00	32.00
DE_3	32.00	32.01	32.00	32.00
CD_0	16.00	16.00	16.00	16.00
CD_1	16.00	15.99	16.00	16.00
CD_2	16.00	15.98	16.00	16.00
CD_3	16.00	15.99	16.00	16.00
AB_0	15.09	15.09	15.09	15.05
AB_1	15.09	15.09	15.09	15.05
AB_2	15.07	15.06	15.07	15.05
AB_3	15.07	15.09	15.07	15.05
AB_4	15.08	15.07	15.08	15.05
AB_5	15.09	15.09	15.09	15.05

PART II

1. TENSION TESTS

1.1 Plane Tension Samples

1.1.1 Testing Procedure

A total of 26 tension tests were conducted on specimens of C1010 and C1020 cold and hot rolled steel sheets. These were milled to dimensions according to the ASTM specifications for tensile specimens(Ref. 1). All heat treating is summarized in Tables 7 and 8. The samples were tested on the Tinius Olsen 12,000-pound testing machine at a cross-head rate of .05 inches per minute, and strain measurements were made with a Tinius Olsen S100 Extensometer with a one-inch gauge length. Friction grips were used for loading the specimen, and were aligned in a vertical plane before testing. Loads vs. strains were recorded automatically on the Tinius Olsen pen graph having a sensitivity setting of .04 in/in; that is, each inch on the graph represented 4 per cent strain in the sample. All tests were carried to complete failure of the specimen.

1.1.2 C1010 Tensile Specimens

The complete results of these tests are given in Table 7. For the C1010 cold rolled samples, no significant difference occurred in yield point or tensile strength between the specimens annealed at 800°F and 1000°F. Samples annealed at 1100° had yield points and tensile strengths lower than the other annealed samples. Yield and ultimate values for the unannealed samples fell within the range of the samples annealed at 800°F and 1000°F. All samples demonstrated a yield point and a yield plateau of approximately 2 per cent strain followed by strain hardening and a total elongation of approximately 34-40 per cent.

1.1.3 C1020 Tensile Specimens

The three annealed C1020 samples, summarized in Table 7, exhibited yield points and tensile strengths higher than those of the C1010 steels. The yield points for the samples varied between 46.6 ksi while the tensile strength varied from 63.9 to 66.0 ksi. The samples exhibited a yield plateau of 2 per cent strain and a total elongation of 32 to 36 per cent.

1.1.4 Flange and Web Specimens from C1020 Steel Model Beams

A total of six samples were prepared from a 14WF103 section, four from the flanges and two from the web. Two flange samples and one web sample were annealed at 1000 degrees F with an oven cool and the remainder received no heat treatment. The results of two of these tests were invalid due to a calibration discrepancy on the Tinius Olsen machine. Results of the four remaining tests (Table 8) show differences between the annealed and non-annealed condition. For the non-annealed samples, yield strengths were determined by the 0.2% offset method. Also a slightly higher tensile strength was obtained for these specimens. The annealed specimens possessed a lower yield point and tensile strength than C1020 tests reported in Part II, section 1.1.3. A yield plateau of 2 per cent strain was obtained with a total average elongation of 32 per cent.

Six web samples from a 21WF62 section were tested with three samples annealed and three non-annealed (Table 8). All six samples demonstrated a higher yield strength and tensile strength than the 14WF103 samples. Again a yield plateau was lacking in the non-annealed samples and yield strength was taken at a .2 per cent offset. For the annealed samples, a yield plateau was taken at a .2 per cent offset. For the annealed samples, a yield plateau of 2 per cent strain was obtained with a total average elongation of 32 per cent.

TABLE 7

RESULTS OF PLAIN TENSION TESTS WITH C1010 AND C1020 STEELS

Material	No.	Annealing	Area (in)x(in)	Yield Stress (ksi)	Tensile Stress (ksi)	Elongation one inch (%)
C1010	1	None	.423x.090	41.2	45.3	36
C1010	2	None	.424x.090	39.1	48.4	40
C1010	3	800°F 60 min.	.423x.090	37.8	47.4	40
C1010	4	800°F 60 min.	.425x.089	44.5	47.6	40
C1010	5	800°F 60 min.	.426x.024	43.5	45.6	38
C1010	6	800°F 60 min.	.426x.024	31.8	44.3	36
C1010	7	1000°F 60 min.	.427x.090	42.2	47.6	40
C1010	8	1000°F 60 min.	.427x.090	43.0	48.4	40
C1010	9	1000°F 60 min.	.427x.024	44.2	45.7	36
C1010	10	1000°F 60 min.	.427x.024	43.4	45.8	36
C1010	11	1100°F 40 min.	.434x.063	35.8	43.9	40
C1010	12	1100°F 40 min.	.434x.062	35.3	42.0	38
C1010	13	1100°F 40 min.	.435x.061	32.6	42.6	34
C1020	1	1100°F 40 min.	.434x.063	46.1	63.9	34
C1020	2	1100°F 40 min.	.434x.063	46.6	66.0	32
C1020	3	1100°F 40 min.	.434x.063	46.1	65.3	36

TABLE 8

RESULTS OF WEB AND FLANGE TENSION TESTS FROM 14WF103 AND 21WF62

MODEL BEAMS C1020 STEEL

Section	Element	Annealing	Area (in)x(in)	Yield Stress (ksi)	Tensile Stress (ksi)	Elongation one inch (%)
21WF62	WEB	None	.033 x .375	48.4	64.0	27
21WF62	WEB	None	.028 x .431	45.7	65.2	25
21WF62	WEB	None	.028 x .435	47.4	64.6	23
21WF62	WEB	1000° F 45 min.	.028 x .436	42.3	61.5	32
21WF62	WEB	1000° F 45 min.	.028 x .436	45.3	61.5	29
21WF62	WEB	1000° F 45 min.	.028 x .437	46.3	62.0	34
14WF103	WEB	None	.028 x .435	34.4	60.0	38
14WF103	FLANGE	None	.053 x .436	35.8	60.2	23
14WF103	FLANGE	1000° F 45 min.	.052 x .436	37.4	58.4	26
14WF103	FLANGE	1000° F 45 min.	.052 x .436	37.8	59.1	39

1.2 Welded Tension Samples

1.2.1 Fabrication

Except for two samples, which were not surface ground after welding, the general method of fabrication was as follows:

1. Milled tension samples were cut at the midpoint of their gauge length.
2. The material was cleaned and degreased in the area of the cut.
3. The two halves were then brought together and clamped.
4. Sections were joined with a single pass of the heliarc pencil welder and specified filler material.
5. Excess weldment was rough ground on a grinding wheel and finish ground on a horizontal grinding machine to form a specimen of constant thickness.
6. Tabs left at the beginning and end of the weld were removed with a steel file.
7. Cross-sectional areas at the center of the gauge length were measured with a one-inch micrometer, and reported yield strengths and tensile strengths are based upon these areas.

1.2.2 C1010 and C1020 Welded Samples with Oxweld 65 Filler Wire

The results for these tests may be found in Table 9. In all cases failure occurred in the base material. Specimens one through six were ground after welding and annealed at 1100 degrees F for 45 minutes and allowed to oven cool. Yield stresses varied from 31.7 to 38.9 ksi and tensile strength from 40.5 to 46.5 ksi. Where yield plateaus were obtained, they averaged 1.75 per cent strain with maximum elongations of thirty per cent.

Specimens seven through ten were not annealed. In two cases, failure occurred outside the gauge length. Those failing inside the gauge length failed adjacent to the gauge edge with measured elongations of eight and ten per cent. In this group, yield stresses from 34.7 to 39.1 ksi and tensile stresses from 40.5 to 47.4 ksi were obtained.

Specimens 11 and 12 were tested in the as-welded condition. Both failed outside the gauge length with yield points of 31.6 ksi and tensile strengths of 42.6 and 43.4 ksi.

Two welded C1020 samples were ground and annealed for testing. Both failed inside the one-inch gauge length with elongations of 12 and 14 per cent. Yield points were 48.8 and 49.4 ksi and tensile strengths 71.0 ksi and 70.4 ksi.

1.2.3 B1113 Welded Samples

The data for these tests are given in Table 9. Three samples were ground and annealed at 1525°F for 40 minutes and oven cooled. An extremely hard scale was produced on the specimens which had to be removed before applying the extensometer. Yield plateaus averaged 2.5 per cent strain and total elongations 22 to 26 per cent strain. Yield stresses were 33.0 ksi and 42.8 ksi, well below the yield stress found on plain tension tests (Part I), and tensile strengths were 57.3 ksi and 78.2 ksi. One sample was not annealed and had a yield stress of 57.3 ksi and a tensile strength of 79.7 ksi. Failure occurred outside the gauge length.

2. JOINT TESTS

2.1 Testing Procedure

A total of nine tests were planned, the joints to be fabricated with Heliarc welding employing Industrial Stainless 410 filler wires. The fabrication procedure for these joints was as follows:

1. Sections were cleaned and clamped to form the desired joint.
2. Sections were initially joined by tack welding.
3. Stiffeners were then positioned and tack welded.
4. The beam-to-column flange connection was completed by welding all around the beam flanges and web.
5. The joint was vapor-honed.
6. Stiffeners were finish welded.

The knee tests were designed so that failure would occur at the compression flange of the

TABLE 9

RESULTS OF HELIARC WELDED TENSION SAMPLES

Material	No.	Filler Wire	Annealing	Area (in)x(in)	Yield Stress (ksi)	Tensile Stress (ksi)	Elongation one inch (%)
C1010	1	Oxweld 65	1100° F 45 min.	.425x.057	31.7	41.7	Outside Gauge
C1010	2	Oxweld 65	1100° F 45 min.	.426x.055	37.4	44.0	26
C1010	3	Oxweld 65	1100° F 45 min.	.427x.057	37.6	44.9	30
C1010	4	Oxweld 65	1100° F 45 min.	.432x.055	38.9	46.5	28
C1010	5	Oxweld 65	1100° F 45 min.	.427x.030	34.7	40.5	Outside Gauge
C1010	6	Oxweld 65	1100° F 45 min.	.425x.026	38.8	40.5	12
C1010	7	Oxweld 65	None	.431x.023	40.8	47.4	8
C1010	8	Oxweld 65	None	.422x.027	34.7	40.5	10
C1010	9	Oxweld 65	None	.426x.057	35.0	41.0	Outside Gauge
C1010	10	Oxweld 65	None	.424x.055	39.1	47.4	Outside Gauge
C1010	11	Oxweld 65	None	.434x.061	31.6	42.6	Outside Gauge
C1010	12	Oxweld 65	None	.435x.061	31.6	43.4	Outside Gauge
C1020	1	Oxweld 65	1100° F 40 min.	.430x.113	49.4	70.4	14
C1020	2	Oxweld 65	1100° F 40 min.	.429x.113	48.8	71.0	12
B1113	1	410 Stainless	1525° F 40 min.	.435x.071	33.0	57.3	26
B1113	2	410 Stainless	1525° F 40 min.	.351x.034	42.8	78.2	22
B1113	3	410 Stainless	1525° F 40 min.	.357x.043	38.7	75.0	22
B1113	4	410 Stainless	None	.433x.080	57.3	79.7	Outside Gauge

beam or column due to bending (Ref. 6). For the cantilever tests, column web stiffeners were provided to prevent a shear failure.

All of the tests were conducted on the Instron Testing Machine Model TT-C with an Instron F tension-compression load cell. Calibration of the machine was carried out before each test and a cross head movement of .002 inches per minute was used in all tests. The test set-ups for the three types of connections are shown in Figures 40 and 41. The model joint was placed on the base plate and the loading rod through aluminum channels was attached to the load cell of the Instron machine. The base plate was placed on the Instron moving cross head, which was raised until the drill holes in the beams and the radial bearings were aligned. One-quarter-inch-diameter pins were then inserted through the radial bearings and beams. For the knee tests, a right angle drafting triangle was used in positioning the pins in the column and pins in the beam in a vertical plane. For the cantilever tests, the triangle was used in centering the loading rod over the centerline of the column. The base plate was then clamped to the cross head with "C" clamps. Load was applied to the joints by raising the moving cross head. Deflection readings were taken for every 50 pounds of load up to yielding. For the knee tests, load readings were taken at specified deflection intervals after yielding had occurred. Because there were two deflection readings to be taken in the cantilever tests, deflection readings were taken at specified deflection intervals after yielding had occurred. All tests were continued until the sections began to unload and extreme flange and web buckling had occurred.

Moments of inertia used in computing theoretical moments were derived by averaging micrometer readings taken at four points of each delivered section.

2.2 14WF103–14WF103 Connection

The data for this connection are given in Table 10. The non-annealed joint attained an ultimate moment of 2690 inch pounds as compared to a predicted ultimate moment of 2070 inch pounds. For the annealed joint, an ultimate moment of 2275 inch pounds was obtained, as compared to a predicted ultimate moment of 2210 inch pounds. The difference in computed ultimate moments between the annealed and non-annealed joint tests is due to a difference in yield stresses between the annealed and non-annealed tension samples taken from a 14WF103 section. For the non-annealed joint, failure occurred in the beam compression flange adjacent to the column flange. For the annealed joint, failure again occurred in the compression flange but in the column, just outside the web stiffener. Soon after unloading of the joints occurred, web buckling was noticeable, although this probably coincided with the peak moment value and was the cause of the unloading of the joints. Figures 42 through 45 give the progression of this buckling.

2.3 14WF103–21WF62 Connection

The data for this connection are given in Table 11. Predicted moments are based upon failure of the 21WF62 section. The non-annealed specimen reached the highest ultimate moment at 2410 inch pounds versus a predicted ultimate moment of 2360 inch pounds. Little effect was seen from pre-annealing, since an ultimate moment of 2370 inch pounds was observed as compared to a predicted ultimate moment of 2190 inch pounds. The annealed joint attained an ultimate moment of 2275 inch pounds as compared to a predicted moment of 2190 inch pounds. Unloading of all the specimens began immediately after web buckling of the 21WF62 had occurred, followed shortly by buckling of its compression flange adjacent to the knee. Although yielding of the 14WF103 was also apparent, buckling of this section did not occur throughout the three tests. Horizontal joint deflections were less for this section, with ultimate moments occurring at about .060 inches horizontal deflection versus approximately 0.12 inches horizontal deflection for the 14WF103–14WF103 connection.

TABLE 10

DATA FOR 14WF103–14WF103 JOINT TESTS

Post-Annealed		Non-Annealed	
Haunch Moment (in. lbs.)	Horizontal Def. (in.)	Haunch Moment (in. lbs.)	Horizontal Def. (in.)
0	0	0	0
283	.0012	283	.0012
566	.0034	566	.0032
848	.0062	848	.0051
1132	.0085	1132	.0071
1414	.0105	1415	.0092
1700	.0122	1700	.0117
1770	.0136	1912	.0143
1840	.0154	2055	.0168
1935	.0240	2125	.0202
1938	.0280	2190	.0260
1955	.0360	2230	.0320
2070	.0560	2270	.0420
2240	.1000	2410	.0600
2265	.1120	2505	.0800
2275	.1280	2550	.0900
2215	.1600	2650	.1200
1903	.2000	2690	.1500
1660	.2400	2620	.1680
1121	.3200	2310	.1900
		1835	.2300
		1320	.2800

TABLE 11

DATA FOR 14WF103–21WF62 JOINT TESTS

Post-Annealed		Pre-Annealed		Non-Annealed	
Haunch Moment (in. lbs.)	Horizontal Deflection (in.)	Haunch Moment (in. lbs.)	Horizontal Deflection (in.)	Haunch Moment (in. lbs.)	Horizontal Deflection (in.)
0	0	0	0	0	0
274	.0011	274	.0013	274	.0029
548	.0025	548	.0021	548	.0061
822	.0051	822	.0036	822	.0102
1095	.0083	1095	.0053	1095	.0118
1370	.0108	1370	.0064	1370	.0137
1645	.0125	1645	.0077	1645	.0159
1780	.0137	1780	.0083	1780	.0174
1918	.0162	1918	.0100	1918	.0191
1972	.0210	1974	.0120	1974	.0200
2000	.0250	2010	.0140	2130	.0290
2070	.0310	2080	.0200	2225	.0350
2140	.0370	2190	.0260	2385	.0530
2190	.0410	2265	.0300	2410	.0620
2275	.0490	2325	.0350	2385	.0710
2250	.0555	2370	.0440	2185	.0860
2165	.0610	2000	.0820	1900	.0980
1835	.0690	1685	.1080	1830	.1040
1625	.0970	1355	.1400	1565	.1220
1495	.1090	1123	.1650	1150	.1680
1327	.1250	1042	.1750	989	.1960
1150	.1470				
986	.1650				

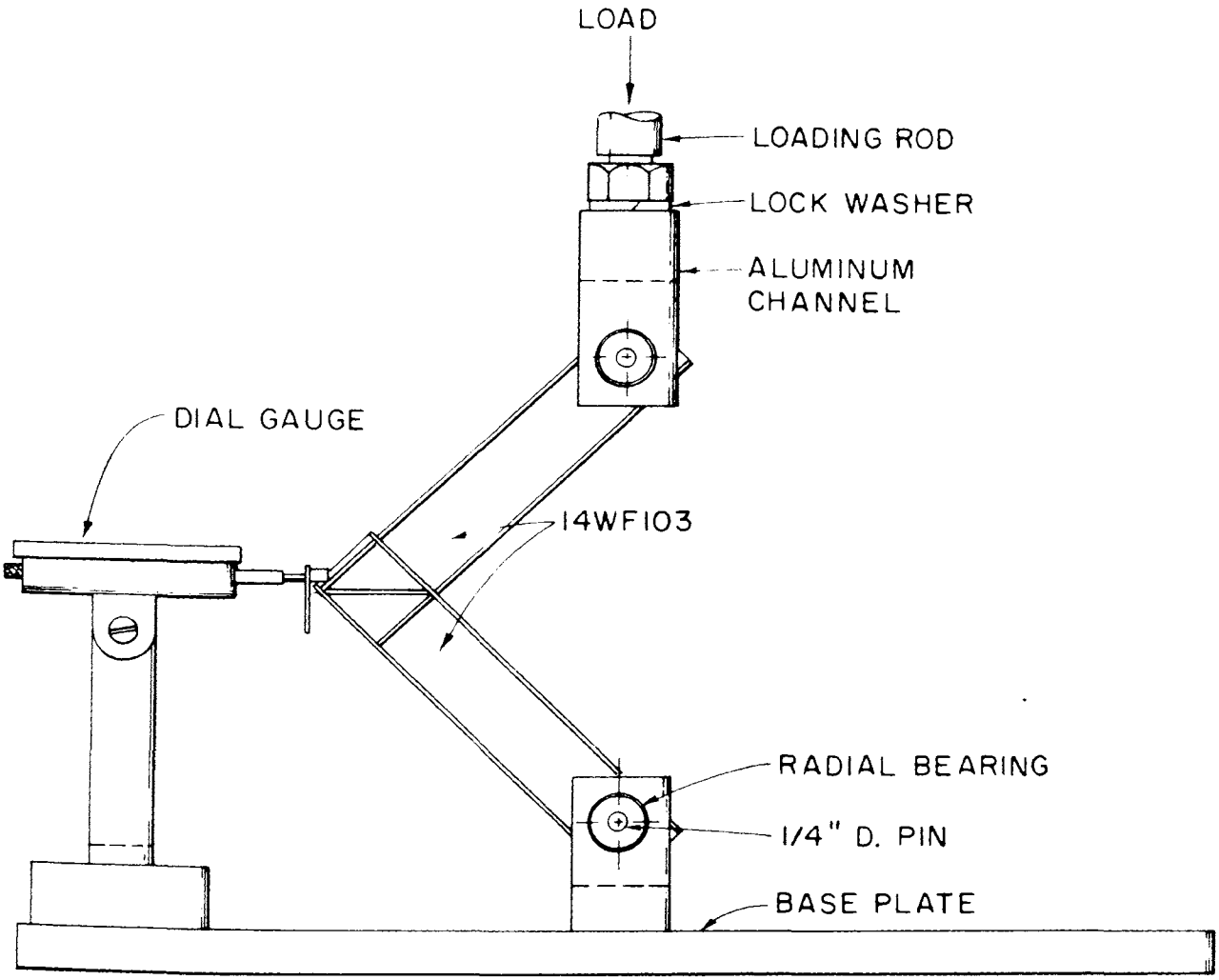

FIGURE 40—TEST SETUP FOR KNEE JOINT TEST

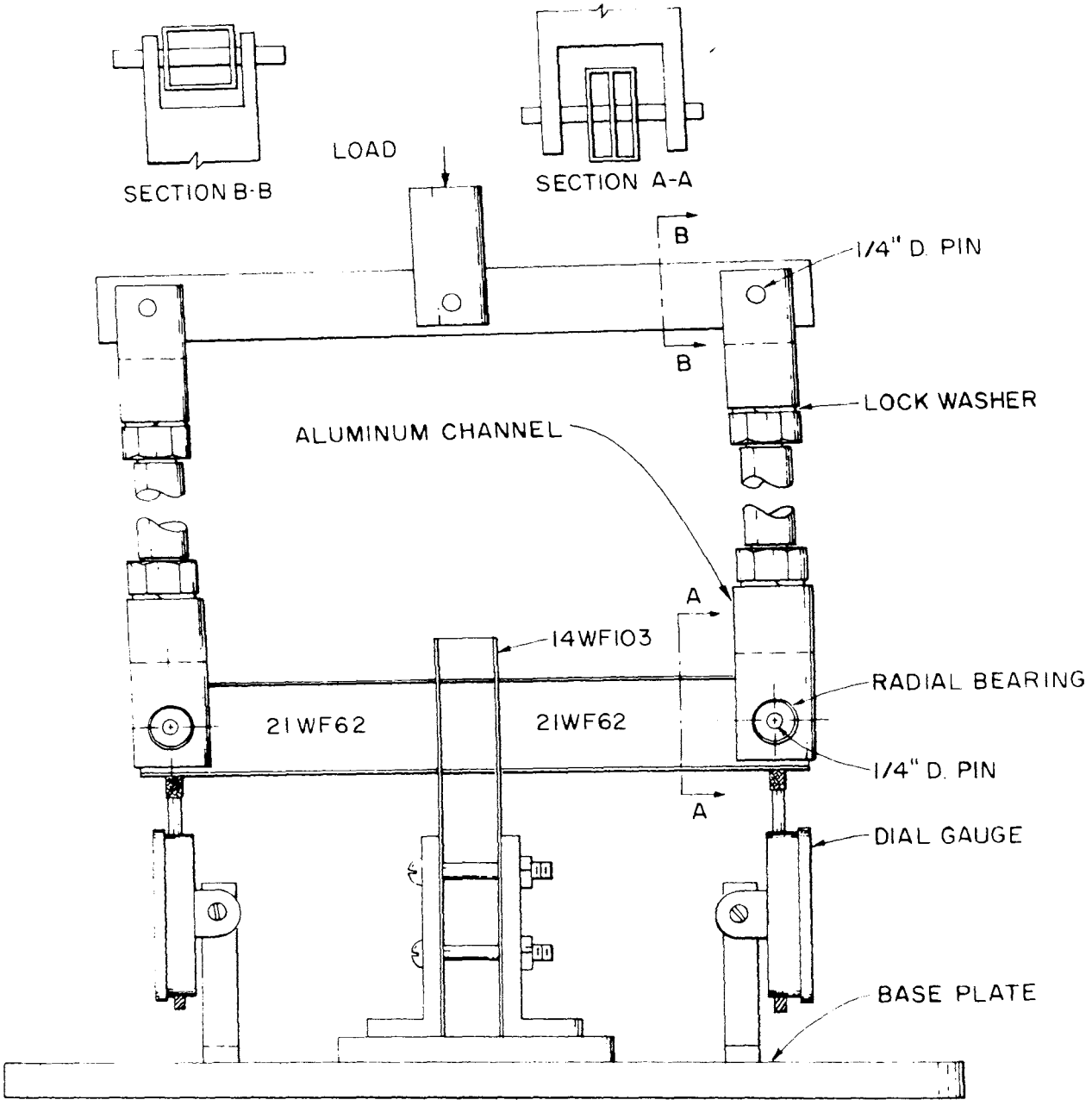

FIGURE 41—TEST SETUP FOR CANTILEVER CONNECTION

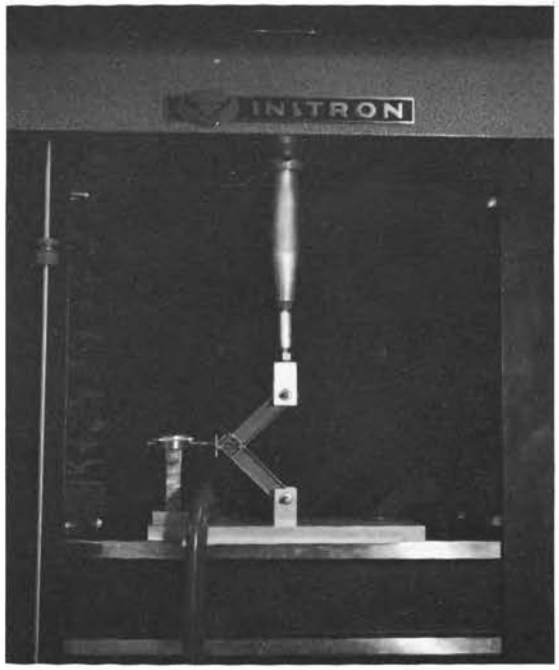

FIGURE 42–BEGINNING OF 14WF103–14WF103 JOINT TEST

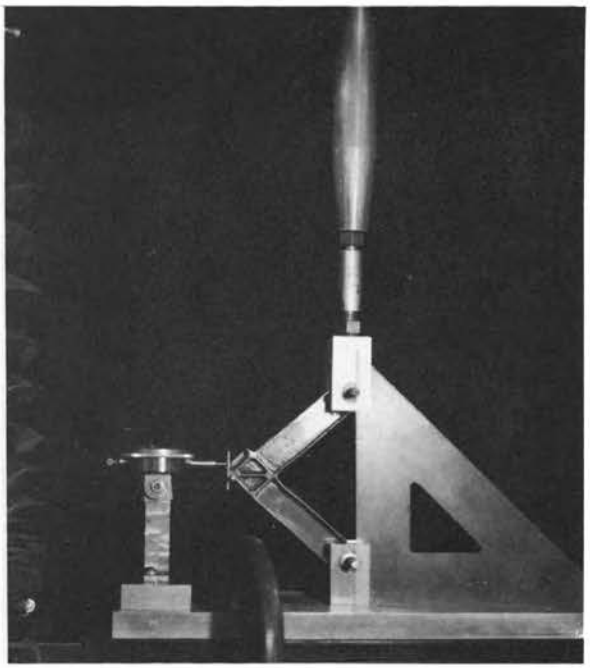

FIGURE 43–INITIATION OF WEB BUCKLING AFTER FLANGE BUCKLING

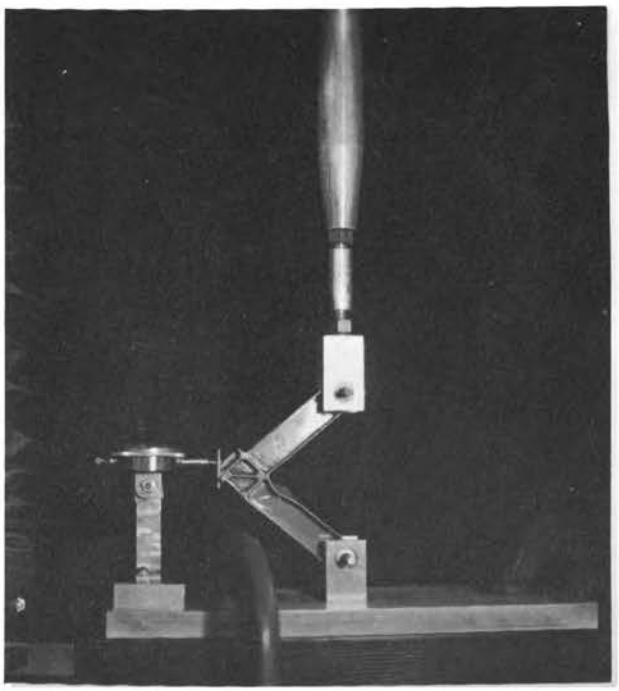

FIGURE 44–UNLOADING OF THE JOINT

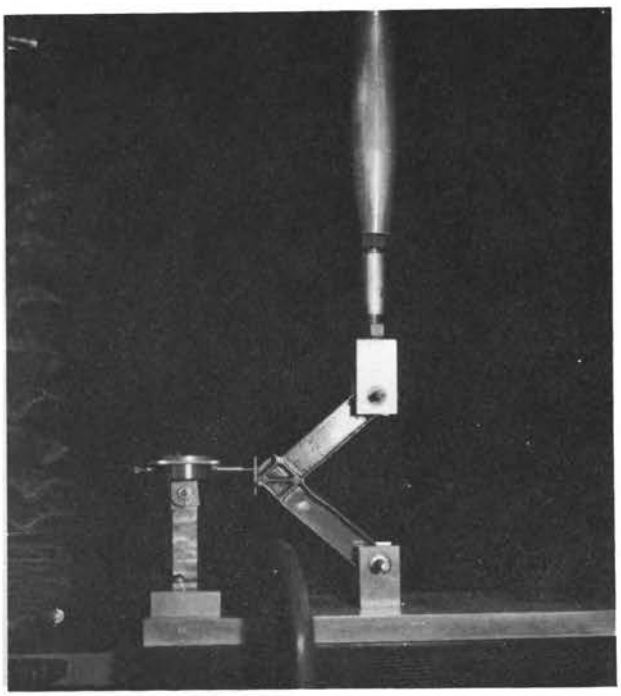

FIGURE 45–BUCKLING AT COMPLETION OF TESTING

2.4 Cantilever Connection

The data for this connection are given in Table 12. Deflections of one cantilever remained constant after unloading of the other cantilever began.

As in the previous joint tests, the non-annealed specimen reached the highest ultimate strength at 3210 inch pounds versus predicted ultimate strength of 2310 inch pounds. The pre-annealed specimen reached an ultimate value of 2630 inch pounds as opposed to a predicted ultimate moment of 2150 inch pounds. Upper yield points were present in both of the annealed beams; however, no yield plateau occurred and loading of the specimens resumed immediately after the lower yield point was reached. An ultimate moment of 2210 inch pounds was observed compared to the predicted value of 2150 inch pounds. In the pre- and post-annealed joints, web buckling was initiated first followed shortly by flange buckling and the unloading of the specimen. For the non-annealed case, flange buckling occurred first, adjacent to the weld. Photographs of the pre-annealed specimen are shown in Figures 46 and 47.

3. BEAM TESTS

3.1 Testing Procedure

Four beams were prepared for testing under the condition of constant moment across the middle third of their lengths (Fig. 48). Two beams were 14WF103 sections and two were 21WF62 sections. One beam of each section was annealed at 1000 degrees F for one hour and allowed to oven cool, while the remaining beams had no heat treatment. Figure 49 gives dimensions for the beams and positions of the web stiffeners and v blocks. These were silver-soldered into position for the annealed tests and held in place with 2.56 screws for the non-annealed tests.

The testing equipment is extensive and only a summary of it will be given here (see Ref. 4). Load to the beams was applied through a one inch diameter piston rod attached to a gas cylinder. The load was distributed to the third points of the beams by means of a small loading beam (Fig. 50). Applied load was measured by a load cell (full Wheatstone bridge consisting of four strain gauges) attached to the piston rod. The calibrated load cell output was monitored by an oscilloscope. Deflection readings were taken with an Ames four-inch, one-thousandth graduation-dial gauge located under the lower flange at midspan. The load was applied in increments up until yield, and thereafter load was determined for specified increments of midspan deflection.

Supports for the beams were a knife edge at one end and a roller at the other (Fig. 50). Lateral bracing, as shown in Figures 50, 51, and 52, was provided at cross sections 7/8 inch inside the third points.

3.2 Beam Test Results

3.2.1 14WF103

The data for these tests are given in Table 13. The linear behavior of these beams followed closely the theoretically predicted behavior. The non-annealed section yielded first at about 1475 inch pounds versus 1700 inch pounds for the annealed beam. Both of these values are lower than calculated values, which were 1665 inch pounds and 1780 inch pounds respectively. Strain hardening of the sections began after approximately 0.5 inches mid-span deflection. Here flange buckling began to develop, but the sections continued to accept load with the annealed beam reaching an ultimate moment of 1775 inch pounds and the non-annealed beam an ultimate moment of 1761 inch pounds. Collapse of the sections then occurred due to extensive flange buckling (Fig. 51).

3.2.2 21WF62

The results of these tests are given in Table 14. The linear behavior of these beams also followed quite closely their theoretical behavior. Both the annealed and non-annealed sections yielded at approximately 1640 inch pounds. This value is lower than the theoretical values, which were 1690 for the annealed and 1780 for

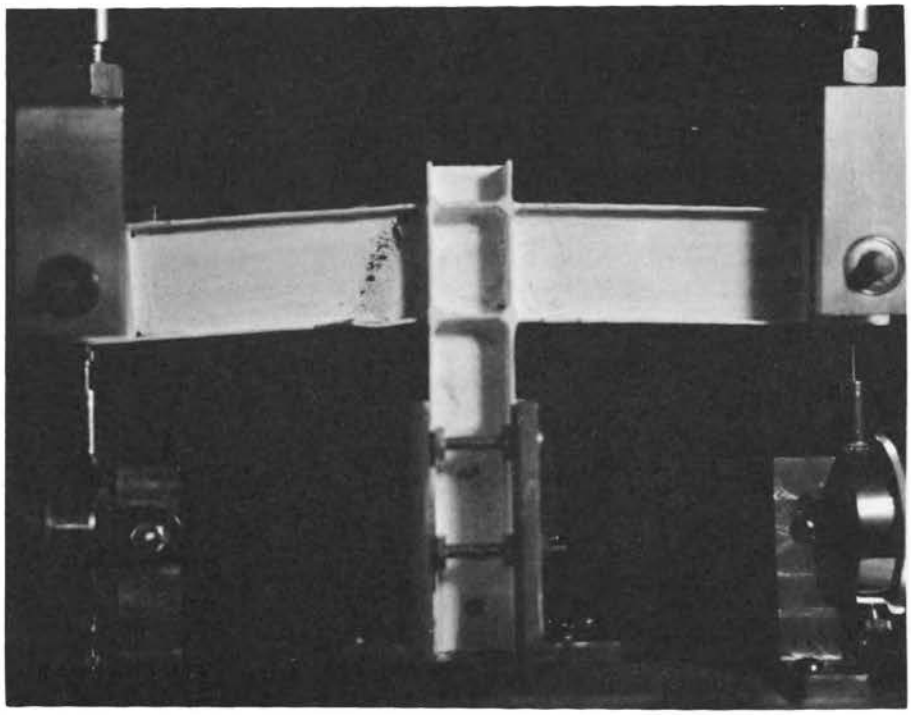

FIGURE 46–YIELD LINES AND THE INITIATION OF WEB AND FLANGE BUCKLING IN THE PRE-ANNEALED CANTILEVER TEST

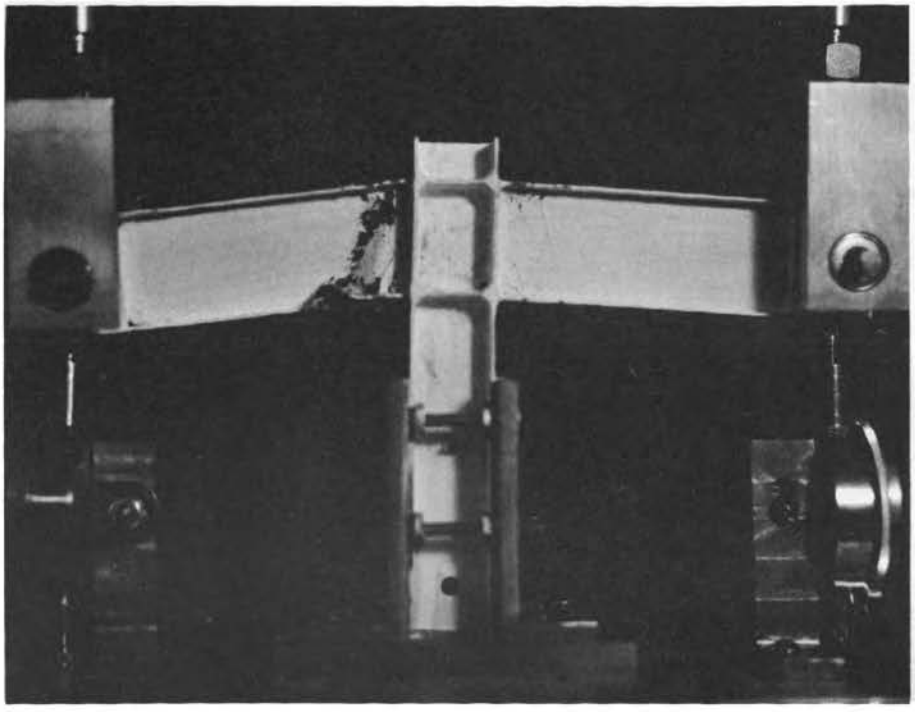

FIGURE 47–EXTREME BUCKLING OF CANTILEVER
(Note the Formation of Yield Lines in the Column)

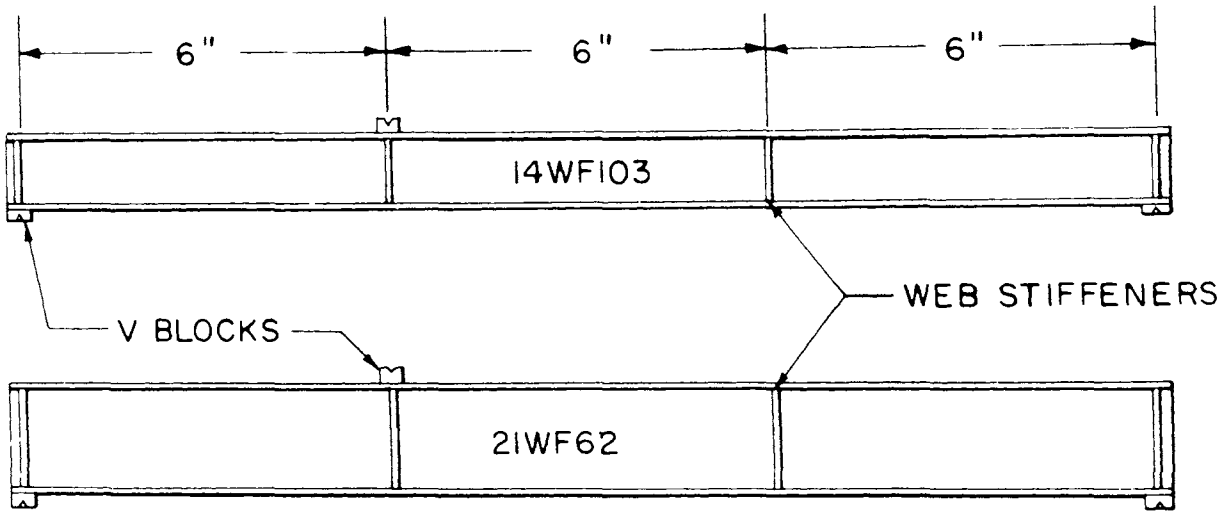

FIGURE 48–POSITION OF WEB STIFFENERS AND LOADING BLOCKS

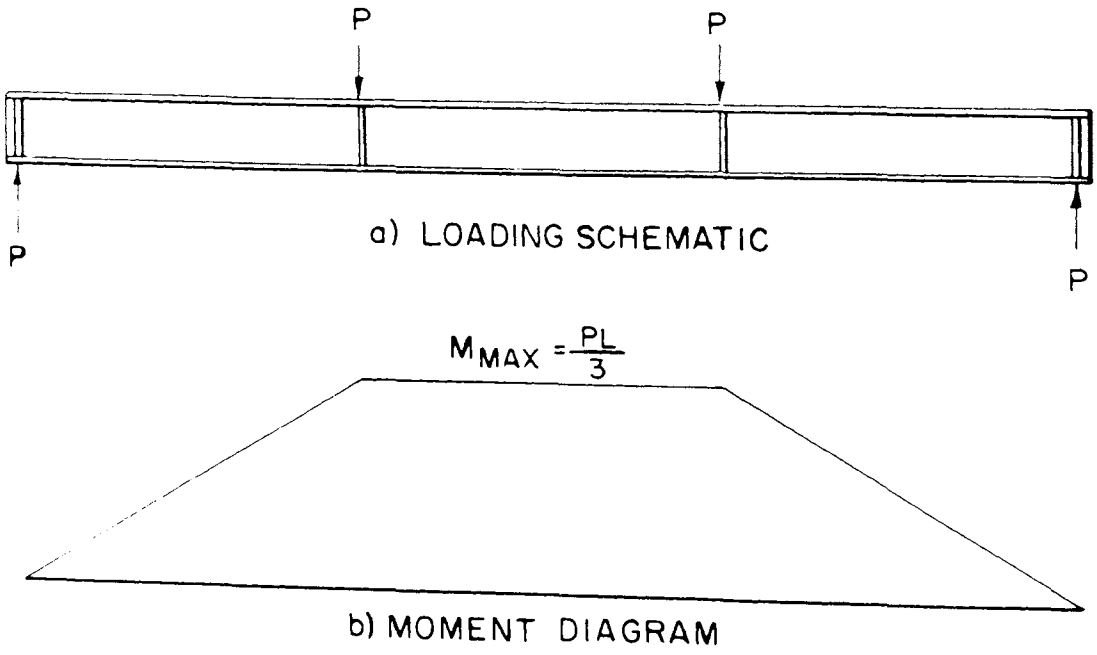

FIGURE 49–LOADING SCHEMATIC AND MOMENT DIAGRAM FOR BEAM TESTS

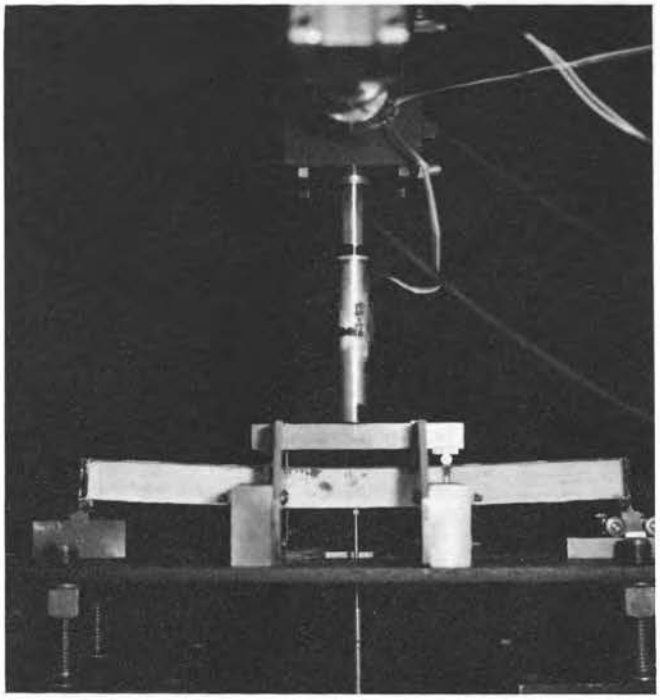

FIGURE 50–21WF62 BEAM TEST SHOWING LOADING BEAM, KNIFE EDGE AND ROLLER SUPPORTS

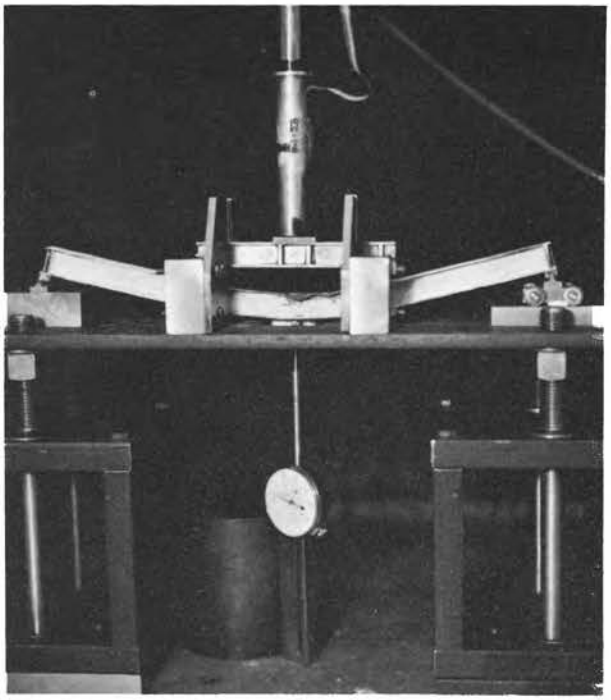

FIGURE 51–FLANGE BUCKLING IN 14WF103 BEAM TEST

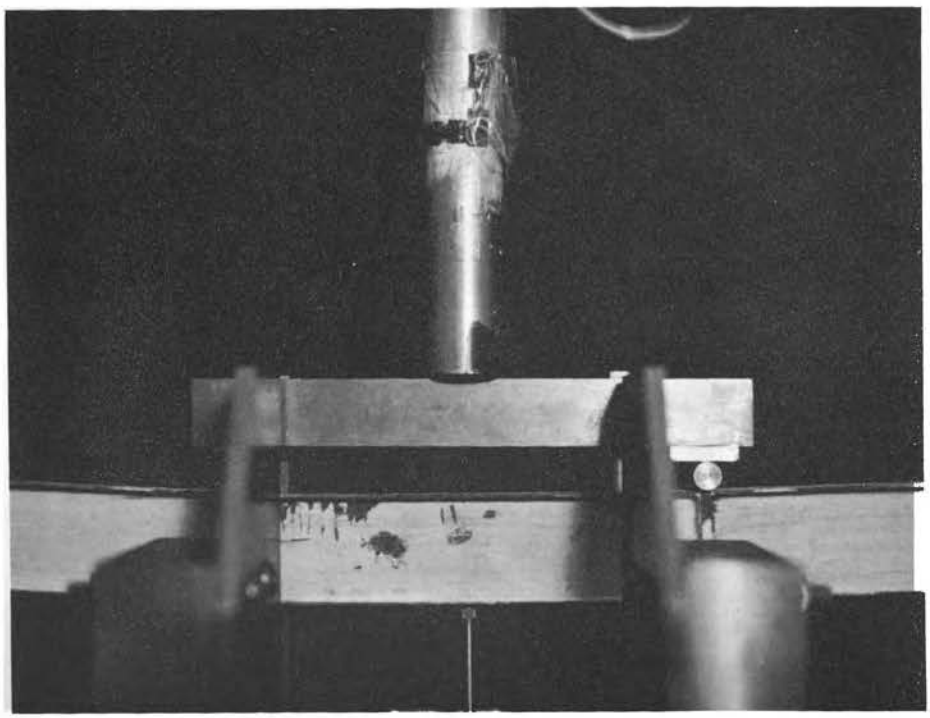

FIGURE 52–DEVELOPMENT OF YIELD LINES IN 21WF62 BEAM TEST

TABLE 12

DATA FOR CANTILEVER TESTS

Post-Annealed				Pre-Annealed				Non-Annealed			
$Moment_A$ (in.lbs.)	ΔV (in.)	$Moment_B$ (in.lbs.)	ΔV (in.)	$Moment_A$ (in.lbs.)	ΔV (in.)	$Moment_B$ (in.lbs.)	ΔV (in.)	$Moment_A$ (in.lbs.)	ΔV (in.)	$Moment_B$ (in.lbs.)	ΔV (in.)
0	0	0	0	0	0	0	0	0	0	0	0
225	.0023	225	.0022	225	.0029	225	.0020	225	.0026	225	.0016
450	.0070	450	.0041	450	.0057	450	.0043	450	.0054	450	.0034
675	.0113	675	.0059	675	.0086	675	.0068	675	.0085	675	.0052
900	.0155	900	.0077	900	.0122	900	.0092	900	.0115	900	.0069
1125	.0193	1125	.0099	1125	.0160	1125	.0114	1125	.0143	1125	.0088
1350	.0228	1350	.0123	1350	.0195	1350	.0144	1350	.0171	1350	.0108
1685	.0294	1685	.0161	1685	.0246	1685	.0177	1685	.0213	1685	.0140
1800	.0323	1800	.0174	1800	.0265	1800	.0214	1800	.0228	1800	.0151
1915	.0359	1915	.0187	1915	.0284	1915	.0236	1915	.0244	1915	.0162
2025	.0490	2050	.0206	2025	.0306	2025	.0263	2025	.0279	2025	.0184
2080	.0635	2080	.0337	2140	.0331	2140	.0294	2250	.0301	2250	.0196
2140	.0802	2140	.0518	2250	.0371	2250	.0335	2470	.0350	2470	.0224
2180	.0990	2180	.0697	2470	.0621	2470	.0613	2700	.0409	2700	.0256
2210	.1370	2210	.0879	2565	.0884	2565	.0820	2930	.0507	2930	.0355
2160	.1694			2630	.1267	2630	.1179	3150	.0880	3150	.0757
2050	.2180			2470	.2180			3210	.1224		
1915	.2718			2250	.2990			2930	.2275		
1685	.3604			2030	.4075			2470	.3598		
								2250	.4165		

TABLE 13

DATA FOR 14WF103 BEAM TESTS

Non-Annealed		Annealed	
Bending Moment (in. lbs.)	Midspan Deflection (in.)	Bending Moment (in. lbs.)	Midspan Deflection (in.)
0	0	0	0
189	.013	189	.012
378	.027	378	.023
567	.041	567	.035
696	.051	693	.045
912	.064	882	.055
1116	.073	1008	.064
1290	.084	1192	.076
1449	.095	1386	.086
1605	.120	1572	.098
1638	.128	1698	.104
1650	.137	1635	.281
1638	.490	1635	.338
1662	.648	1698	.540
1725	.802	1775	1.260
1761	.956		
1698	1.060		
1636	1.180		
1575	1.245		

TABLE 14

DATA FOR 21WF62 BEAM TESTS

Non-Annealed		Annealed	
Bending Moment (in. lbs.)	Midspan Deflection (in.)	Bending Moment (in. lbs.)	Midspan Deflection (in.)
0	0	0	0
378	.021	189	.011
756	.039	378	.022
1134	.058	567	.034
1512	.075	756	.043
1635	.082	945	.053
1635	.149	1134	.064
1635	.190	1323	.075
1635	.216	1533	.089
1635	.277	1596	.096
		1602	.106
		1692	.127
		1722	.167
		1722	.212

the non-annealed. Figure 52 shows yield lines forming in the web of the non-annealed beam. Soon after reaching the yield point these sections evidenced lateral buckling, followed by the collapse of the sections.

REFERENCES

1. ASTM Standards 1961 "Part 3–Metals Tests Methods", Philadelphia, 1961.

2. Building Design Data, United States Steel Corporation, Section II, "Steel Properties", October, 1963.

3. McCoy, R. H., Development of Modeling Techniques for Steel Structures, Technical Report to the United States Steel Corporation, M.I.T. Department of Civil Engineering, R63–34: August, 1964.

4. Rowe, P. E., Stewart, W. L., Dynamic Tests of Model Steel Structures, Technical Report to the U.S. Naval Civil Engineering Laboratory, M.I.T. Department of Civil Engineering, R65–32, July, 1965.

5. SAE Handbook 1963, Society of Automotive Engineers Inc., New York 17, New York, 1963.

6. Topractsoglou, A. A., Beedle, L. S., and Johnston, B. G., "Connection for Welded Continuous Portal Frames," The Welding Journal Supplement, July 1951, Welding Research Council of the Engineering Foundation, Progress Report No. 4 (Part II): Theoretical Analysis of Straight Knees, pp. 397S–405S.

Ultimate Strength Behavior of Small-Scale 8WF31 Beam-Columns

by

WILLIAM A. LITLE

DUKE OAKES

ACKNOWLEDGEMENT

This research project was carried out in the Structural Models Laboratory of the Department of Civil Engineering at the Massachusetts Institute of Technology. The project was sponsored by the Committee of Structural Steel Producers and the Committee of Steel Plate Producers of American Iron and Steel Institute, and the Structural Steel Fabricators of New England.

The authors wish to acknowledge the contributions of the design and construction of the beam-column loading device by P. Starin, of the development by Y. Nakamuri of a computer program for the analytical predictions of the beam-column behavior, and of the continued help of D. Foster during all phases of the research.

TABLE OF CONTENTS

ABSTRACT

This project was conducted to determine the behavior of model steel wide flange columns subjected to different combinations of axial load and end moments. Forty-eight beam-column tests were conducted on one-tenth scale models of an 8WF31 section having an L/r_x ratio of fifty-five.

The beam-columns were tested with equal end moments in both single and double curvature for a wide range of P/P_y ratios. One half of the members were annealed before testing and the others were tested in an as-received and fabricated condition.

It is concluded that:

1. The models show reasonable correlation with mathematical predictions.
2. Annealing is necessary when critical portions of the members are heat affected by the method of fabrication used.
3. Duplicate cases should be investigated when mathematical checks are not available to insure reliable results.

NOMENCLATURE

D = Depth of section

B = Width of flange

W = Thickness of web

T = Thickness of flange

A = Area of cross-section

Z = Plastic section modulus = $(A - WD)\left(\frac{D-T}{2}\right) + \frac{WD^2}{4}$

σ_y = Yield stress level

M_p = Plastic moment = $\sigma_y Z$

M_{PC} = Plastic moment modified to include the effect of axial compression

Neutral axis in web:

$$M_{PC} = M_p - \frac{P^2}{4\,\sigma_y W} \qquad \text{where:} \quad [\,P \leq \sigma_y W(D-2T)\,]$$

Neutral axis in flange:

$$M_{PC} = \frac{\sigma_y}{2}\left[D\left(A - \frac{P}{\sigma_y}\right) - \frac{1}{2B}\left(A - \frac{P}{\sigma_y}\right)^2\right]$$

where: $[\,\sigma_y W(D-2T) \leq P \leq P_y\,]$

P_y = Axial yield load

P_{act} = Actual axial load applied

M_u = Ultimate moment

θ = End rotation

$\frac{\text{EXP}}{\text{THEO}}$ = A measure of the experimental – analytical correlation;

$$= \frac{\text{distance origin to experimental point on Figure 2, 3, 4 or 5}}{\text{distance origin to theoretical curve along the same line}}$$

LIST OF TABLES

LIST OF FIGURES

PART I

I INTRODUCTION

1.1 Background

Accurate representation of the behavior of steel prototype structures by means of small scale steel models could be of significant value in research leading to more efficient and new uses of steel and the actual design of unconventional structures.

The purpose of this paper is to determine the behavior of model column members subjected to different combinations of axial load and end moments.

This paper is a part of a larger study being done by the Laboratory for Structural Models of the Department of Civil Engineering under the sponsorship of the Committees of Structural Steel and Steel Plate Producers of American Iron and Steel Institute and the Structural Steel Fabricators of New England. The project consists of the following parts:

1. Model Material Selection
2. Members
   a. Fabrication
   b. Behavior
      i. Beams
      ii. Beam-Columns
3. Frameworks
   a. Fabrication
   b. Behavior
      i. Joint tests
      ii. Frame tests

The first portion of the study, model material selection, member and framework fabrication, and beam and joint behavior was performed by Foster[1] in 1964–65. Reimer and Falcone[2] conducted frame behavior tests in 1965–66.

1.2 Scope

Forty-eight beam column tests were conducted on one-tenth scale models of an 8WF31 section having an L/r_x ratio of fifty-five. Table 1 and Figure 1 contain the loading conditions for each individual test. One-half of the columns were annealed at 1100°F for one-half hour before testing and the others were tested with the same loading conditions, in an as-received and fabricated condition. Nominal dimensions are given in Table 2.

Each test condition was repeated three times so that some measure of reliability could be attached to the results. Note that beam-columns numbers 12, 30 and 32 were improperly loaded and so only forty-five valid tests are included. The individual beam-column was loaded axially with a fraction of the yield load of the member. Then equal end moments causing either single or double curvature bending were applied in the strong direction of bending until failure occurred. The columns were laterally braced to prevent lateral torsional buckling.

II THE TEST PROGRAM

2.1 Theoretical Considerations

The theoretical moment vs. column end rotation values were computed using an iterative program developed for an IBM-360 computer by Y. Nakamura[3]. This program uses a variation of the procedure proposed by N. W. Newark[8] and further developed by R. L. Ketter and others at Lehigh University[9]. The solution assumes bilinear stress-strain curve for the column material and that the column has no residual stresses. With the input of yield stress, cross-section dimensions, length, and applied axial load for each individual column, theoretical curves of moment vs. end rotation were obtained for each test column.

Plastic and reduced moments were calculated using the method given by Beedle[4].

2.2 Model Material Properties

Tentative values for yield stresses of the columns were obtained from tensile specimens cut from each of the approximately twelve-foot long stock sections from which the columns

were taken. These stresses were used to compute the required axial load P for a given P/P_y.

To determine the actual strength of each individual column, a six-inch section was cut from each column after it was tested. The flanges were cut away from the web and machined into tensile specimens. The tensile specimens were cut from the center of the double curvature columns and from one end of the single curvature columns, since these sections were not plastically deformed during the test. The yield stresses of the individual columns were found to vary somewhat from the yield stresses as determined from the stock sections. The individual yield stresses (average of two tests) and dimensions of each column were used to compute the yield loads and plastic moments shown in Table 3.

2.3 Test Procedure

The columns were fabricated as described in Section A, Part II and were placed in the testing apparatus described in Section B, Part II.

An axial load corresponding to a given P/P_y was applied to the column and held throughout the test. Then equal end moments causing either single or double curvature bending were applied incrementally in the strong direction of bending until failure occurred. End rotation measurements were taken after each increment of moment was applied. The columns were laterally braced to prevent lateral torsional buckling. A more complete description of the test procedure is given in Section C, Part II.

2.4 Results

The experimental results are presented in Tables 4 and 5 and are also shown on the interaction diagram plots in Figures 2, 3, 4, and 5.

A theoretical interaction curve is shown in each figure along with a curve plotted from the values of M/M_p and P/P_y taken from tables developed by Galambos and Prasad[5] for steel with a yield strength of 33 ksi and residual stresses of 0.3 σ_y.

Section D, Part II contains moment-end rotation relations for each of the columns along with their theoretical predictions. Because of the large variations in the testing conditions the results are normalized for easier comparison.

Columns 12, 30 and 32 were failed accidentally by an axial overload and are not included in the results.

2.4.1 Double Curvature

The annealed columns, as shown in Figure 2, compare favorably with the theoretical interaction curve in most of the P/P_y range.

The as-received and fabricated columns, as shown in Figure 3, agree closely with each other but in all twelve cases the observed ultimate moment is larger than expected. This result corroborates the experience that Foster[1] observed in his tests on small-scale welded joints. In both cases TIG welding was accomplished in the vicinity of the critical section (in this case the end cross-sections) and in both cases a systematic strength increase was observed.

2.4.2 Single Curvature

The annealed columns, as shown in Figure 4, generally follow the expected interaction curve. However, when compared with the unannealed cases, the experimental results seem somewhat scattered and somewhat under the theoretically predicted values. No explanation for such differences can be offered.

Figure 5 shows very good agreement between experimental and theoretical values throughout the range of P/P_y for the as-received and fabricated columns.

2.5 Conclusions

The described beam-column program was carried out as part of an overall investigation concerning the question "Can small scale models of steel frameworks be fabricated and tested to give reliable results?" A reasonable measure of whether the experiments were successful can be obtained by an examination of the EXP/THEO ratios listed in Tables 4 and 5. Considering separately the double curvature annealed, double curvature nonannealed, single curvature

annealed, and single curvature nonannealed cases, the minimum-average-maximum values of EXP/THEO were 0.90–1.02–1.13, 1.04–1.11–1.20, 0.83–0.96–1.10, and 0.98–1.03–1.08, respectively.

Clearly, the double curvature nonannealed columns were affected by the welding process used to attach the columns to their base plates. Although some care was taken to minimize the heating during the welding operation, the lesson learned by Foster[1] from his joint tests was set aside in the press of time. Several fabrication techniques that would not have involved heat input were considered, but each technique either did not work or promised to be substantially more time consuming and costly than the one adopted. In essence, we gambled here and lost.

The double curvature annealed, single curvature annealed and single curvature nonannealed results, while not superb, are acceptable. The scatter in the results is of the same magnitude as that for full scale tests conducted at Lehigh University[7]. The relative scatter in the annealed cases as compared to the unannealed cases is, at first glance, surprising; however, this fact may again be due to fabrication difficulties. The annealed columns were attached to their base plates and annealed (Part II, Section A) at a local commercial metallurgical company. A fabrication process had been worked out with the employees of that company, but just prior to production the employees went out on strike. Management stepped in and completed the fabrication and annealing of the annealed columns. Although perhaps unlikely, it is possible that the twenty-one columns experienced some fabrication and/or annealing variations.

With regard to the moment vs. end rotation characteristics of the forty-five beam-columns (Part II, Section D), the experimental behavior, with one excepted characteristic, compared well with the analytical predictions. That excepted characteristic is the initial slope of the experimental curve where it was consistently less than predicted in the double curvature columns and often less in the single curvature ones. The fact that the rotation measuring devices were attached to the base plates rather than to the column may have resulted in measurement of not only column rotation but base plate distortions.

The fact that these concluding paragraphs have included reference to fabrication and test procedures indicates the critical relationship between these procedures and the quality of the results. Fundamentally, the small scale models can be reliably used. However, the quality of the results depend, as they do in any tests, on the control of the specimen fabrication, loading, and instrumentation procedures.

TABLE 1

NOMINAL LOADING CONDITIONS

Test Number	Loading Condition	P/P_y	M/M_p	Steel Treatment
1, 2, 3	Double	0.12	(increasing	(annealed
4, 5, 6	Curvature	0.25	from zero	at 1100°F
7, 8, 9		0.50	to	for 1/2
10, 11, 12		0.75	failure)	hour)
13, 14, 15	Double	0.12		(as received
16, 17, 18	Curvature	0.25		and
19, 20, 21		0.50	(")	fabricated)
22, 23, 24		0.75		
25, 26, 27	Single	0.12		(annealed at
28, 29, 30	Curvature	0.25		1100°F for
31, 32, 33		0.50	(")	1/2 hour)
34, 35, 36		0.75		
37, 38, 39	Single	0.12		(as received
40, 41, 42	Curvature	0.25		and
43, 44, 45		0.50	(")	fabricated)
46, 47, 48		0.75		

TABLE 2.

MODEL DIMENSIONS

	Depth (in)	Flange Width (in)	Flange Thickness (in)	Web Thickness (in)	Area (in^2)
Nominal 1/10 scale 8WF31	0.800	0.800	0.0433	0.0288	0.0912
Measured Max.	0.804	0.804	0.044	0.034	0.0942
Measured Min.	0.799	0.800	0.042	0.028	0.0873
Ave. Measured	0.802	0.801	0.043	0.031	0.0914

TABLE 3.

MODEL SECTION PROPERTIES

Column Number	D (inch)	B (inch)	T (inch)	W (inch)	A (inch^2)	σ_y (ksi)	P_y (lbs)	M_P (lb-in)
1	.801	.800	.043	.030	.0903	34.8	3142	1041
2	.800	.802	.043	.030	.0904	31.0	2802	928
3	.803	.800	.044	.030	.0919	35.1	3226	1072
4	.803	.800	.043	.029	.0896	28.0	2509	836
5	.804	.802	.044	.029	.0913	37.1	3387	1133
6	.803	.802	.044	.029	.0913	35.7	3259	1088
7	.804	.800	.042	.030	.0888	29.4	2611	867
8	.801	.801	.043	.030	.0903	29.4	2655	880
9	.800	.801	.043	.030	.0903	30.3	2736	906
10	.800	.802	.043	.031	.0911	32.8	2988	986
11	.800	.802	.043	.031	.0911	32.8	2988	986
13	.802	.800	.043	.030	.0903	38.2	3449	1144
14	.801	.802	.044	.029	.0913	37.4	3415	1137
15	.800	.803	.043	.031	.0912	35.1	3201	1056
16	.801	.800	.044	.029	.0911	34.8	3170	1056
17	.801	.802	.043	.031	.0911	39.2	3571	1180
18	.803	.801	.044	.031	.0926	37.2	3445	1140
19	.803	.801	.043	.032	.0918	38.1	3498	1153
20	.802	.801	.044	.031	.0926	36.9	3417	1132
21	.803	.800	.044	.032	.0933	37.1	3461	1142
22	.800	.803	.042	.032	.0904	34.4	3110	1020
23	.800	.802	.044	.032	.0934	38.8	3624	1192
24	.800	.803	.043	.034	.0933	36.7	3424	1118
25	.801	.800	.042	.028	.0873	36.0	3143	1048
26	.804	.801	.043	.028	.0890	35.8	3186	1068
27	.800	.802	.043	.030	.0904	34.6	3128	1036
28	.803	.801	.043	.029	.0897	29.4	2636	879
29	.803	.800	.043	.030	.0903	32.0	2890	960
31	.801	.801	.044	.030	.0919	37.2	3419	1134
33	.802	.800	.043	.032	.0917	33.1	3035	1000
34	.803	.802	.043	.029	.0898	36.9	3314	1105
35	.800	.802	.043	.030	.0904	34.5	3119	1032
36	.802	.802	.043	.028	.0890	36.2	3222	1077
37	.801	.800	.043	.033	.0924	32.7	3021	991
38	.800	.800	.044	.032	.0932	32.8	3057	1006
39	.802	.802	.044	.033	.0941	36.3	3416	1124
40	.802	.800	.044	.033	.0940	32.7	3074	1010
41	.799	.803	.043	.031	.0912	35.3	3219	1061
42	.802	.803	.044	.032	.0935	34.9	3263	1077
43	.800	.804	.043	.031	.0913	32.5	2967	979
44	.804	.802	.044	.033	.0942	35.0	3297	1087
45	.803	.803	.044	.032	.0935	36.8	3441	1137
46	.803	.800	.044	.032	.0933	31.7	2958	977
47	.803	.803	.044	.032	.0935	34.0	3179	1051
48	.801	.802	.043	.031	.0911	32.0	2915	963

TABLE 4.

LOADING CONDITIONS & RESULTS–DOUBLE CURVATURE

Column Number	P_{act} (1b)	$\frac{P_{act}}{P_y}$	M_{PC} (1b-in)	Ultimate Moment (lb-in) Actual	Theoretical	$\frac{M_{act.}}{M_{theo.}}$	$\frac{M_{act.}}{M_P}$	EXP / THEO
			Annealed					
1	407	.130	1001	1100	994	1.11	1.06	1.10
2	363	.130	892	920	885	1.04	0.99	1.03
3	399	.124	1035	1110	1029	1.08	1.03	1.06
4	590	.235	729	820	719	1.14	0.98	1.10
5	892	.263	951	950	936	1.10	0.84	1.01
6	868	.266	910	880	896	0.98	0.81	0.97
7	1470	.563	445	410	429	0.96	0.47	0.97
8	1480	.558	456	430	440	0.98	0.49	0.98
9	1520	.555	471	430	455	0.95	0.47	0.97
10	2540	.850	177	320	168	1.90	0.32	1.13
11	2230	.747	298	170	284	0.60	0.17	0.90
			Nonannealed					
13	371	.108	1114	1340	1108	1.21	1.17	1.20
14	422	.124	1096	1230	1088	1.13	1.08	1.11
15	377	.118	1023	1200	1018	1.18	1.14	1.17
16	880	.278	870	1080	855	1.16	1.02	1.18
17	813	.228	1044	1160	1030	1.13	0.98	1.09
18	863	.250	981	1200	966	1.24	1.05	1.18
19	1770	.506	670	740	650	1.14	0.64	1.07
20	1785	.523	632	720	612	1.18	0.64	1.08
21	1636	.472	705	740	684	1.08	0.65	1.04
22	2340	.753	302	340	288	1.18	0.33	1.04
23	2610	.723	393	460	375	1.23	0.39	1.07
24	2630	.768	313	440	298	1.48	0.39	1.11

TABLE 5.

LOADING CONDITIONS & RESULTS–SINGLE CURVATURE

Column Number	P_{act} (1b)	$\frac{P_{act}}{P_y}$	M_{PC} (1b-in)	Ultimate Moment (1b-in) Actual	Ultimate Moment (1b-in) Theoretical	$\frac{M_{act.}}{M_{theo.}}$	$\frac{M_{act.}}{M_P}$	EXP / THEO
				Annealed				
25	393	.125	1009	1010	892	1.13	0.96	1.10
26	395	.124	1029	980	911	1.08	0.92	1.06
27	395	.126	998	780	881	0.89	0.75	0.90
28	720	.273	731	580	566	1.02	0.66	1.01
29	603	.209	865	610	708	0.86	0.64	0.90
31	1455	.425	754	460	521	0.88	0.41	0.94
33	1200	.395	704	340	497	0.68	0.34	0.83
34	2480	.749	328	160	184	0.87	0.14	0.96
35	2580	.828	213	110	115	0.96	0.11	0.99
36	2506	.778	283	80	157	0.51	0.074	0.089
				Nonannealed				
37	386	.128	956	870	843	1.03	0.88	1.03
38	360	.118	975	890	867	1.03	0.88	1.02
39	430	.126	1085	960	959	1.00	0.85	1.00
40	820	.267	855	710	666	1.06	0.70	1.04
41	790	.245	918	710	730	0.97	0.67	0.98
42	893	.274	900	780	697	1.12	0.72	1.08
43	1580	.533	536	410	348	1.18	0.42	1.07
44	1790	.543	586	420	375	1.12	0.39	1.05
45	1778	.517	645	460	419	1.10	0.40	1.04
46	2460	.832	197	90	106	0.85	0.092	0.98
47	2670	.840	203	160	110	1.45	0.15	1.07
48	2350	.806	224	140	123	1.14	0.15	1.02

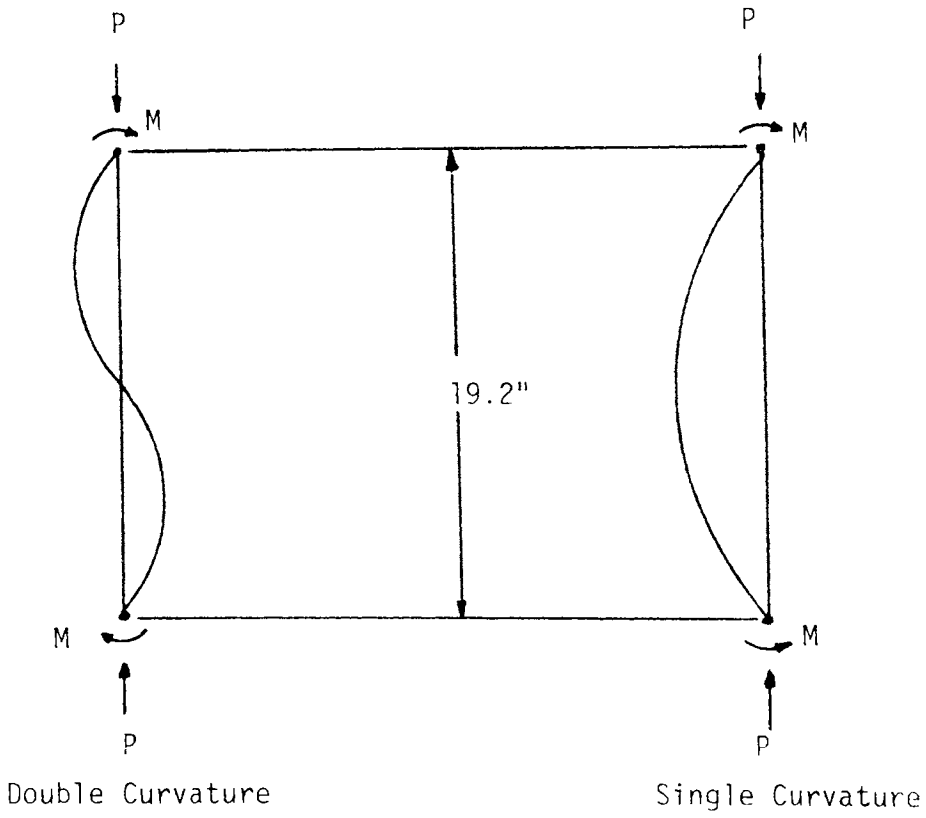

FIGURE 1–MOMENT APPLICATION

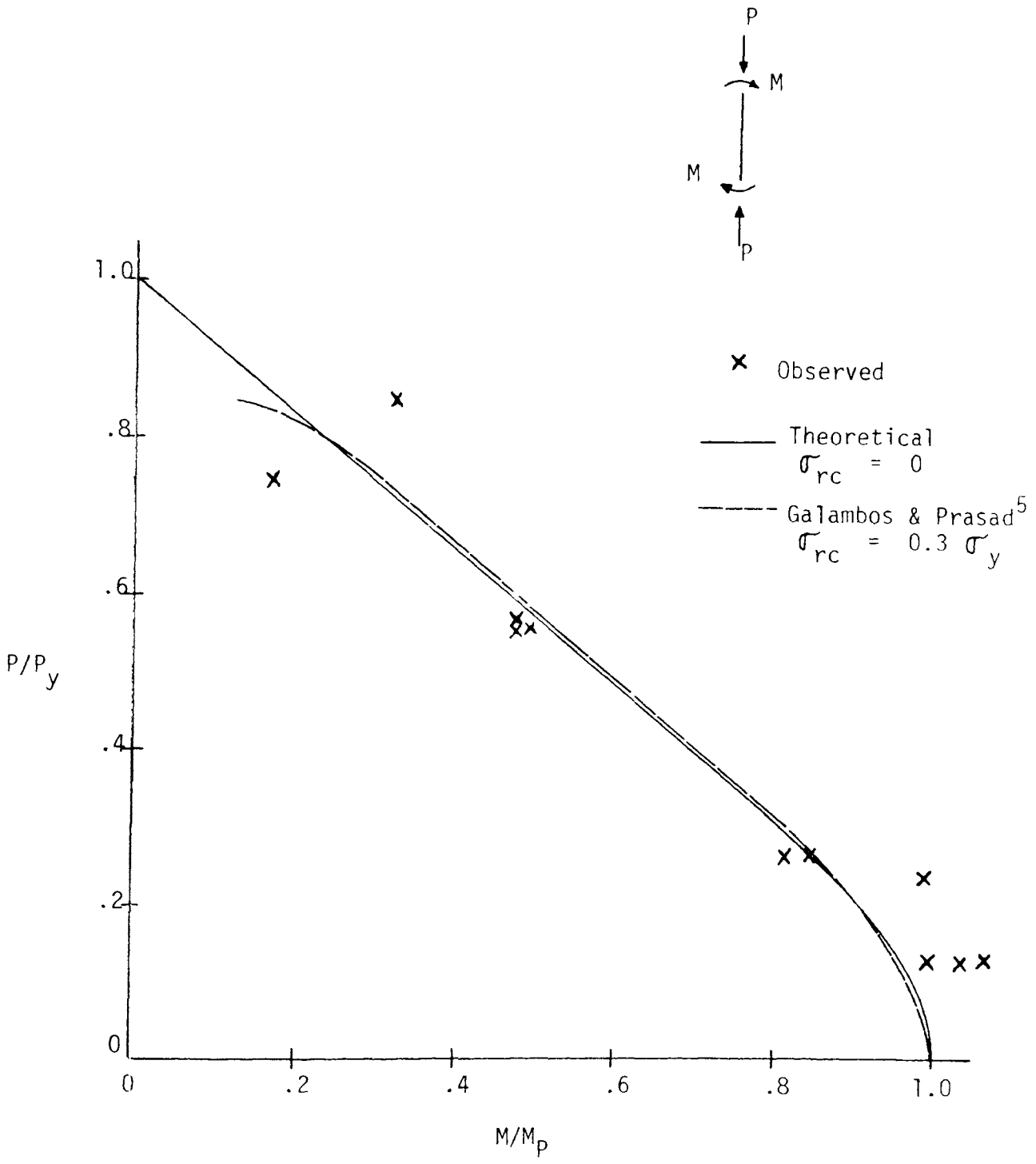

FIGURE 2–INTERACTION DIAGRAM – COLUMNS 1-11 (ANNEALED)

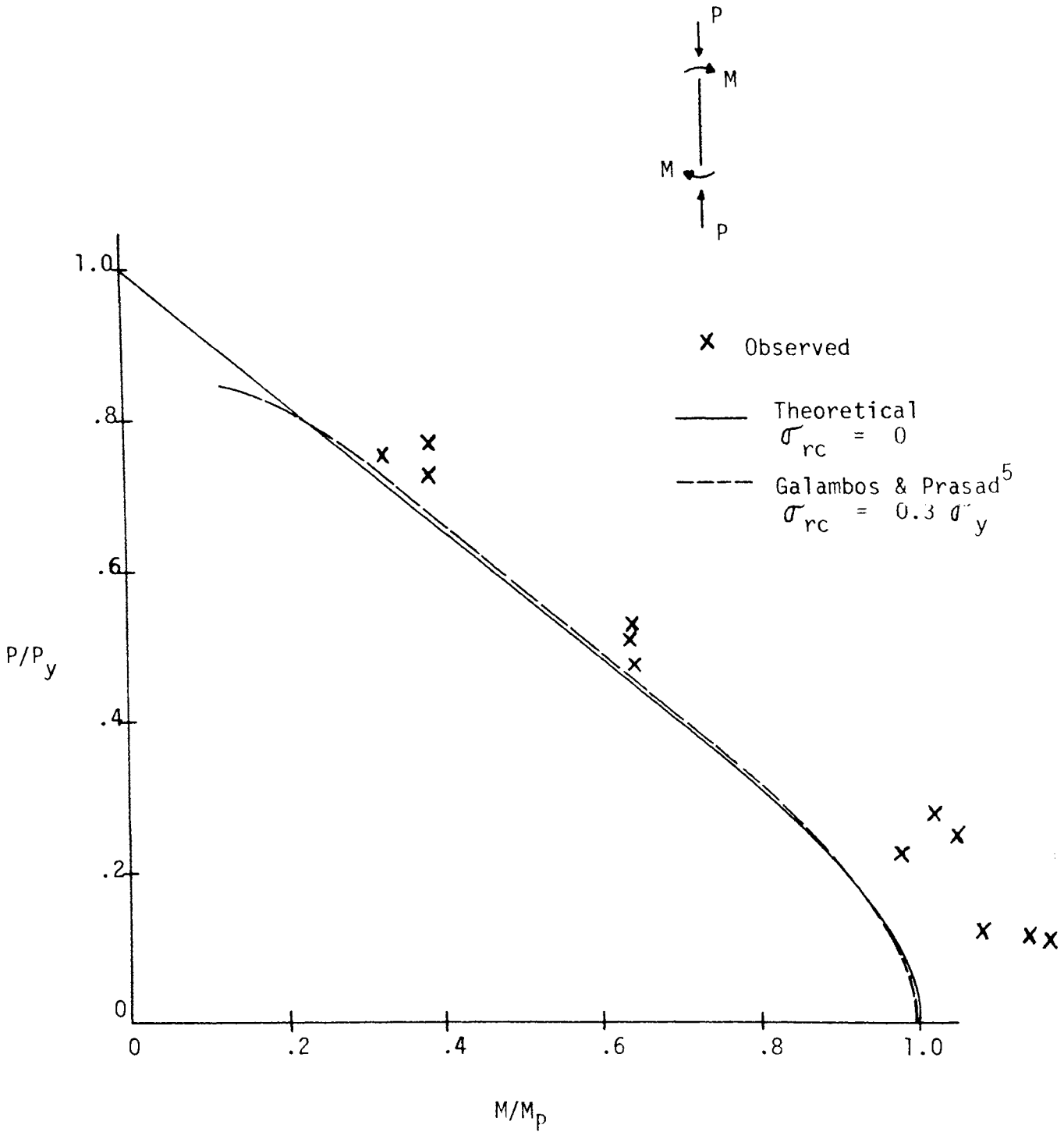

FIGURE 3–INTERACTION DIAGRAM – COLUMNS 13-24 (UNANNEALED)

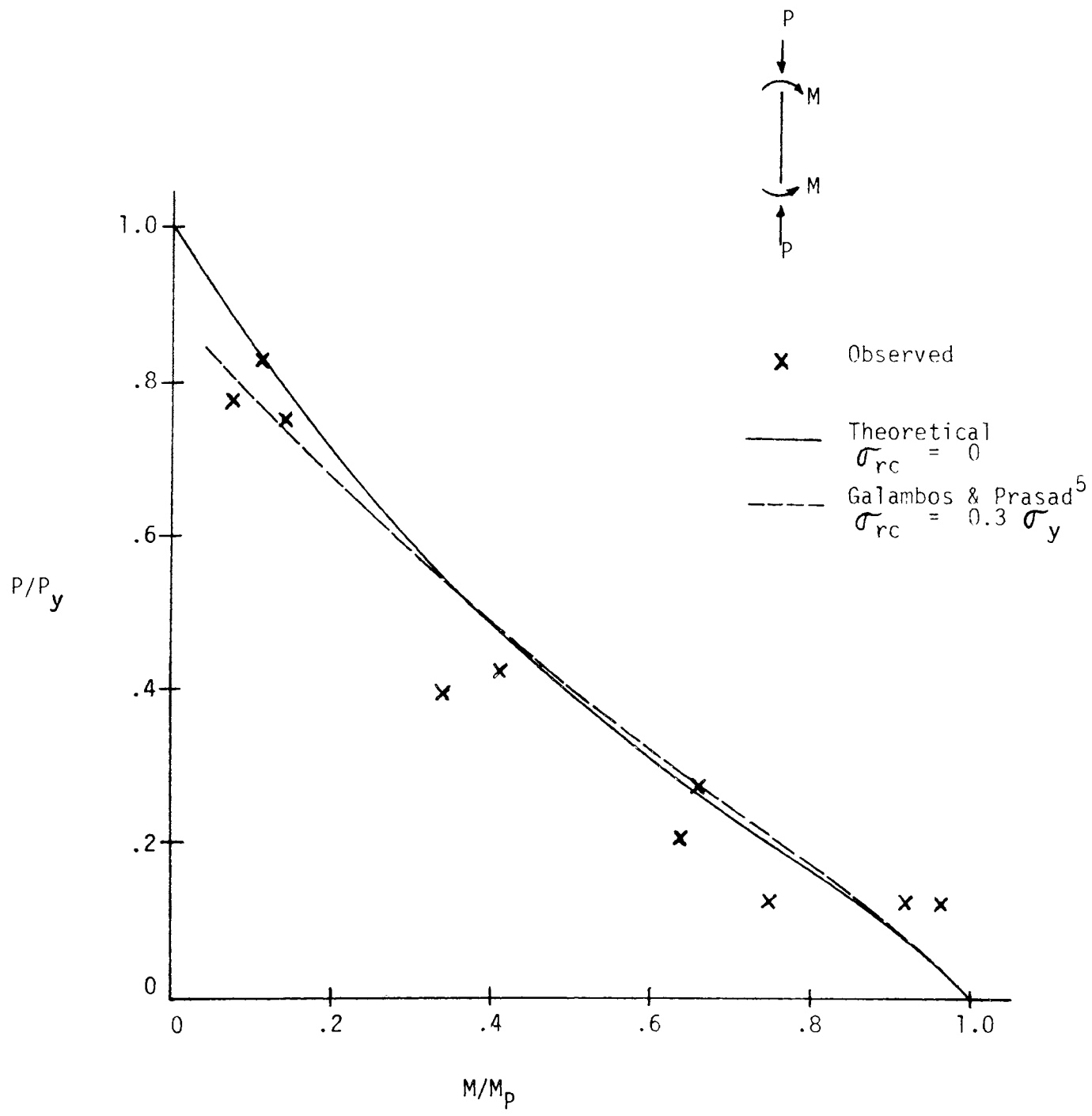

FIGURE 4—INTERACTION DIAGRAM — COLUMNS 25-36 (ANNEALED)

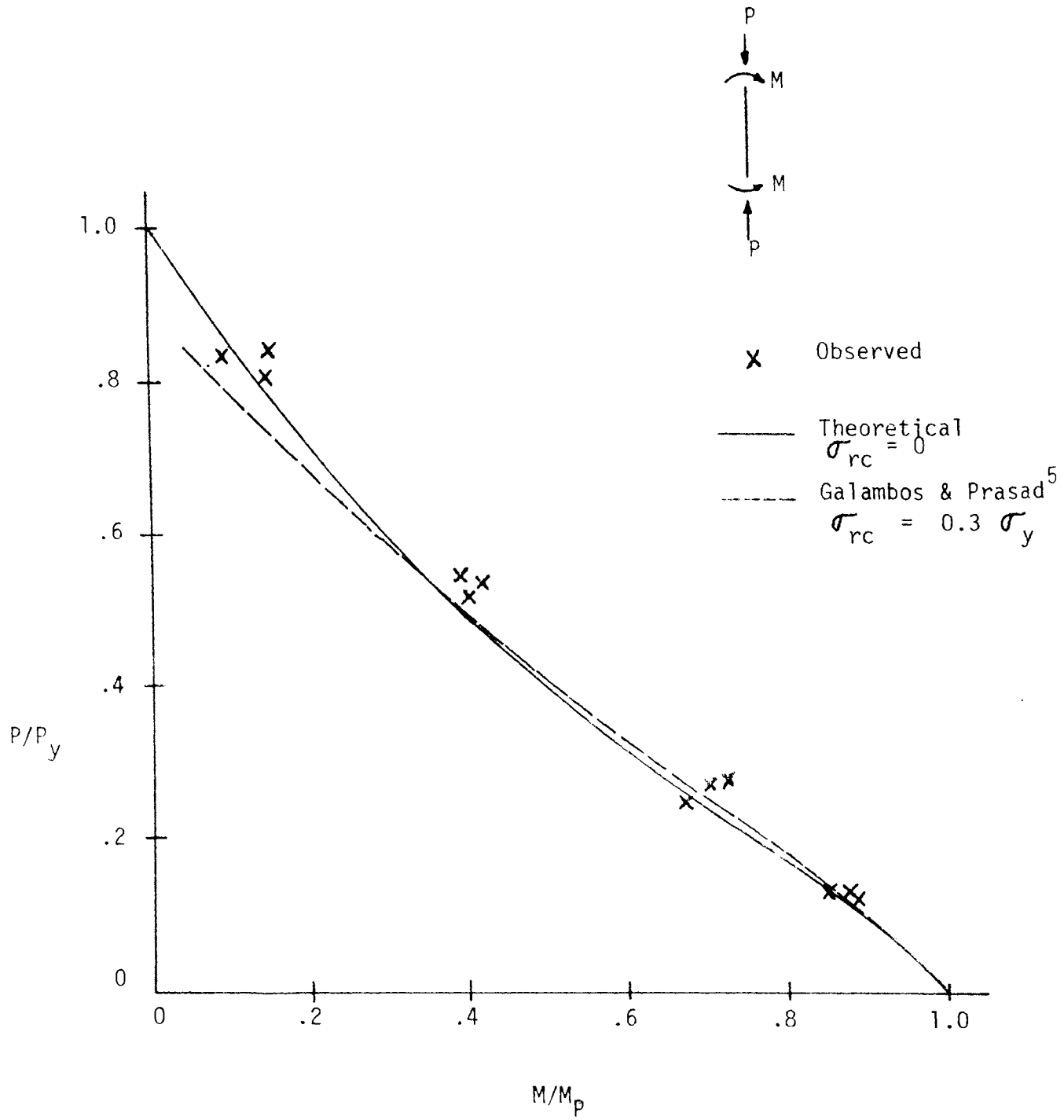

FIGURE 5–INTERACTION DIAGRAM – COLUMNS 37-48 (UNANNEALED)

PART II

A. MODEL FABRICATION

A.1 Column Sections

The column sections were milled from SAE C1020 by Precision Shapes, Inc., Suffern, N. Y. Each column was cut 19.2 inches long, giving an L/r_x ratio of approximately 55 (bending about the strong axis).

A.2 End Plates

Three-inch-square end plates were cut from 3/8-inch-thick steel stock for attaching the columns to the loading apparatus. Electron discharge machining was used to cut an H-slot, the shape of the column cross section, in the center of the plate. Four 3/8-inch drill holes were located at the corners of the plates for bolting the columns securely to the loading device. A hole was provided near the center of each plate for attaching the end rotation measuring gages.

A.3 Assembly

To produce the annealed columns, the sections and plates were annealed at 1100°F for about 20 minutes. Then the column end was inserted into the plate until the end of the column was flush with the bottom of the plate. The column and plate assembly was aligned in a jig to insure that the finished column would be normal to the plates. While still in the jig, the column was tack welded to the bottom surface of the plate. Finally, the sections were brazed to the plates at a temperature of 1100°F for ten minutes.

The as-received and fabricated columns presented the problem of attaching the base plates so that a heat affected zone was not introduced in the finished column. Starin[6] had shown that neither lead solder nor epoxies furnished enough strength to securely fix the column in the hole. It was decided to try heliarc welding the end of the column to the bottom of the plate with as little heat as possible and filling the small spaces where the column enters the plate with epoxy (see Figure A1). This worked well for the single curvature cases (columns 37-38) since very little heat was conducted to the midsection of the column where the critical stresses occur. Although Foster had shown increased strength near welded connections, the same method of attachment was used for the double curvature unannealed columns. It was thought that the thick base plate would remove much of the heat developed in the welding process.

Web stiffeners were cut from 1/16-inch stock and placed at the one-third points to stiffen the webs at the points where the lateral bracing was attached. Since the forces on the stiffeners were not expected to be very large, they were epoxied in place. This method was used for both the annealed and the unannealed columns because it could be done rapidly and presented no heating problems.

A.4 Strain Gages

Four epoxy-backed, foil strain gages (Baldwin Lima Hamilton FA-25-12 S6) at each end of each column (see Figure A2) were used to help in centering the applied axial load and to provide some insight into the column behavior throughout the test. Figure A3 shows a beam-column ready for testing.

B. TEST APPARATUS

B.1 Loading Device

Moment was applied to the ends of the column with a set of bearing mounted lever arms developed by Starin[6] (see Figure B1). Starin calibrated the loading heads and showed that the moment required to overcome friction in the bearings is less than 10 in-lb when the axial load is 2500 lbs. As an upper error limit, it is thought

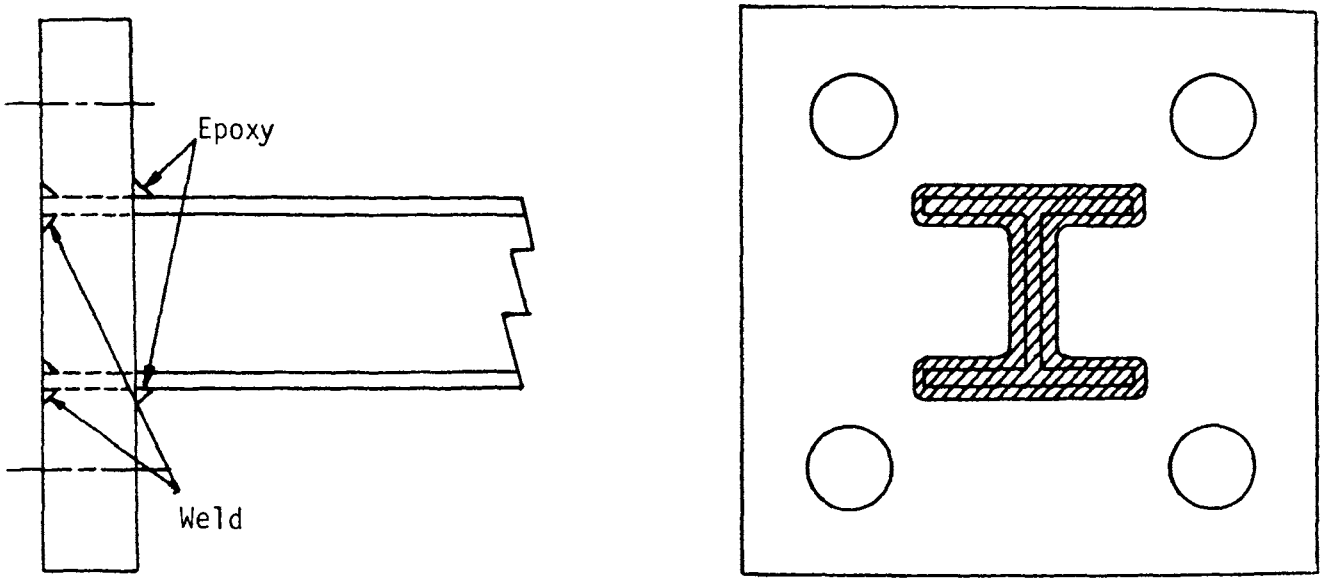

FIGURE A1–ATTACHMENT OF BASE PLATES – NON-ANNEALED COLUMNS

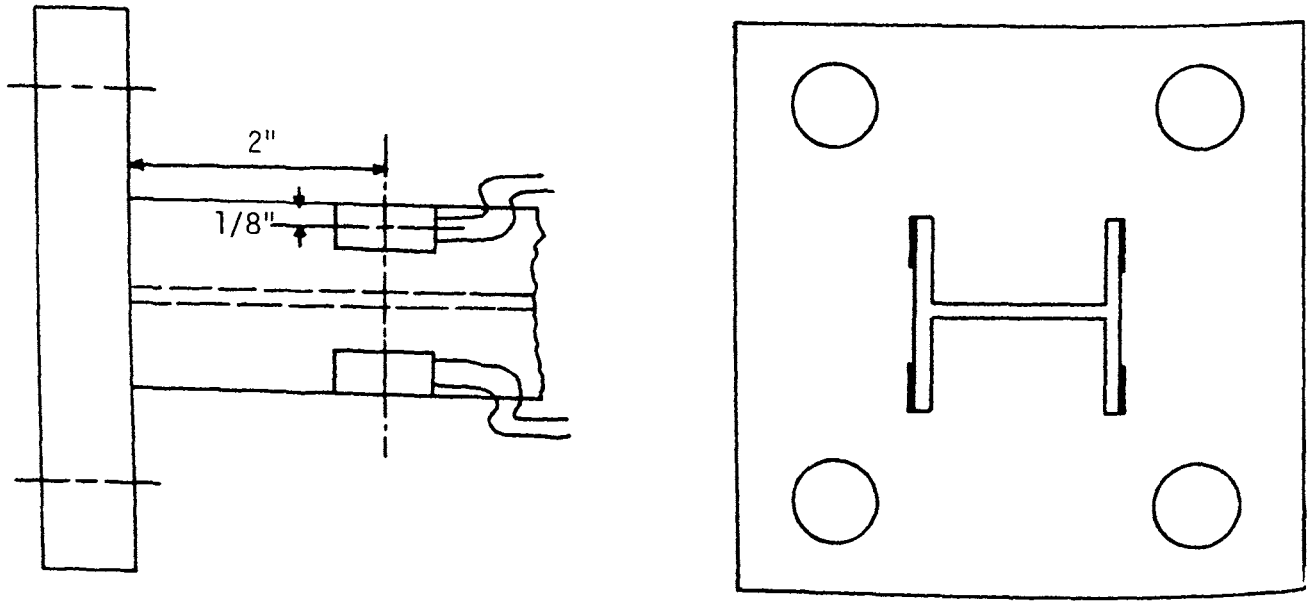

FIGURE A2–STRAIN GAGE LOCATION

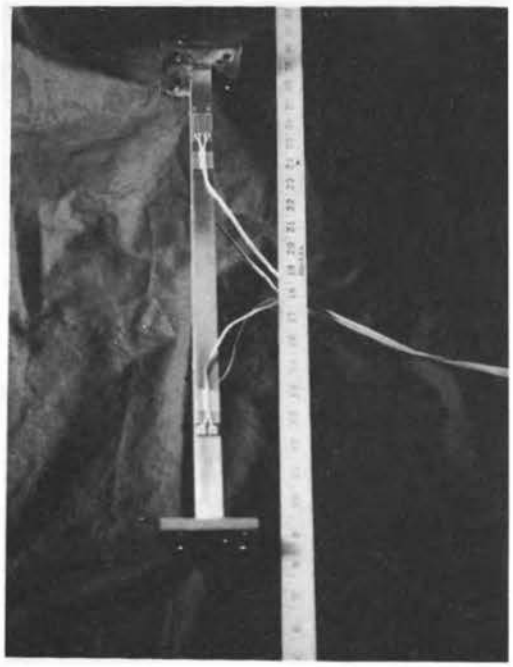

FIGURE A3–BEAM COLUMN READY FOR TESTING

that with column 36 (see Table 5) this friction might amount to ten percent. For lower P/P_y values and for double curvature cases the error would be less.

By hanging weights on the top and bottom arms on the same side of the column, double curvature bending was introduced into the column. And by using opposite lever arms, the column was subjected to single curvature bending.

The mounted lever arms were fitted in a 60-kip Baldwin Lima Hamilton universal testing machine which was used to apply the axial load. With the machine set on low range, the full scale reading is 6000 pounds. Since the smallest scale division is five pounds, the axial load (P) can be estimated within approximately 2.5 pounds.

B.2 Lateral Bracing

The columns were braced laterally at the third points to prevent failure by lateral torsional buckling. The bracing consisted of a linkage, one end of which was attached to the compression flange and the other to a rigid frame surrounding the column. The linkage was pinned so that movement of the compression flange was not restricted in any direction except laterally (see Figures B2 and B3).

B.3 Rotation Measurement Devices

A rotation gage consisting of a bubble level, a deflection measuring dial gage, and a six-inch lever was connected to each base plate. The dial gage measured the deflection of the lever arm away from the level. A change in deflection of 0.0001 inch, the smallest division on the dial, is equivalent to an 0.0000167 radian rotation of the column end. The instruments are capable of measuring rotations accurately up to about 0.08 radian. A view of the rotation gage during a test is shown in Figure B4.

C. TEST PROCEDURE

C.1 Column Alignment

The column was first bolted to the top loading head and the eight strain gages were zeroed with a switching and balancing box connected to an SR-4 strain indicator. The bottom was then bolted in place and a small test load was applied and the gages read to check for any large variations in strains which would indicate the column was not properly aligned. In this case, the column was adjusted using the method given by Starin[6].

Once the column was aligned, the bracing and rotation measuring instruments were attached and testing began.

C.2 Loading

A specified (see Table 1, Part I) fraction of the axial yield load was applied carefully, with occasional checks on the strains to insure that the loading did not induce bending moments into the column. Holding the axial load, weights were added in increments to the lever arms, thus applying the top and bottom end moments. After each increment of applied moment, readings were taken. When the column became strained past the elastic limit it was necessary to wait for creep to stop before taking readings. This creep behavior lasted from a few minutes to as long as thirty minutes, depending upon the loading conditions. Weights were added until column failure, which was evident by a continuous end rotation without the addition of additional moments.

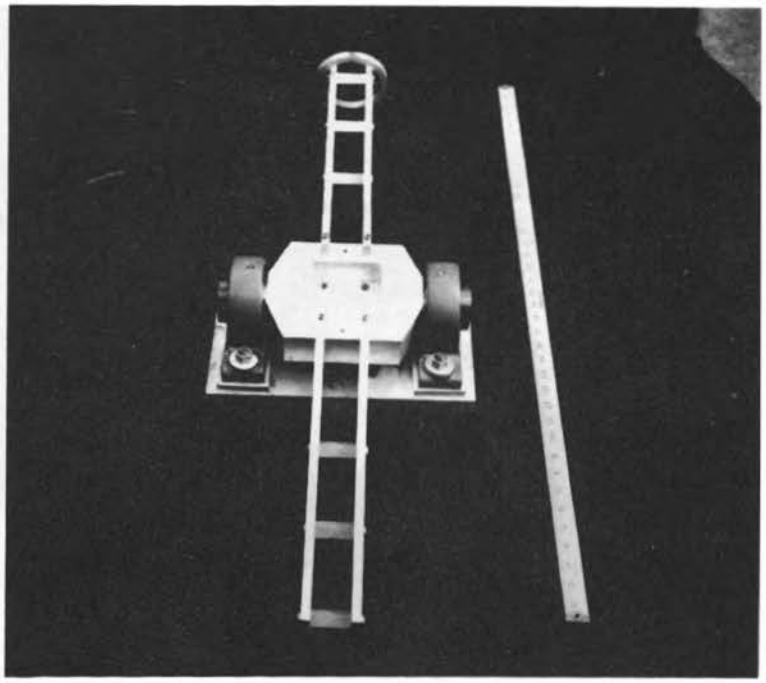

FIGURE B1–LOADING DEVICE

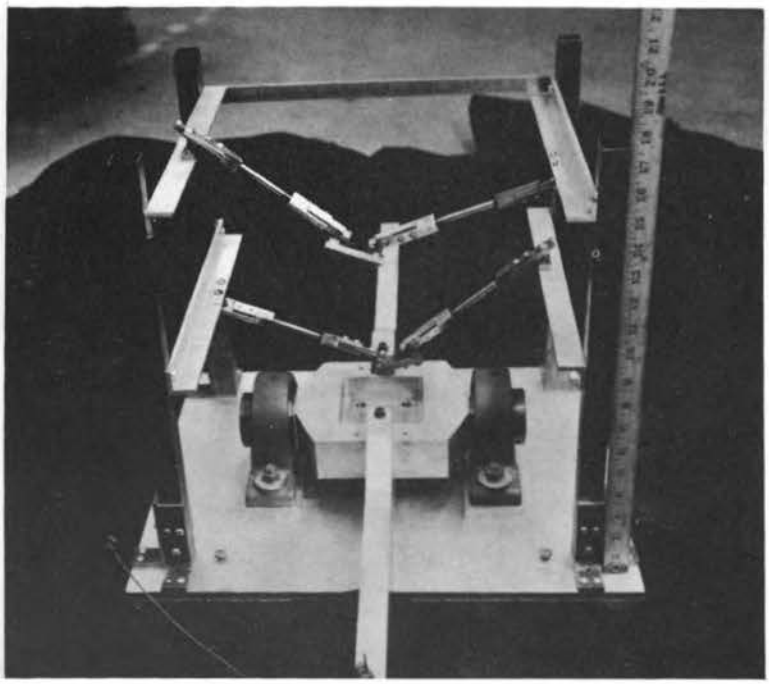

FIGURE B2–LATERAL BRACING

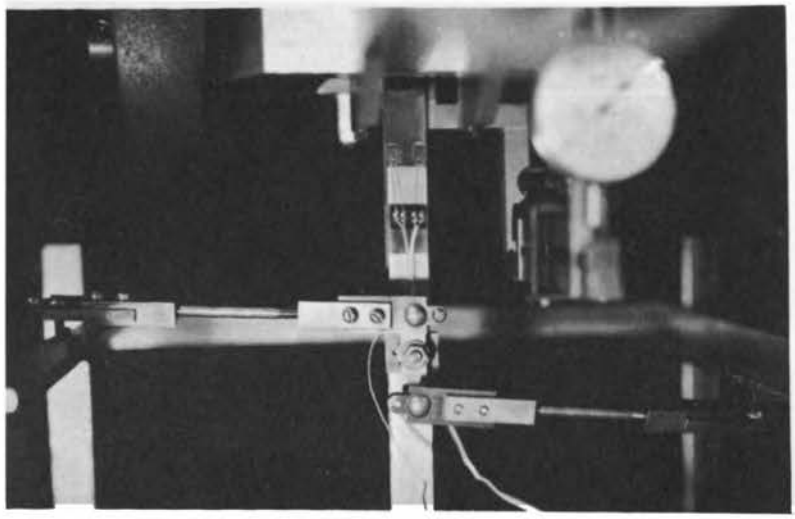

FIGURE B3–LATERAL BRACING CLOSEUP

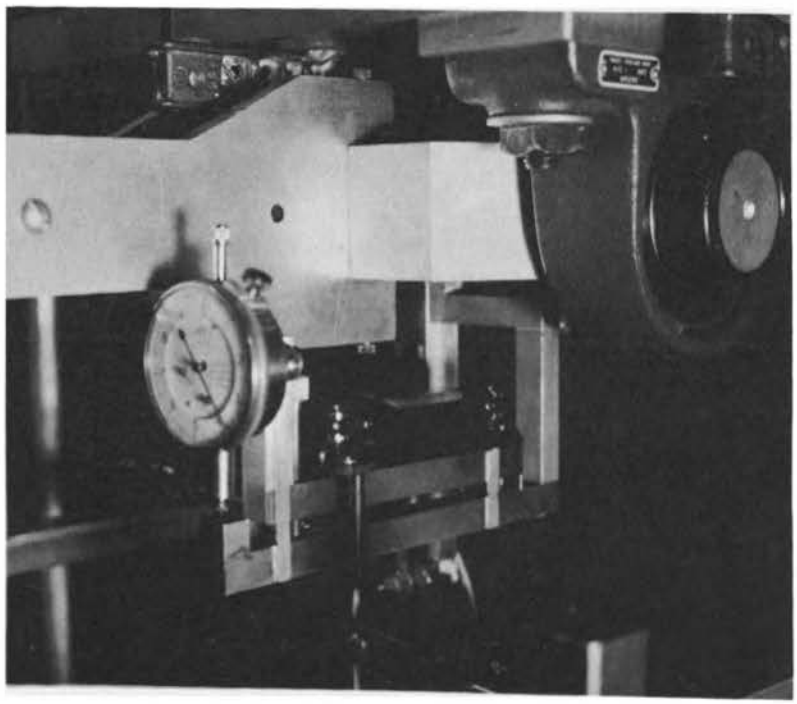

FIGURE B4–ROTATION GAGE

D. MOMENT vs. END ROTATION PLOTS

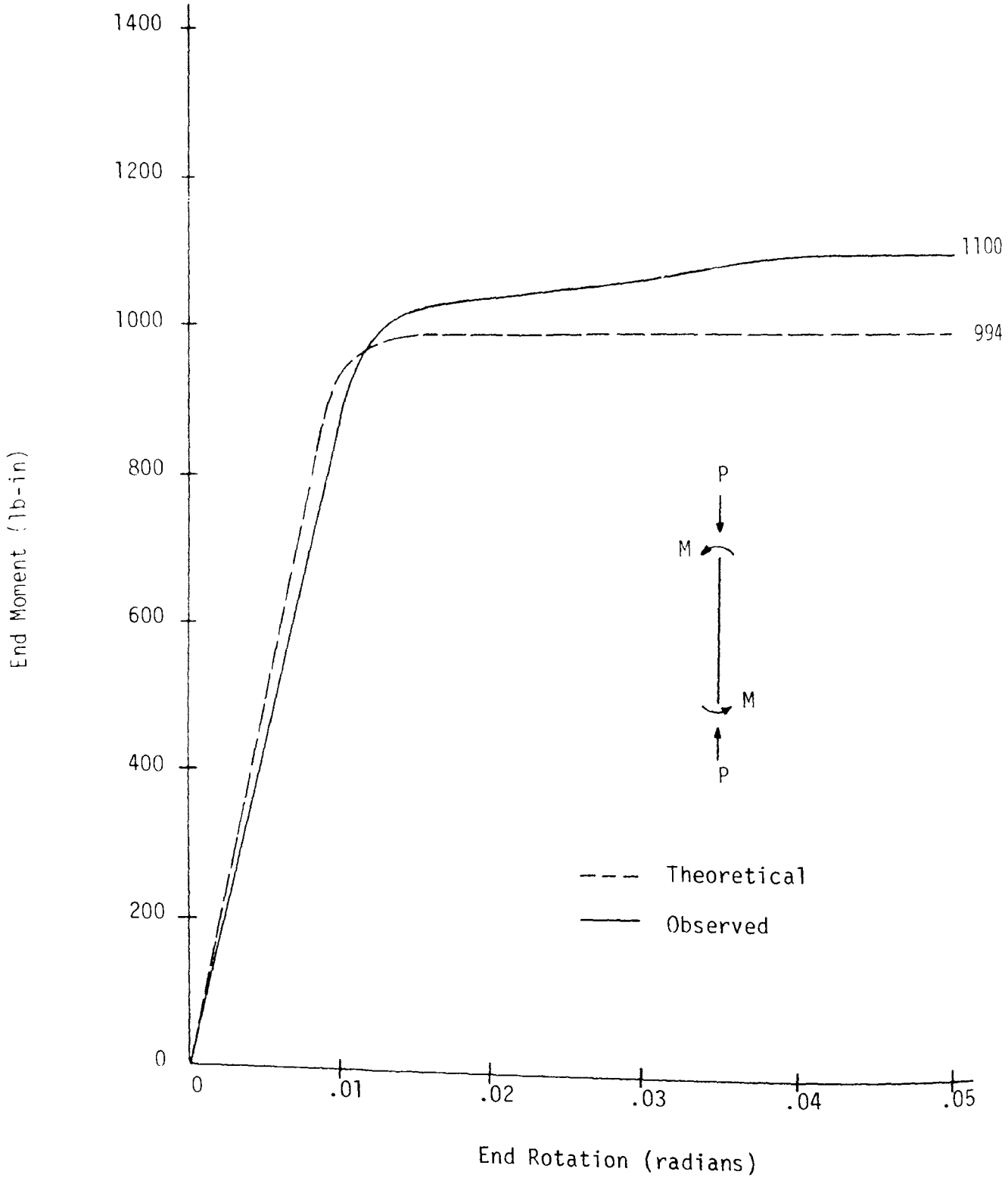

FIGURE D1–BEAM COLUMN 1 MOMENT vs. ROTATION

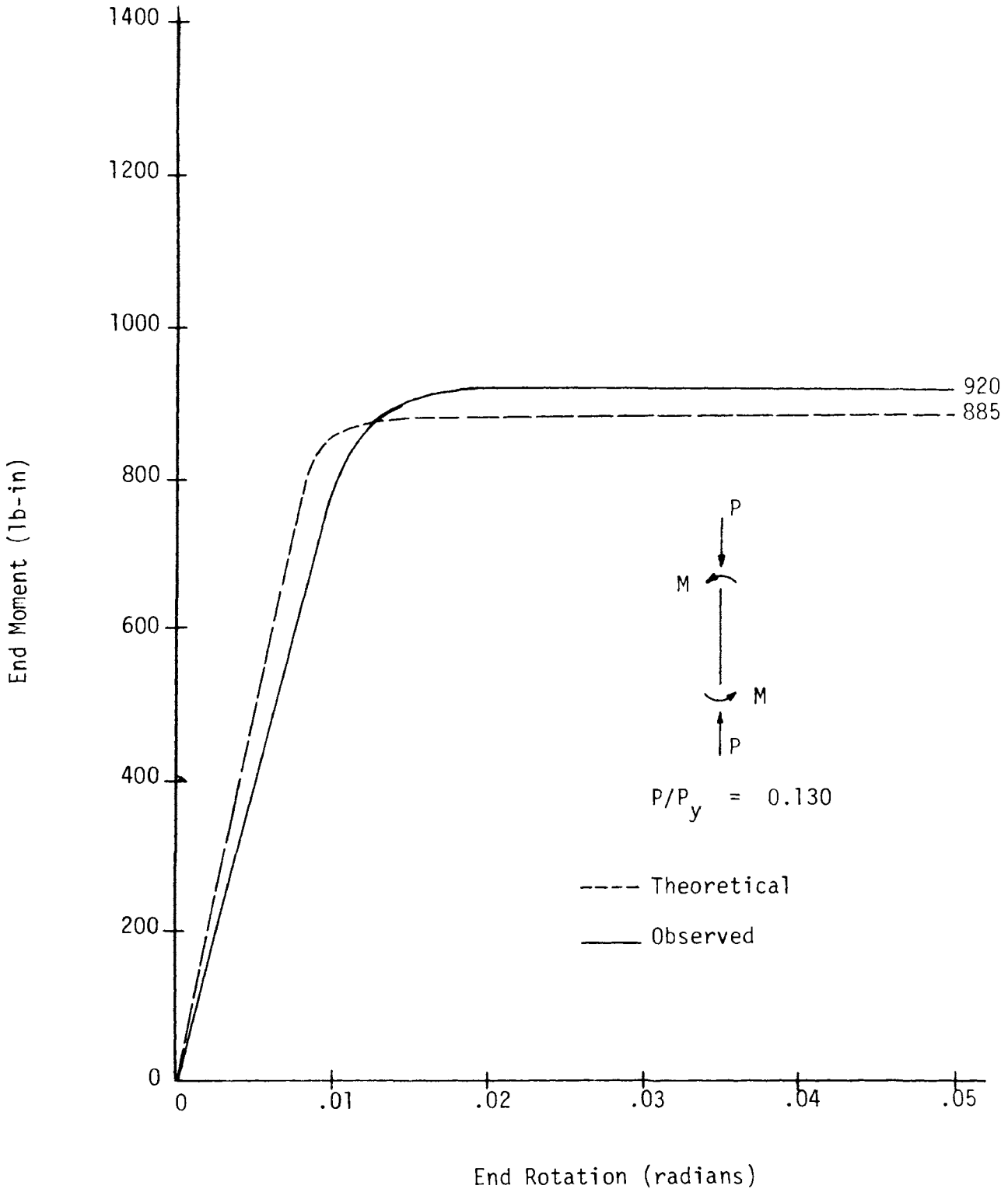

FIGURE D2–BEAM COLUMN 2 MOMENT vs. ROTATION

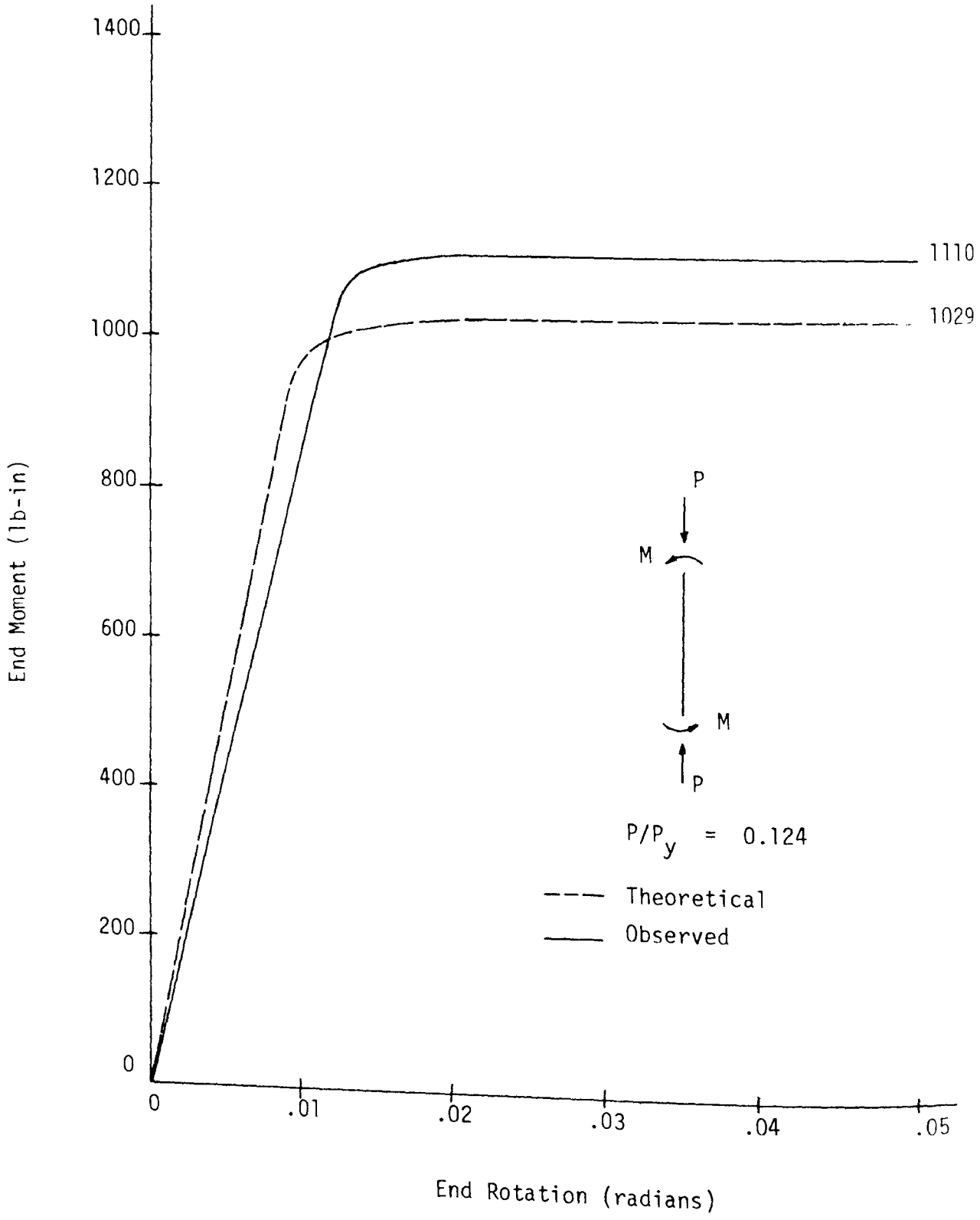

FIGURE D3–BEAM COLUMN 3 MOMENT vs. ROTATION

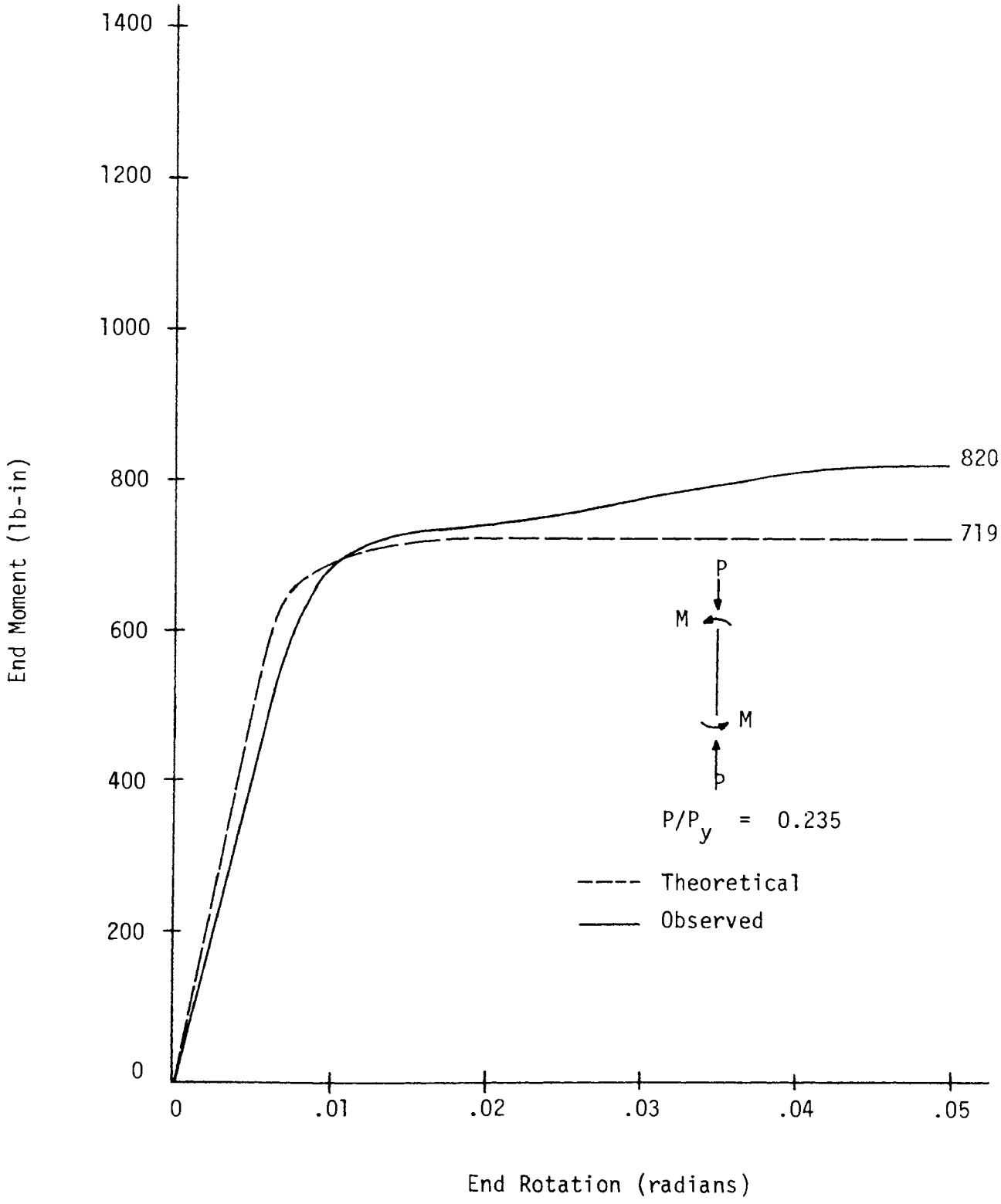

FIGURE D4—BEAM COLUMN 4 MOMENT vs. ROTATION

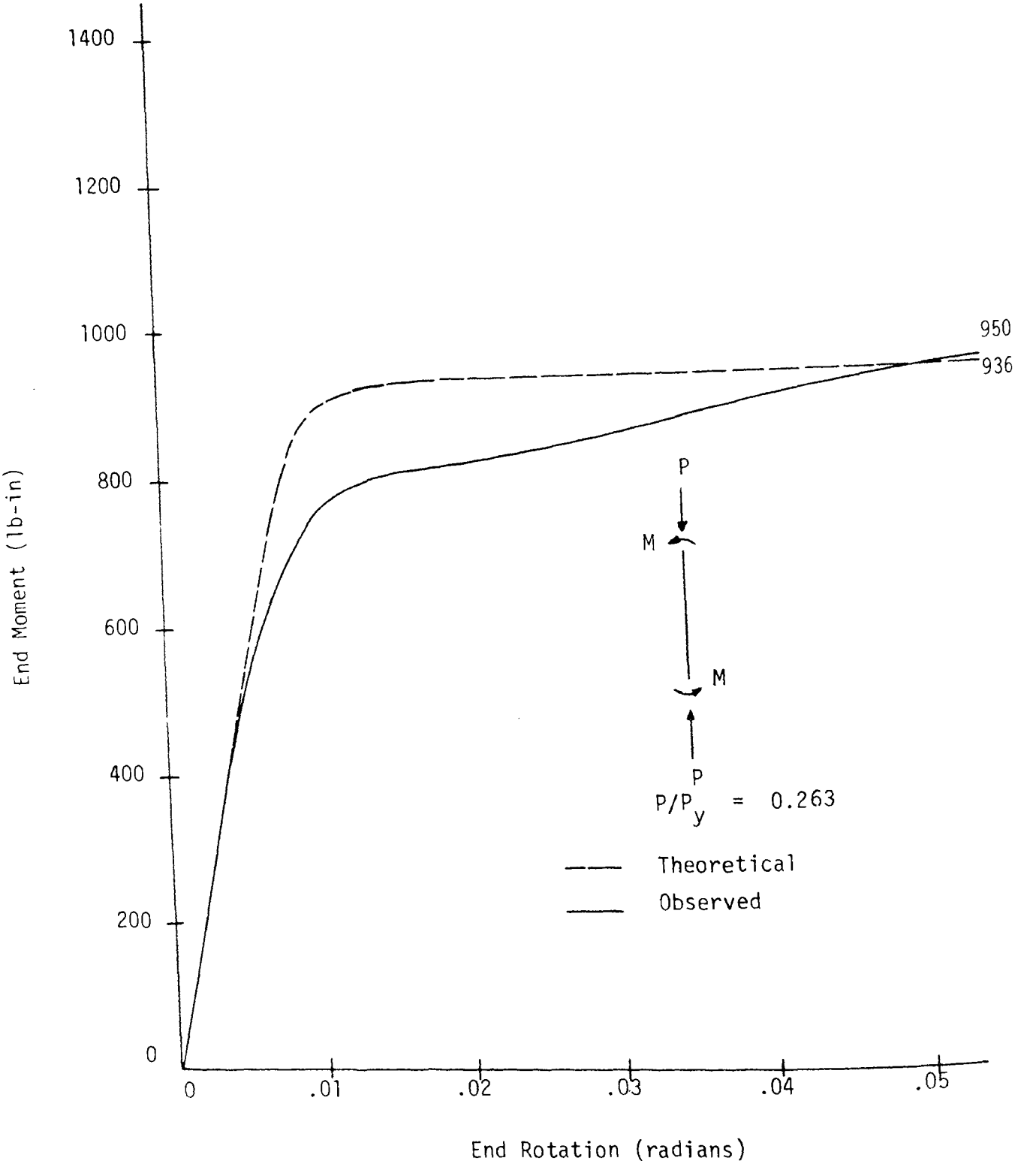

FIGURE D5–BEAM COLUMN 5 MOMENT vs. ROTATION

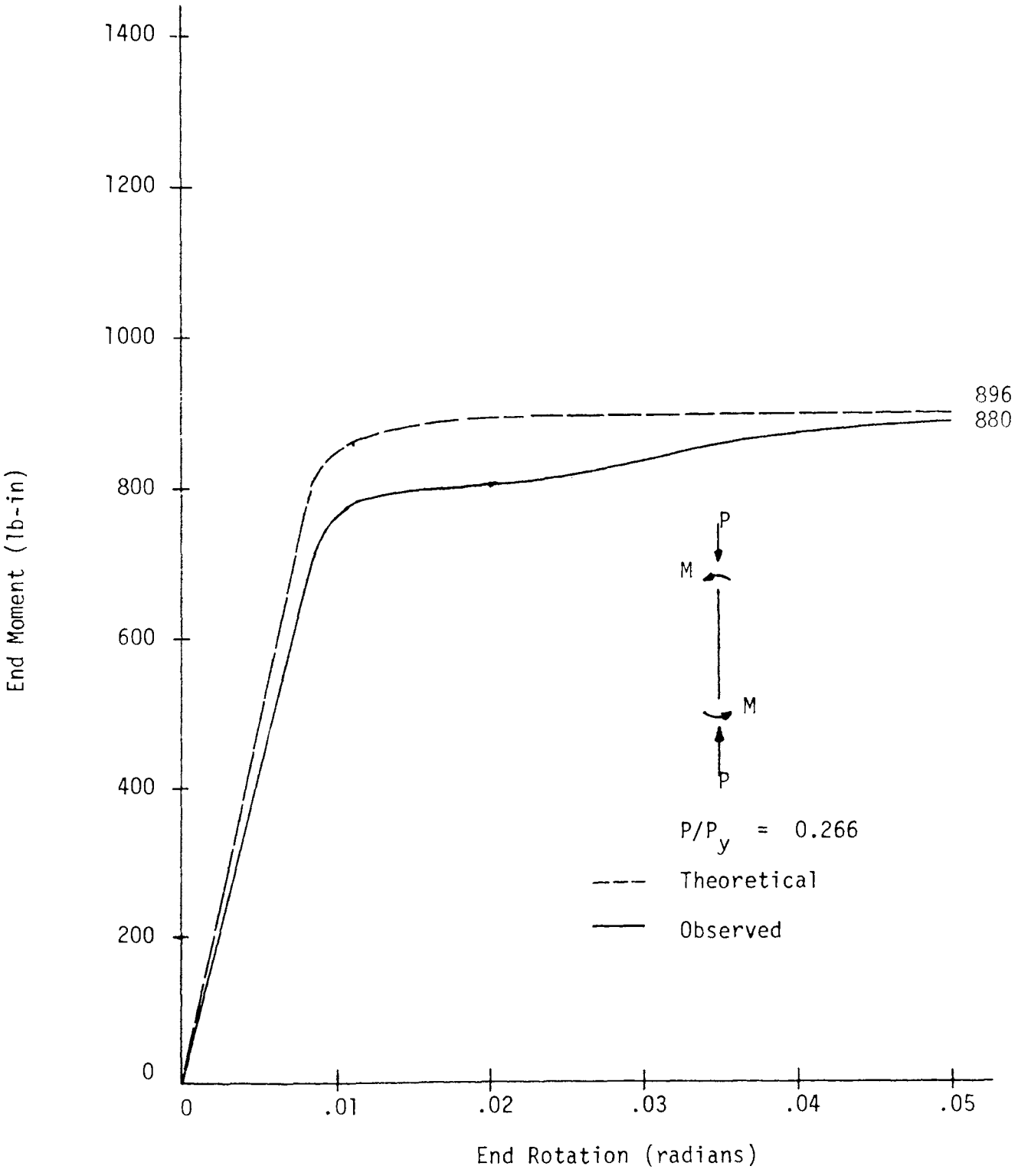

FIGURE D6–BEAM COLUMN 6 MOMENT vs. ROTATION

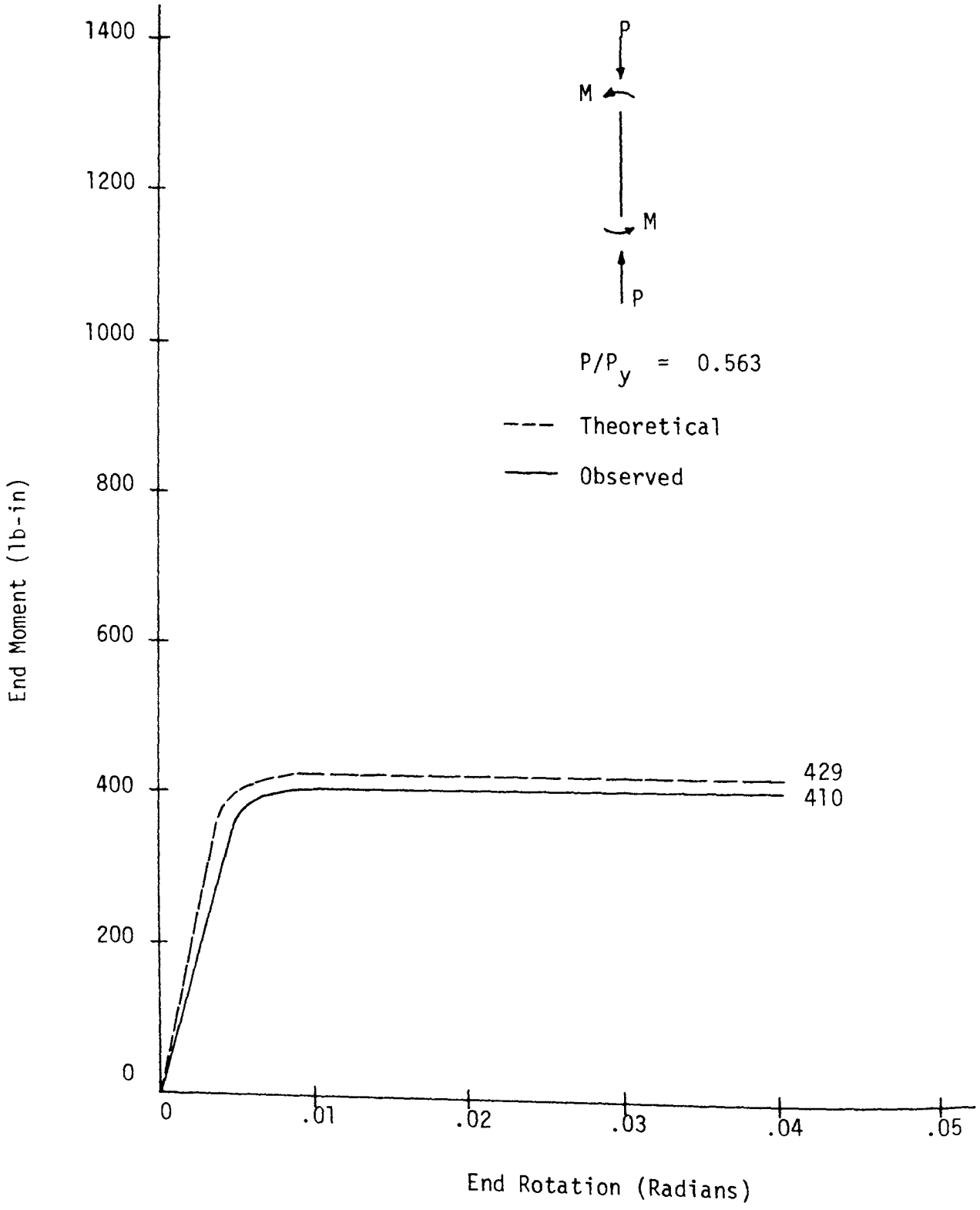

FIGURE D7—BEAM COLUMN 7 MOMENT vs. ROTATION

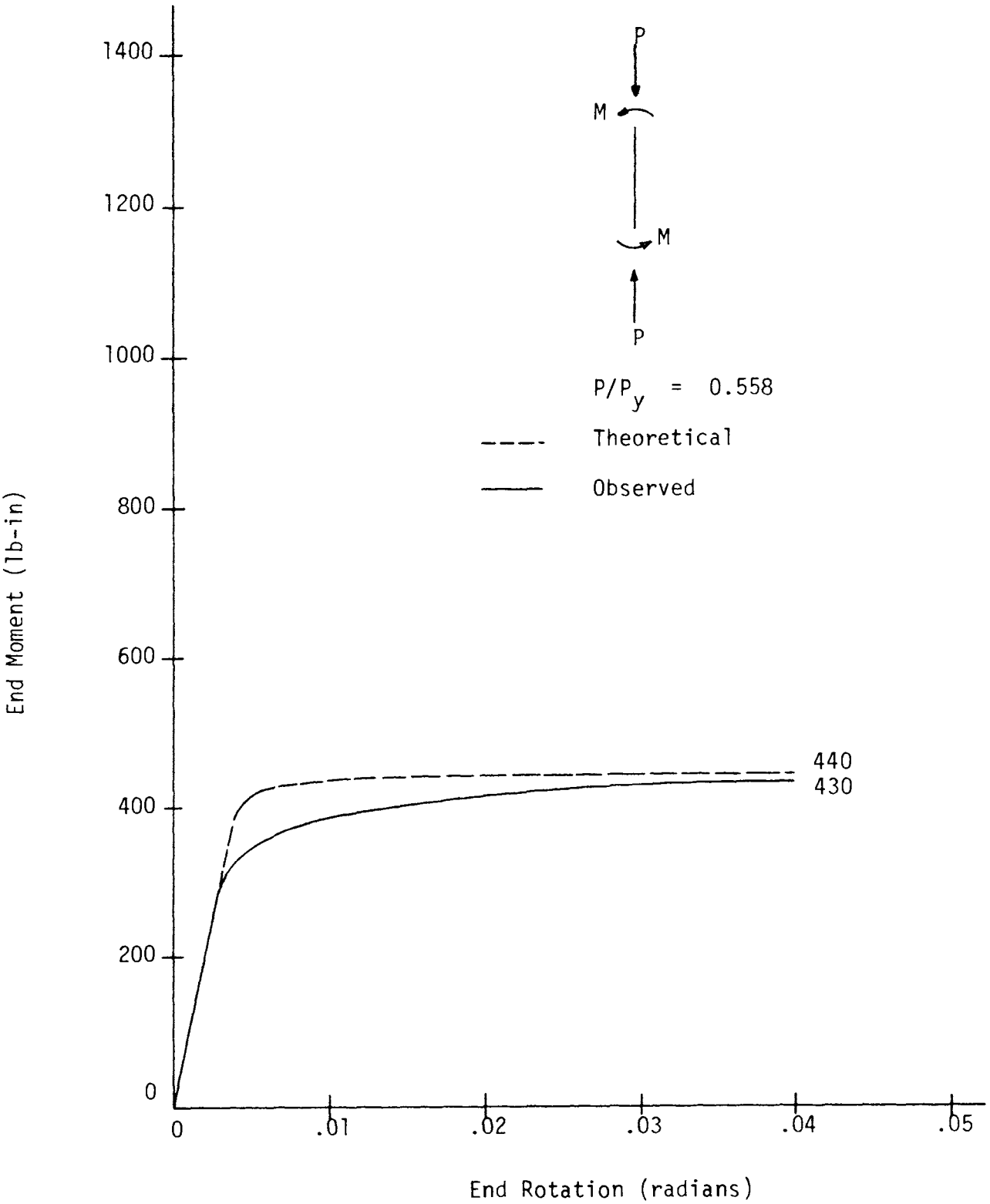

FIGURE D8–BEAM COLUMN 8 MOMENT vs. ROTATION

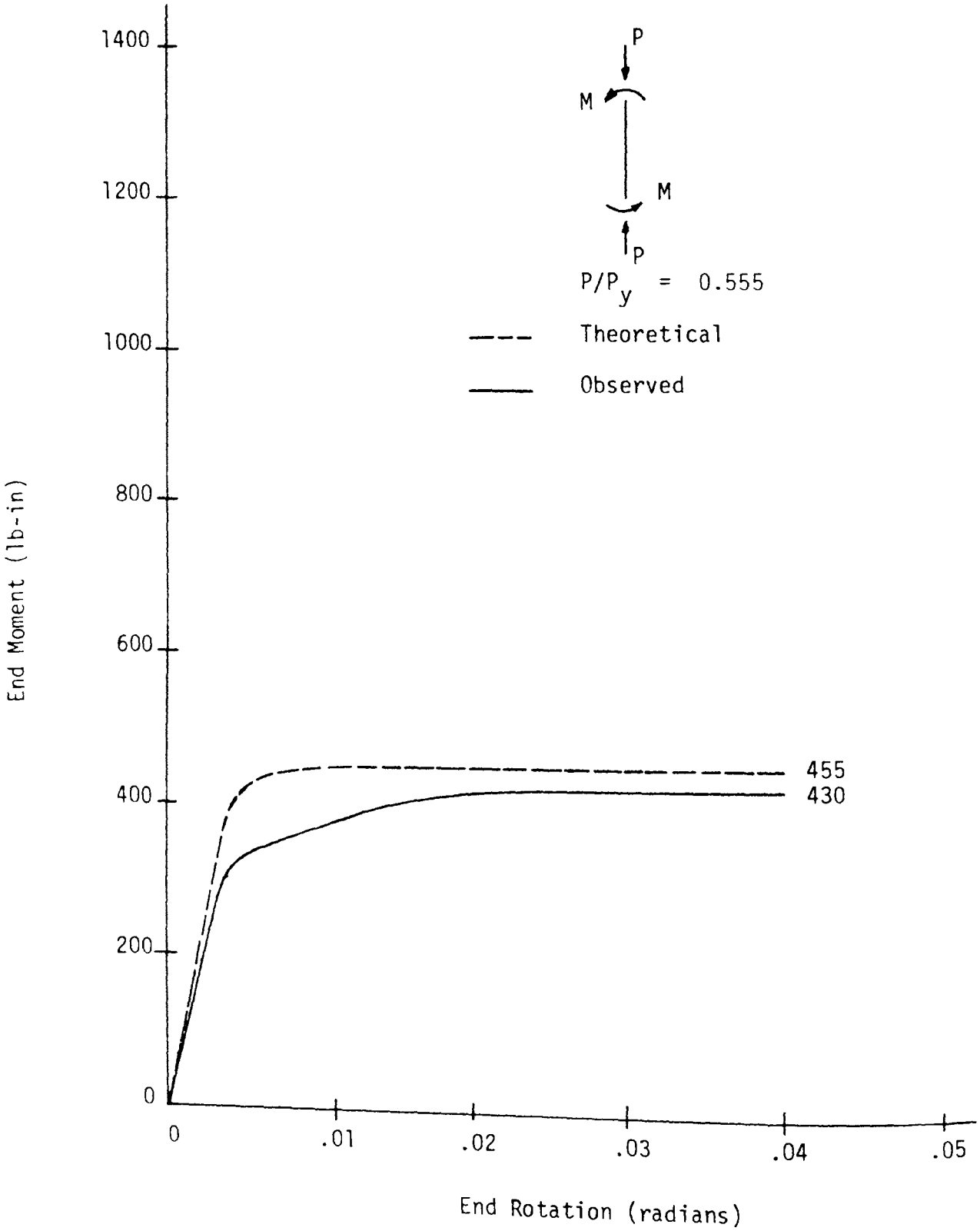

FIGURE D9–BEAM COLUMN 9 MOMENT vs. ROTATION

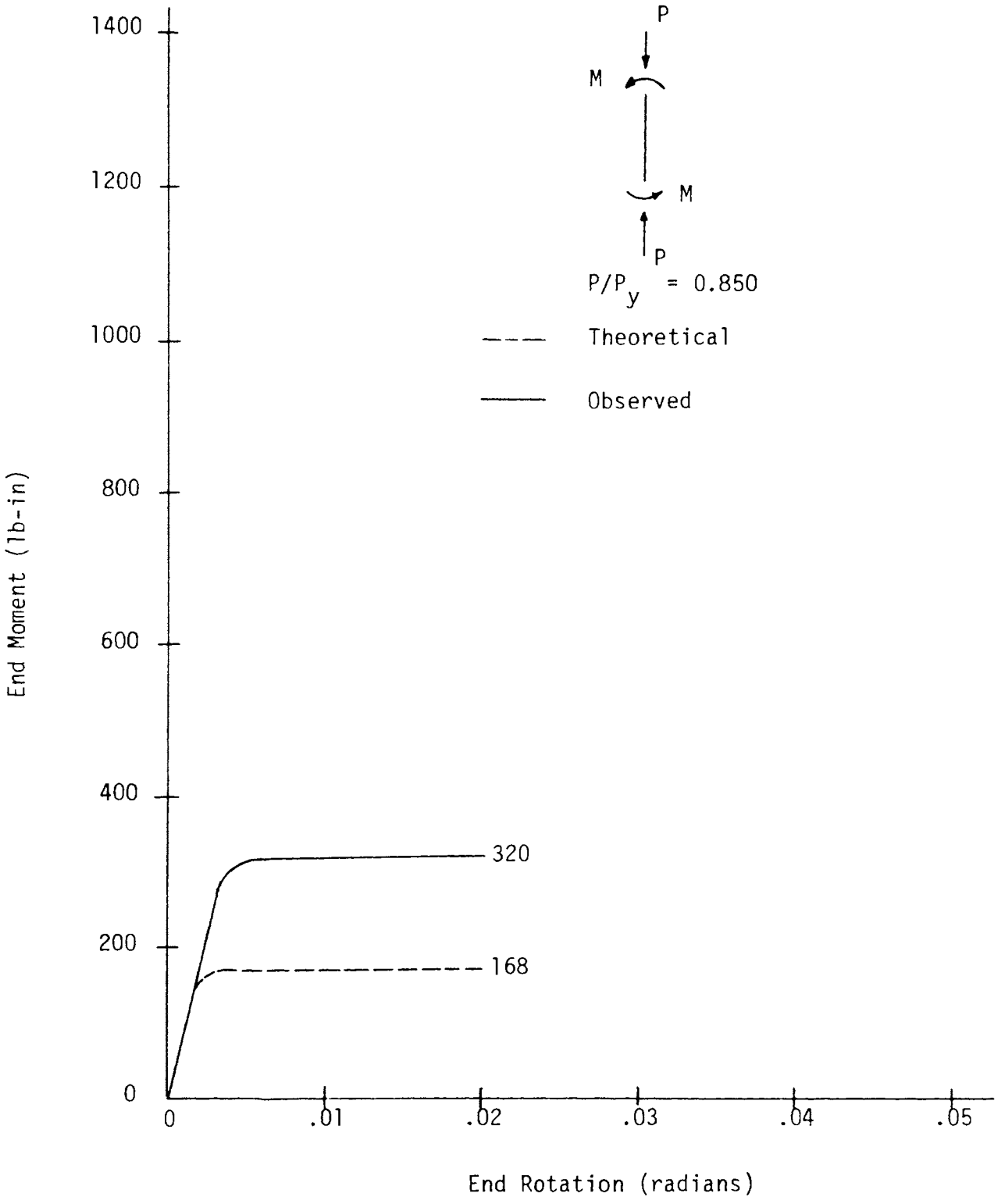

FIGURE D10–BEAM COLUMN 10 MOMENT vs. ROTATION

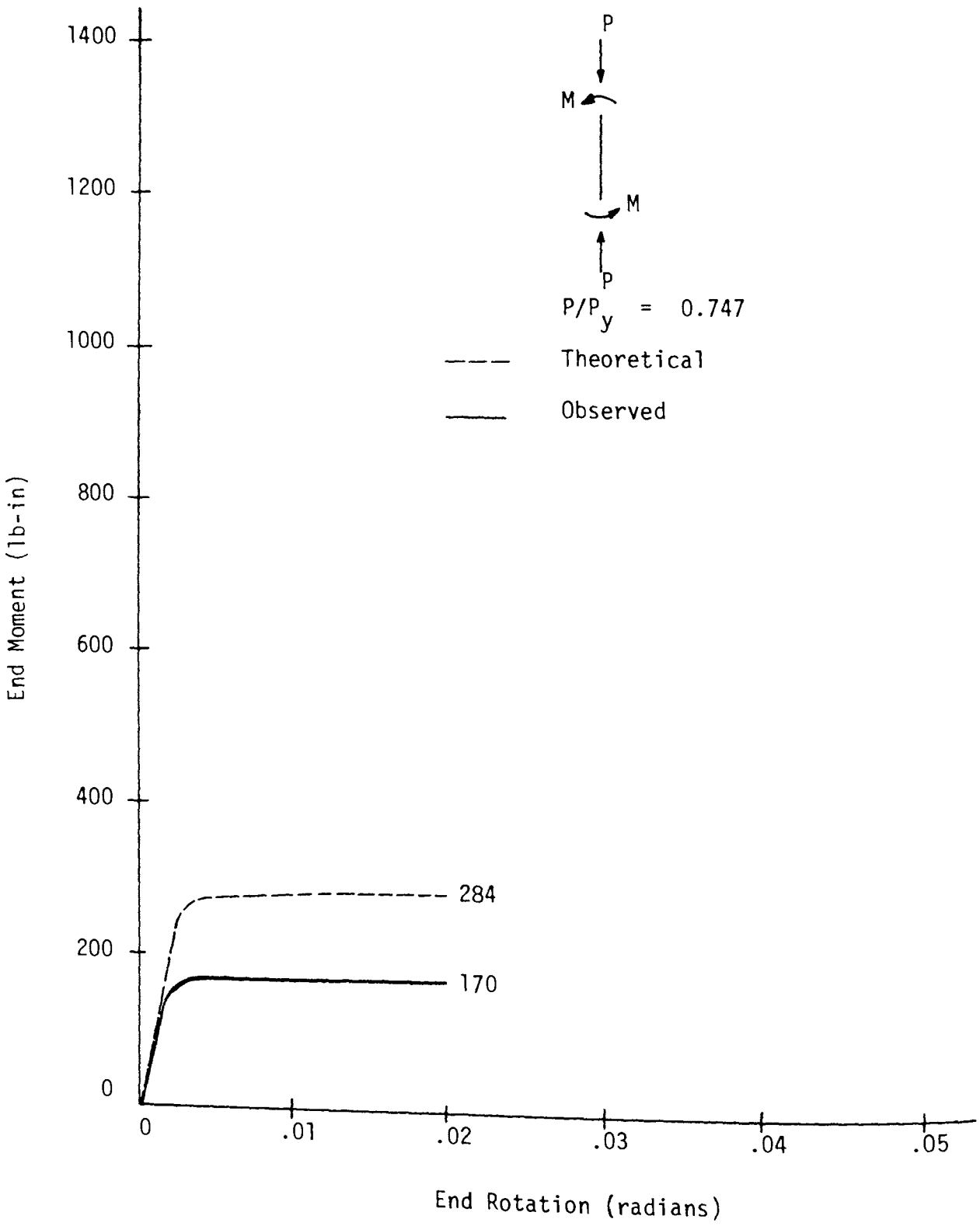

FIGURE D11–BEAM COLUMN 11 MOMENT vs. ROTATION

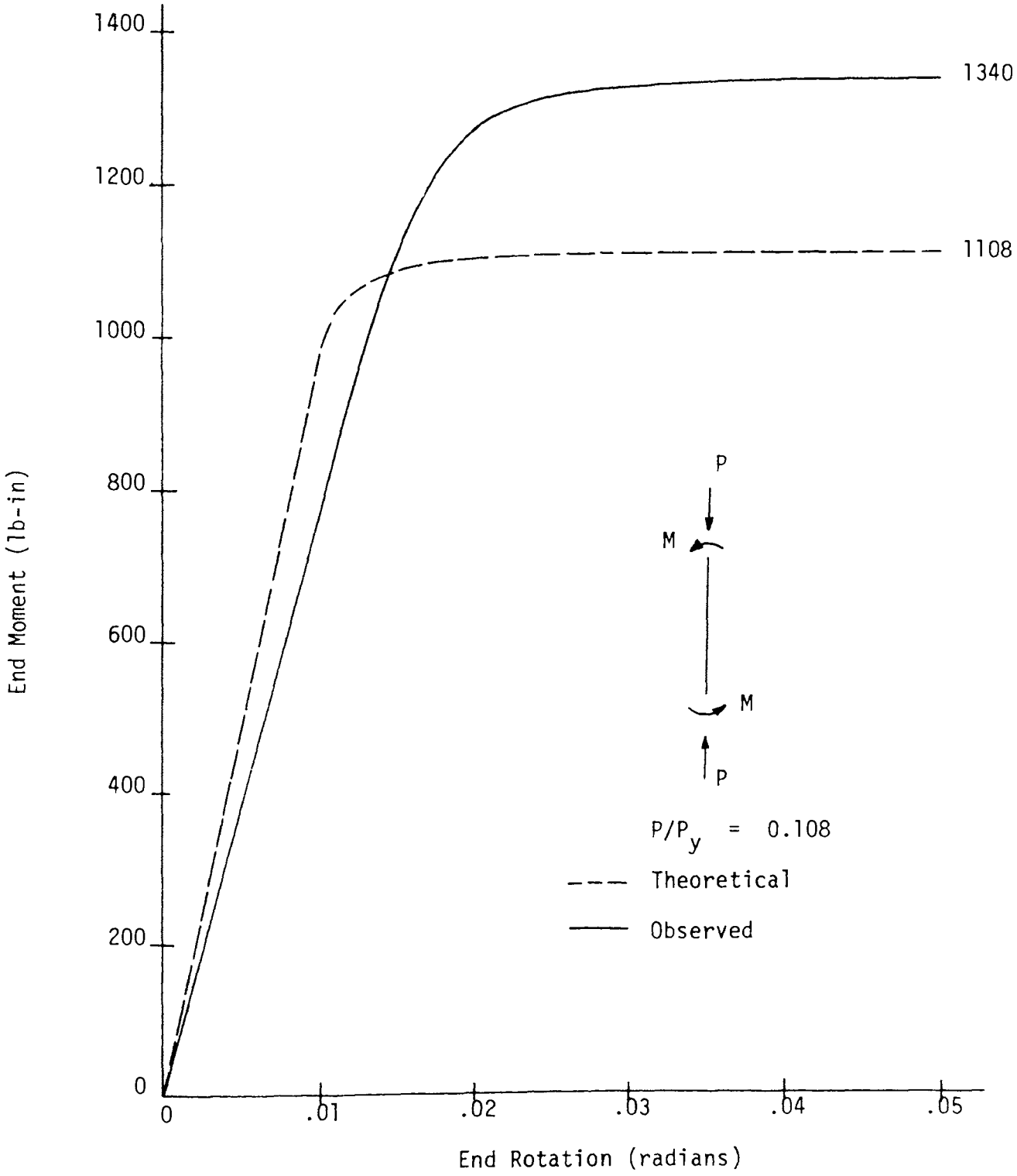

FIGURE D13–BEAM COLUMN 13 MOMENT vs. ROTATION

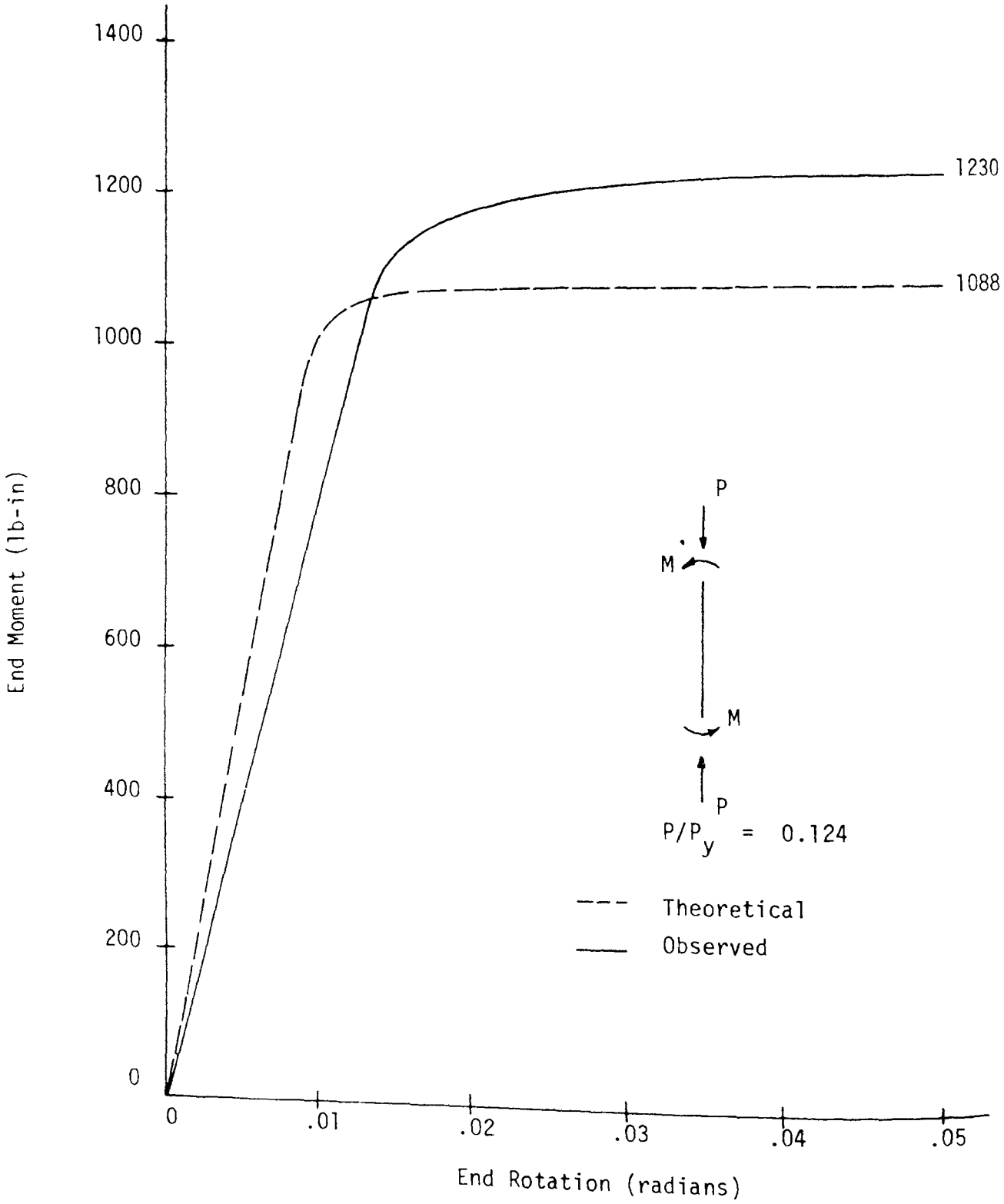

FIGURE D14—BEAM COLUMN 14 MOMENT vs. ROTATION

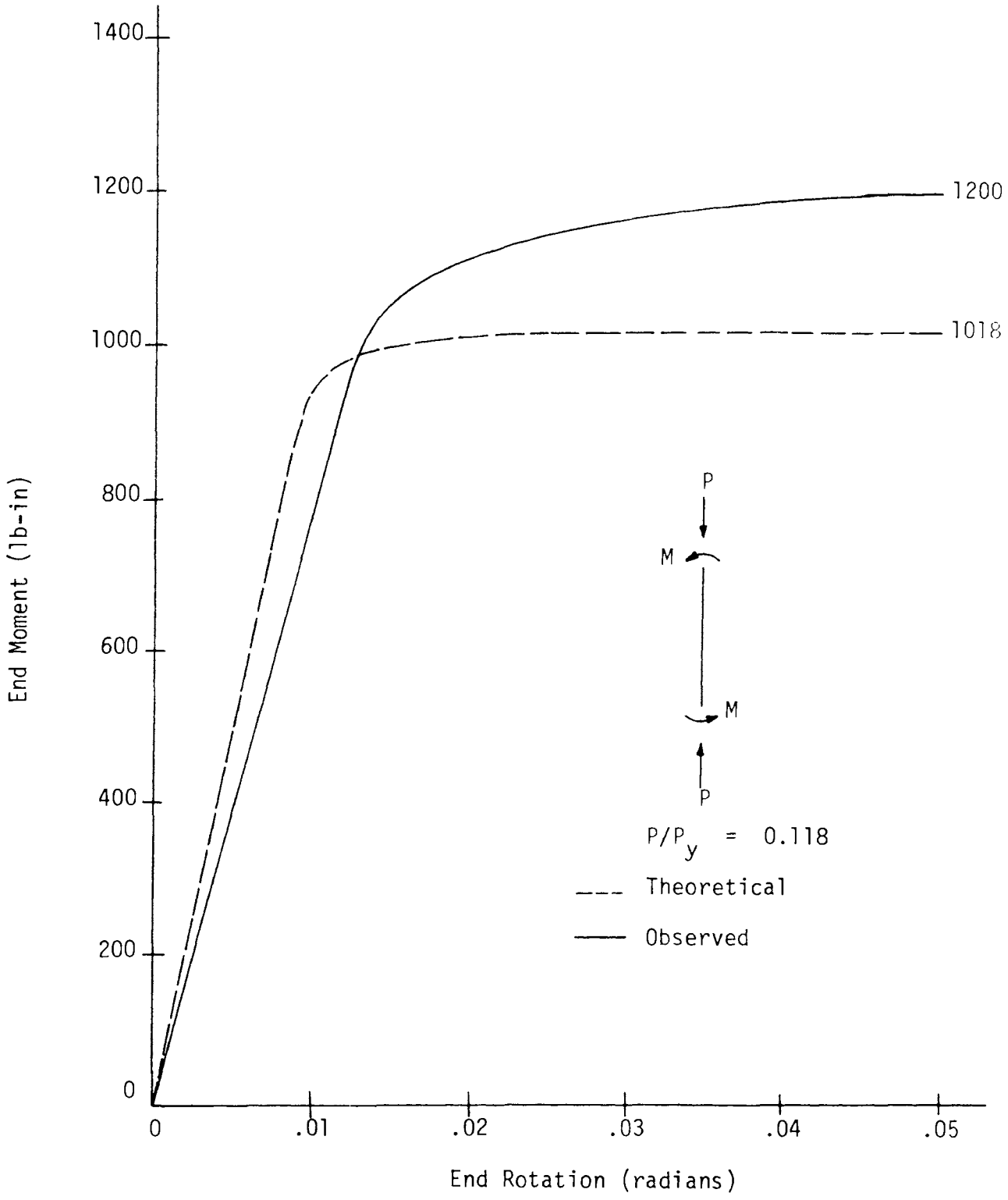

FIGURE D15—BEAM COLUMN 15 MOMENT vs. ROTATION

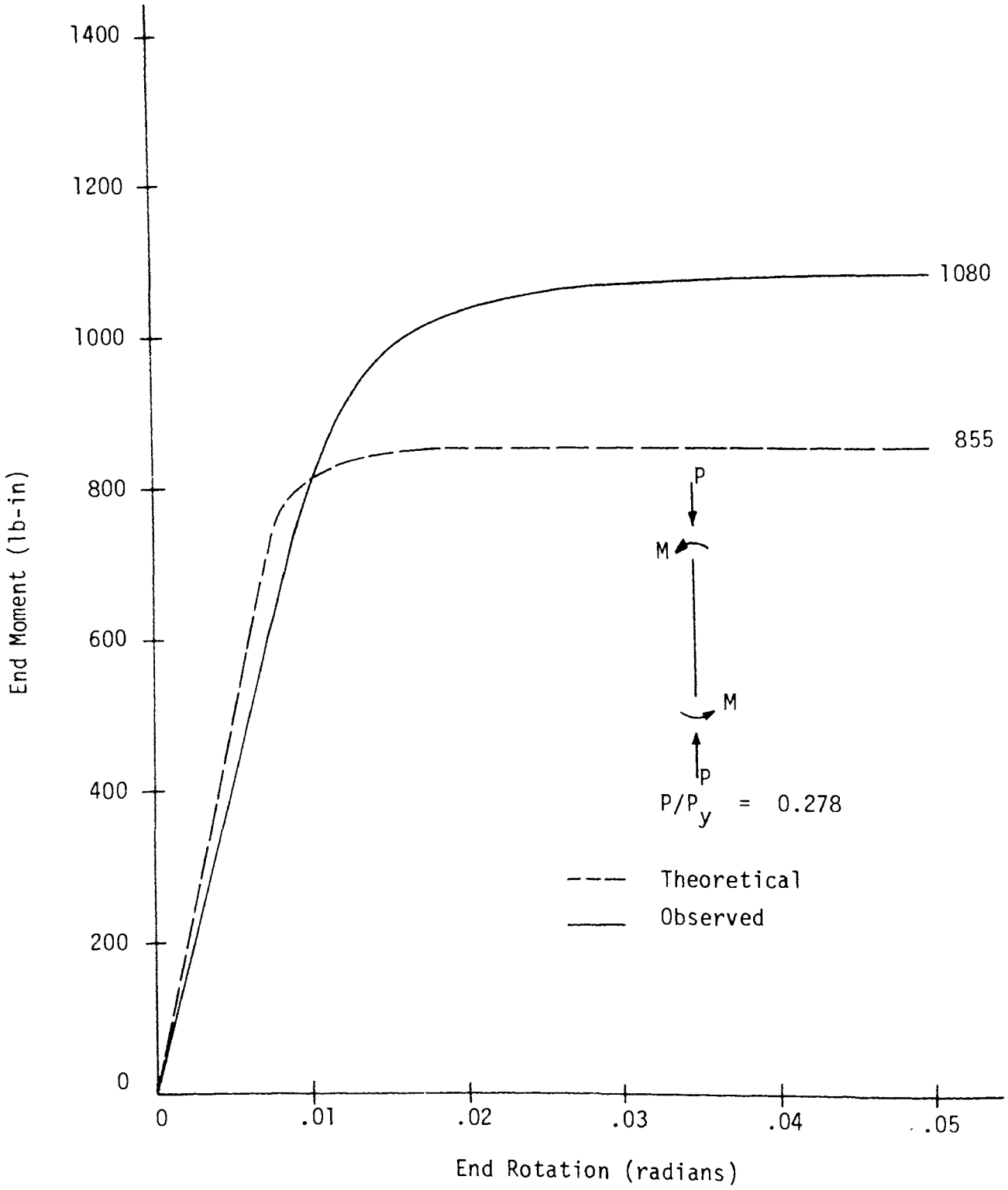

FIGURE D16–BEAM COLUMN 16 MOMENT vs. ROTATION

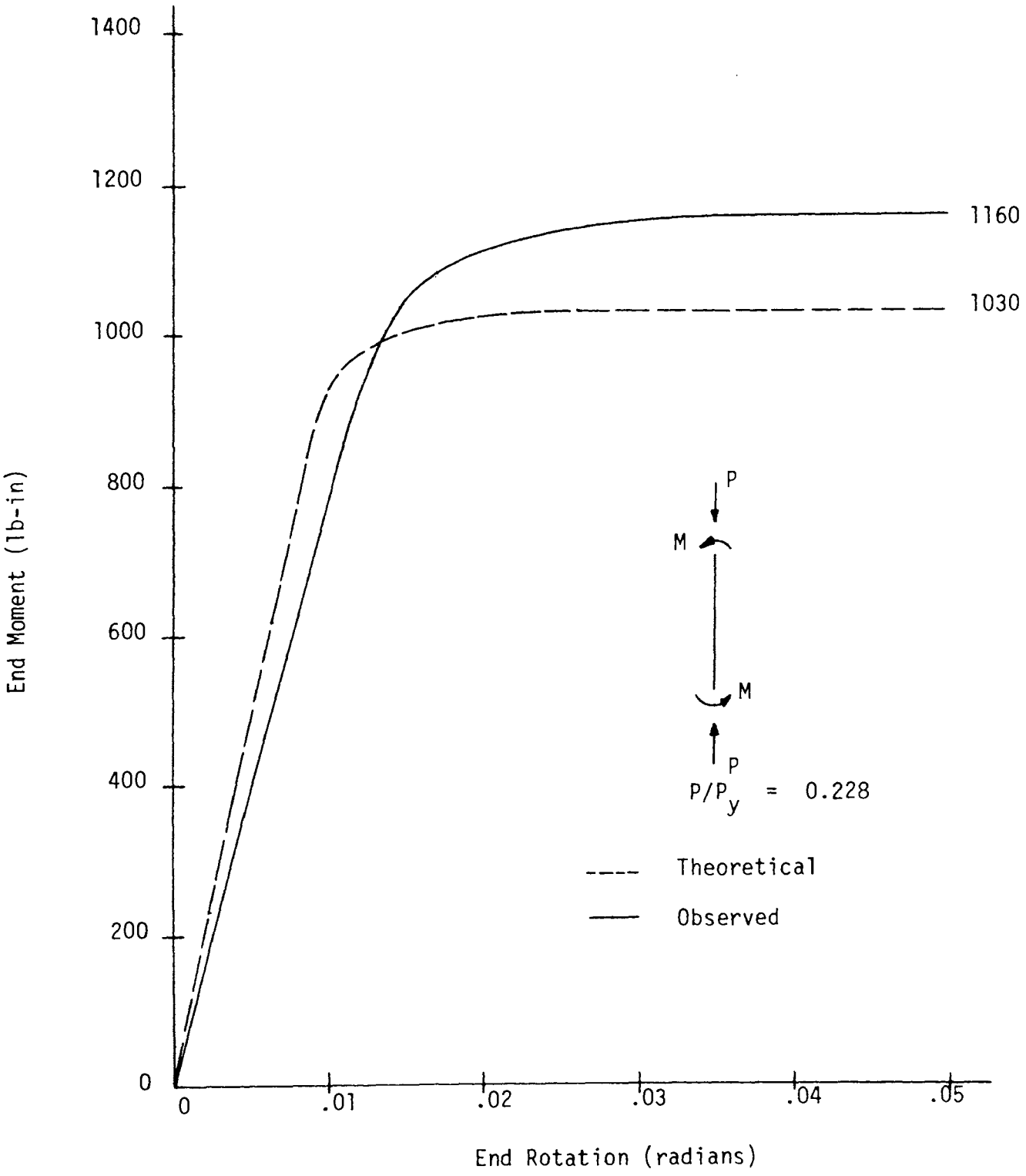

FIGURE D17—BEAM COLUMN 17 MOMENT vs. ROTATION

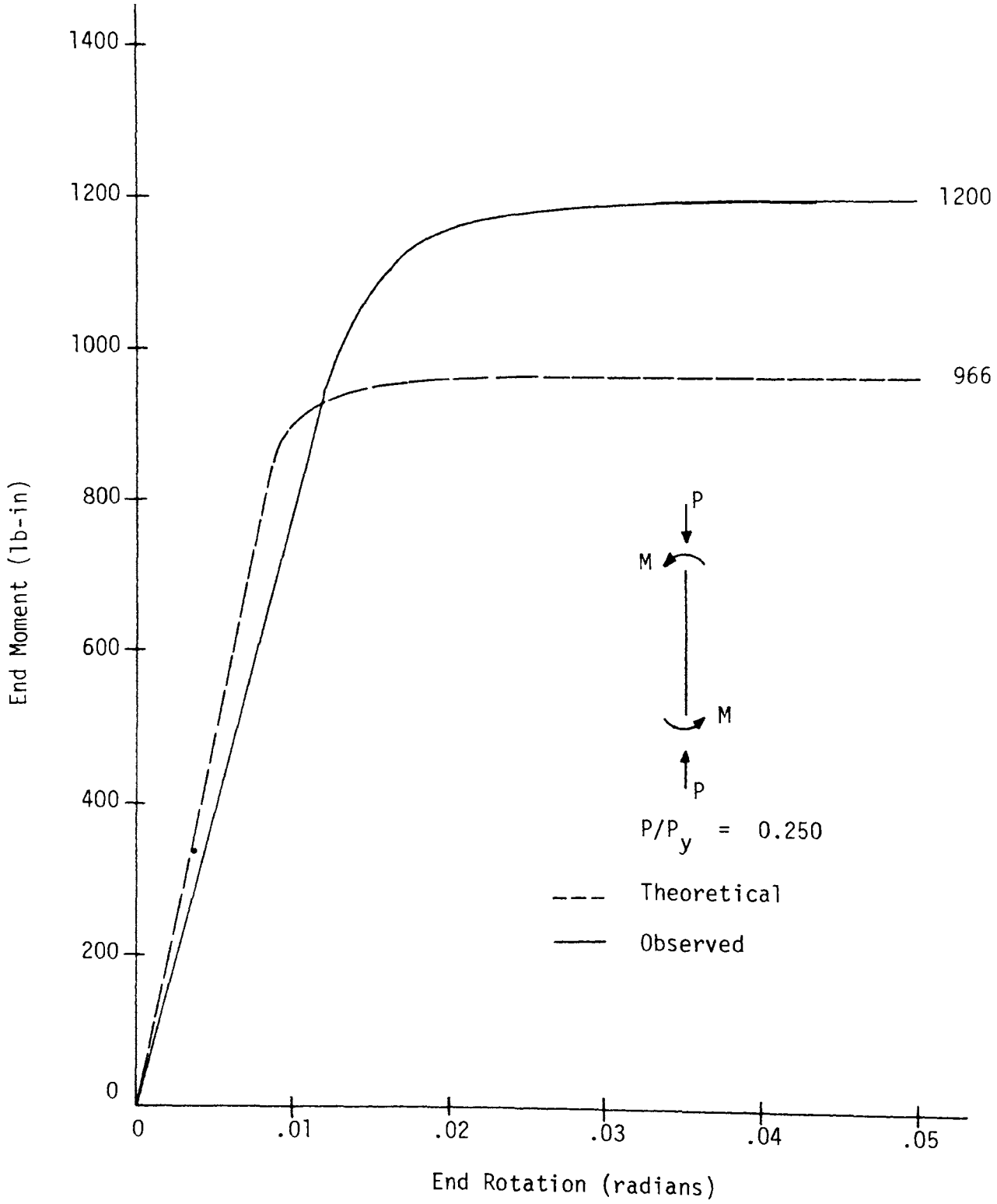

FIGURE D18—BEAM COLUMN 18 MOMENT vs. ROTATION

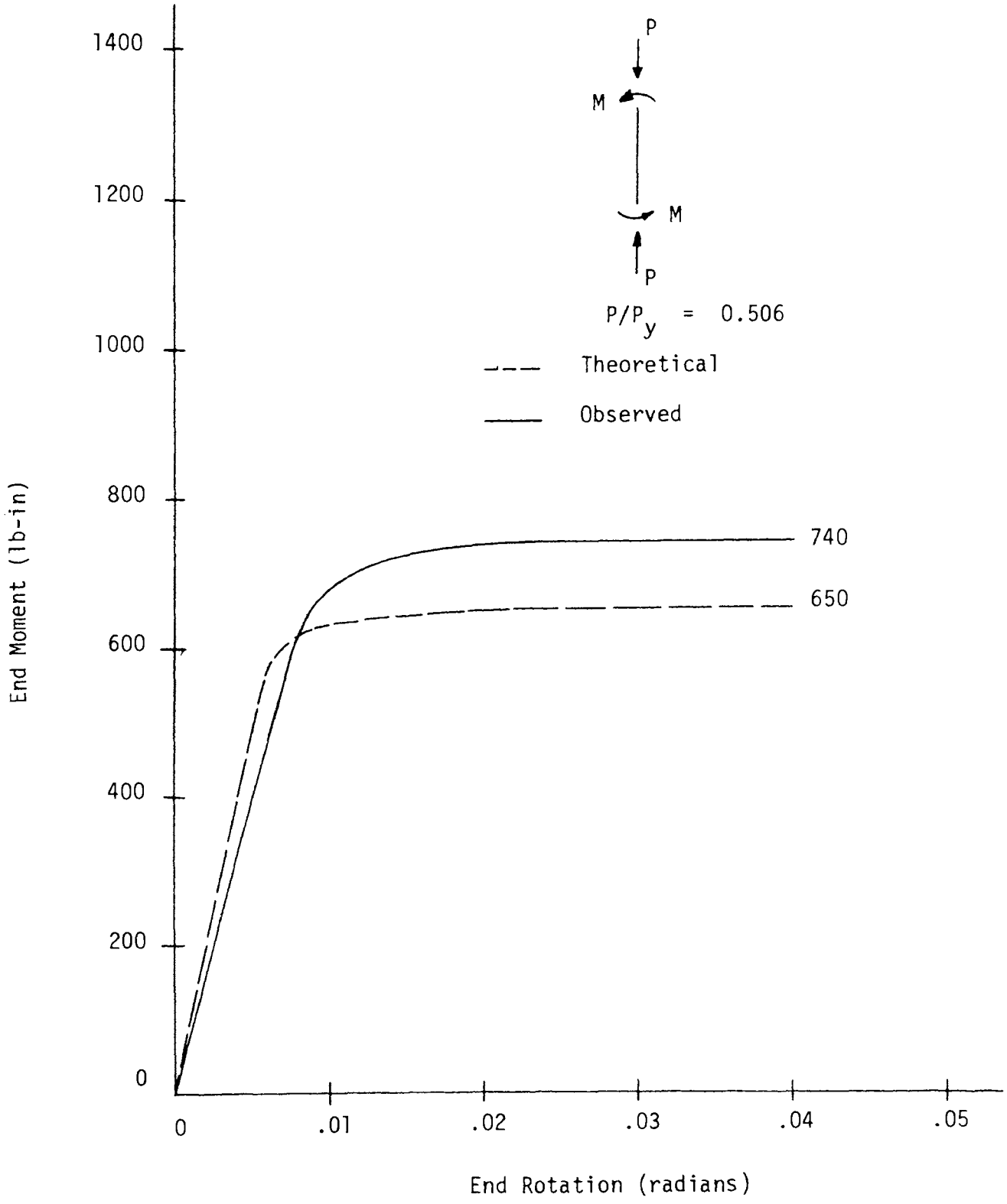

FIGURE D19–BEAM COLUMN 19 MOMENT vs. ROTATION

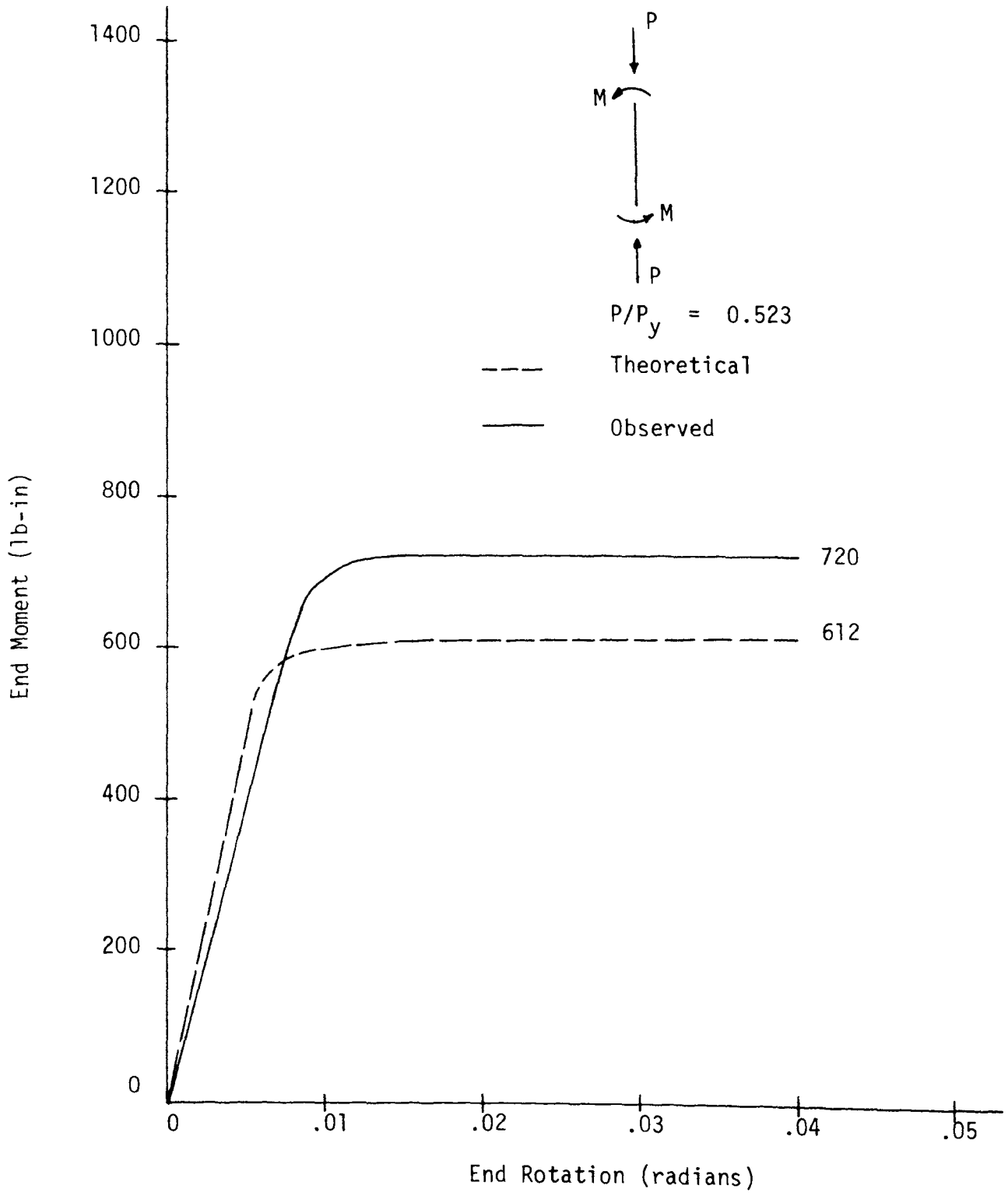

FIGURE D20–BEAM COLUMN 20 MOMENT vs. ROTATION

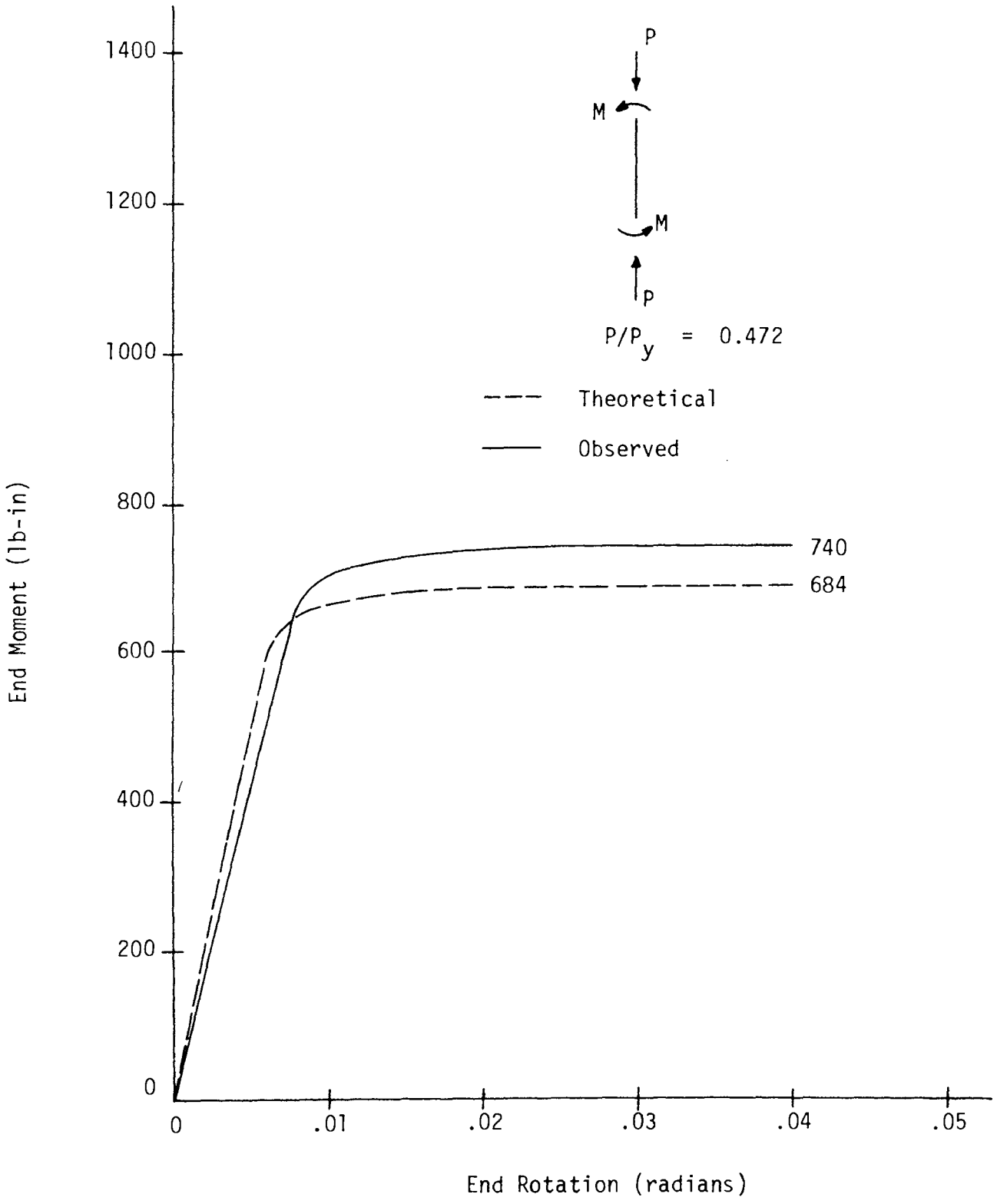

FIGURE D21–BEAM COLUMN 21 MOMENT vs. ROTATION

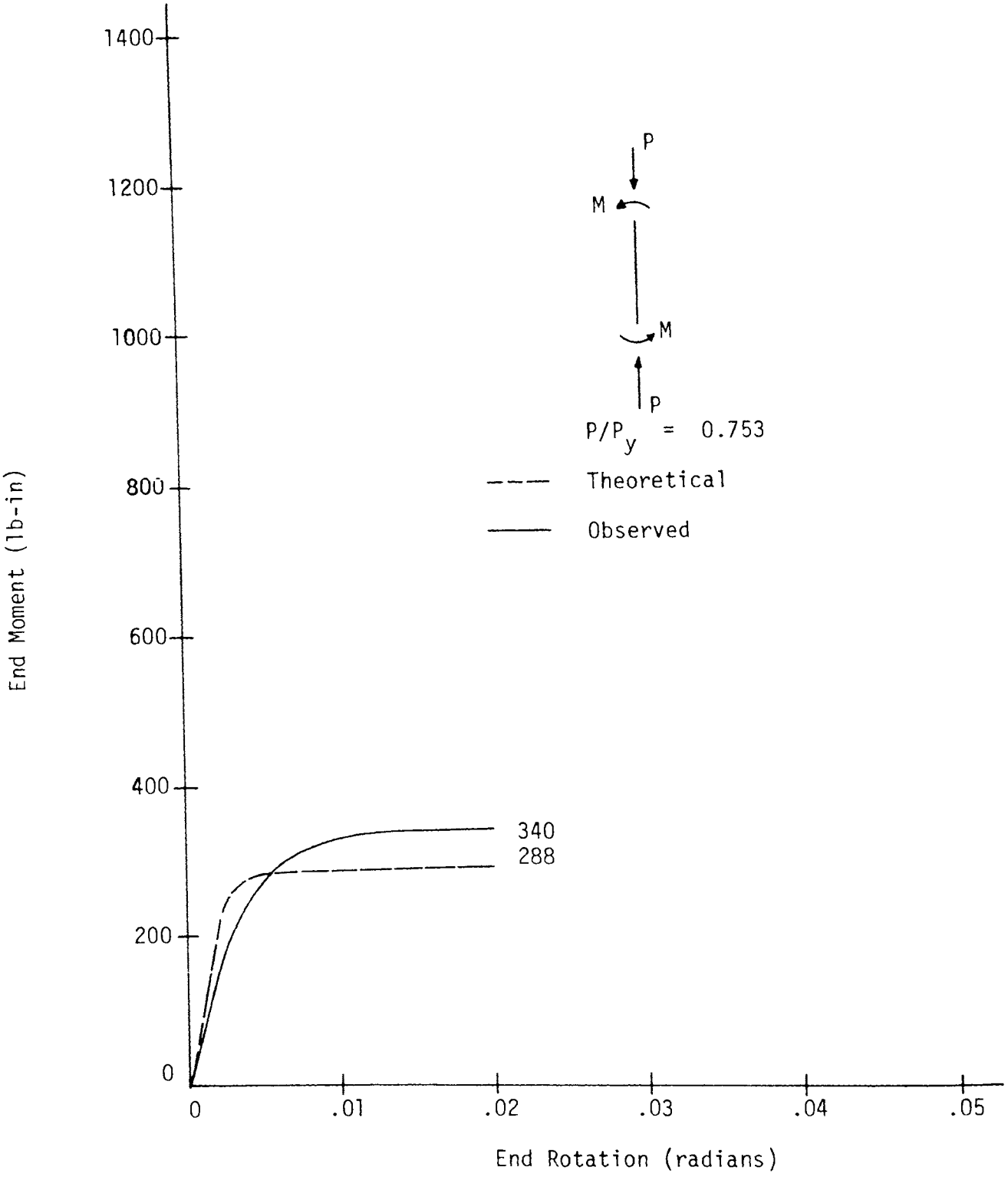

FIGURE D22—BEAM COLUMN 22 MOMENT vs. ROTATION

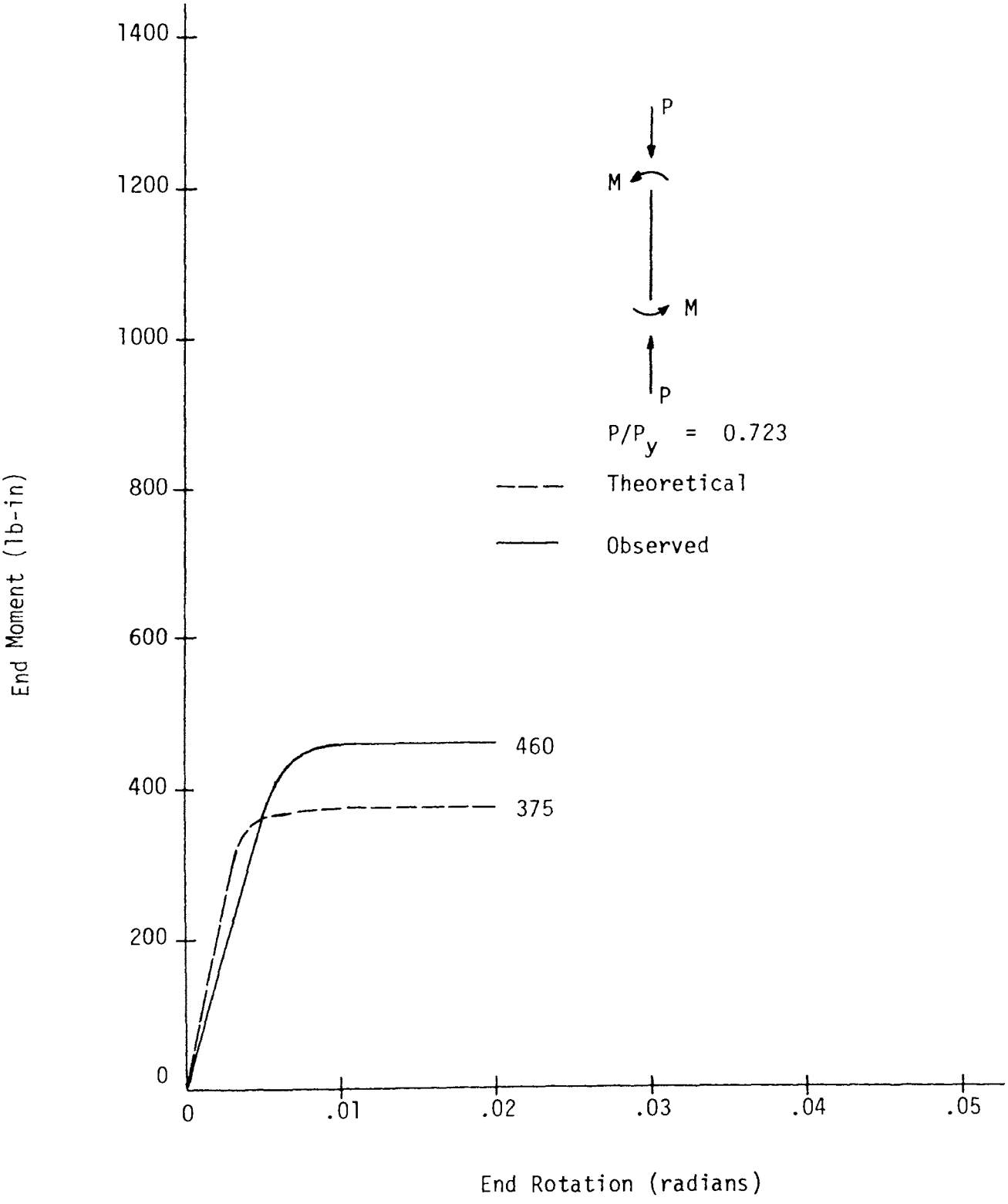

FIGURE D23–BEAM COLUMN 23 MOMENT vs. ROTATION

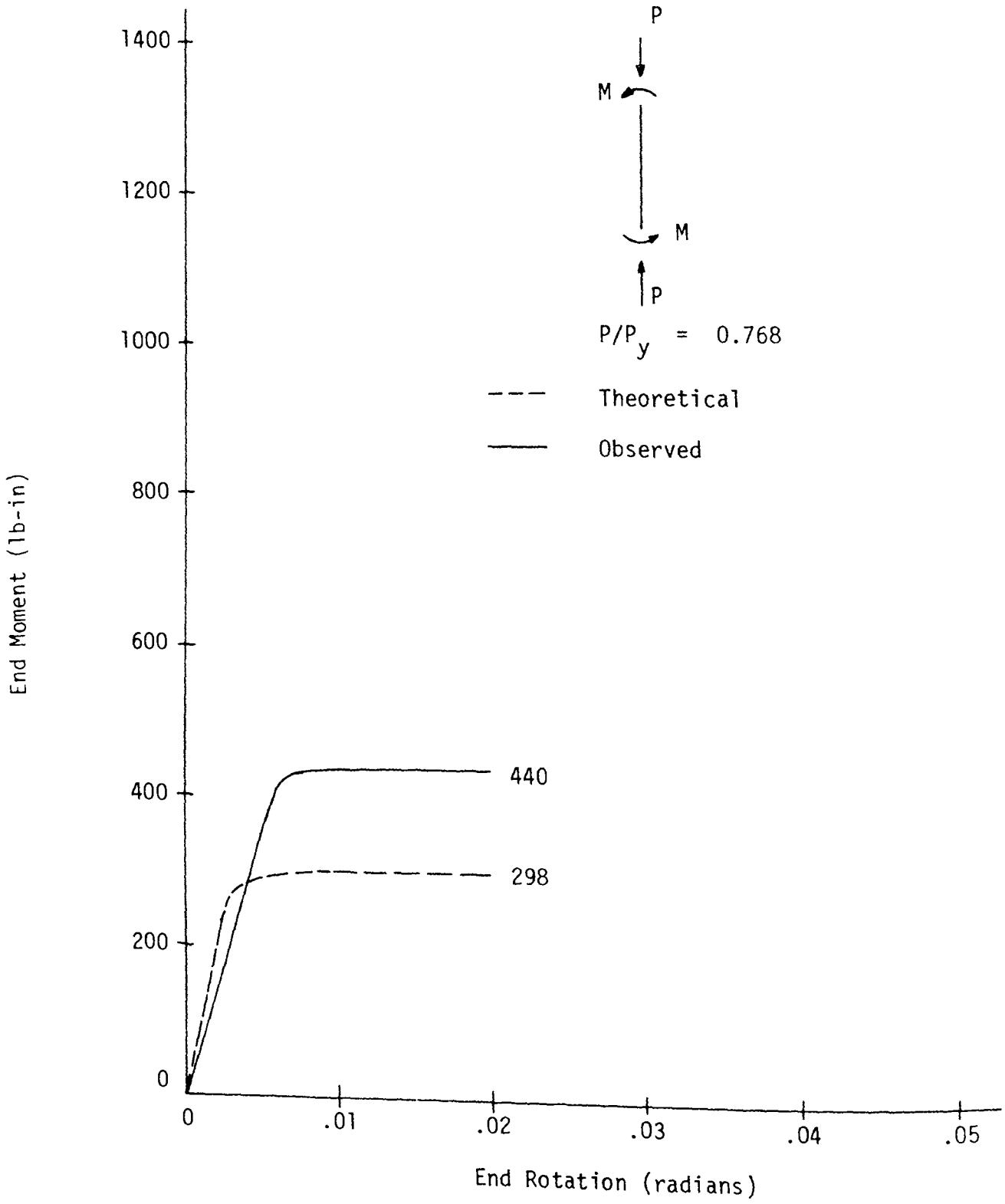

FIGURE D24—BEAM COLUMN 24 MOMENT vs. ROTATION

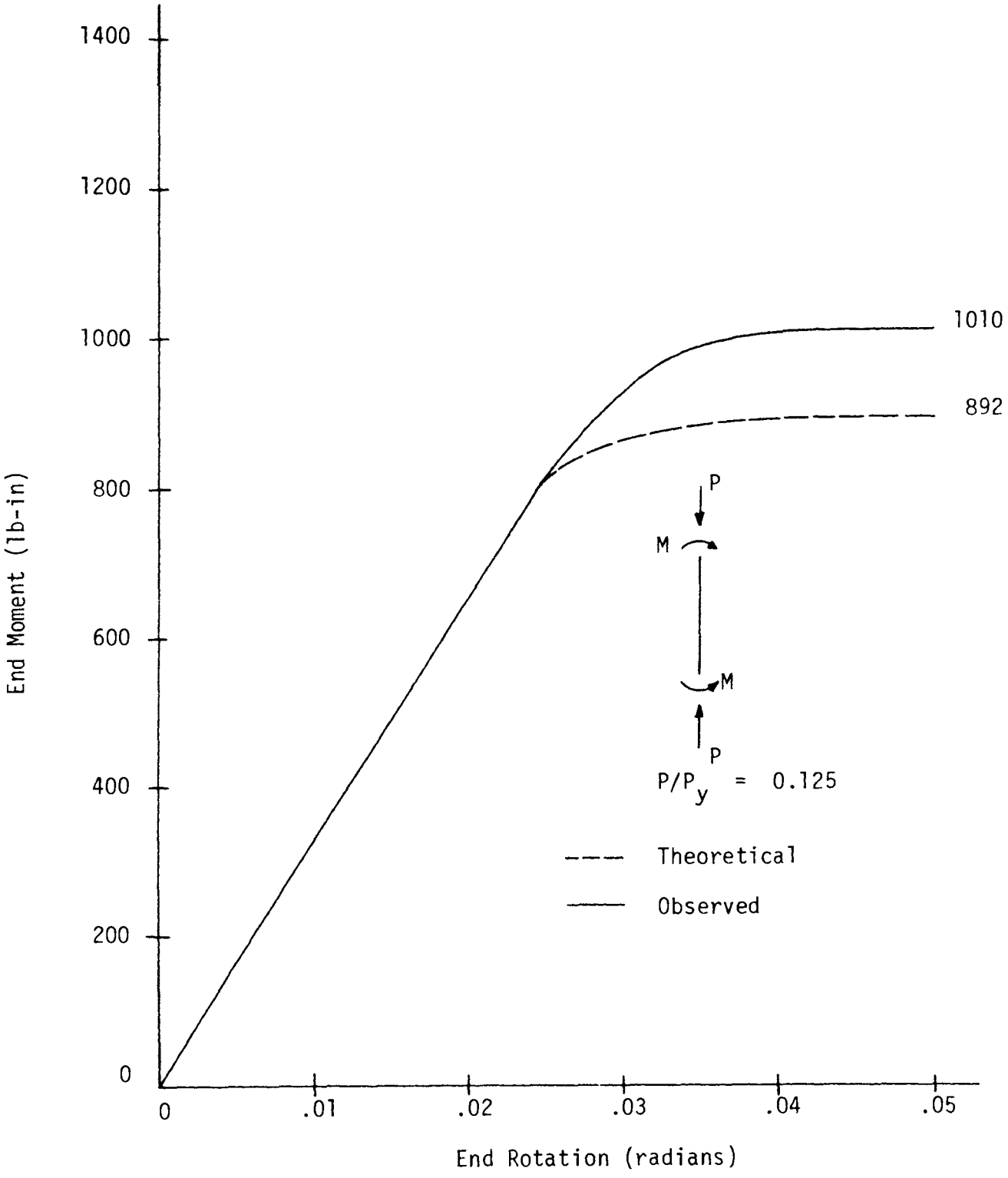

FIGURE D25–BEAM COLUMN 25 MOMENT vs. ROTATION

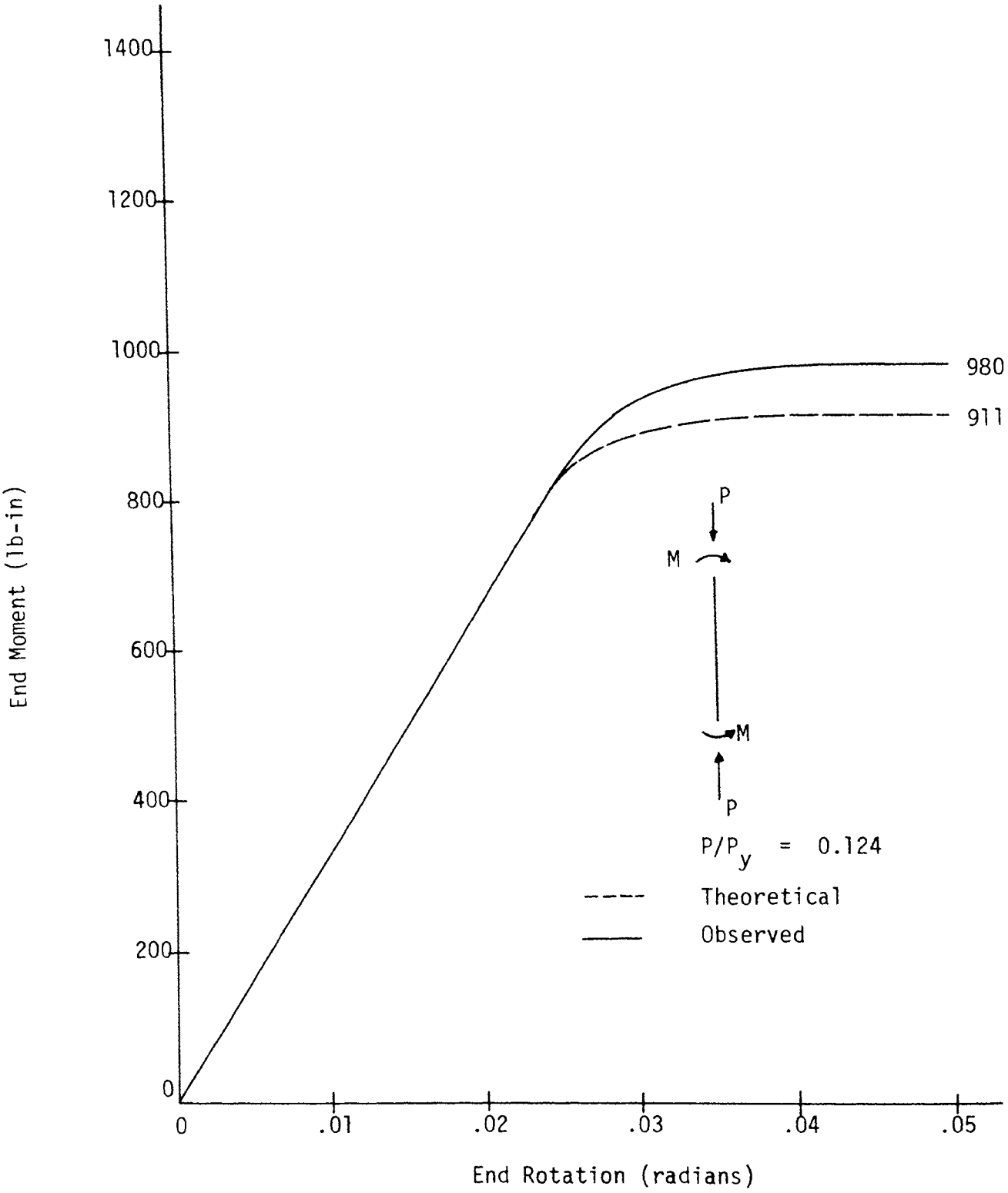

FIGURE D26–BEAM COLUMN 26 MOMENT vs. ROTATION

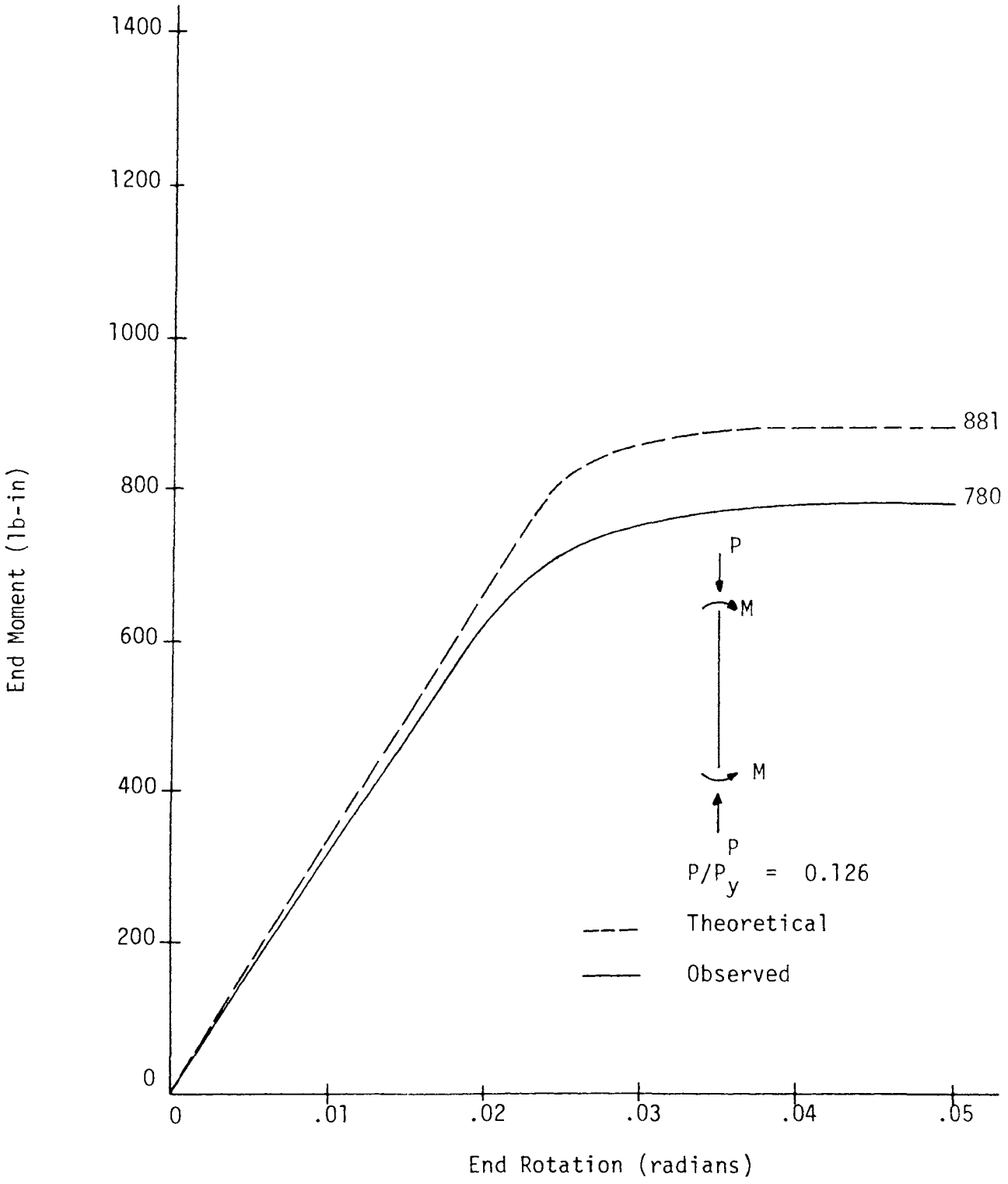

FIGURE D27–BEAM COLUMN 27 MOMENT vs. ROTATION

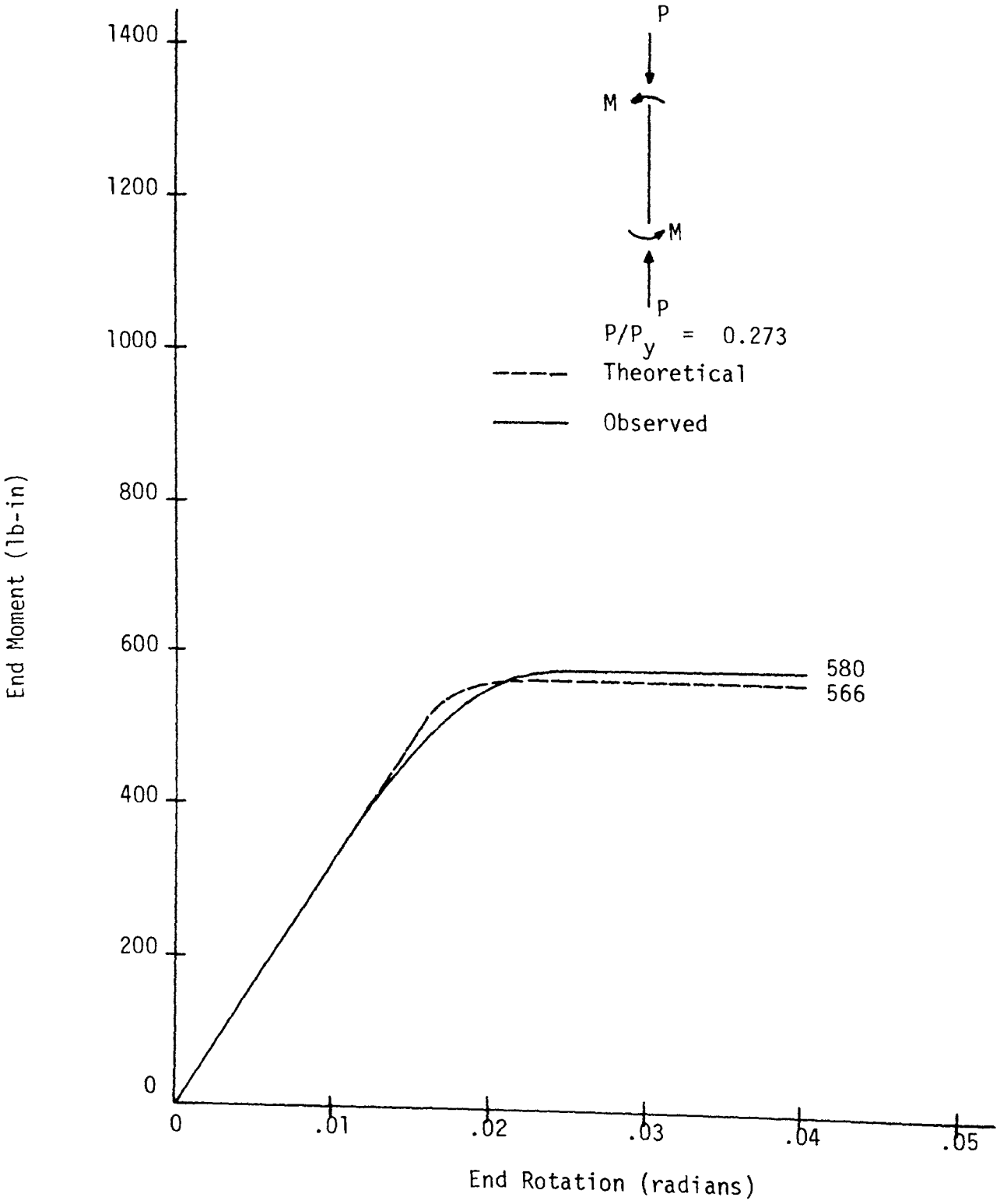

FIGURE D28—BEAM COLUMN 28 MOMENT vs. ROTATION

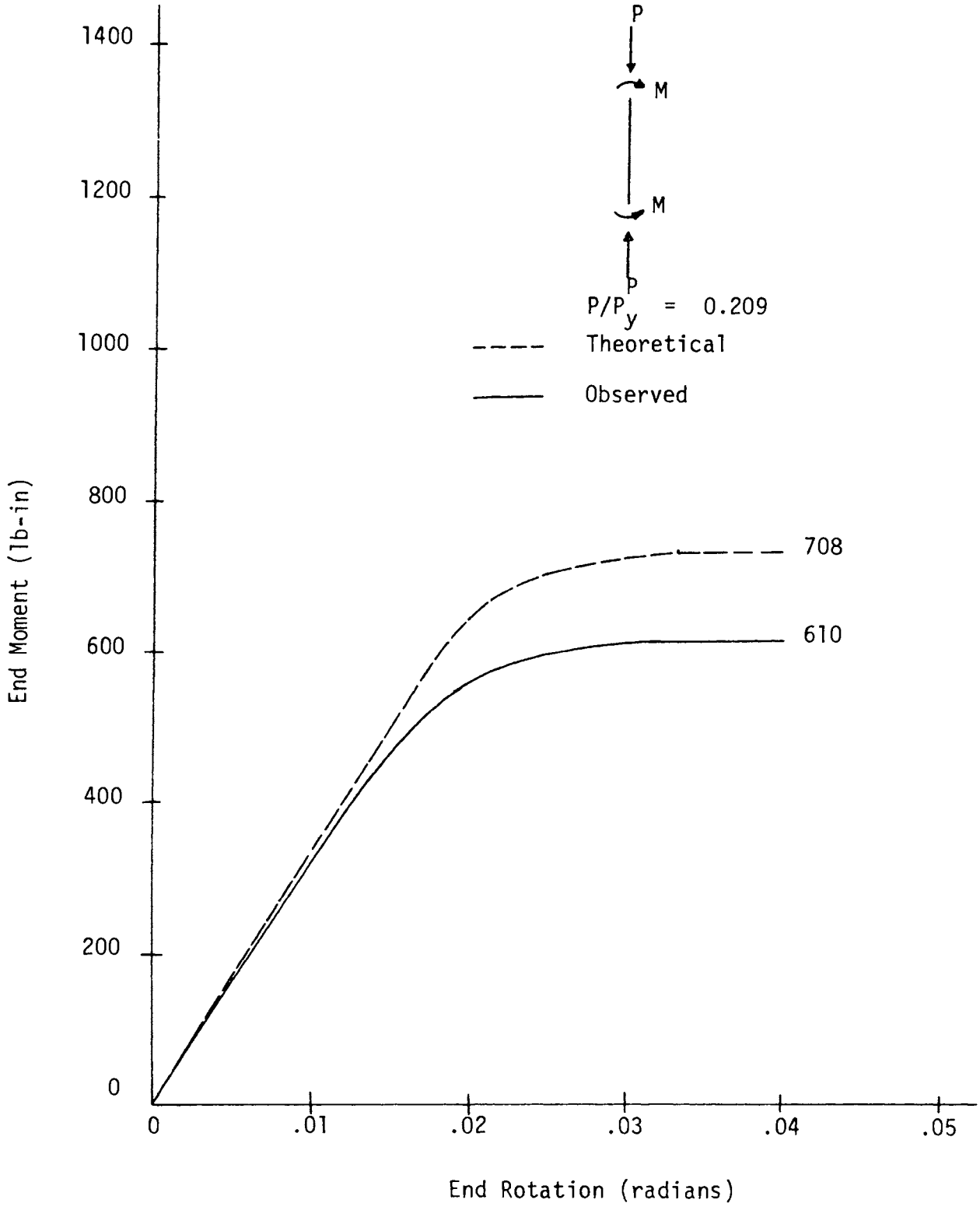

FIGURE D29–BEAM COLUMN 29 MOMENT vs. ROTATION

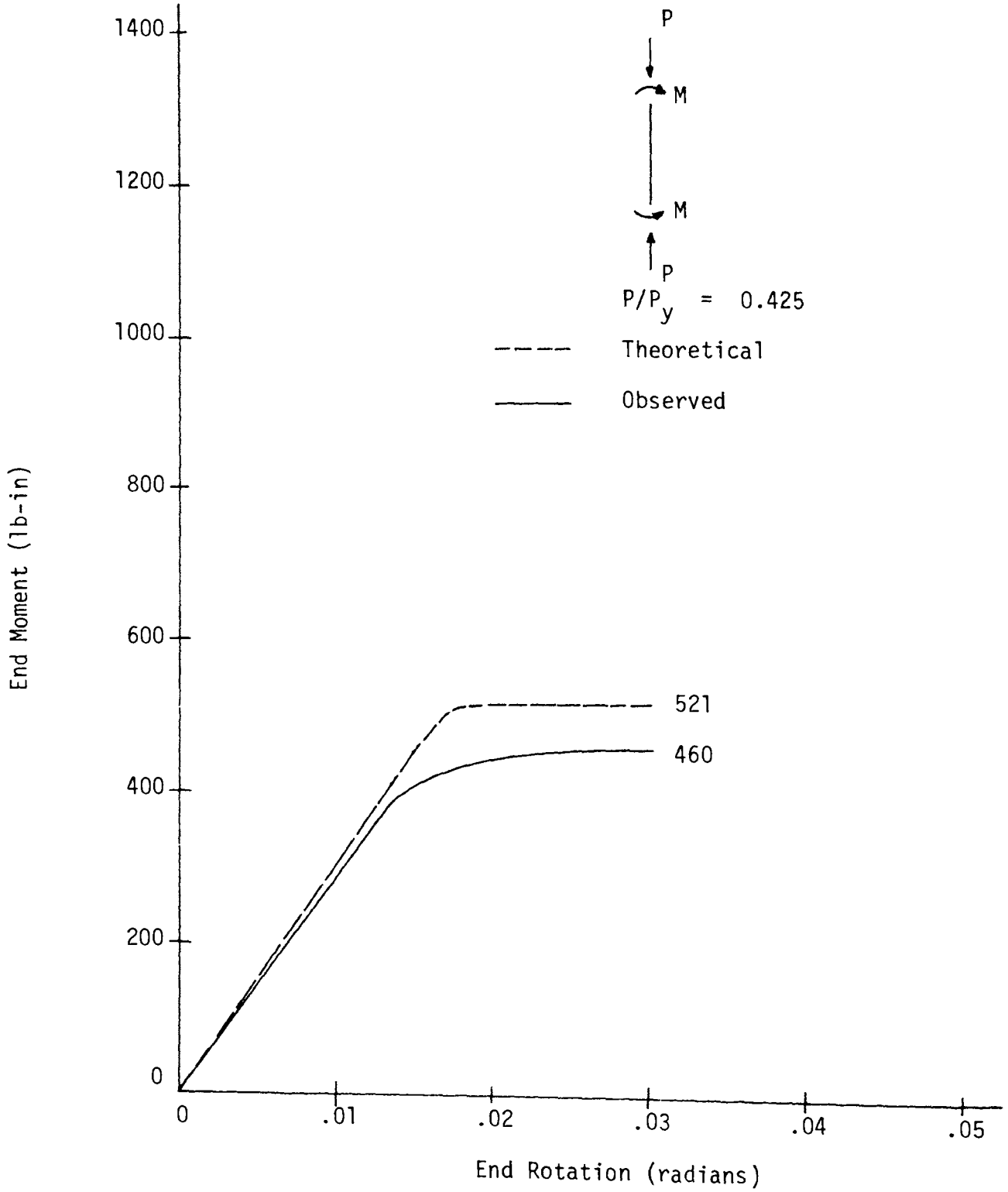

FIGURE D31–BEAM COLUMN 31 MOMENT vs. ROTATION

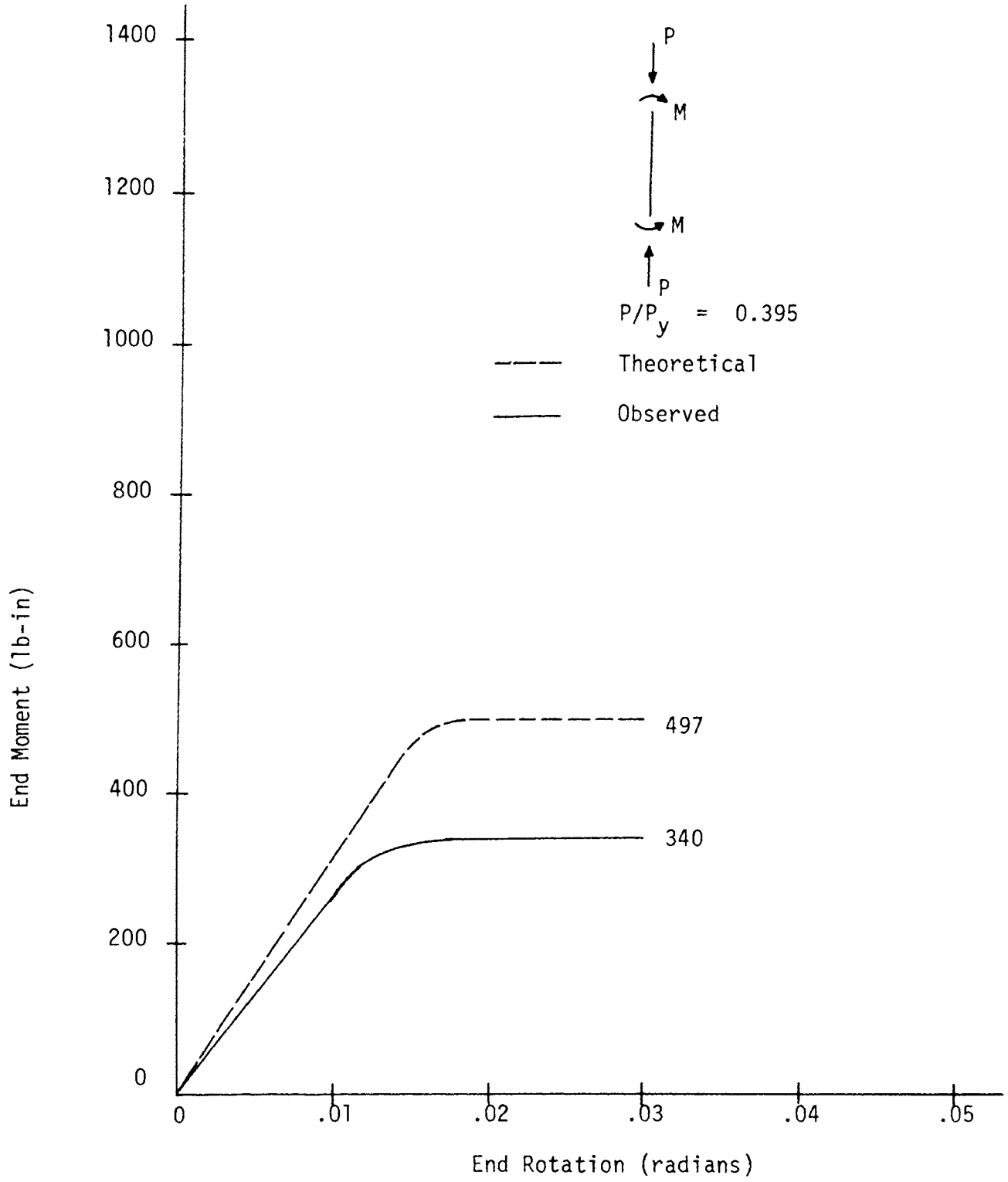

FIGURE D33—BEAM COLUMN 33 MOMENT vs. ROTATION

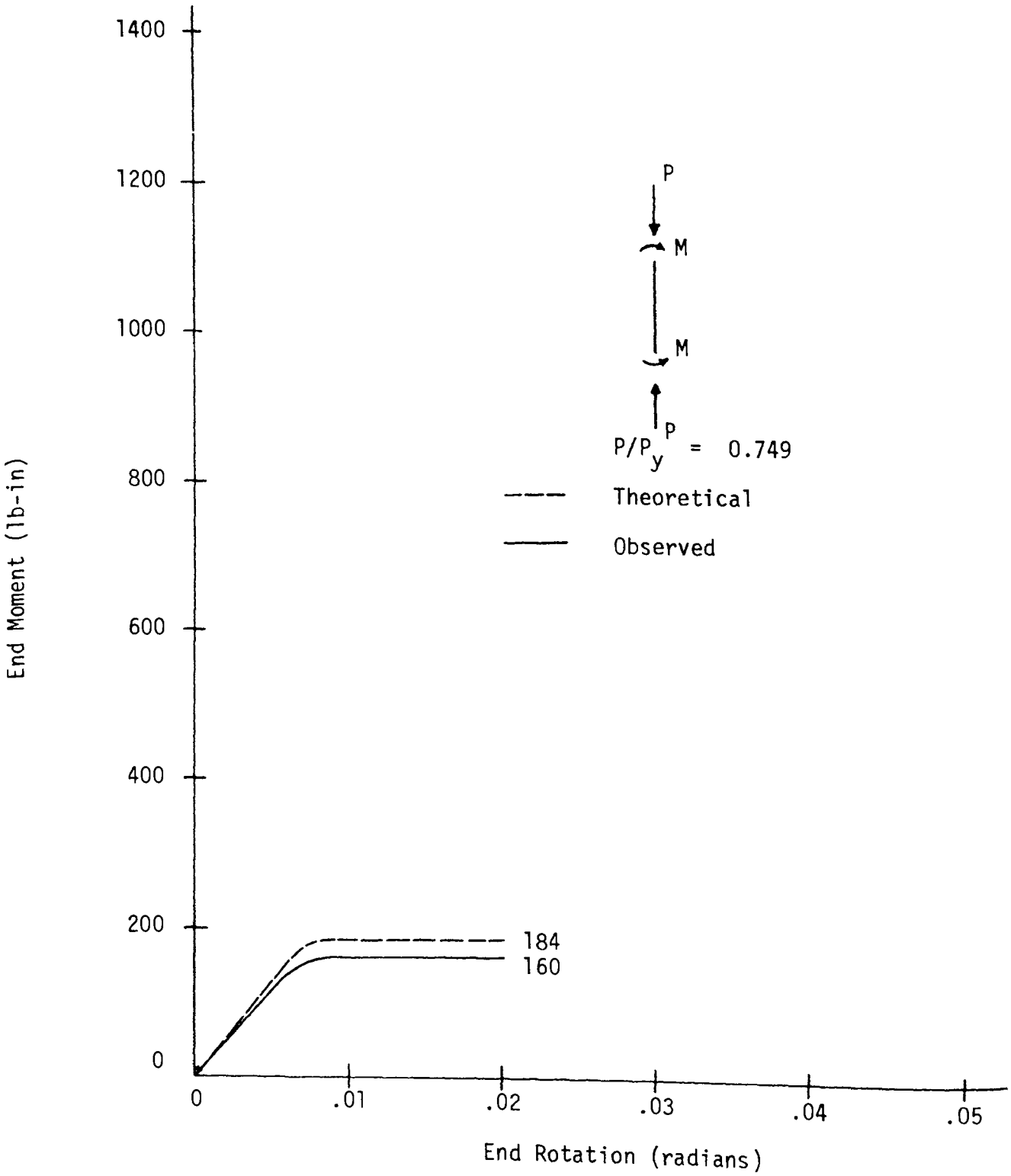

FIGURE D34—BEAM COLUMN 34 MOMENT vs. ROTATION

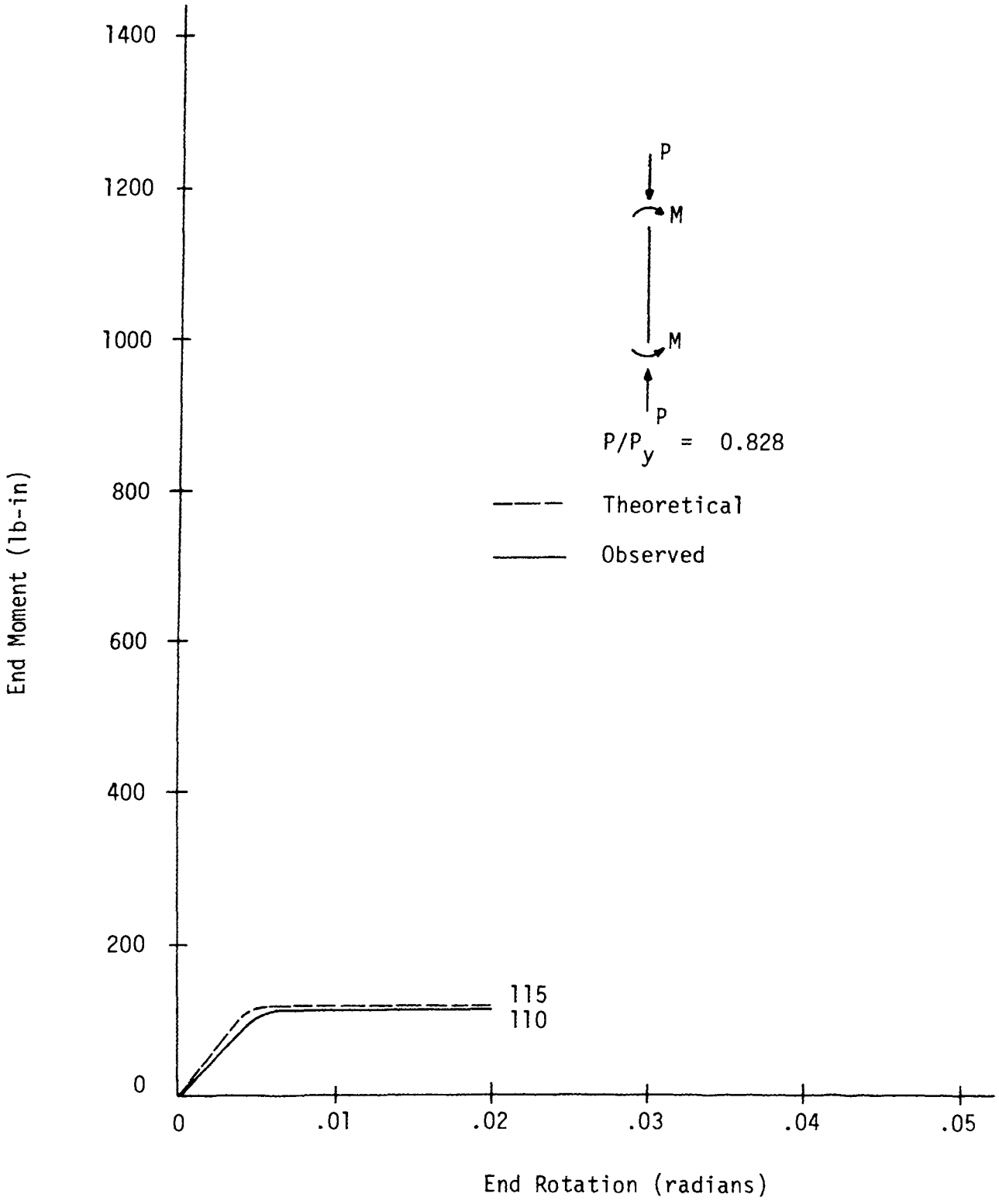

FIGURE D35–BEAM COLUMN 35 MOMENT vs. ROTATION

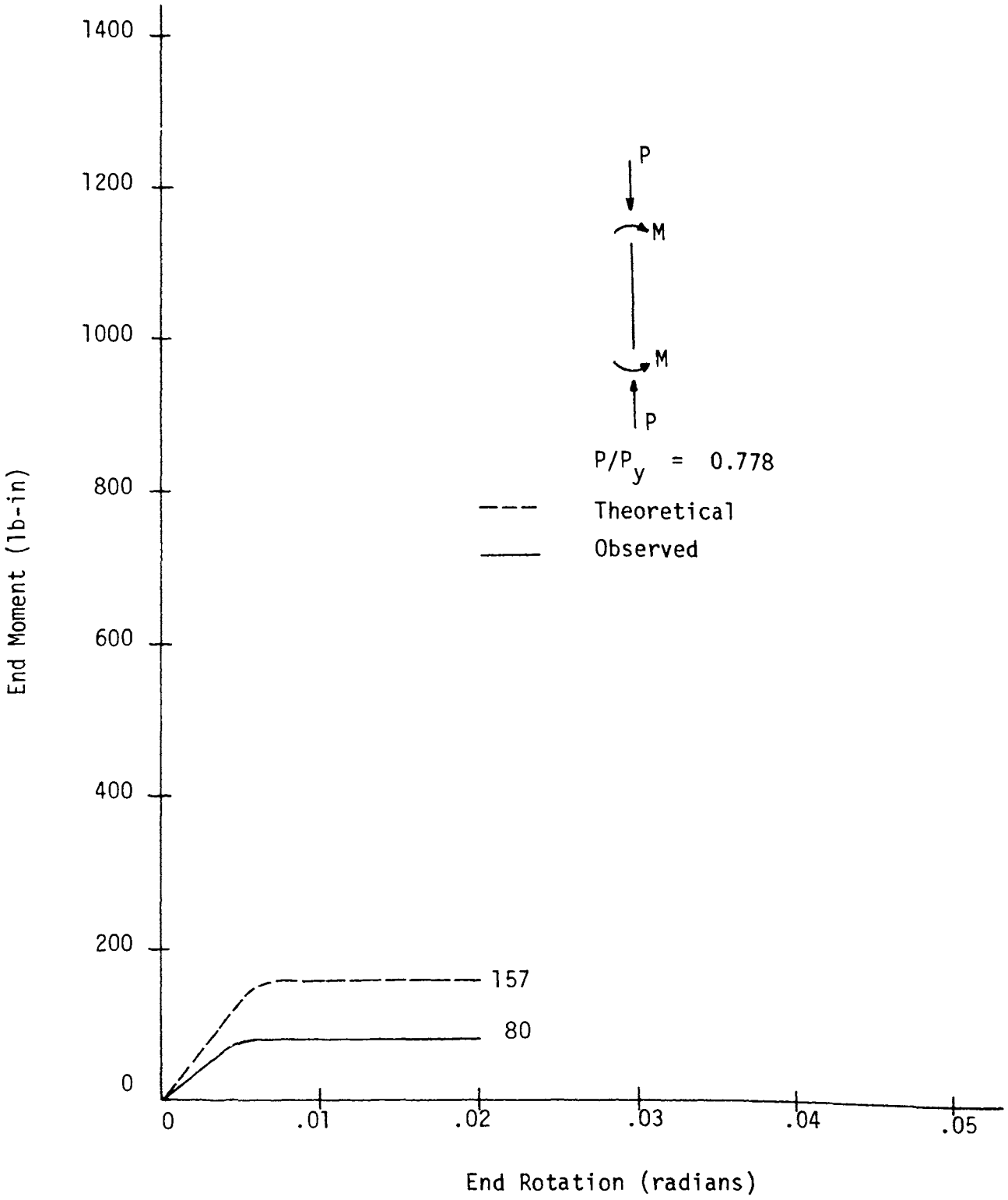

FIGURE D36–BEAM COLUMN 36 MOMENT vs. ROTATION

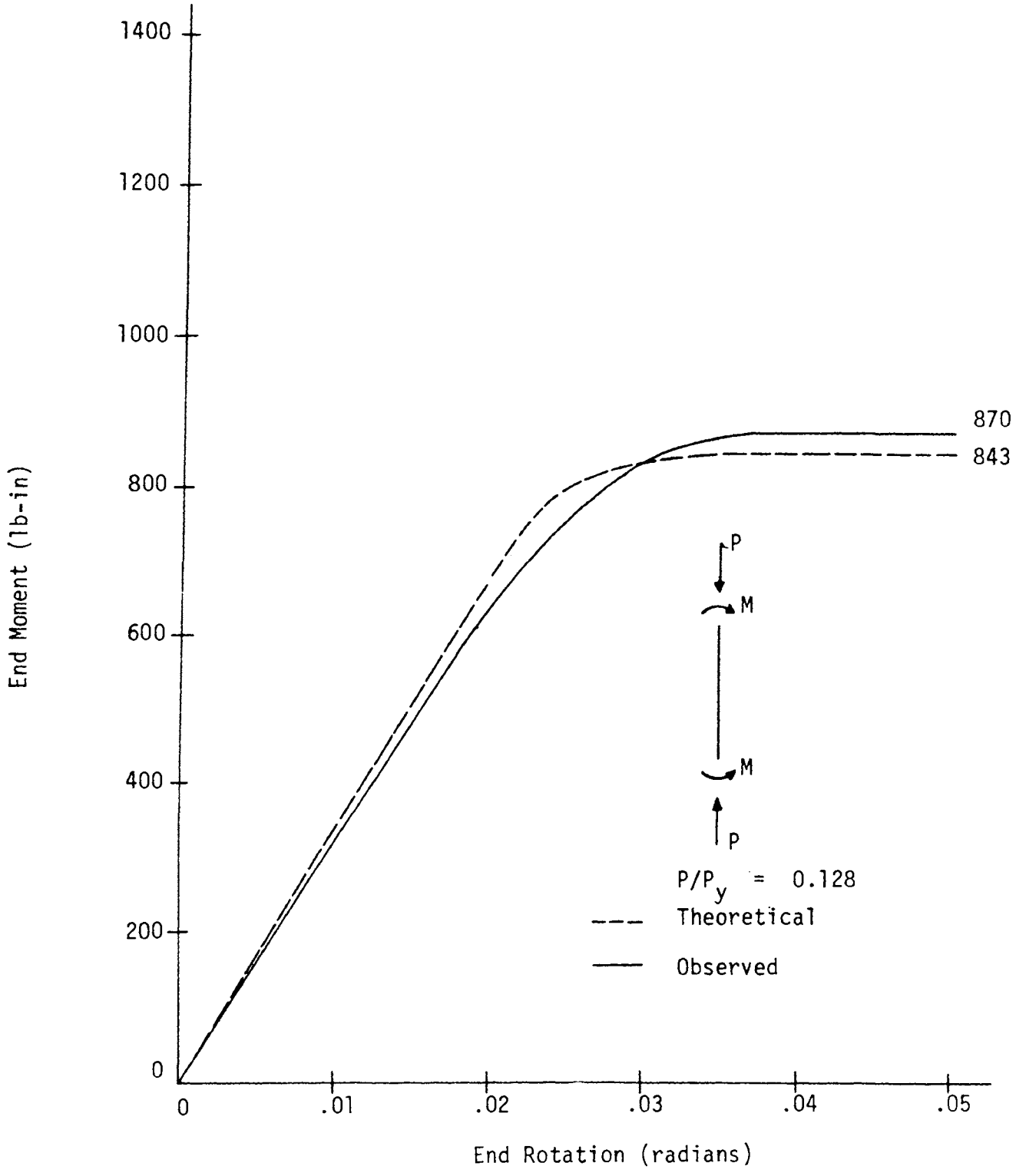

FIGURE D37–BEAM COLUMN 37 MOMENT vs. ROTATION

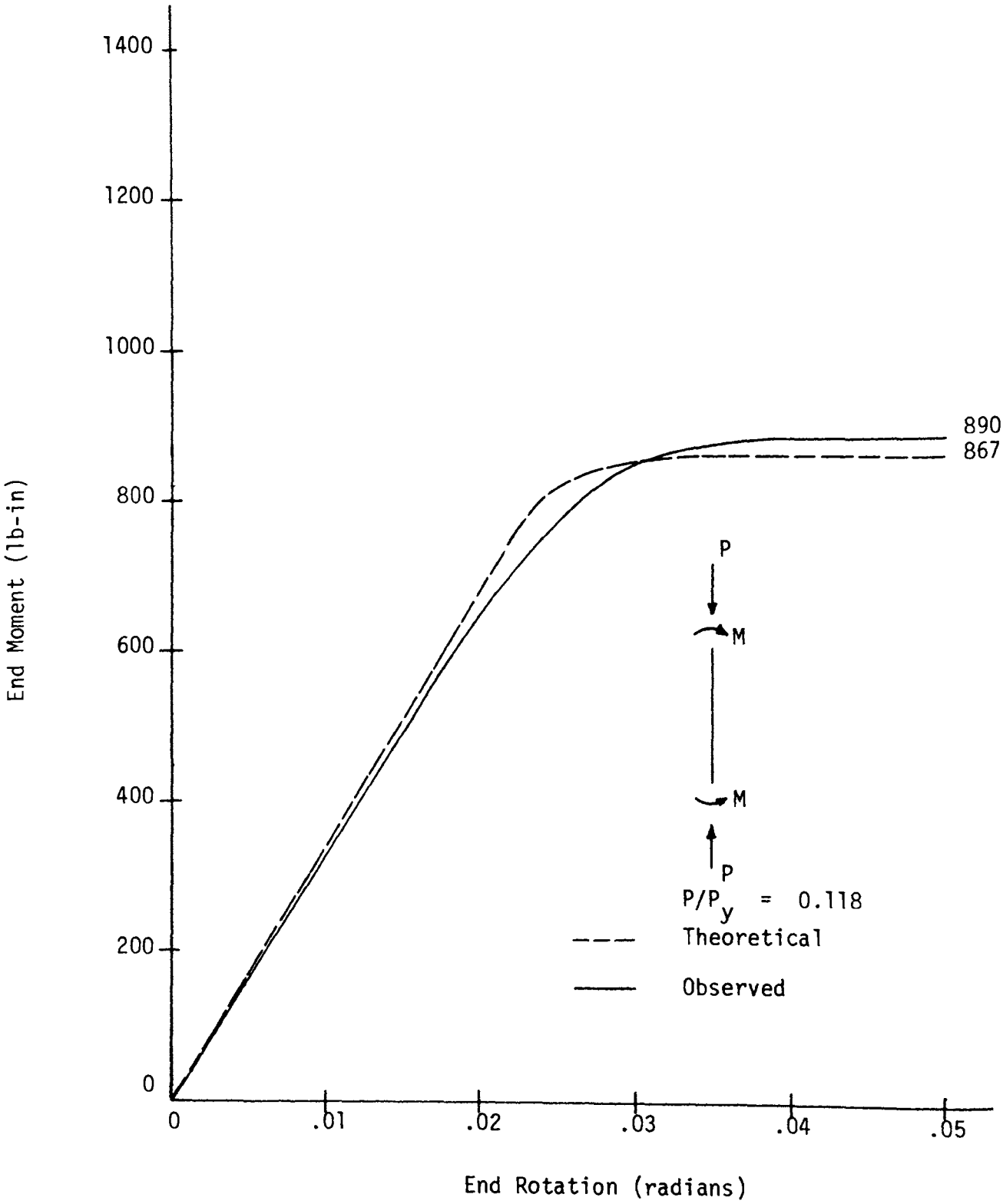

FIGURE D38–BEAM COLUMN 38 MOMENT vs. ROTATION

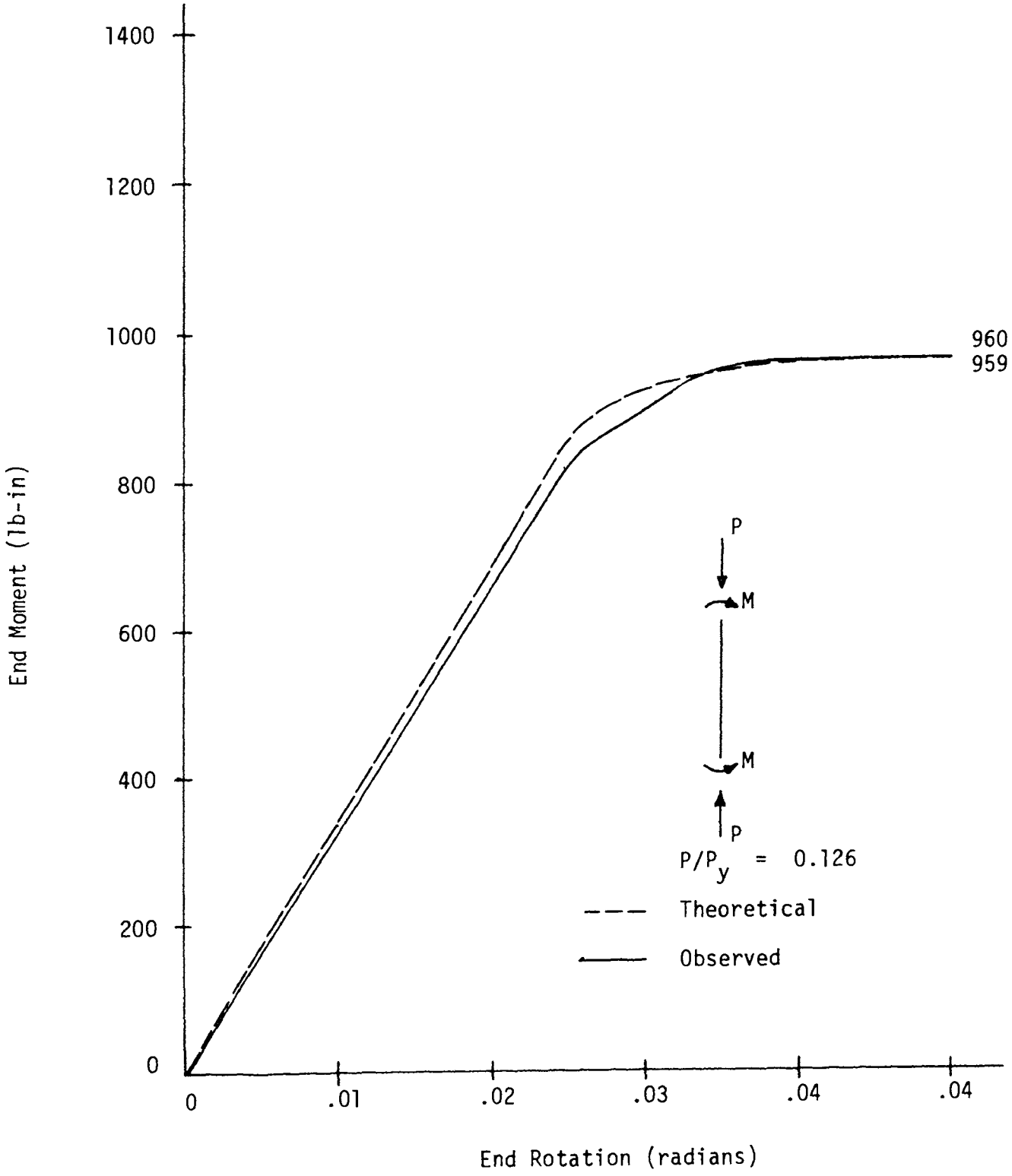

FIGURE D39—BEAM COLUMN 39 MOMENT vs. ROTATION

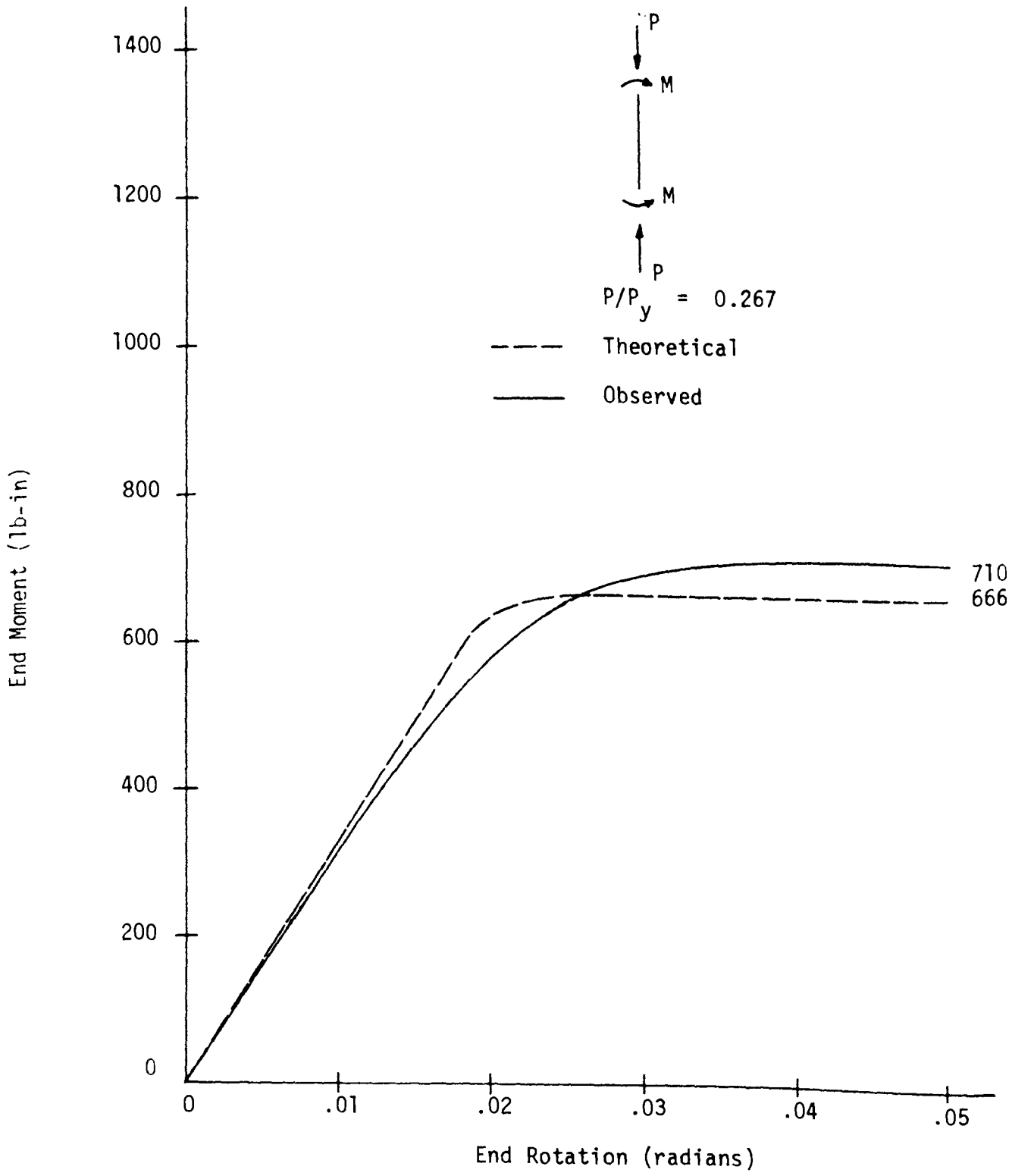

FIGURE D40—BEAM COLUMN 40 MOMENT vs. ROTATION

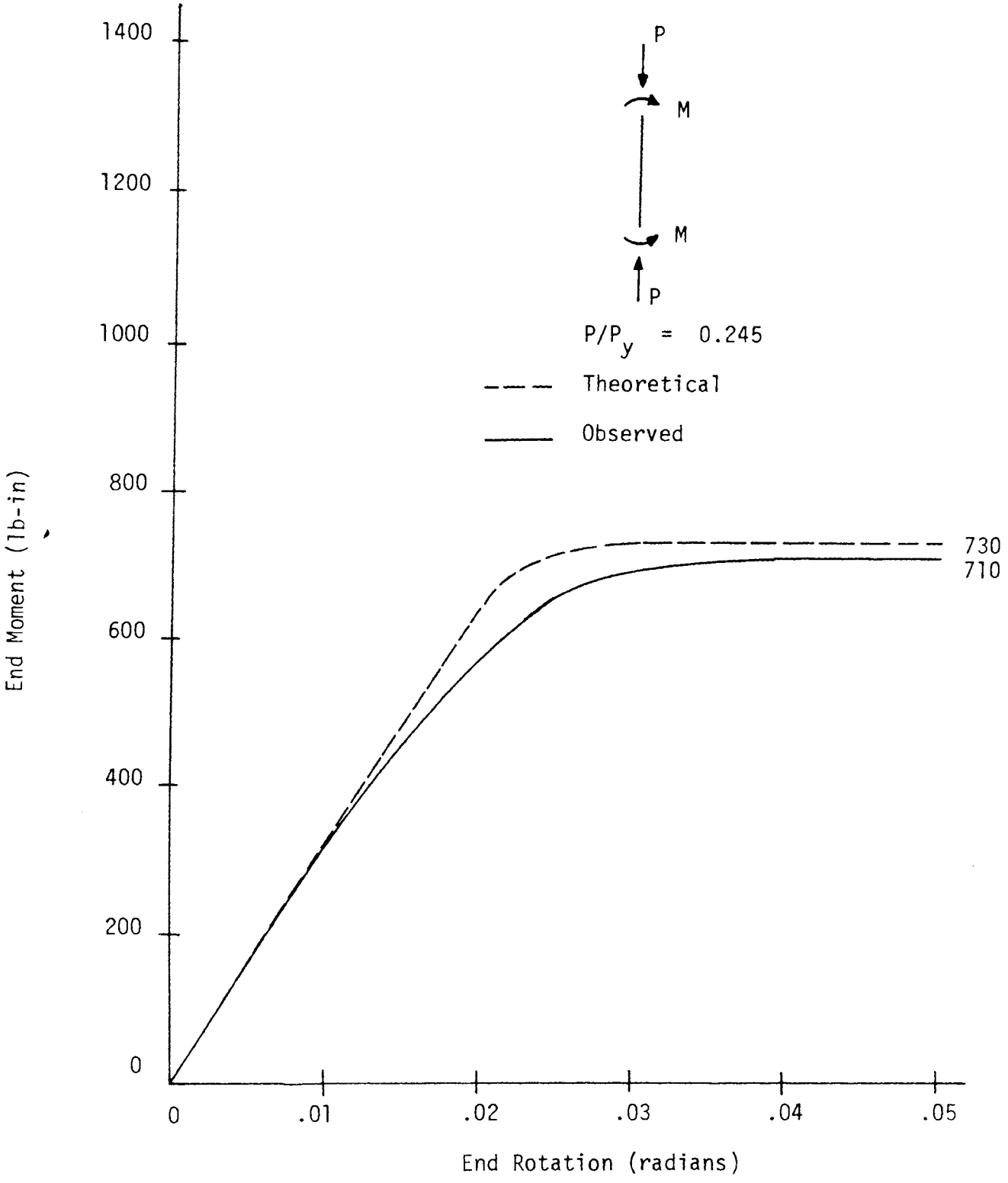

FIGURE D41–BEAM COLUMN 41 MOMENT vs. ROTATION

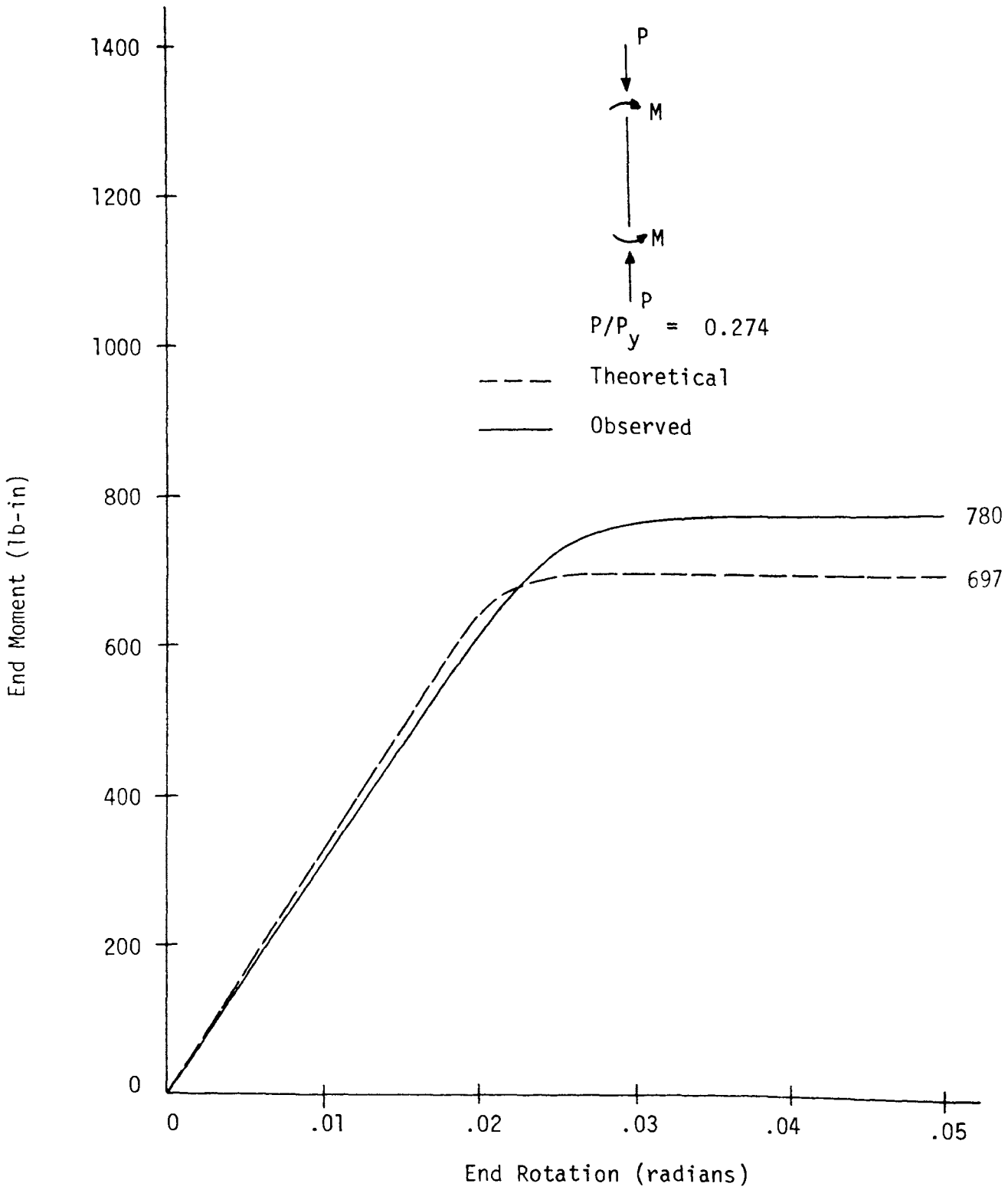

FIGURE D42–BEAM COLUMN 42 MOMENT vs. ROTATION

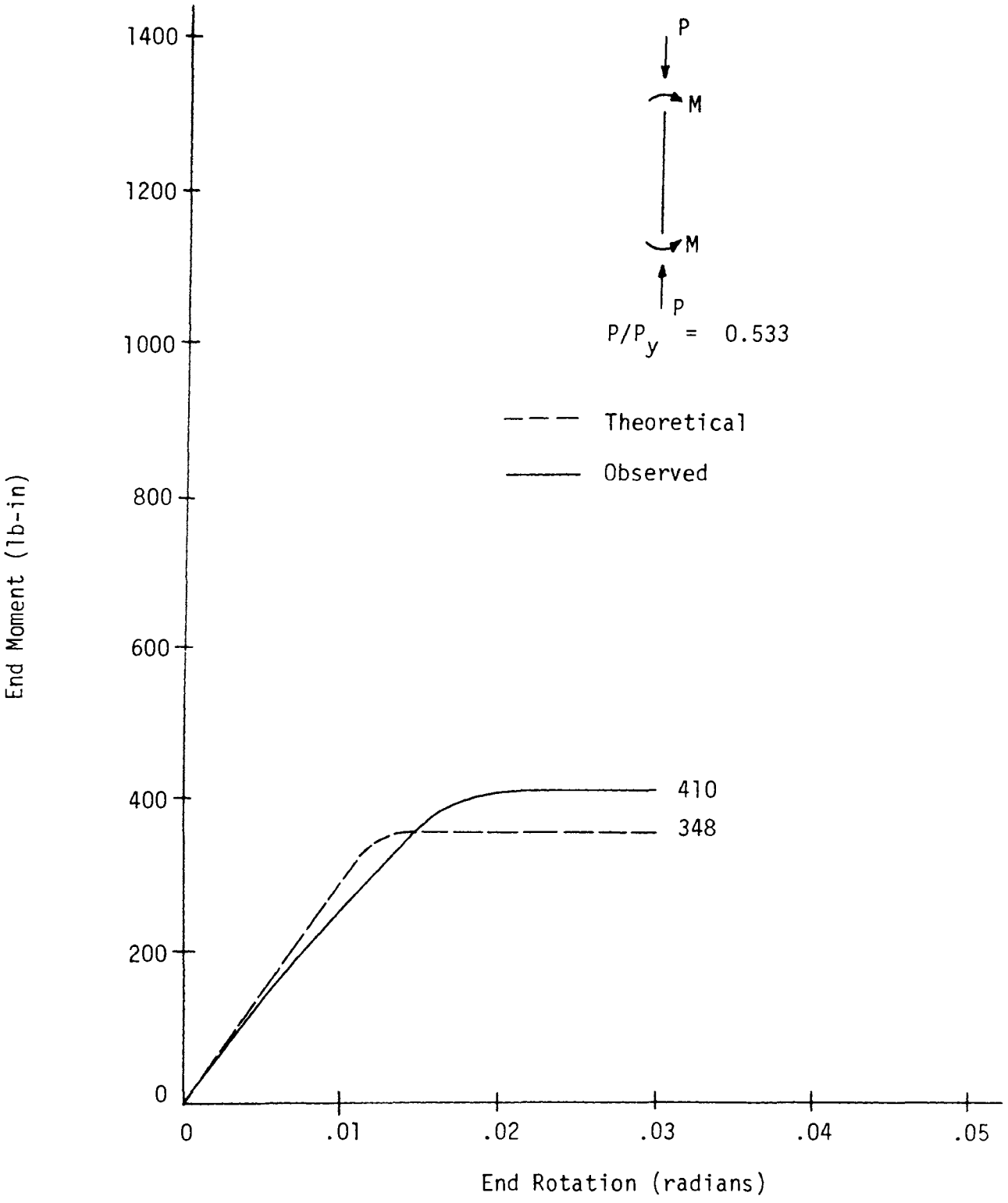

FIGURE D43—BEAM COLUMN 43 MOMENT vs. ROTATION

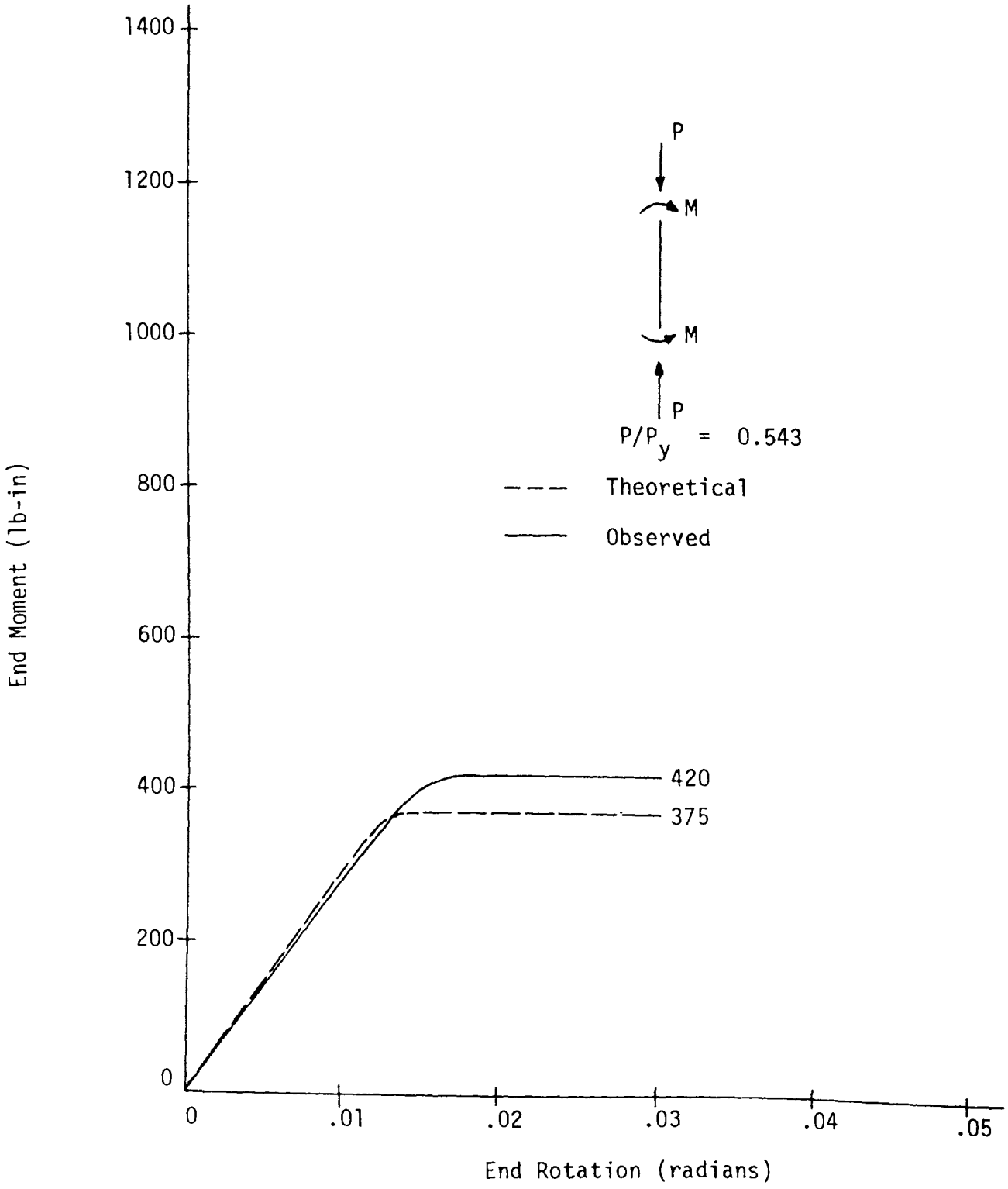

FIGURE D44–BEAM COLUMN 44 MOMENT vs. ROTATION

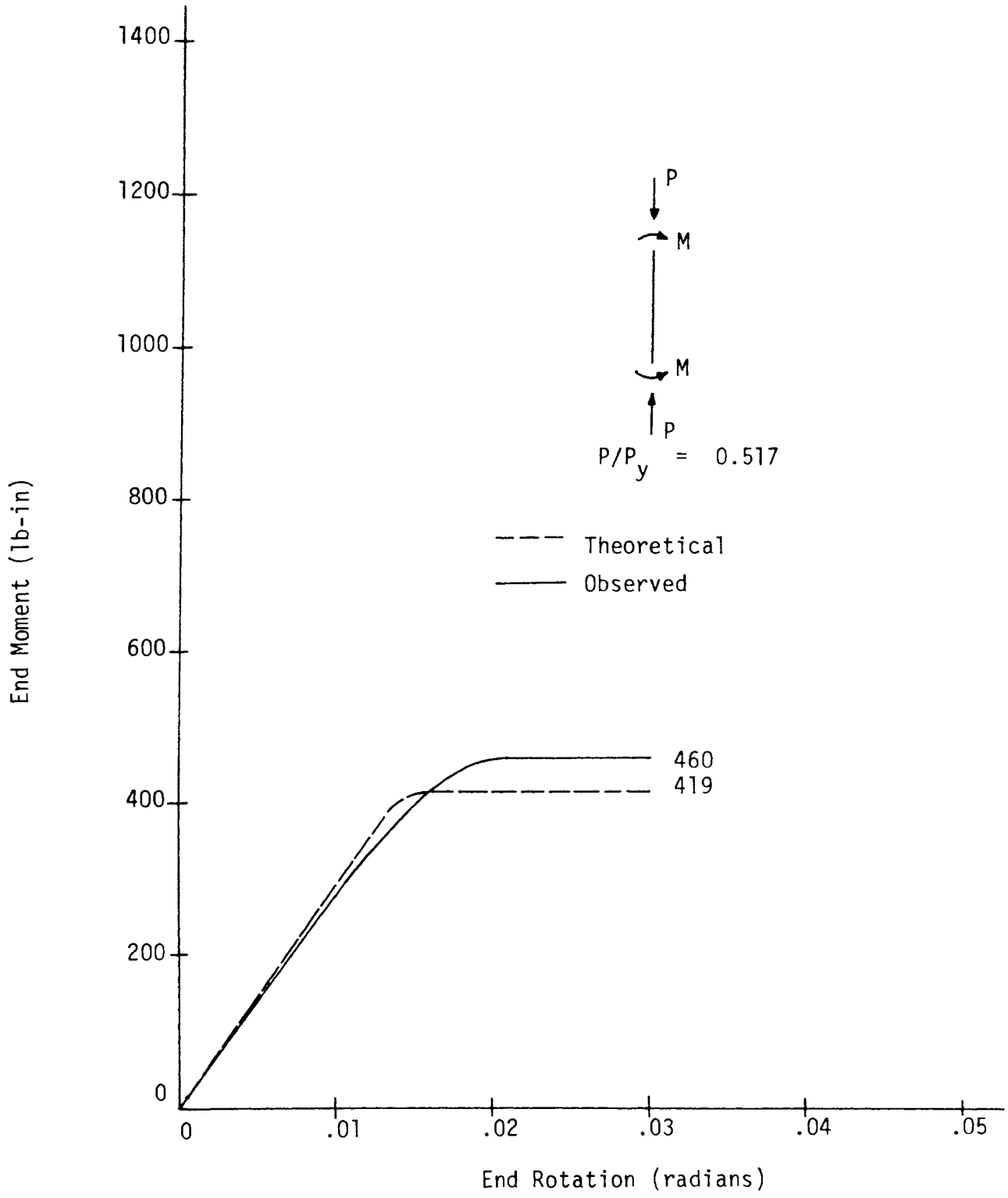

FIGURE D45–BEAM COLUMN 45 MOMENT vs. ROTATION

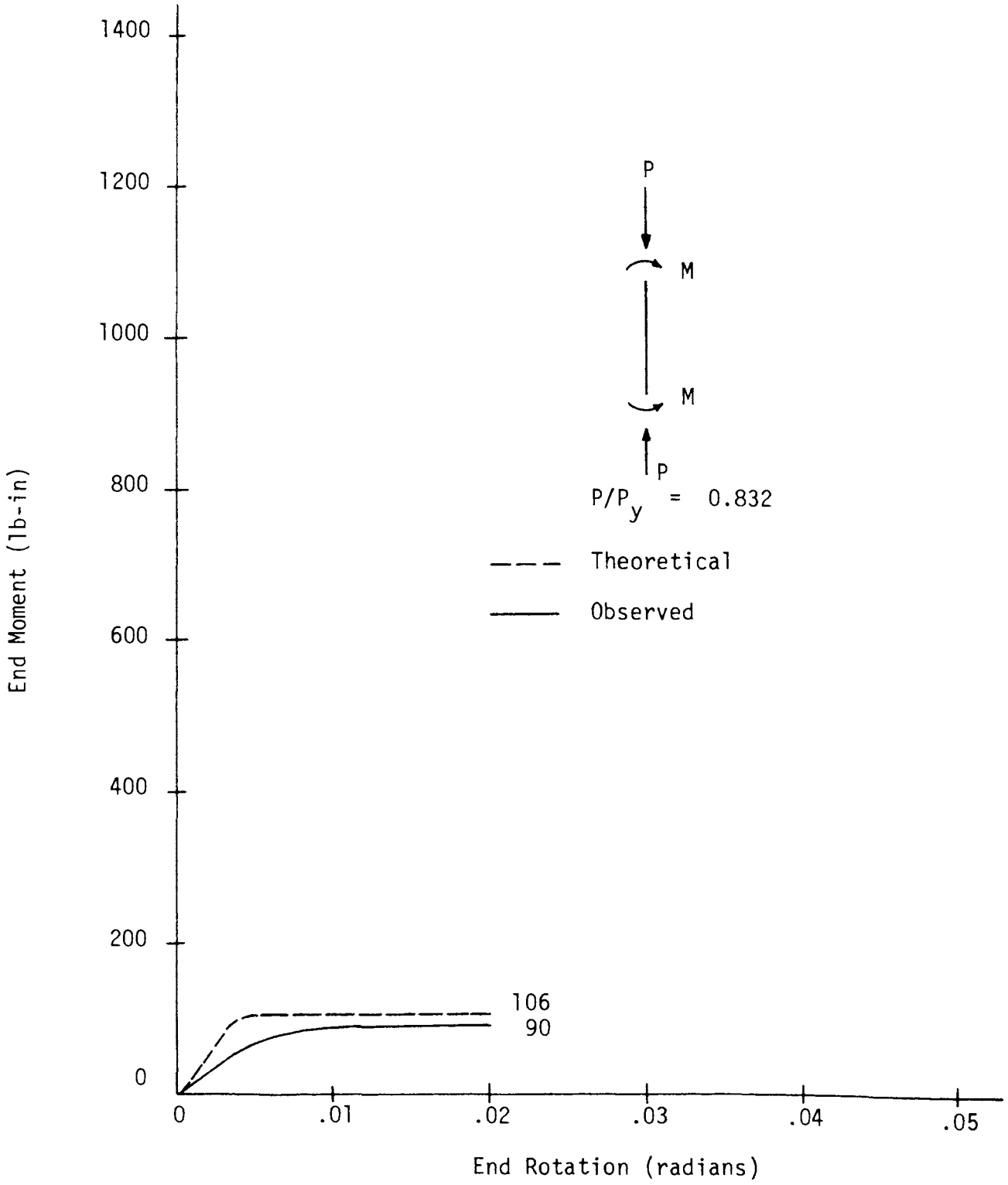

FIGURE D46–BEAM COLUMN 46 MOMENT vs. ROTATION

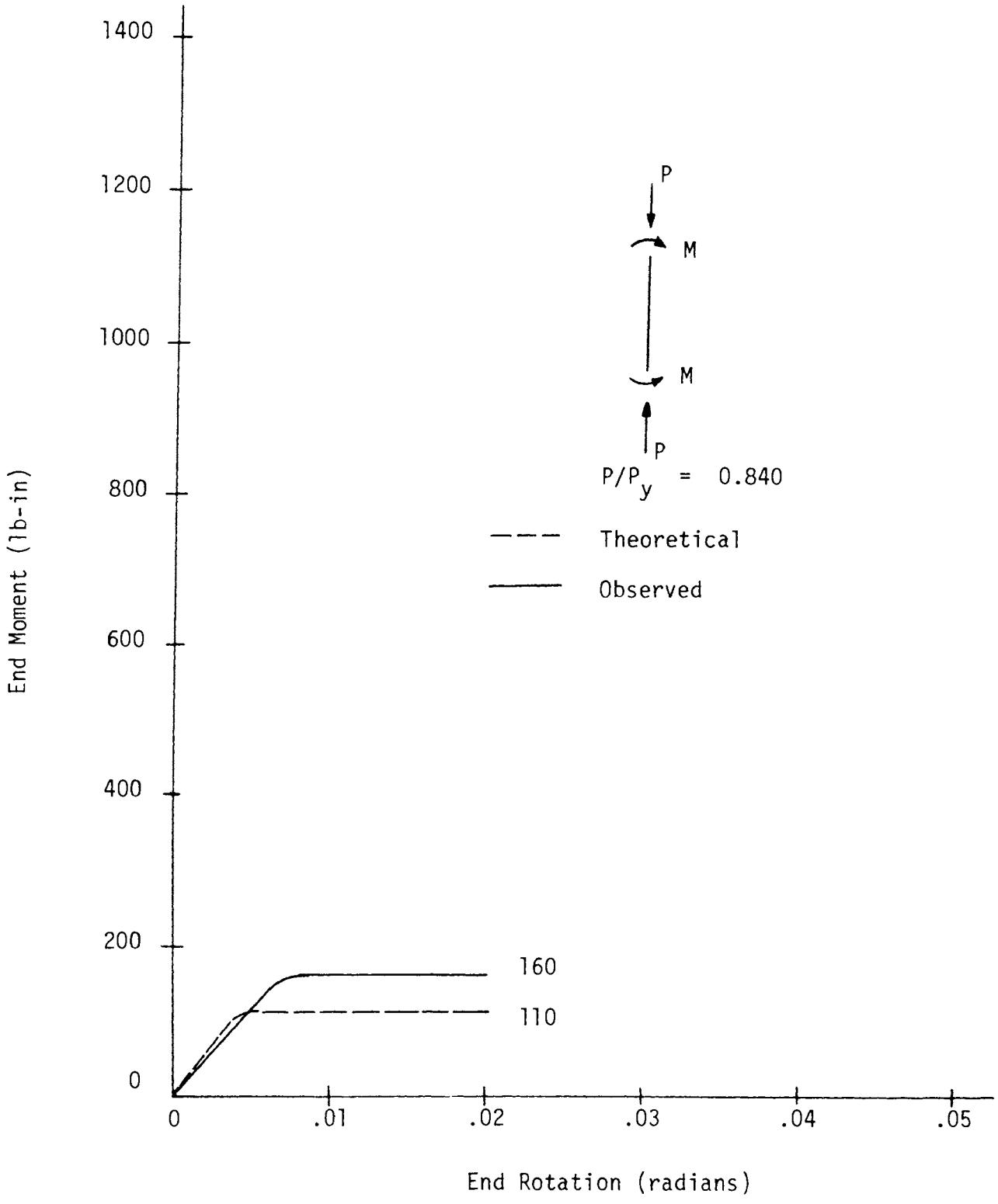

FIGURE D47–BEAM COLUMN 47 MOMENT vs. ROTATION

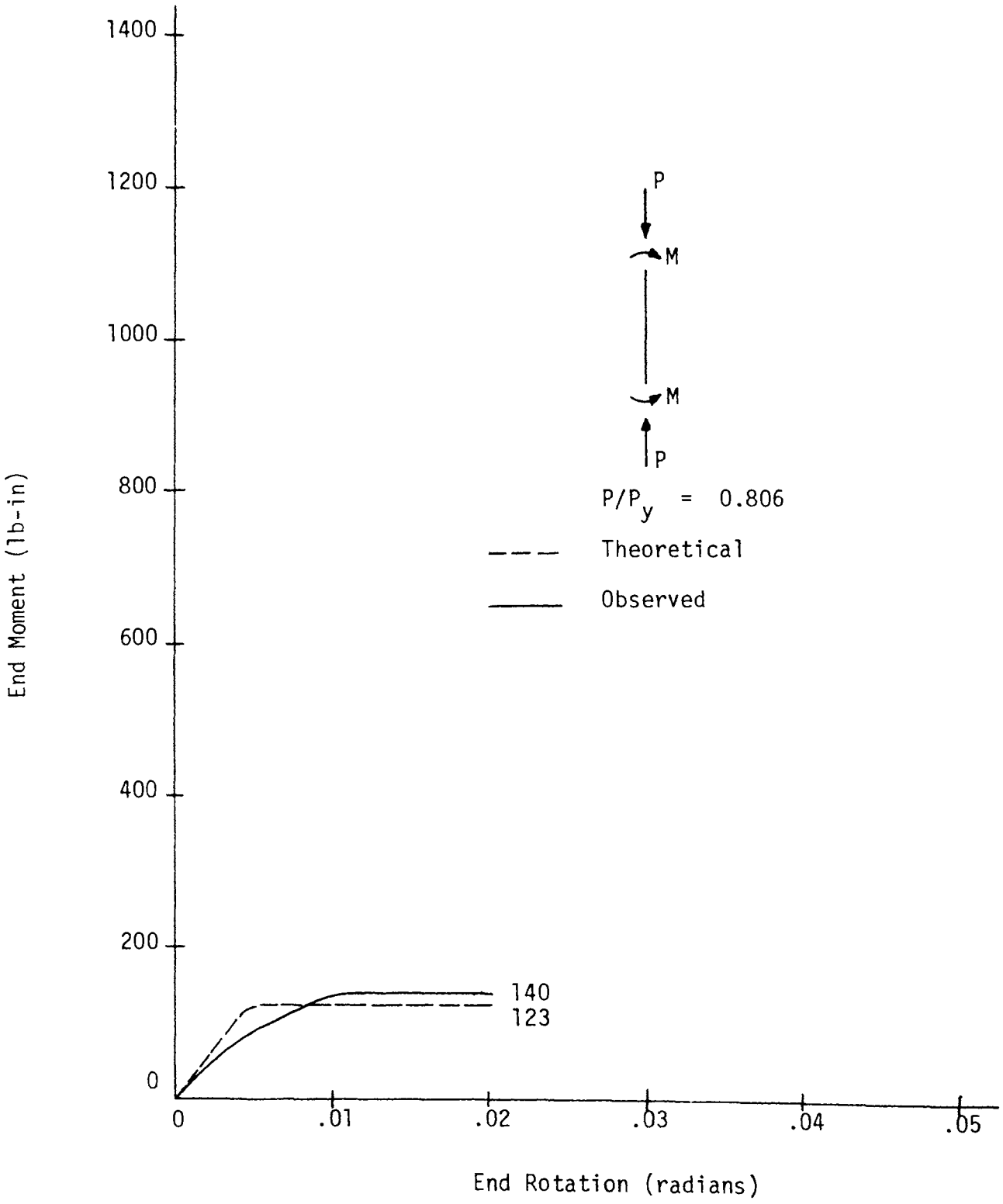

FIGURE D48–BEAM COLUMN 48 MOMENT vs. ROTATION

REFERENCES

1. Foster, D. C., "Fabrication Techniques for Small Scale Models," unpublished M.S. Thesis, Department of Civil Engineering, M.I.T., June 1966.

2. Reimer, R., and Falcone, P., "Ultimate Strength Behavior of Small Scale Steel Frameworks," unpublished M.S. Thesis, Department of Civil Engineering, M.I.T., June 1966.

3. Nakamura, Y., "Beam-Column Behavior," a report prepared in subject 1.531 Special Problems in Structural Engineering, M.I.T., May 1966.

4. Beedle, L. S., "Plastic Design of Steel Frames," John Wiley & Sons, Inc., New York, N.Y. 1958 pg. 108.

5. Galambos, T. V., and Prasad, J., "Ultimate Strength Tables for Beam-Columns," Weld, Res. Council Bull. 78, June 1962.

6. Starin, P., "Device for Testing Small Scale Columns Under Combined Thrust and End Moment," unpublished M.S. Thesis, Department of Civil Engineering, M.I.T., January 1966.

7. Van Kuren, R. C., and Galambos, T. V., "Beam Column Experiments," Proceedings of the American Society of Civil Engineers, Vol. 90, No. ST2, April 1964.

8. Ketter, R. L., and Galambos, T. V., "Columns Under Combined Bending and Thrust," Transactions American Society of Civil Engineers, Vol. 126, 1961.

9. Ojalvo, M., "Restrained Columns," Proceedings of the American Society of Civil Engineers, Vol. 86, No. EM5, October 1960.

Ultimate Strength Behavior of Small-Scale Steel Frameworks

by

WILLIAM A. LITLE

PHILIP FALCONE

RICHARD B. REIMER

ACKNOWLEDGEMENT

This research project was carried out in the Structural Models Laboratory of the Department of Civil Engineering at the Massachusetts Institute of Technology. The project was sponsored by the Committee of Structural Steel Producers and the Committee of Steel Plate Producers of American Iron and Steel Institute, and the Structural Steel Fabricators of New England.

TABLE OF CONTENTS

ABSTRACT

This project was conducted to determine the behavior of two, two-bay, three-story model steel frames. One frame was loaded with varying vertical loads only, while the other was loaded with indicated vertical loads and varying horizontal loads.

It is concluded that:

1. The vertically loaded frame showed close agreement between the theoretical predictions and the experimental results.
2. All data retrieved from any test are dependent upon the accuracy of the instrumentation used to obtain such data.
3. Additional comparison with the Lehigh frame is needed.

LIST OF TABLES

LIST OF FIGURES

PART I

I. INTRODUCTION

In the past, theories explaining the ultimate strength of structures have been proven by full scale tests. These full scale tests, where feasible, will continue to be the final proof of new theories. On the other hand such full scale tests have many limitations. They are expensive and require large testing facilities and loading systems. Furthermore, because of these size and cost limitations, the number of tests which can be performed is small. Consequently, any test program calling for only full scale tests cannot be very exhaustive.

Realizing the advantages which may be achieved by using small scale models, the Civil Engineering Department at M.I.T. undertook a research project to investigate techniques for fabricating and testing small scale models of steel frameworks. This research project consisted of:

1. Model Material Selection
2. Members
   a. Fabrication
   b. Behavior
      i. Beam Tests
      ii. Beam-Column Tests
3. Frameworks
   a. Fabrication
   b. Behavior
      i. Beam Tests
      ii. Frame Tests

During 1964/65 Foster worked on Parts 1, 2a, 2b Beams, 3a, and 3b Joints.[1]* During 1965/66 Foster and Oakes worked on 2b Beam-Columns.[2] This report covers 3b Frame Tests.

* Superscript refers to references at the end of this report.

The results of the 1964/65 study indicated that acceptable small scale WF steel shapes could be milled from SAE C1020 hot rolled bar stock, that TIG (tungsten inert gas) welded joints possessed adequate strength and ductility, and that it was desirable to anneal such welded joints.

This present study begins with findings of the above-mentioned work and uses the techniques described therein to build and test two, two-bay, three-story steel frames. The frames are 1/8 scale replicas of frames tested at Lehigh University.

Frame A, shown in Figure 1a, was loaded with vertical loads only. The loads P were increased from 0 to failure. Theoretical predictions of the behavior of Frame A were obtained from a piece-wise linear elastic analysis which is explained in Section II. Section III represents the experimental results. Section IV interprets the results and explains what conclusions may be drawn from this study.

Frame B, shown in Figure 1b, was loaded with the indicated vertical loads and, holding these constant, the horizontal loads, H, were increased from 0 to failure. Section III presents the experimental results. The same kind of piece-wise linear analysis used for Frame A was performed for Frame B. The fact that the "$P\ \Delta$" effect was not accounted for in the analysis was shown to be important. Some conclusions are presented in Section IV.

II. THEORETICAL ANALYSIS

Theoretical predictions of the load-displacement behavior of Frame A were based on a piece-wise linear elastic analysis. Using the M.I.T. STRESS program[3], loads were incremented until the first plastic hinge was formed. With successive modifications of the structure, the sequence of hinge formation was determined and load versus displacement behavior was obtained.

The criterion for plastic hinge formation was the interaction curve plotted in Figure 2, and it was assumed that the moment-thrust-curvature relationships were bilinear (see Figure 3).

Values for P_y and M_p were determined from 1/8 scale nominal section properties in conjunction with yield stresses from tensile coupons taken from each length of material. These P_y and M_p values are shown in Figure 4.

Thus the analysis for the gravity-loaded Frame A was quite straightforward. Gravity loads were proportionally applied until the first plastic hinges were found. Frictionless hinges were then inserted at these points and equal and opposite concentrated moments were applied to the members on either side of the hinge. The load was again increased until new hinges were found and the procedure continued. The ultimate load occurred when a beam mechanism formed in the first and second story beams. Section A in Part II shows a sample of the analysis procedure. Figures 11, 12, and 13 show the determined load versus midspan beam displacement curves for each of the three stories, respectively.

The analysis of Frame B was performed using a piece-wise linear elastic method similar to that described above for Frame A. Reduction for column plastic moment capacity due to axial load was accounted for, but the stiffness reductions were not. More importantly the effect of the vertical loads acting in a horizontally displaced position (sometimes called the "$P-\Delta$" effect) were not considered. A proper analysis to account for these important secondary effects has not yet been made.

III. EXPERIMENTAL ANALYSIS

3.1 BACKGROUND

Frames A and B each consisted of milled steel members with TIG welded joints, and both were annealed at 1000°F for one hour (furnace cooled) before testing. Frame A was loaded in the vertical direction only, while Frame B was loaded vertically to 1.3 times the design service loads, and then horizontally while holding the vertical loads constant. In both cases, the top story vertical loads were 75 percent of the lower story loads. Frame B, ready for testing is shown in Figure 5.

The cross-section dimensions of the members used in Frames A and B are included in Table B1, Section B, Part II. Also tabulated in Section B are measured yield stress values of tension coupons taken from beam and column lengths. With these geometrical properties and yield stresses, values of M_p and P_y were calculated. The results of these calculations appear in Figure 4 and were used in the theoretical analysis (Section II). In addition to this investigation of member properties, simple beam tests of individual members were made and the measured plastic moments are presented in Table B4, Section B, Part II. Beam moment vs. mid-span displacement curves are shown in Figures B3 through B11, Section B, Part II.

The frames were loaded vertically using hydraulic pull-jacks acting through "gravity load simulators". The purpose of these devices is to support the jacks and allow them to remain vertical while experiencing horizontal motion due to any sidesway of the frame. The gravity load simulators are further described in Section C, Part II. Horizontal loads were applied to Frame B by a dead weight and pulley system also described in Section C, Part II.

Bracing of the beams was accomplished using mechanisms modeled after a concept originally developed at Lehigh University. The devices permit complete freedom of the beams in the plane of the frame but restrain them from displacing out of this plane. Four braces were attached between the loading points on each beam. Column bracing consisted of teflon-covered aluminum blocks placed in pairs against each column at every story level. Figures 6 and 7 illustrate bracing details of the top story.

Loading instrumentation consisted of load cells at the quarter points of each beam (Section D, Part II). Three additional load cells were employed at the points of application of the horizontal loads on Frame B. Checks on the magnitude of applied loads were provided by

pressure gages for the vertical loads and a previous calibration of the dead weight and pulley systems for the horizontal loads. Dial gages are used for all translational displacement measurements. Vertical displacements were measured at the midspan of all beams and horizontal displacements at the three story levels. A measure of the degree of fixity achieved at the "fixed" bases was obtained by measurements of column rotations at the bases. These displacements were obtained from linear variable displacement transformers. Four electric resistance strain gages were attached to each column in each story (total of 36 gages). Two gages on the outside face of the flanges at a cross section near the top, and two similarly placed gages at a cross section near the bottom, enable one to calculate the actual moments, shears, and axial loads in each column at all times. A more detailed description of the instrumentation used may be found in Section D, Part II. Figure 8 locates all instrumentation points.

3.2 TEST PROCEDURE AND RESULTS

3.2.1 Frame A

Vertical loads were applied proportionally from zero, initially in approximately 100 pound increments based on pressure gage readings. At each increment the pressures were held constant and readings taken of load cells, displacements, rotations and strains. At every stage, loads and displacements were compared to the predicted values obtained from the theoretical analysis. The increments of applied loads were decreased to approximately five pounds as the frame approached its ultimate load. Finally, when sustained creep was noted in the vertical displacement of several lower story beams, the loads were held constant.

Failure was initiated by lateral-torsional buckling in beam b-2-c (see Figure 8 for notation). This beam is shown in Figure 9. Immediately thereafter, beams a-2-b, a-1-b, and b-1-c failed in a similar manner. The collapsed frame is shown in Figure 10.

The results of all load, displacement, rotation, and strain readings are presented in Section E, Part II. The load vs. displacement results are presented in Figures 11, 12, and 13.

3.2.2 Frame B

Vertical loads were applied in three steps from zero to full load of 388 pounds. Thereafter, the vertical loads were held as constant as possible. Horizontal loads were applied by placing pre-weighted quantities of steel punchings in buckets that were suspended from pulleys (see Figure C3, Part II). Ten-pound increments were applied up to a total of 80 pounds. One six-pound increment was then applied, and thereafter two-pound increments up to failure. At every loading stage horizontal displacements were measured. Load cells, rotations and strains were recorded at ten-pound increments. The results of all load, displacement, strain and rotation readings are presented in Section F, Part II, and in Figure 14 load versus horizontal displacement curves are shown. In plotting the load ordinates in Figure 14, the three horizontal loads as determined by the load cells were averaged and then a deduction of from one to three pounds for friction losses in the gravity load simulators (see Section C, Part II) was made. The resulting loads are given in Section F, Part II.

At a load of 94 pounds, the top story displacement was 0.592 inch. On increasing the load to 96 pounds the top story displacement gradually increased to over 1 inch, the limit of travel of the lateral braces. Severe local buckling in the compression flanges at load point 1 (see Figure 10) and in the first floor beams on the windward side of columns b and c occurred, but no lateral buckling. The failed frame is shown in Figure 15.

IV. DISCUSSION OF RESULTS AND CONCLUSIONS

4.1 FRAME A

In looking at Figures 11, 12 and 13, one can note close agreement between the theoretical predictions and the experimental results.

As noted in Section B, Part II, the actual section moduli were about 3 per cent lower than the 1/8 scale nominal section properties used in the theoretical analysis. This would mean that the predicted ultimate load of 547 pounds should be shifted down to about 530 pounds.

Beam b-2-c of Frame A reached an ultimate average load of 589 pounds, 11 per cent higher than the modified prediction. The only plausible explanation of this behavior was that the material reached the strain-hardening region, which fact was not accounted for in the theoretical prediction.

The question arises, "Can the results of a small scale model be projected to some prototype structure?" In an attempt to answer this question, the behavior of the 1/8 scale model framework was compared to the prototype, a full scale frame tested at Lehigh University[4]. Figure 16 compares the first story load vs. deflection curves of the two frames in question. Beam b-1-c agrees almost exactly with its counterpart, Beam A-1-B of Lehigh's frame. Beam a-1-b yields an ultimate strength 5 per cent higher than its counterpart, beam B-1-C. In terms of an experimental study, the correlation between these two tests is excellent, perhaps fortuitously so since the member strengths and loading locations do not satisfy exactly the conditions of similitude (nor was any attempt made to do so). For example, the critical Lehigh beam had an M_p = 773 kip inches.[4] Scaled down, this would imply an M_p = 1.51 kip inches for the MIT beam. Actually the MIT beams were slightly weaker than this (see Figure 4). Also, the distance between load points in the Lehigh test was 81 inches. Scaled down, this calls for 10.125 inches, whereas the value of 10.875 inches used in the MIT test is one-half of the distance between column faces. There are other dissimilar material property characteristics and support characteristics as well. It is emphasized, however, that the model tests were intended only to "nominally" simulate the Lehigh test. Exact scaling of each Lehigh frame characteristic would have been impossible.

All data retrieved from any test are dependent upon the accuracy of the instrumentation used to obtain such data. One such problem with Frame A involved the loading system. The first and second story jacks were controlled by one valve and composed a closed system. The third story jacks were controlled by another valve and comprised another closed system. Ideally, every jack in the first-second story system had the same applied load. Similarly, every jack in the third story system should have had the same applied load. In fact, the piston-to-cylinder friction in each jack varied, thus making the applied loads different. For example, loads A, B, C and D should have been identical. However, the data in Section E, Part II shows that a difference in jack friction caused loads C and D to be about 20 pounds less than A and B at load levels of 100-200 pounds, and about 40 pounds less at load levels of 400-500 pounds. Also, the valves were supposed to keep the pressure within each system constant, which they did not. At the higher load levels, fluctuations of up to 10 pounds in the applied loads were noted. This inadequacy in the valves necessitated adjustments of pressure when a constant load on Frame A was required for an extended period of time.

Figure 17 presents a typical reduction of the strain gage data. It has been assumed that the modulus of elasticity is 29,600,000 psi and the areas and section moduli of the column sections were taken to be 0.112 in^2 and 0.032 in^3, respectively (see Section B, Part II). Shown are the moment, thrust and shear at each gaged cross section. With these forces it is possible to make a variety of static checks or to compute the moment, thrust or shear at any other cross section. For example, the check on vertical forces shown at the left of the figure indicates that the values deduced from the strain gages are within a few per cent of the load cell results. As another example, the moment in beam a-1-b (see Figure 16) at the face of the center column, calculated by isolating beam a-1-b, is 1065 inch pounds. Although the values shown in Figure 17 may be correct within a few per cent, this moment is obtained by taking the difference between computed clockwise and counterclockwise moments at the face of the column. Taking

such a difference between two large numbers inherently risks substantial error in the result even though the starting values are believed to be reasonably correct. Thus we know in this case that, at this load, the moment at the point in question has already reached the plastic moment of 1450 inch pounds. Strain-gaged cross sections in the beams (as was done in the Lehigh tests) would permit one to obtain the indicated moment without involving the deduced column gross internal forces.

4.2 FRAME B

Figure 14 presents load vs. displacement curves for each of the three stories of Frame B. (The predicted curves were obtained using the piece-wise linear elastic approach described in Part I, Section II.) It can be seen that the correspondence between predicted and observed behavior is very close for low values of load, but becomes poorer as the load becomes greater. It is felt that this can be attributed mainly to the "P–Δ effect" (see Part I, Section II) that was not considered in the analytic procedure.

Plotting only the top story displacements, Figure 18 shows the experimental behavior and the simple plastic theory prediction for the Lehigh prototype. The model (both experimental and analytical) overestimates the strength of the prototype. (Note that comparison of the M.I.T. and Lehigh experimental behavior beyond the peak load is not fair since Lehigh employed a displacement controlled loading system whereas M.I.T. used dead weight loading.)

At the time this report was released the data from the Lehigh frame had not been published. However, it seems likely that the principal reason for the dissimilar behavior lay in the fact that the roof beams in the prototype were 10B15 members whereas they were 1/8 scale 12B16.5 in the model. These beams did participate significantly in the plastic behavior of the prototype whereas the "oversized" beams in the model did not. Of course, this hypothesis must be verified when the details of the Lehigh test become known.

(a) FRAME A

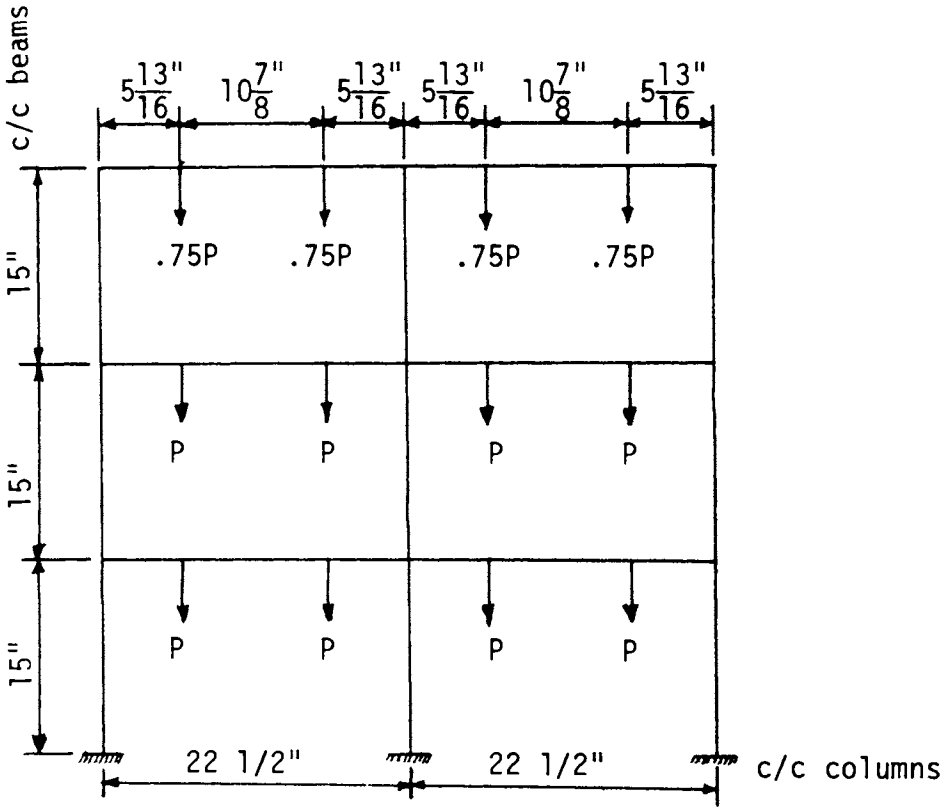

Note:
1. All beams are 1/8 scale 12B16.5
2. All columns are 1/8 scale 6WF25
3. Vertical Load only P increased from zero to failure

(b) FRAME B

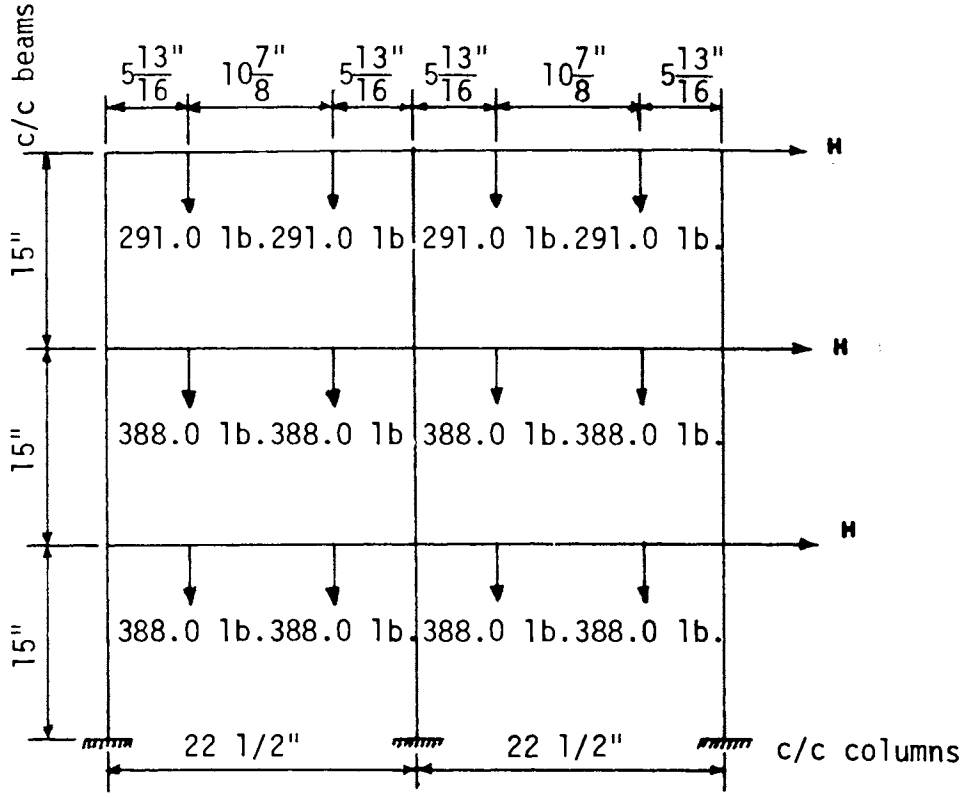

Note:
1. All beams 1/8 scale 12B16.5
2. All columns 1/8 scale 6WF25
3. Constant vertical load with horizontal load H increased from zero to failure

FIGURE 1—LOADING SCHEMES FOR FRAMES A AND B

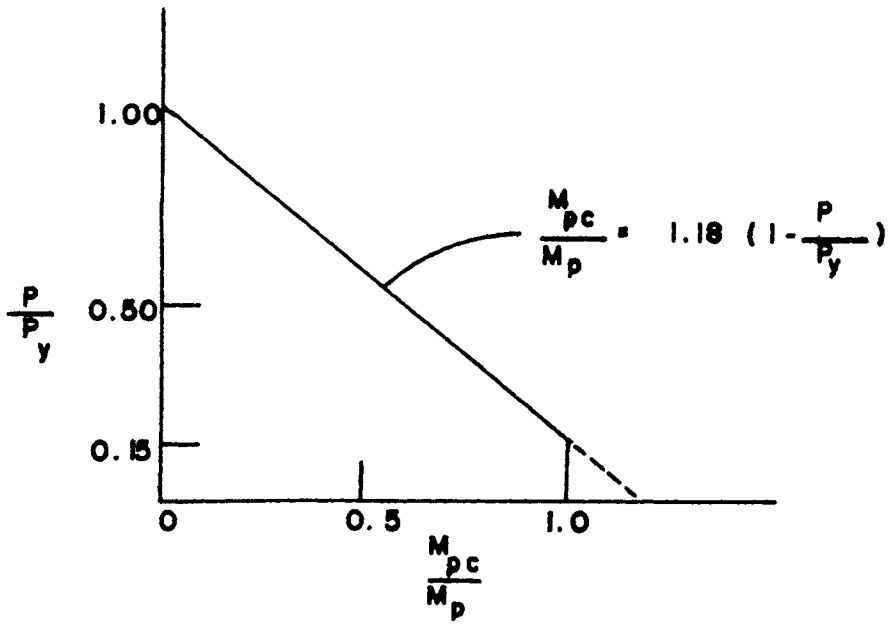

FIGURE 2–BEAM-COLUMN INTERACTION CURVE USED IN THEORETICAL ANALYSIS

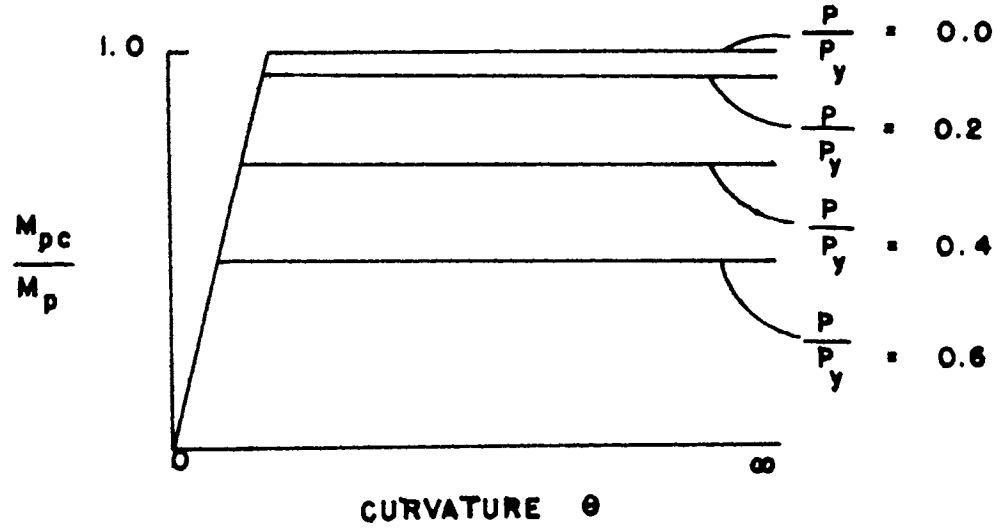

FIGURE 3–ASSUMED MOMENT-THRUST-CURVATURE BEHAVIOR FOR THEORETICAL ANALYSIS

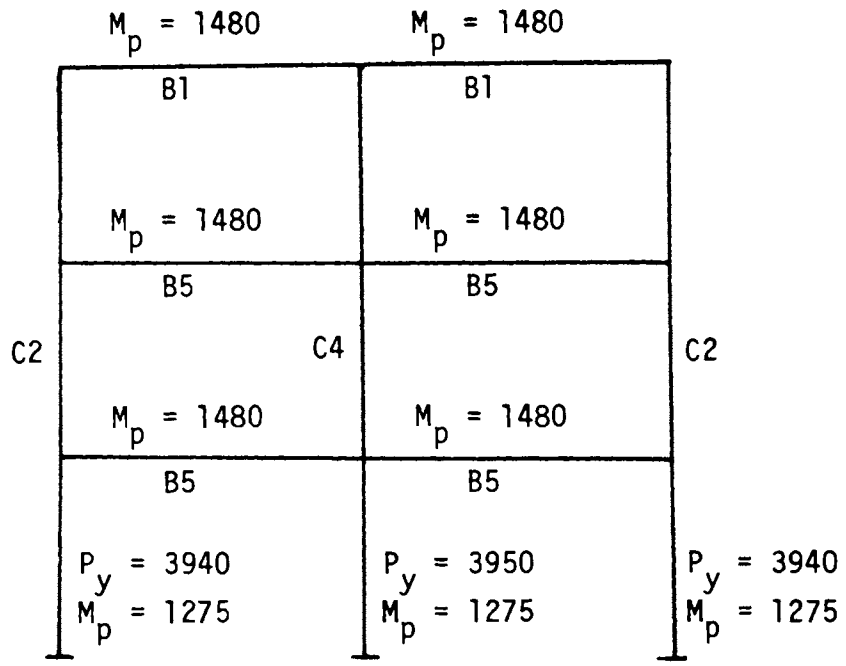

(a) FRAME A

Note: M_p's given in inch-pounds
P_y's given in pounds
C1,..B1,..refer to lengths of material used (See Appendix B)

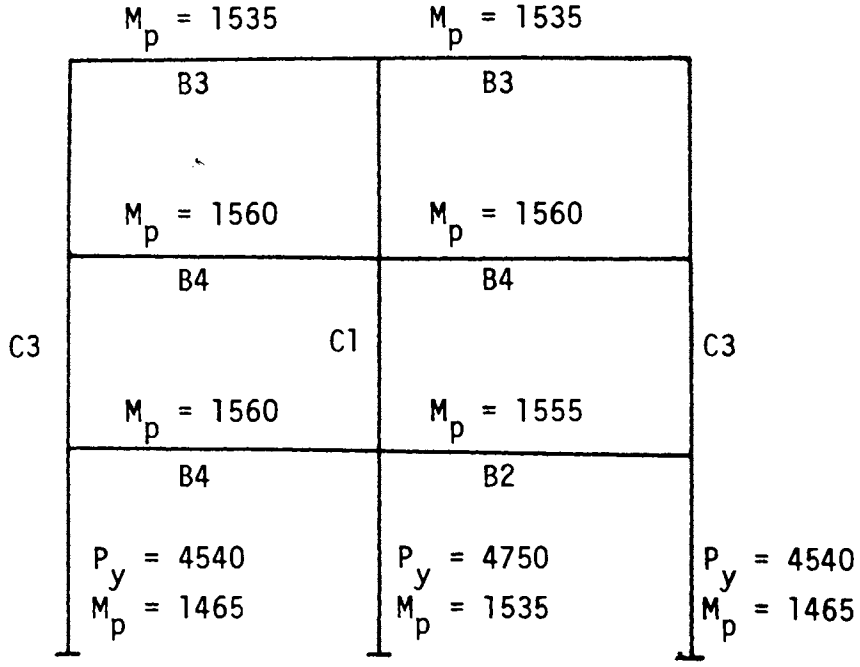

(b) FRAME B

FIGURE 4–MEMBER PROPERTIES OF FRAMES A AND B

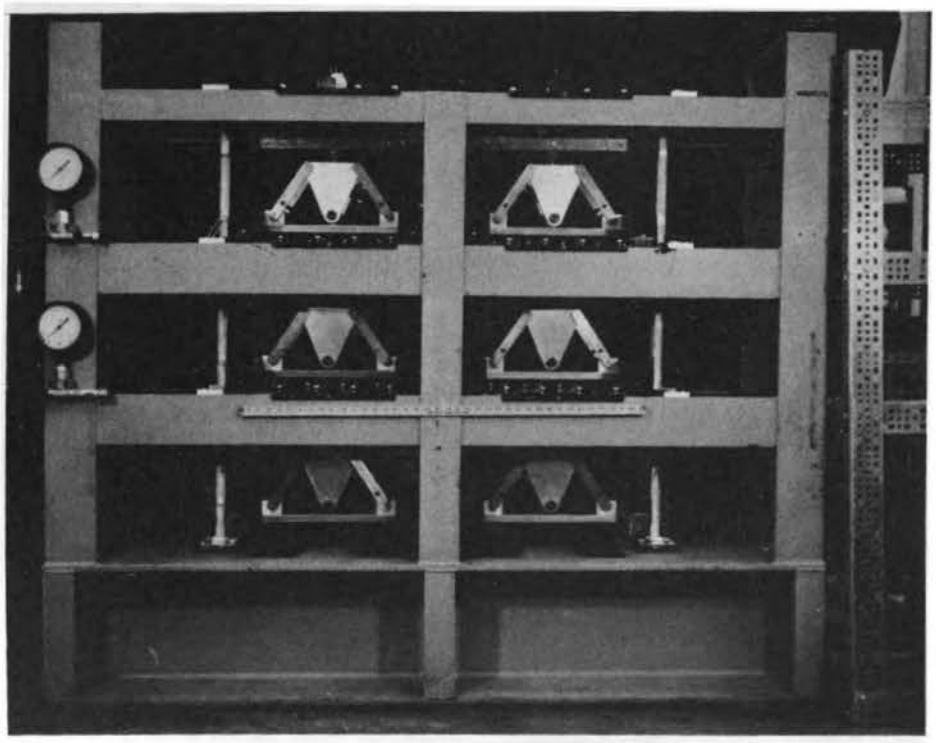

FIGURE 5–FRAME B READY FOR TESTING

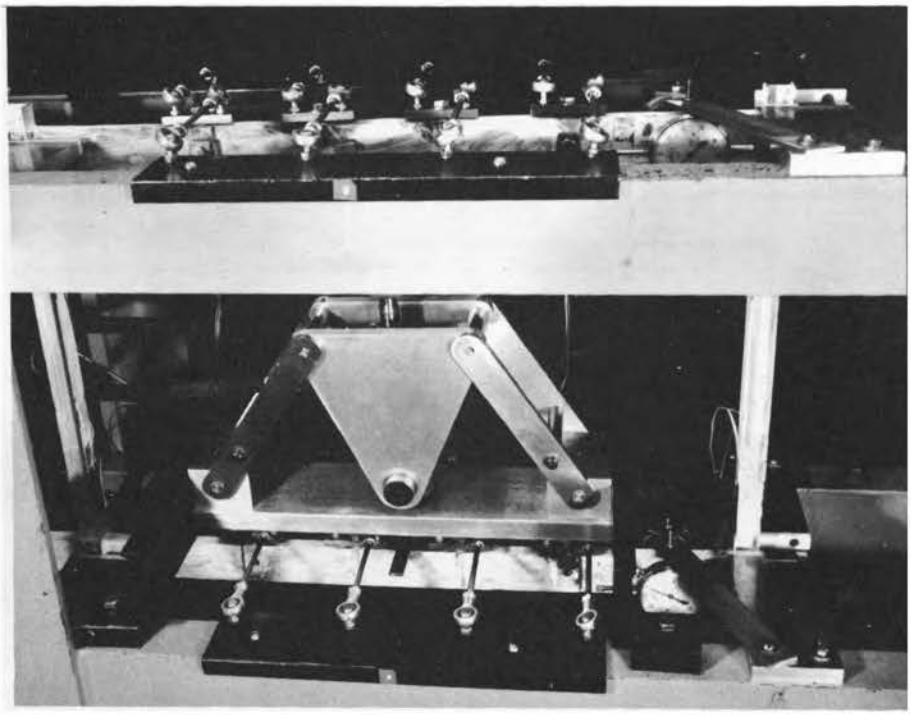

FIGURE 6–TOP STORY OF FRAME B

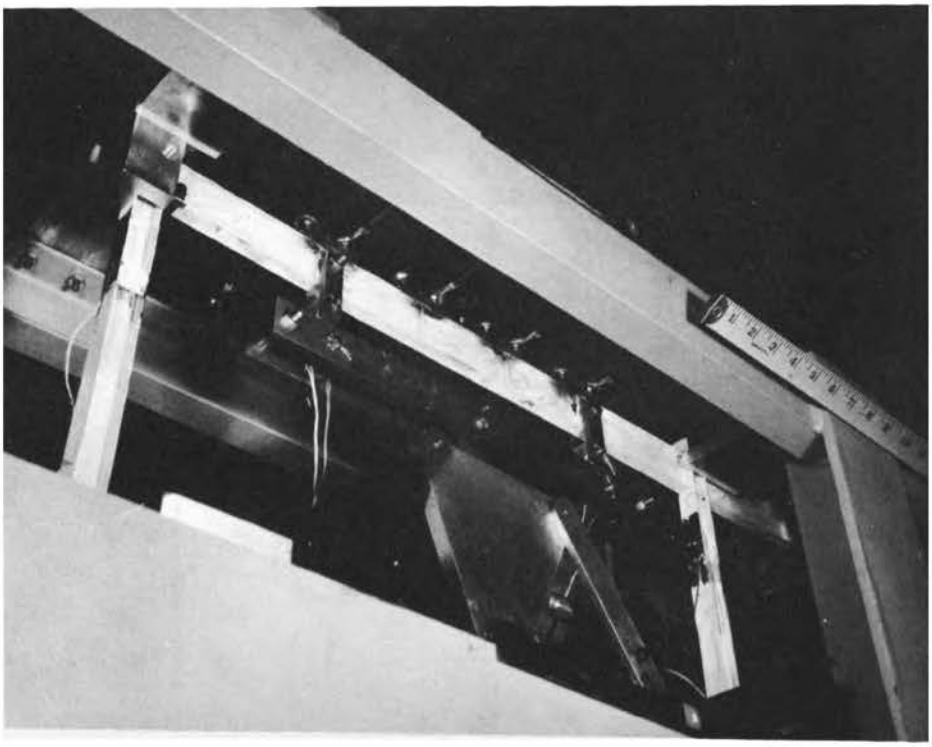

FIGURE 7–TOP STORY OF FRAME B

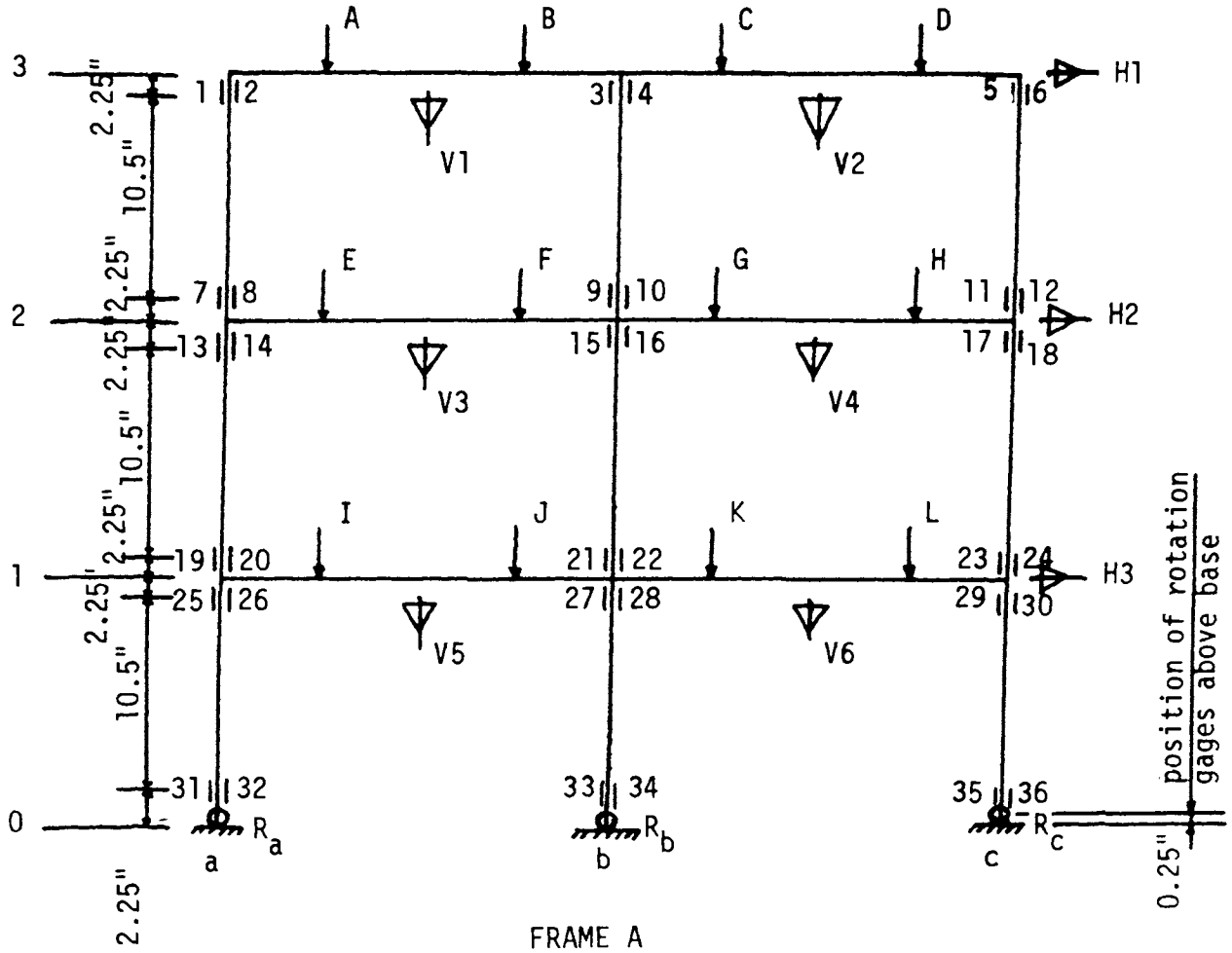

FRAME A

		Symbol	Range
12 Loads	Load Cells	↓X	A THRU L
9 Displacements	Ames Dial Gages	↑V-	V1 " V6
		→H-	H1 " H3
36 Strains	SR-4 Strain Gages	i ii	1 " 36
3 Rotations	Metripak Rotary Position LVDT	Φ R-	R_a " R_c

FIGURE 8—MEASUREMENTS TAKEN ON FRAME A

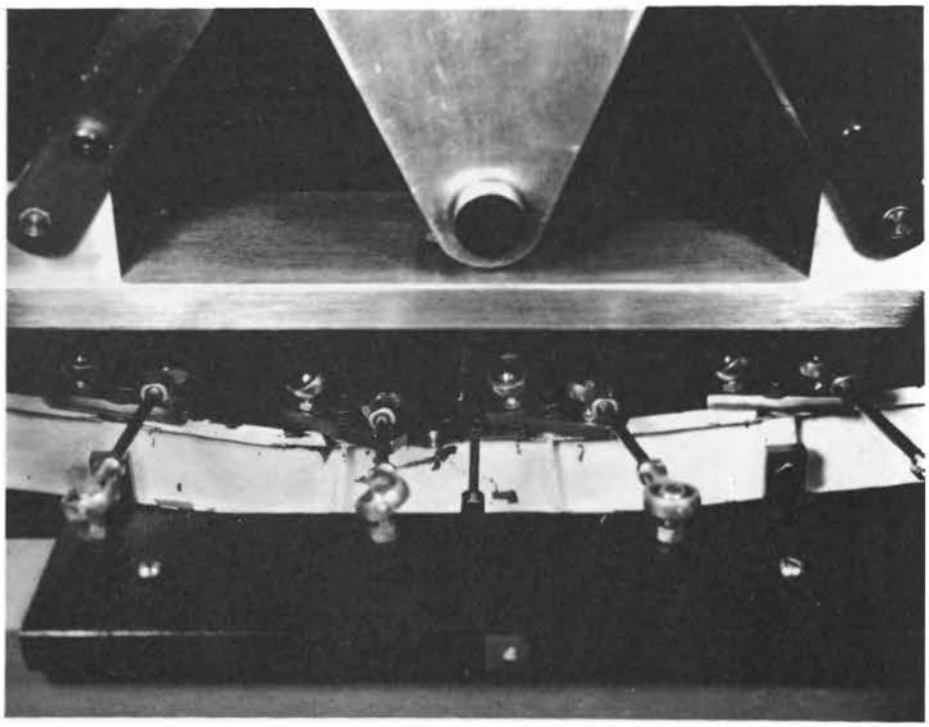

FIGURE 9—FLANGE BUCKLING IN BEAM b-2-c OF FRAME A

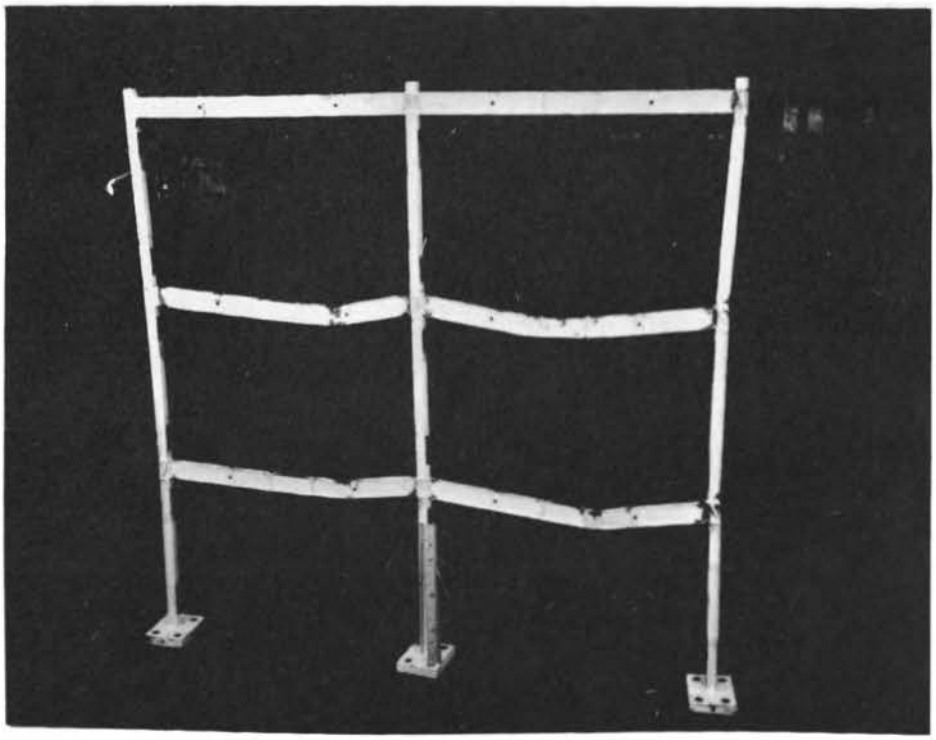

FIGURE 10—FRAME A AFTER TESTING TO ULTIMATE STRENGTH

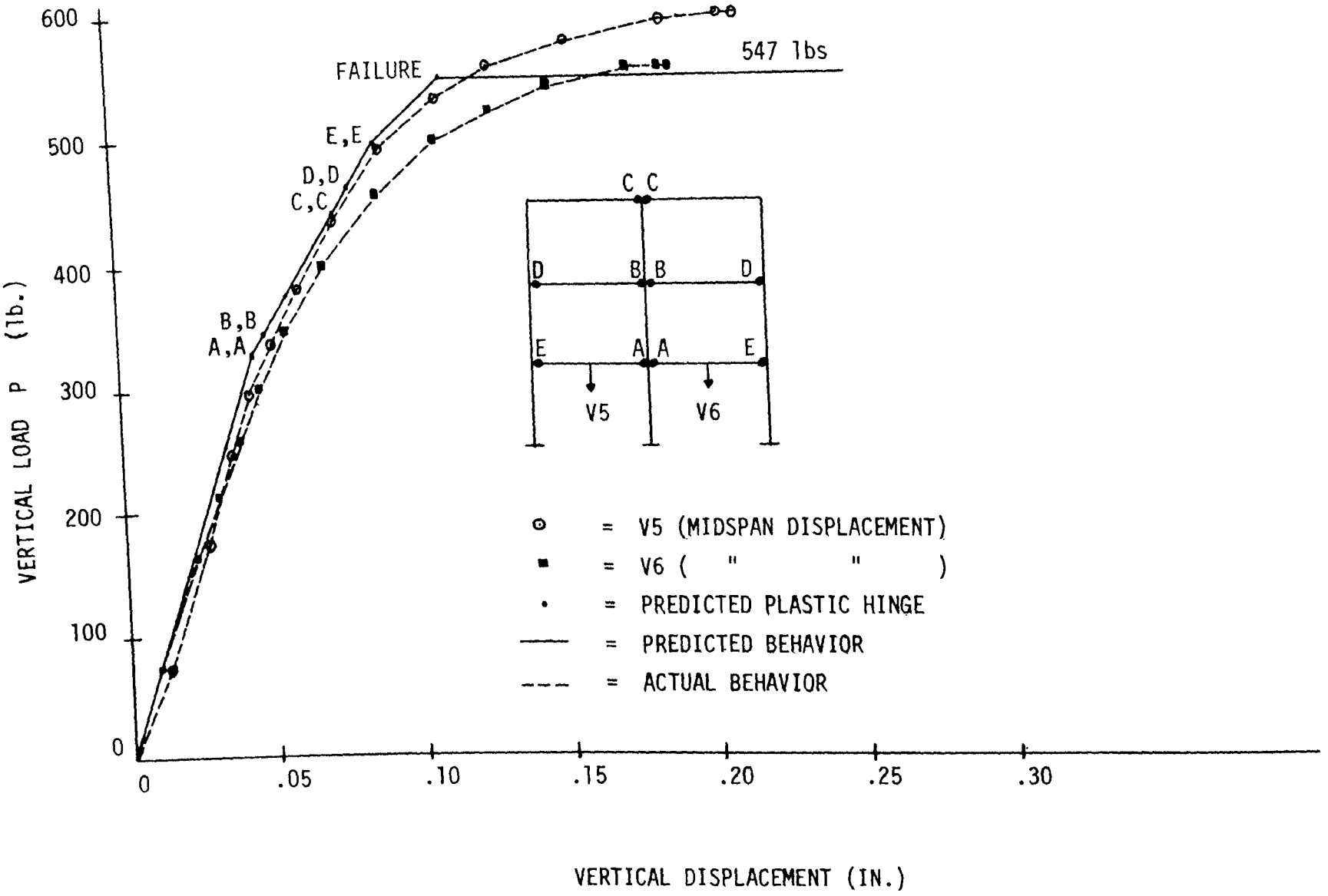

FIGURE 11–LOAD-DISPLACEMENT CURVES FOR FIRST STORY OF FRAME A

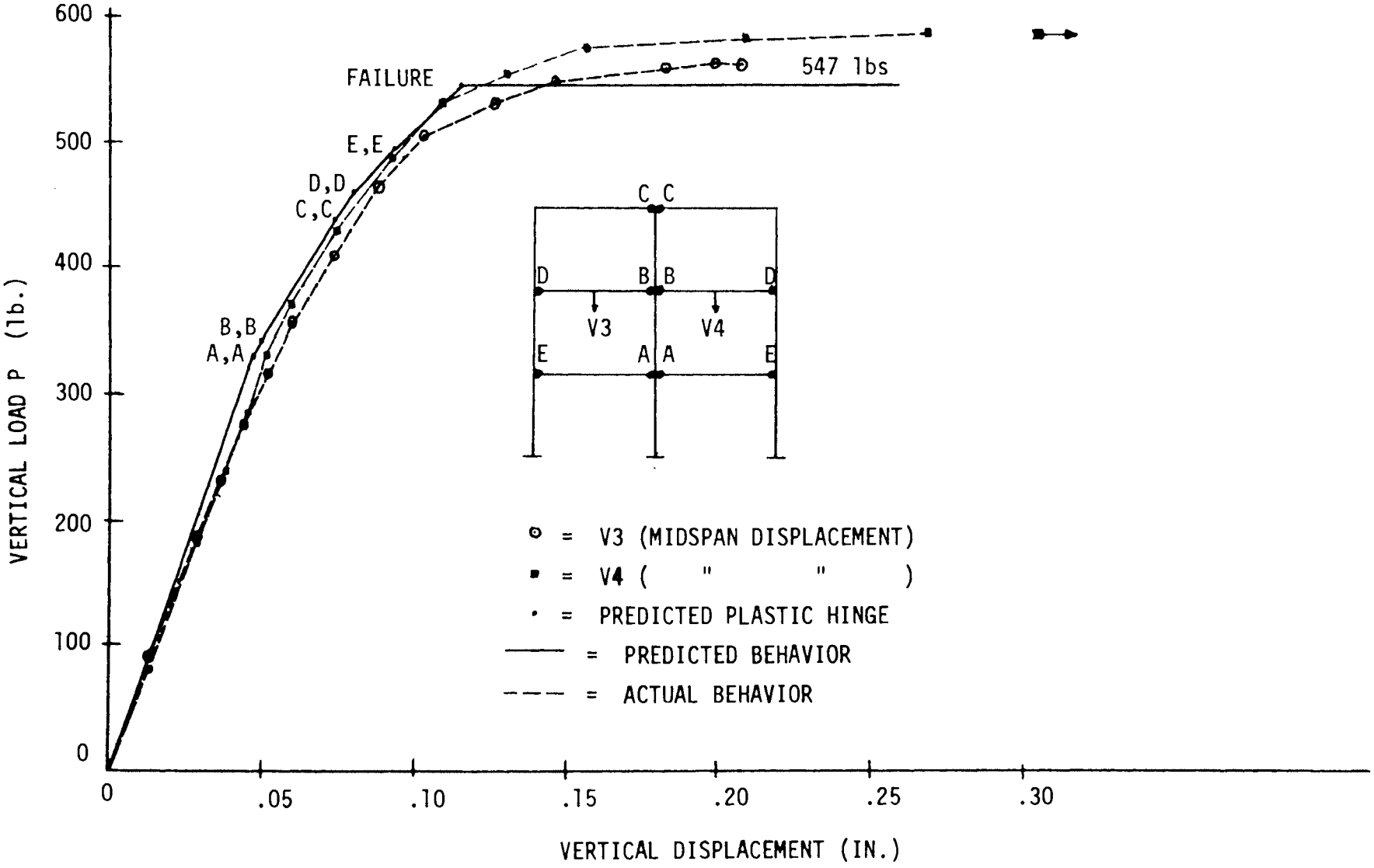

FIGURE 12–LOAD-DISPLACEMENT CURVES FOR SECOND STORY OF FRAME A

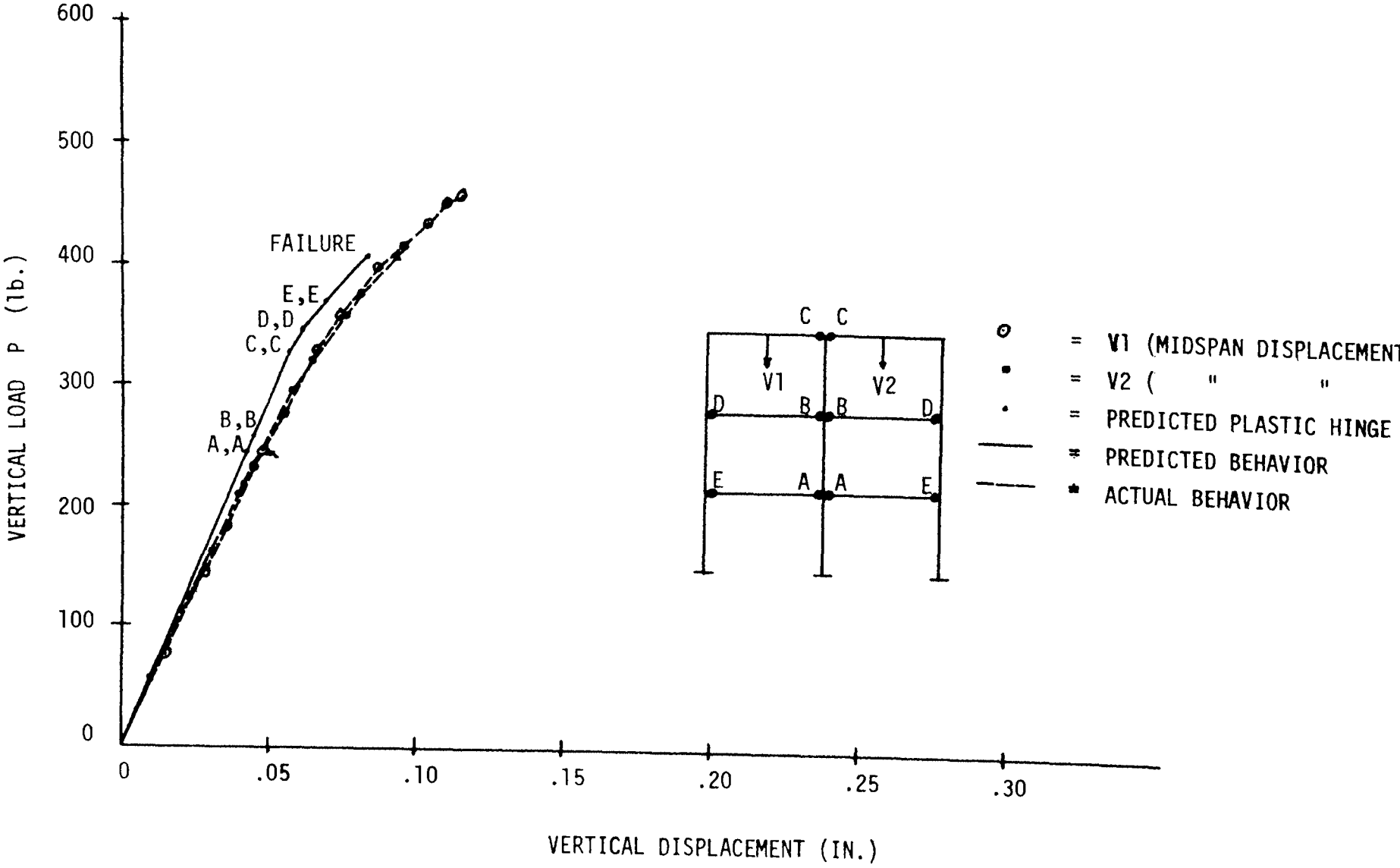

FIGURE 13—LOAD-DISPLACEMENT CURVES FOR THIRD STORY OF FRAME A

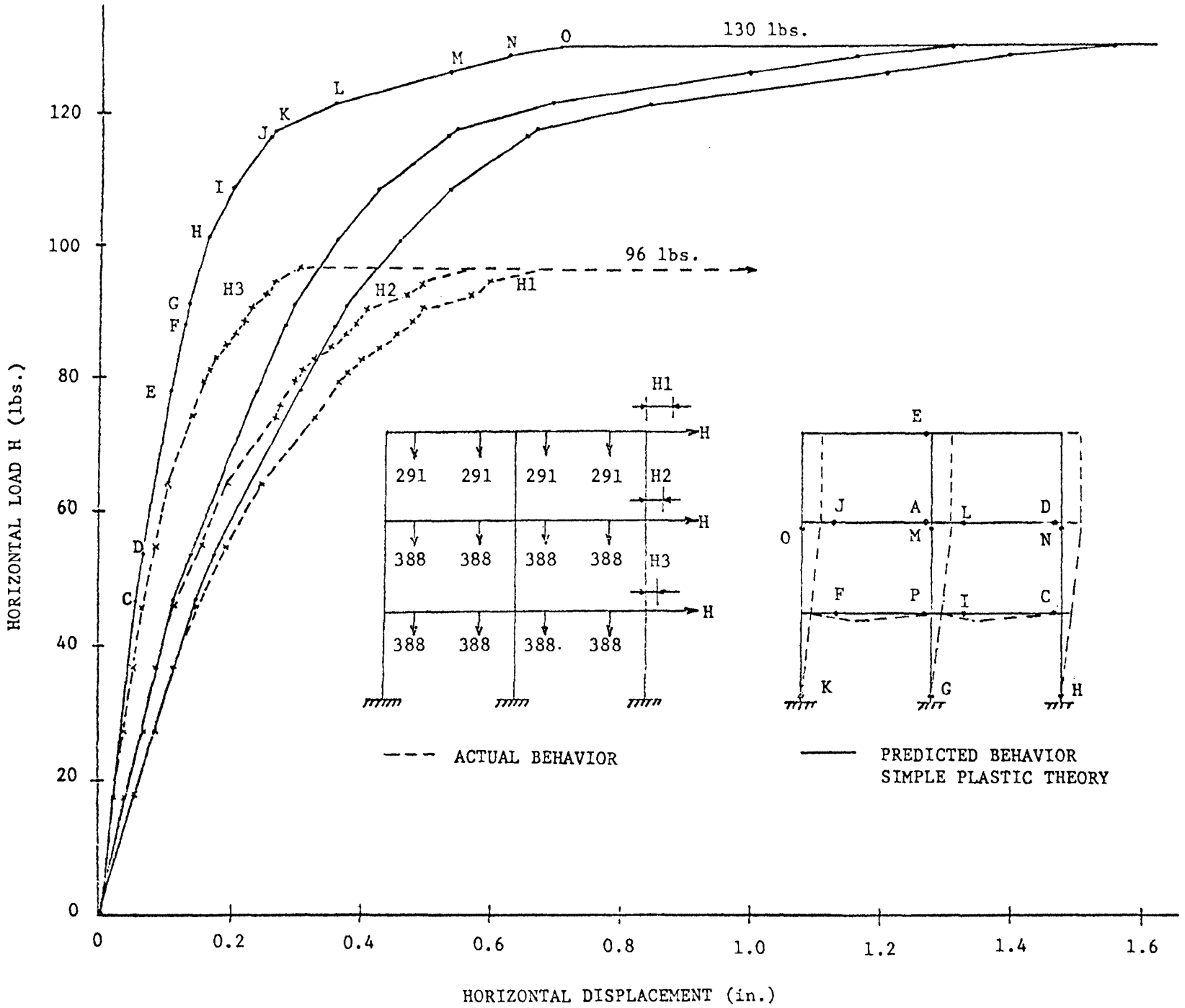

FIGURE 14–LOAD vs. DISPLACEMENT CURVES, MODEL FRAME B

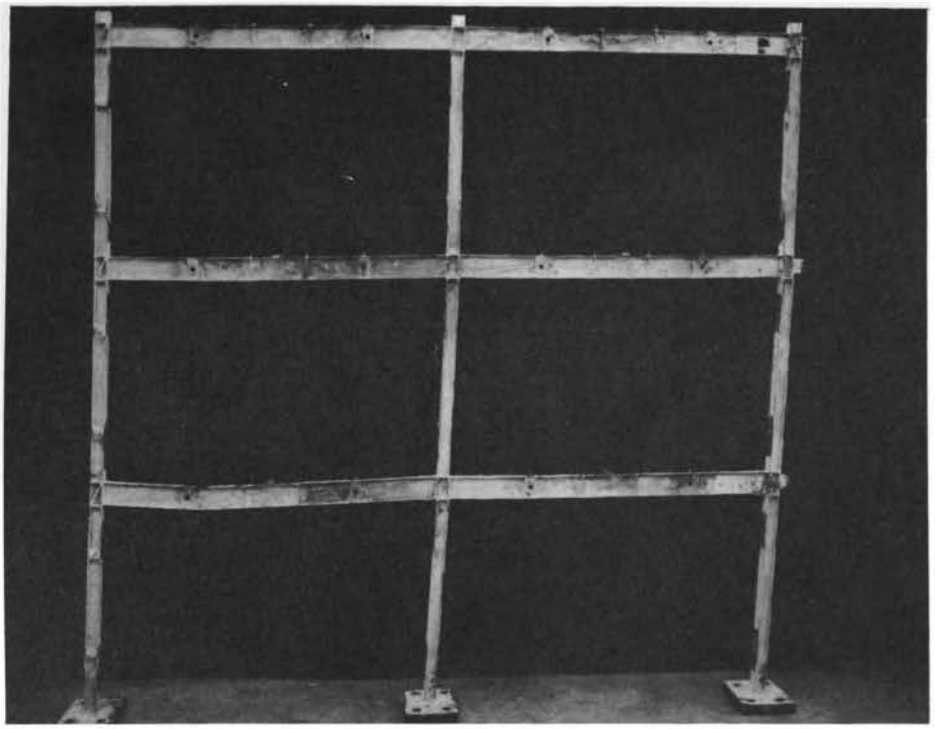

FIGURE 15—FRAME B AFTER TESTING ULTIMATE STRENGTH

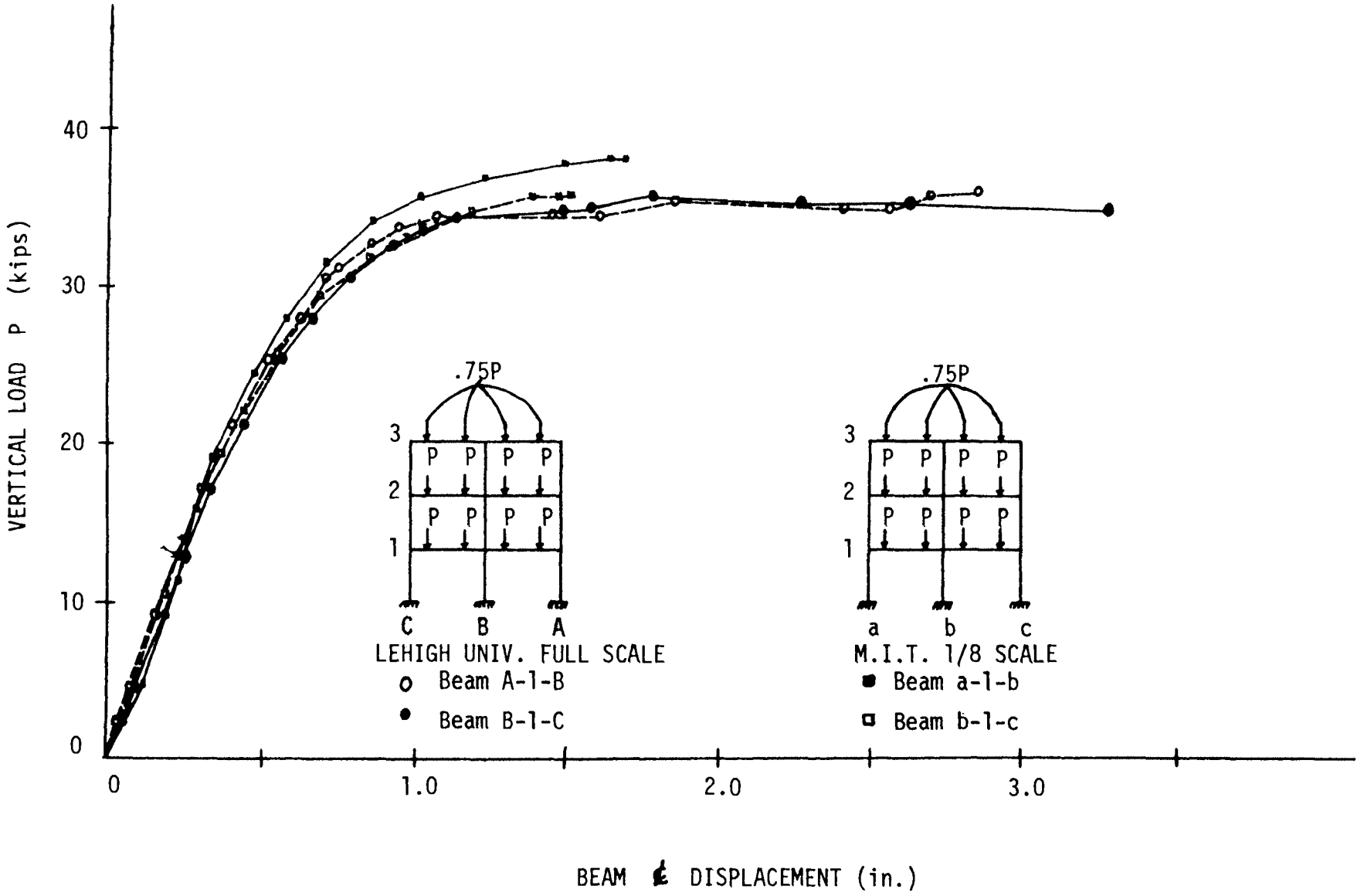

FIGURE 16—PROTOTYPE-MODEL COMPARISON FOR FRAME A

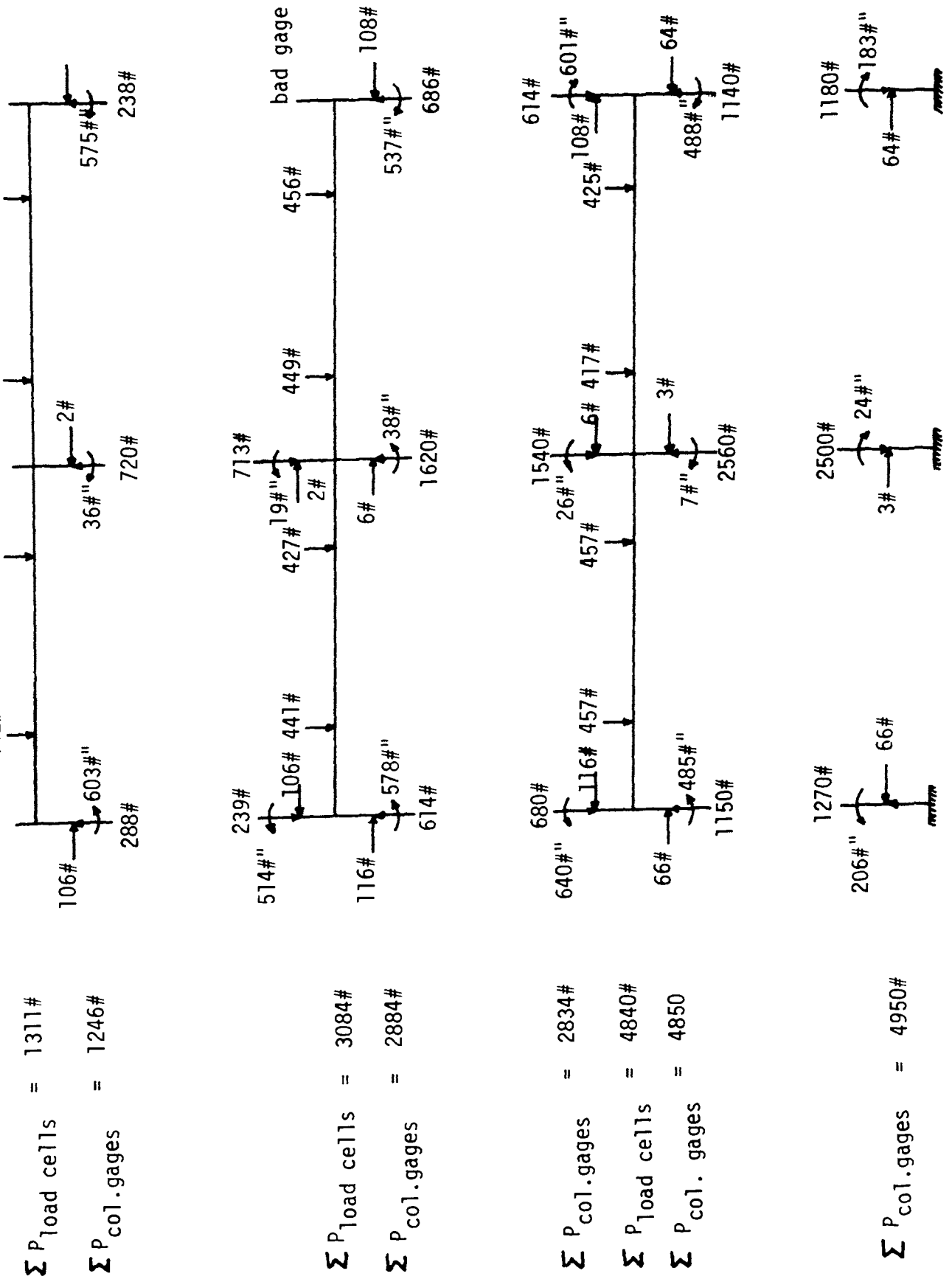

FIGURE 17–STRAIN GAGE DATA REDUCTION, FRAME A LOADING 9

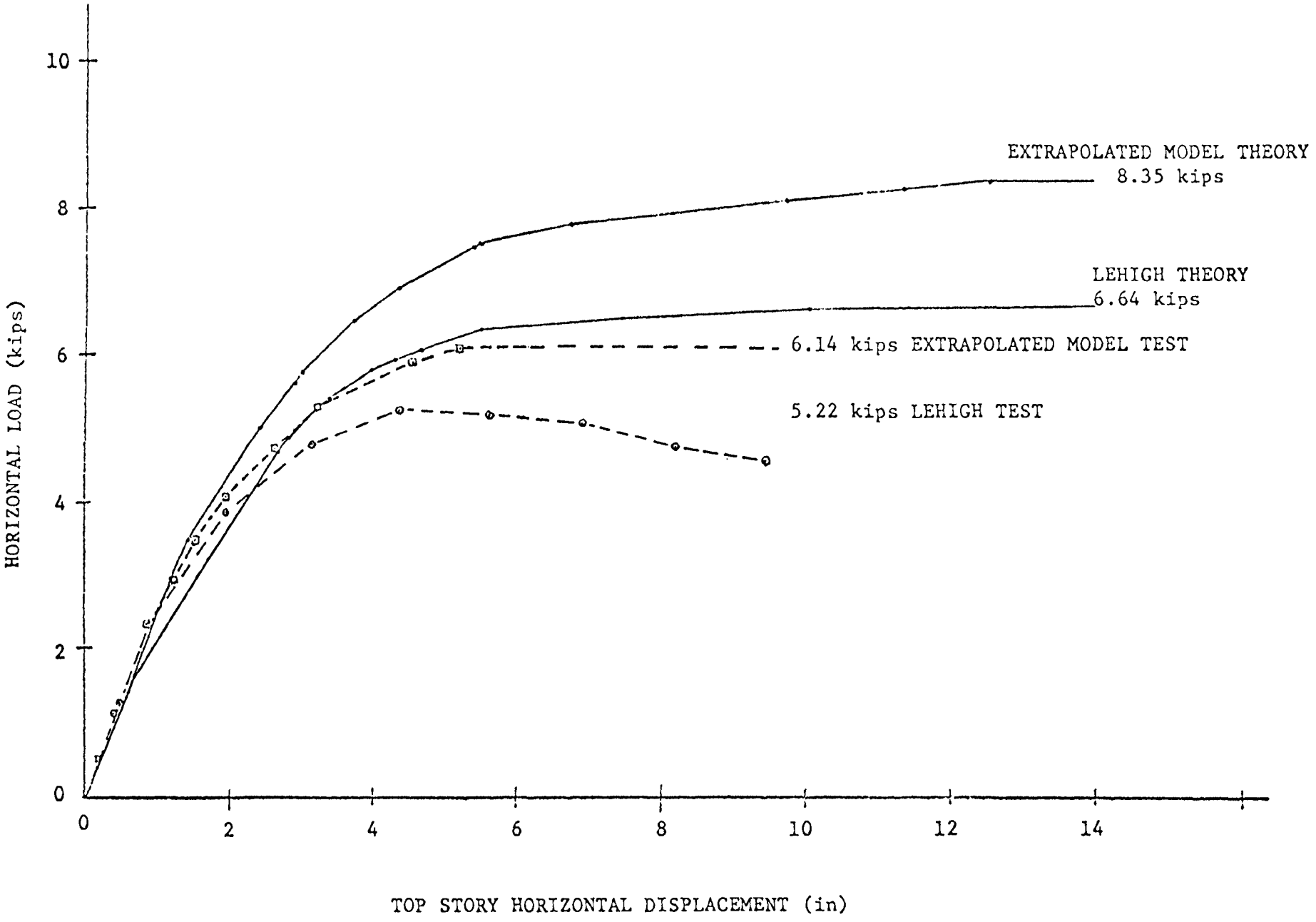

FIGURE 18—FRAME B, LOAD vs. DISPLACEMENT COMPARISONS

PART II

A. SAMPLE CALCULATIONS FRAME A

As described in Section II, Part I, the analysis of this case consisted mainly of inserting hinges and concentrated moments in a structure that was assumed to be behaving in an elastic manner. Consequently, it was only necessary to obtain a solution for two loadings in order to interpolate the magnitude of load when the next plastic hinge formed. For example, the calculations for the load-deflection curve for the lower story beams, when hinges CC (see Figure A2) are about to form, are shown below.

The structure with the hinges shown in Figure A1 exists when P=342.5 lb. With P=425.0 lb., it is found that the moment is largest at the interior column faces of the top story beams. Computer output indicates that the magnitude of these moments and the vertical displacements at midspan of the lower story beams are:

@ P = 425.0 lb., M = -1431 lb.-in., Δ = 0.0683 in.
@ P = 450.0 lb., M = -1518 lb.-in., Δ = 0.0746 in.

From control tests, it is predicted that the plastic moment in the upper story is ± 1480 lb.-in. Therefore, for M_p = -1480 lb.-in.,

$$P = 425.0 + \frac{(1480-1431)\,(25.00)}{(1512-1431)} = 439.0 \text{ lb.}$$

$$\Delta = 0.0683 + \frac{(1480-1431)\,(0.0063)}{(1518-1431)} = 0.0718 \text{ in.}$$

The structure shown in Figure A2 is in equilibrium when P = 439.0 lb.

B. MATERIAL AND SECTION PROPERTIES

The 1/8 scale 6WF25 and the 1/8 scale 12B16.5 sections used in the fabrication of the two frames were milled from solid stock and delivered in lengths of 6 to 10 feet. Each length of material was subjected to cross-section measurements, tension tests, and beam tests as described below.

Cross-Section Measurements

The cross-sectional dimensions of each length of WF shape were measured with micrometers at a cross section near each end and at the mid-length. The dimensions appear in Table B1. The corresponding dimensions as published in the AISC Manual, and scaled to 1/8 actual size, also appear in Table B1 for comparison. From the dimensions given in Table B1, the area, plastic section modulus, elastic section modulus, and moment of inertia in the strong direction were computed. These section properties appear in Table B2.

Tension Tests

To determine the strength properties of each length of material, three tension coupons were cut from one end and one beam specimen from the other end.

A summary of the tension tests conducted is given in Table B3. The average values of yield stress σ_y, tensile stress, σ_u, yield strain, ϵ_y, and the strain at the initiation of strain hardening, ϵ_{sh}, are tabulated.

For each length of material, three sheet metal coupons with the dimensions shown in Figure B1 were cut, one from each flange and one from the web. Each specimen was annealed at 1000°F for one hour (oven cooled). The coupons were tested on the Tinius Olsen testing machine, with a Tinius Olsen S-100 electromechanical extensometer used to measure the strains.

The average yield stress from 12 coupons taken from the 6WF25 shapes varies from 34.3 ksi to 41.3 ksi. The average yield stress from 15 coupons taken from the 12B16.5 shapes varied from 36.9 ksi to 38.8 ksi. The fact that there existed a large variation in the yield stress of the 6WF25 shapes as compared to the 12B16.5

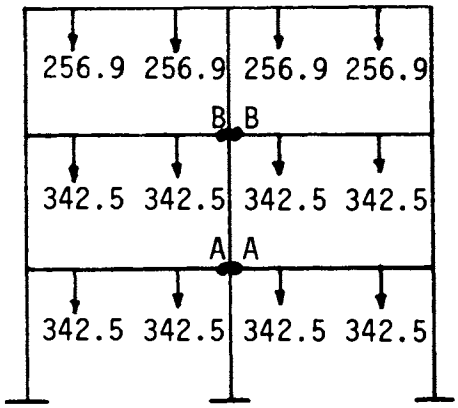

• = PLASTIC HINGE

FIGURE A1–FRAME A WITH P = 342.5 LB.
(LOADS SHOWN ARE IN POUNDS)

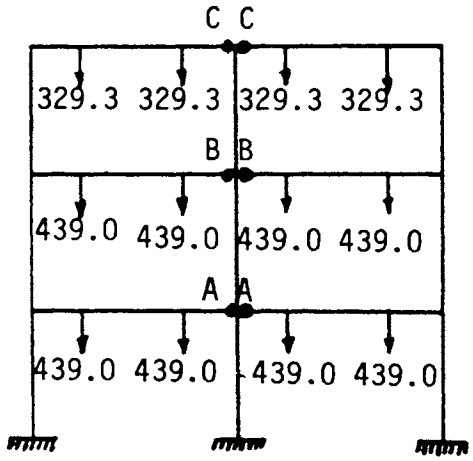

• = PLASTIC HINGE

FIGURE A2–FRAME A WITH P = 439.0 LB.
(LOADS SHOWN ARE IN POUNDS)

shapes can only be explained by considering the random nature of the stock selection.

The results of the tension tests were combined with the scaled handbook section properties to obtain values of P_y and M_p. Based on these P_y and M_p values, the location of beams and columns in Frames A and B was established (see Figure 4, Part I) and these values were then used for the theoretical analysis.

Beam Tests

In order to determine the plastic moment, M_p, of each length of WF shape used, simply supported 12-inch beams loaded at their quarter points were tested. The beams were laterally braced as shown in Figure B2. The lateral bracing was spaced the same as the corresponding lateral bracing of Frames A and B, to check if lateral, local and/or web buckling occurred in the 12B16.5 specimens. No buckling was noted for the 6WF25 specimens.

The beam specimens were tested in an Instron testing machine at a cross-head speed of 0.05 inches per minute. The displacements at midspan were measured with a dial gage. The tests were run until the midspan of the beams deflected one inch, at which time the material was well into the plastic range.

The results of the beam tests are plotted in Figures B3 through B11. Values of M_p for the following cases are compared in Table B4:

1. the tension test results and the handbook section properties,
2. the tension test results and the measured section properties, and
3. the beam test results.

C. LOADING

C.1 VERTICAL LOAD

Vertical loads were applied by means of hydraulic jacks mounted in gravity load simulators (Figure C1). The basis of the design of these mechanisms came from Lehigh University, where similar devices were used in full scale tests of steel frameworks.

The system for supplying hydraulic fluid to the jacks can be seen in Figure C2. For simplicity, it was decided to use hydraulic accumulators which could be pressured up and would supply oil at a varying pressure to a pressure reducing valve. This valve was designed to maintain an adjustable downstream pressure independent of the upstream pressure providing, of course, that the upstream pressure never falls below the required downstream value.

C.2 HORIZONTAL LOAD

Horizontal loads were applied by means of dead weights acting over ball bearing pulleys. The loading set-up is shown schematically in Figure C3. Calibration tests were performed to determine the friction losses in the pulleys. In all three cases the friction loss was less than 10 per cent. Load cells would sense the horizontal load actually applied to the frame.

Even though the gravity load simulators had roller bearings at each pivot point, calibrations showed that they offered resistance to horizontal motion in proportion to the amount of vertical applied load and to the magnitude of horizontal movement. The simulators that offered the least resistance were placed in the top story and those with the most friction were placed in the bottom story, where they would undergo smaller displacements. Used in this way, it is estimated that each pair of simulators (with full vertical load for the Frame B test acting) would absorb four pounds of horizontal shear with a top story displacement of 1.0 inch. At intermediate displaced positions it could be assumed that each pair absorbed one, two or three pounds of horizontal shear. (Subsequent checks, or the actual column shears in Frame B as determined from the strain gages on the columns, verified such friction losses.)

D. INSTRUMENTATION

Loads, deflections, strains and rotations were measured as illustrated in Figure 8, Part I. The loads were measured through tension load cells

utilizing four electrical resistance strain gages. The calibration factors used to convert the output of the load cells to pounds appear in Table D1. The output of the vertical load cells was read on a digital voltmeter and the horizontal ones on a BLH Type N strain indicator.

Deflections were read by means of dial gages used in pairs, one on either side of the member, to account for any twisting of the member.

The strains at the outside of each flange, top and bottom of the columns for each story, were measured by means of electrical resistance strain gages (Baldwin Lima Hamilton FAB-25-12 gages for Frame A and FA-25-12 gages for Frame B). The strains were measured to enable the determination of the axial load, bending moments and shears present in each column. This afforded a check on the total applied story load, and also enabled the distribution of the total load to each column to be checked.

The rotations of the column bases were measured by means of rotary position LVDT's. Since the column bases were theoretically "fixed", these measurements provided an experimental check on the degree of fixity achieved. The calibration factors for the rotation transducers are listed in Table D2. Their output was read on a digital voltmeter.

TABLE B1

CROSS-SECTIONAL DIMENSIONS

Member	Depth (inch)	Top Flange Width (inch)	Bottom Flange Width (inch)	Top Flange Thickness (inch)	Bottom Flange Thickness (inch)	Web Thickness (inch)
6WF25						
Handbook	.796	.760		.057		.040
C-1						
left end	.800	.763	.763	.055	.054	.043
	.797			.056	.055	.042
	.792					
mid length	.809	.763	.766	.057	.055	.042
	.804			.055	.055	.042
	.797					
right end	.809	.763	.764	.057	.057	.042
	.803			.055	.055	.042
	.797					
average	.801	.764		.055		.042
C-2						
left end	.797	.769	.763	.055	.054	.041
	.801			.056	.056	.041
	.807					
mid length	.799	.765	.762	.056	.056	.041
	.799			.055	.054	.041
	.804					
right end	.803	.765	.762	.055	.056	.042
	.799			.055	.055	.041
	.799					
average	.801	.764		.055		.041
C-3						
left end	.804	.755	.760	.055	.053	.041
	.798			.055	.053	.041
	.797					
mid length	.803	.761	.756	.056	.056	.041
	.802			.055	.054	.041
	.800					
right end	.799	.764	.759	.055	.056	.041
	.801			.055	.054	.041
	.802					
average	.799	.759		.055		.041

TABLE B1 (Cont'd)

Member	Depth (inch)	Top Flange Width (inch)	Bottom Flange Width (inch)	Top Flange Thickness (inch)	Bottom Flange Thickness (inch)	Web Thickness (inch)
C-4						
left end	.803	.761	.762	.055	.055	.041
	.799			.054	.053	.041
	.797					
mid length	.800	.765	.763	.056	.055	.042
	.799			.054	.053	.041
	.804					
right end	.796	.764	.763	.055	.054	.041
	.798			.054	.055	.041
	.802					
average	.799		.763		.055	.041
12B16.5						
Handbook	1.500		.500		.034	.029
B-1						
left end	1.505	.499	.501	.032	.033	.030
	1.505			.035	.033	.030
	1.504					
mid length	1.505	.501	.503	.032	.033	.030
	1.505			.035	.033	.029
	1.505					
right end	1.505	.501	.502	.032	.033	.029
	1.504			.034	.032	.029
	1.505					
average	1.505		.501		.033	.030
B-2						
left end	1.500	.499	.502	.031	.034	.029
	1.500			.033	.033	.030
	1.501					
mid length	1.508	.496	.499	.033	.032	.029
	1.504			.034	.033	.028
	1.499					
right end	1.506	.499	.501	.032	.035	.028
	1.504			.033	.033	.028
average	1.502		.499		.033	.029

TABLE B1 (Cont'd)

Member	Depth (inch)	Top Flange Width (inch)	Bottom Flange Width (inch)	Top Flange Thickness (inch)	Bottom Flange Thickness (inch)	Web Thickness (inch)
B-3						
left end	1.499	.501	.500	.034	.034	.027
	1.500			.033	.033	.028
	1.496					
mid length	1.500	.500	.500	.034	.033	.027
	1.500			.033	.033	.028
	1.497					
right end	1.498	.501	.500	.034	.034	.027
	1.500			.033	.033	.028
	1.497					
average	1.499	.500		.034		.028
B-4						
left end	1.500	.503	.502	.033	.032	.031
	1.501			.035	.034	.029
	1.501					
mid length	1.501	.503	.501	.033	.032	.030
	1.502			.035	.033	.029
	1.502					
right end	1.499	.503	.496	.031	.031	.031
	1.501			.034	.034	.030
	1.501					
average	1.501	.501		.033		.030
B-5						
left end	1.501	.504	.503	.032	.033	.029
	1.501			.035	.034	.029
	1.499					
mid length	1.505	.504	.502	.032	.034	.028
	1.504			.034	.031	.029
	1.500					
right end	1.509	.504	.502	.033	.033	.030
	1.505			.033	.034	.029
	1.498					
average	1.502	.503		.033		.029

TABLE B2. CROSS-SECTIONAL PROPERTIES

Member	Area (inch^2)	Z_x (inch^3)	S_x (inch^3)	I_x (inch^4)
6WF25				
Handbook	.115	.0372	.0328	.0131
C-1	.113	.0363	.0321	.0128
C-2	.112	.0362	.0320	.0128
C-3	.112	.0359	.0317	.0126
C-4	.112	.0360	.0319	.0127
12B16.5				
Handbook	.076	.0402	.0342	.0259
B-1	.076	.0398	.0337	.0253
B-2	.075	.0391	.0331	.0249
B-3	.074	.0392	.0334	.0250
B-4	.076	.0397	.0335	.0252
B-5	.075	.0393	.0333	.0250

TABLE B3. TENSILE TEST RESULTS

Member	σ_y (ksi)	σ_u (ksi)	ϵ_y (in/in)	ϵ_{sh} (in/in)
6WF25				
C-1	41.3	61.5	.0014	.022
C-2	34.3	50.1	.0012	.025
C-3	39.5	60.0	.0014	.021
C-4	34.3	49.9	.0012	.024
12B16.5				
B-1	37.0	56.2	.0013	.017
B-2	38.8	56.8	.0013	.015
B-3	38.3	56.9	.0013	.015
B-4	38.8	57.0	.0013	.014
B-5	36.9	56.2	.0013	.016

TABLE B4. COMPARISON OF PLASTIC MOMENTS

Member	$M_p(1)$ (lb-in)	$M_p(2)$ (lb-in)	$M_p(3)$ (lb-in)
6WF25			
C-1	1535	1500	1450
C-2	1275	1240	1200
C-3	1465	1420	1440
C-4	1275	1230	1160
12B16.5			
B-1	1480	1450	1464
B-2	1555	1495	1462
B-3	1535	1455	1470
B-4	1560	1520	1476
B-5	1480	1450	1450

$M_p(1)$ = Tensile Test results x 1/8 scale handbook plastic section modulus.

$M_p(2)$ = Tensile Test results x computed plastic section modulus.

$M_p(3)$ = Beam Test results.

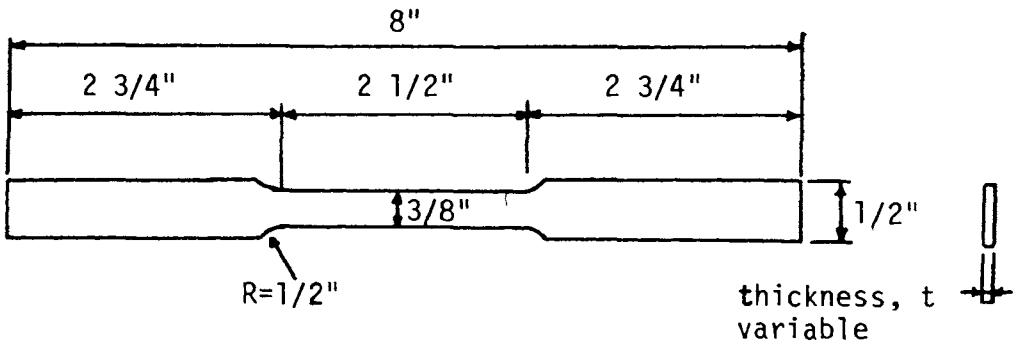

FIGURE B1—TENSION COUPON

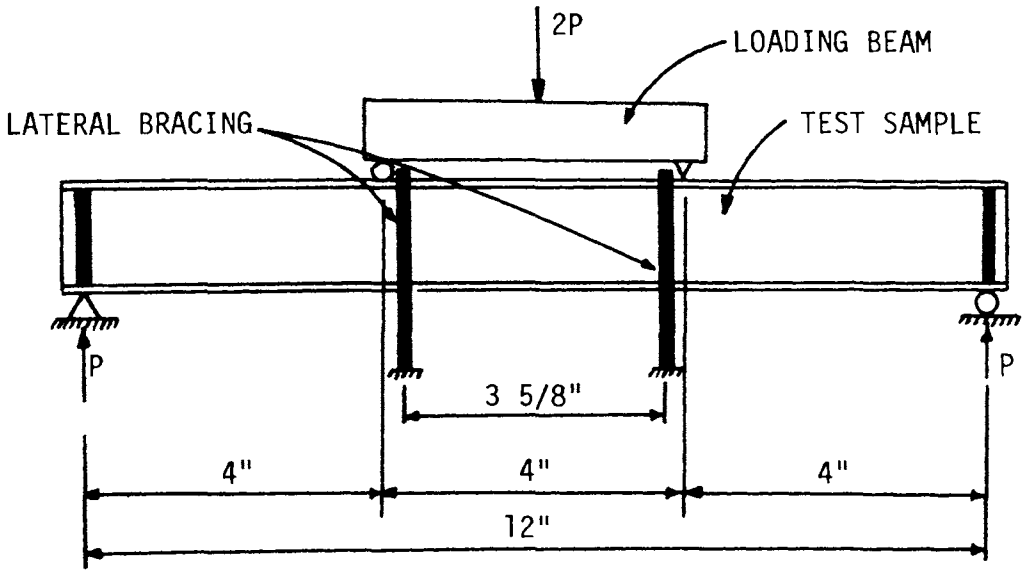

FIGURE B2—SETUP OF BEAM TEST

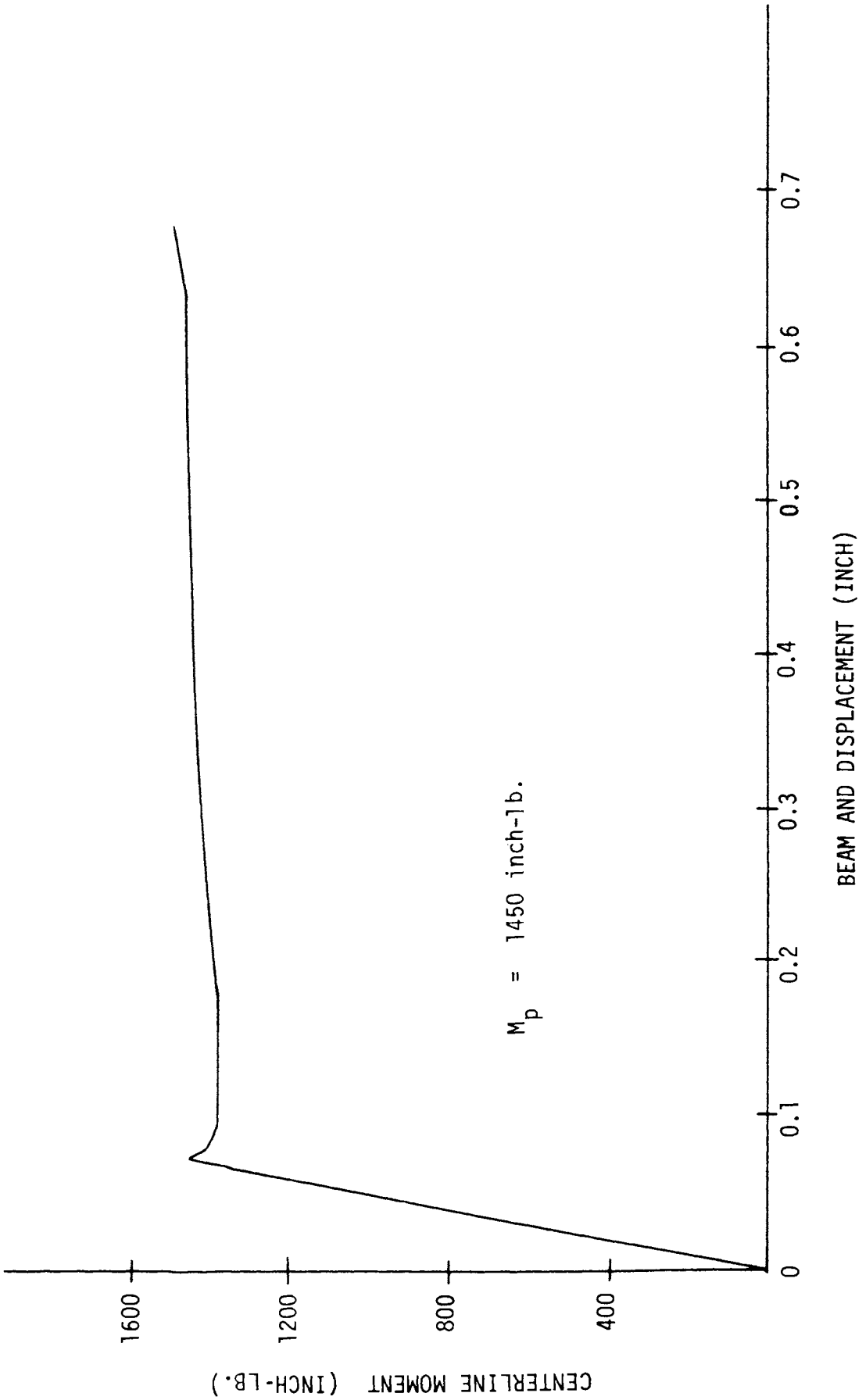

FIGURE B3–BEAM TEST RESULT FOR SAMPLE C1

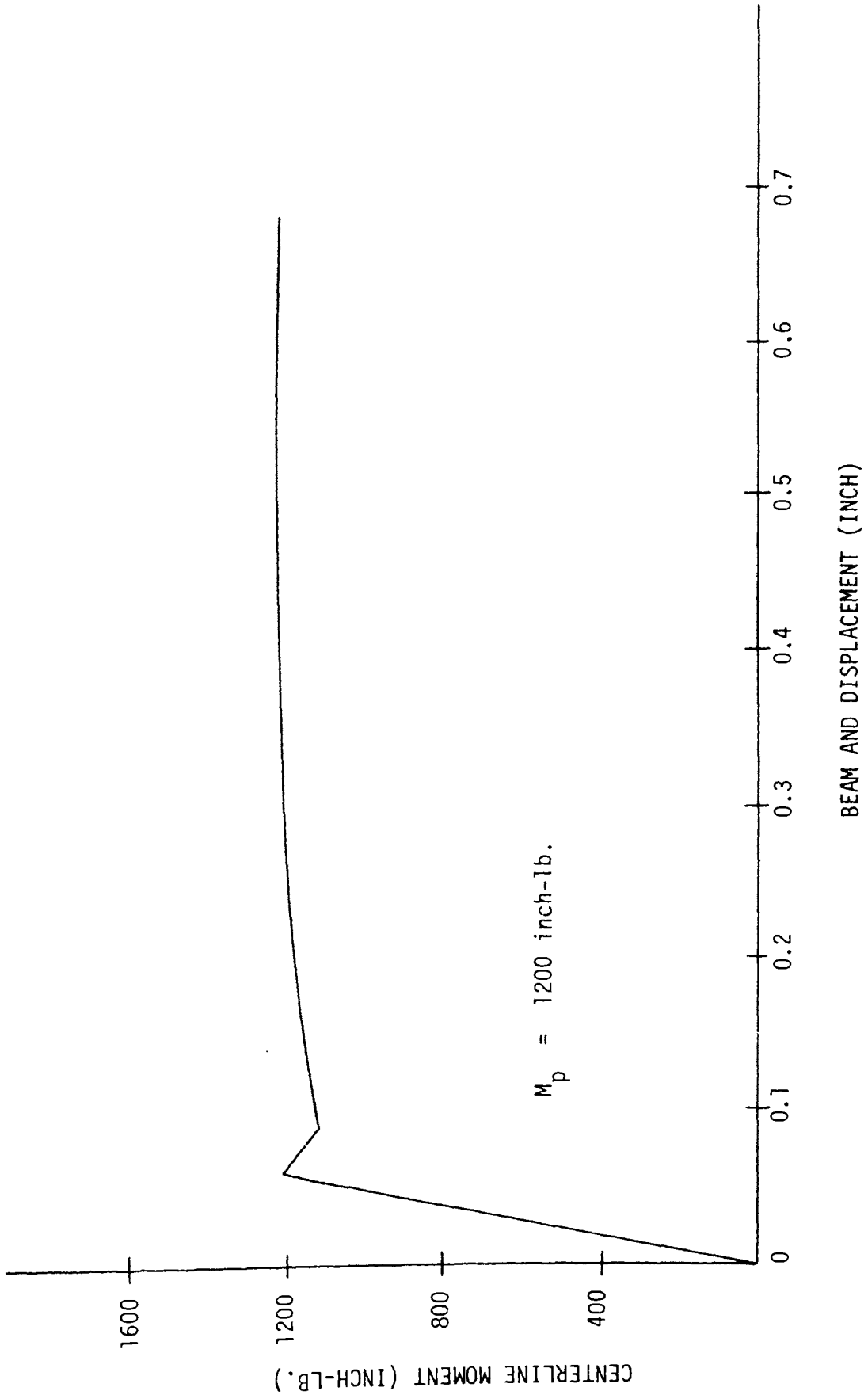

FIGURE B4–BEAM TEST RESULTS FOR SAMPLE C2

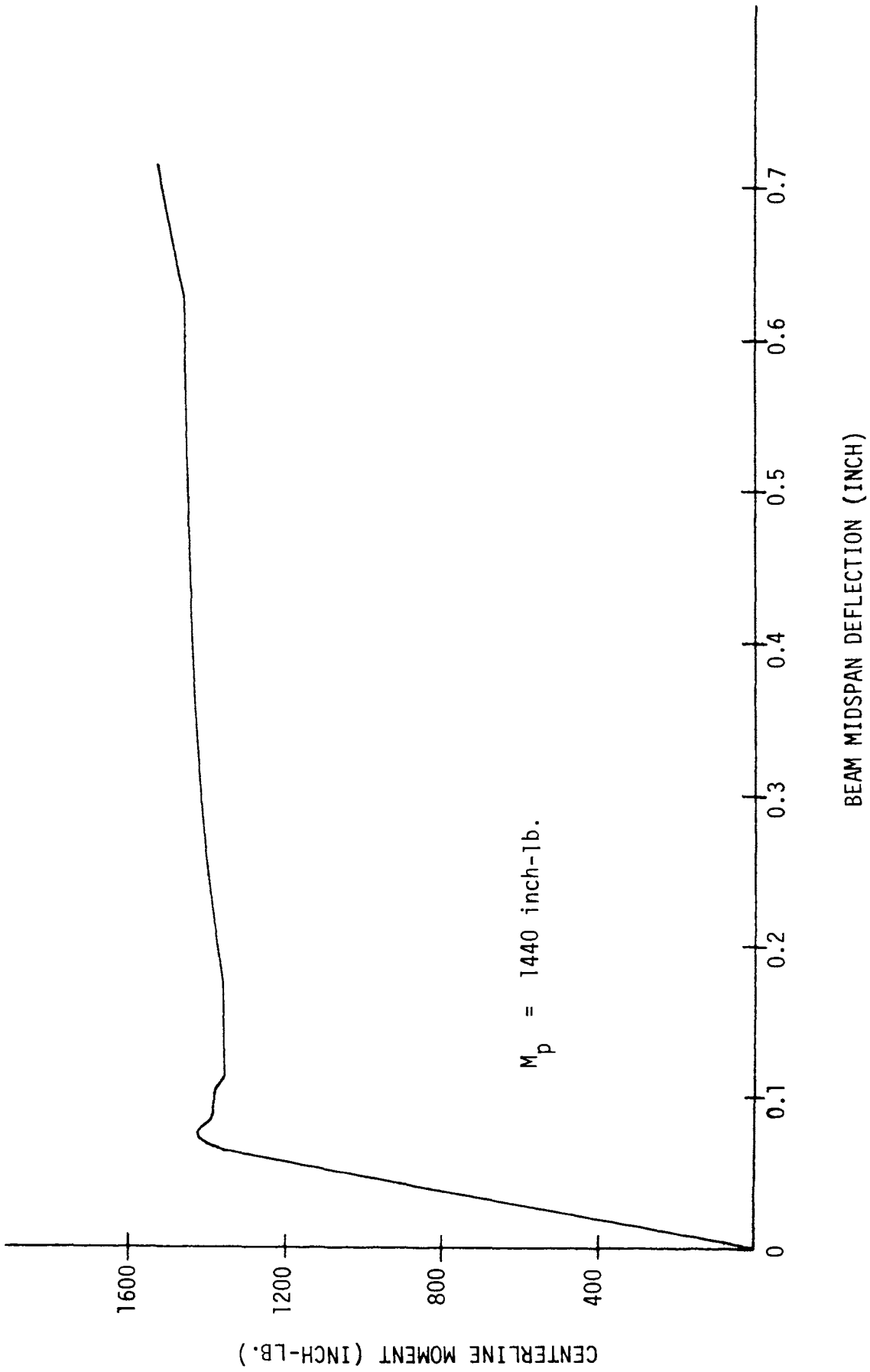

FIGURE B5–BEAM TEST RESULTS FOR SAMPLE C3

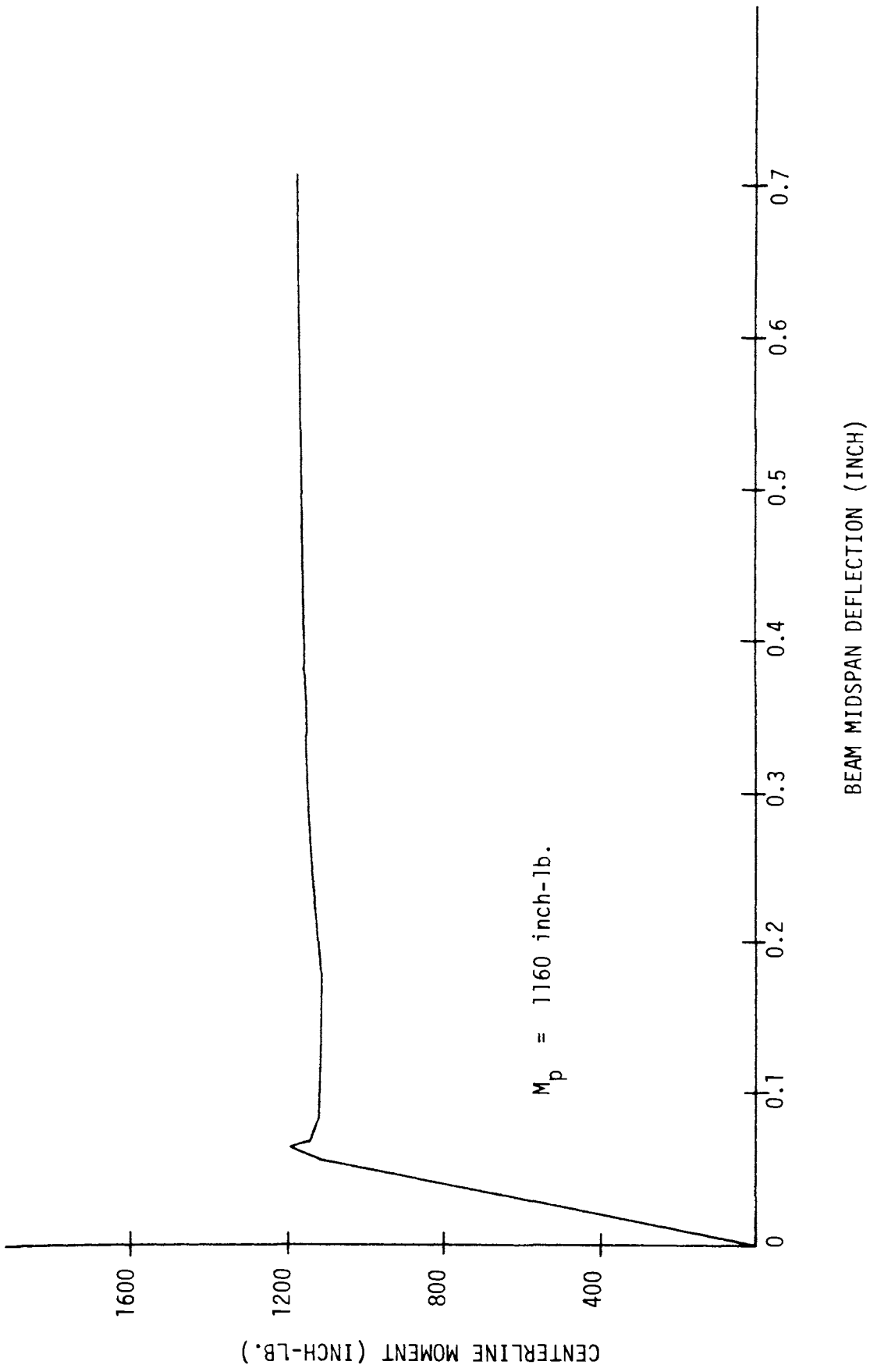

FIGURE B6–BEAM TEST RESULTS FOR SAMPLE C4

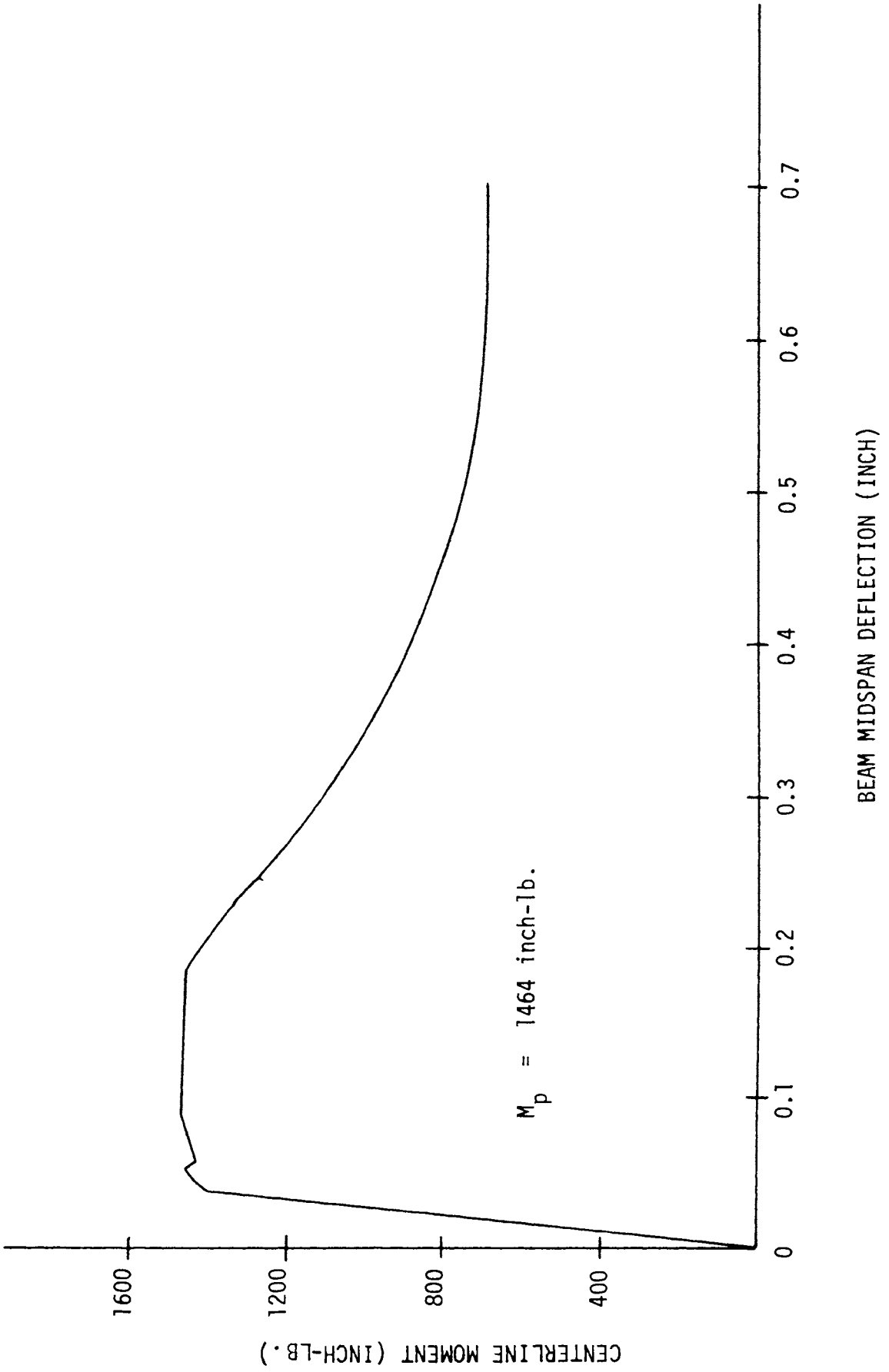

FIGURE B7–BEAM TEST RESULTS FOR SAMPLE B1

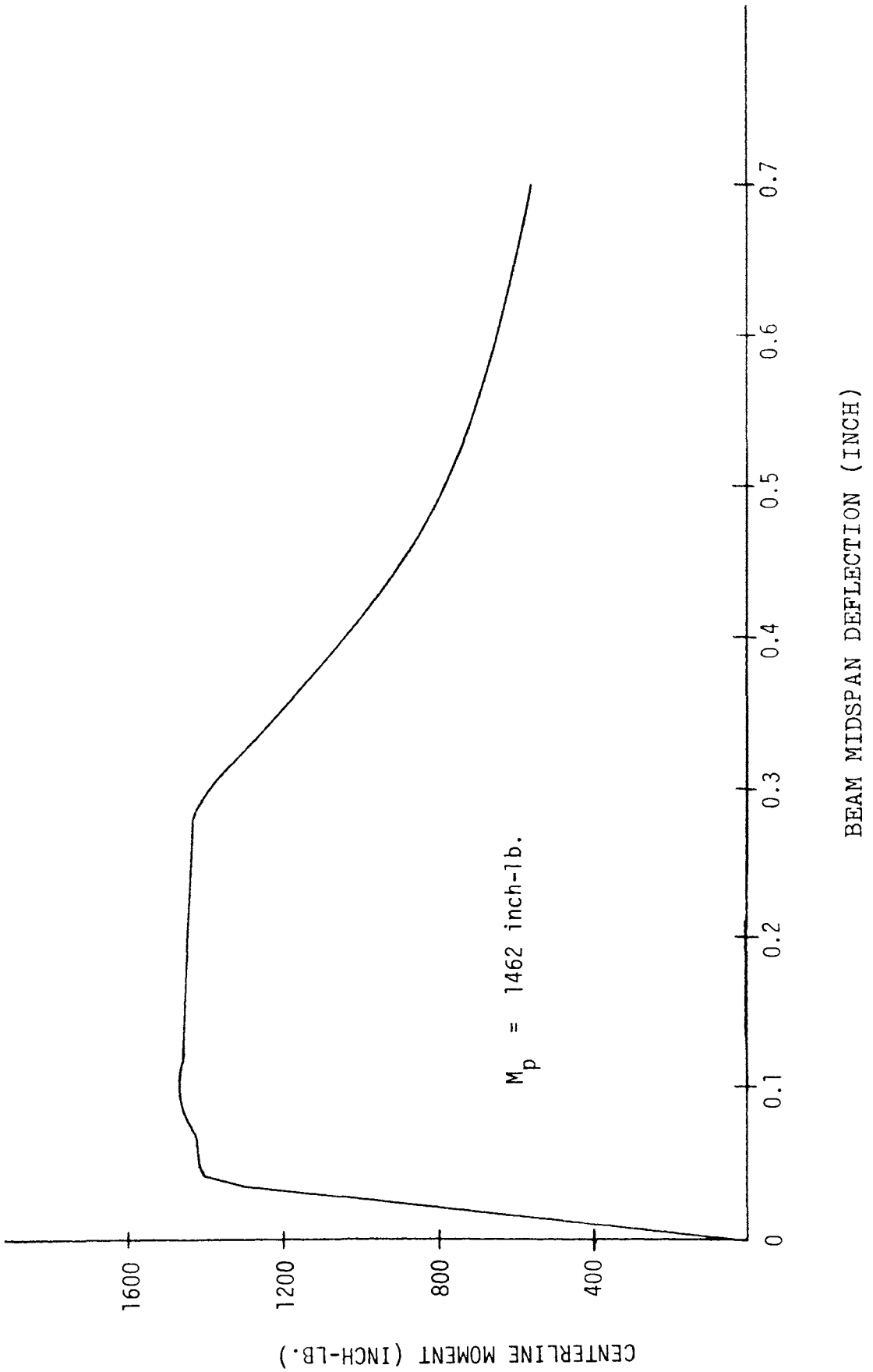

FIGURE B8–BEAM TEST RESULTS FOR SAMPLE B2

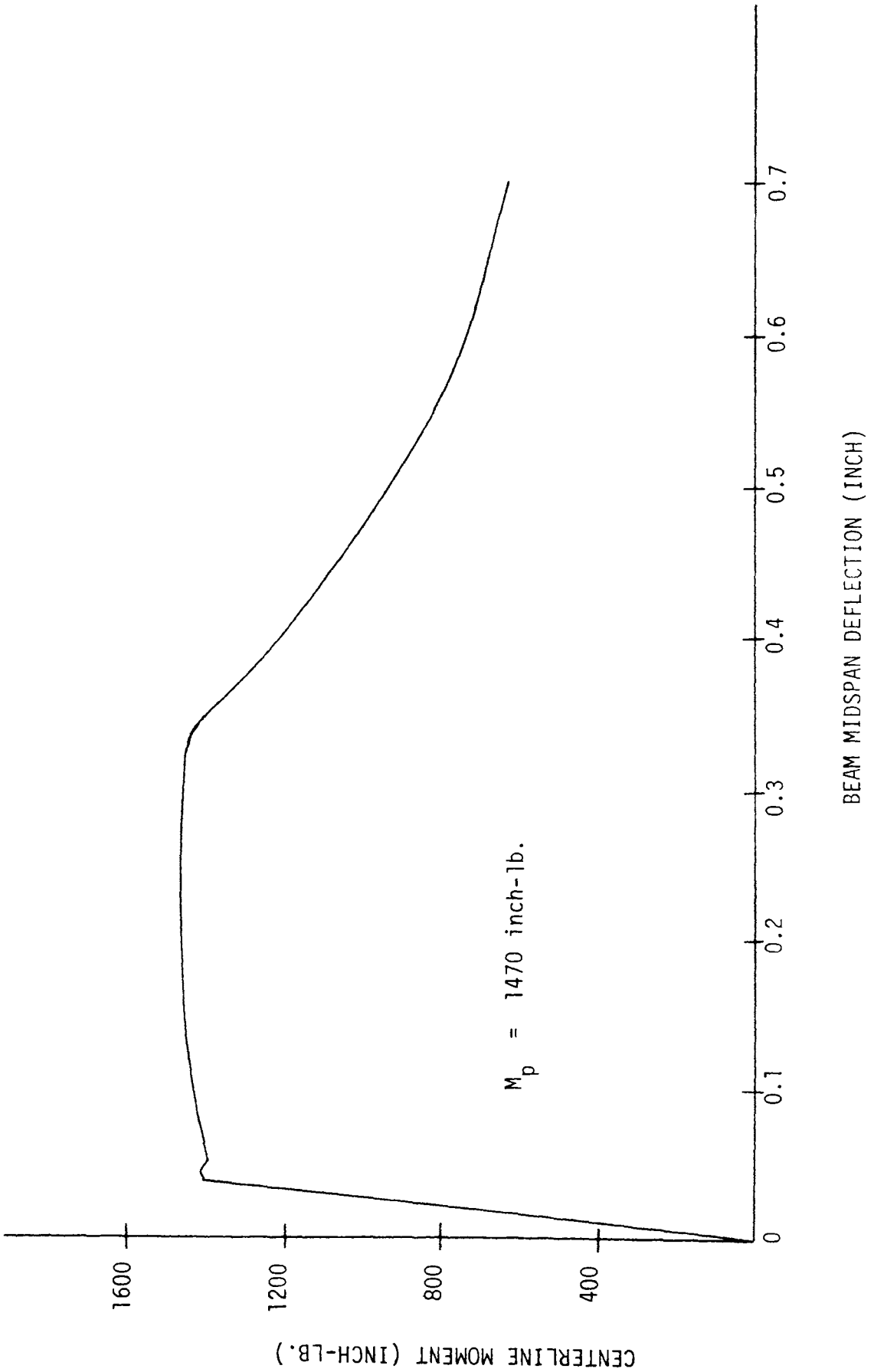

FIGURE B9—BEAM TEST RESULTS FOR SAMPLE B3

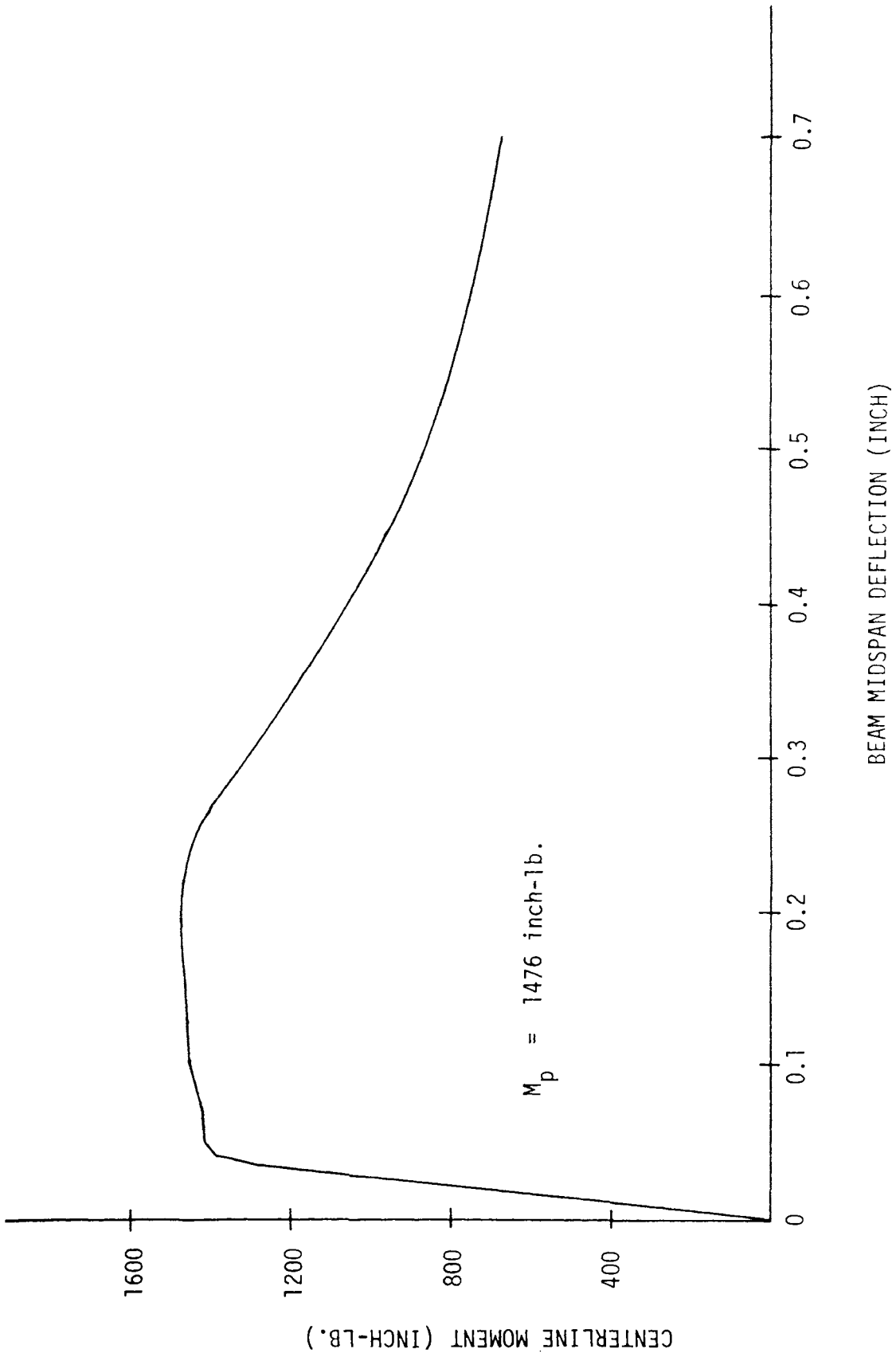

FIGURE B10–BEAM TEST RESULTS FOR SAMPLE B4

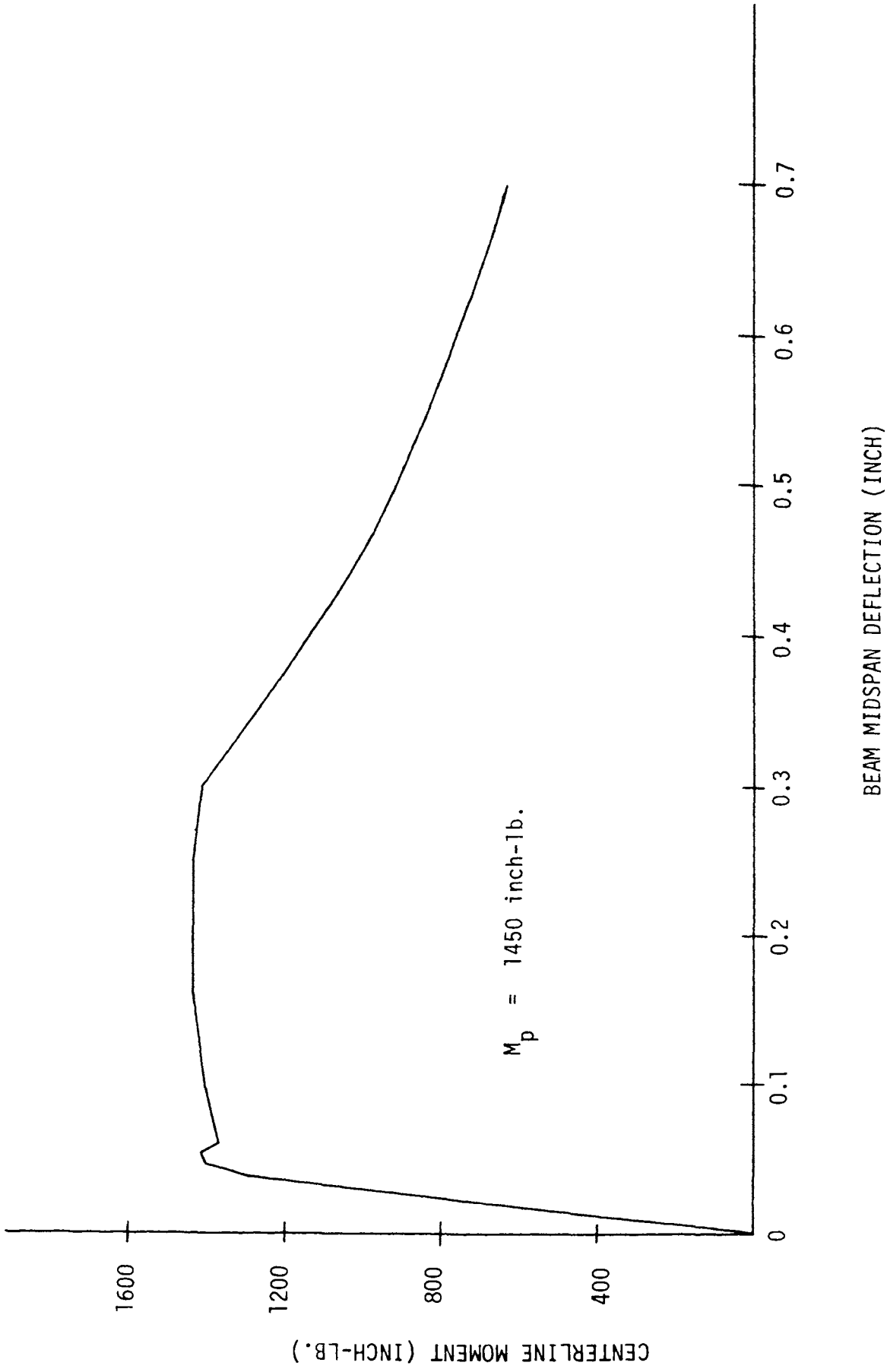

FIGURE B11—BEAM TEST RESULTS FOR SAMPLE B5

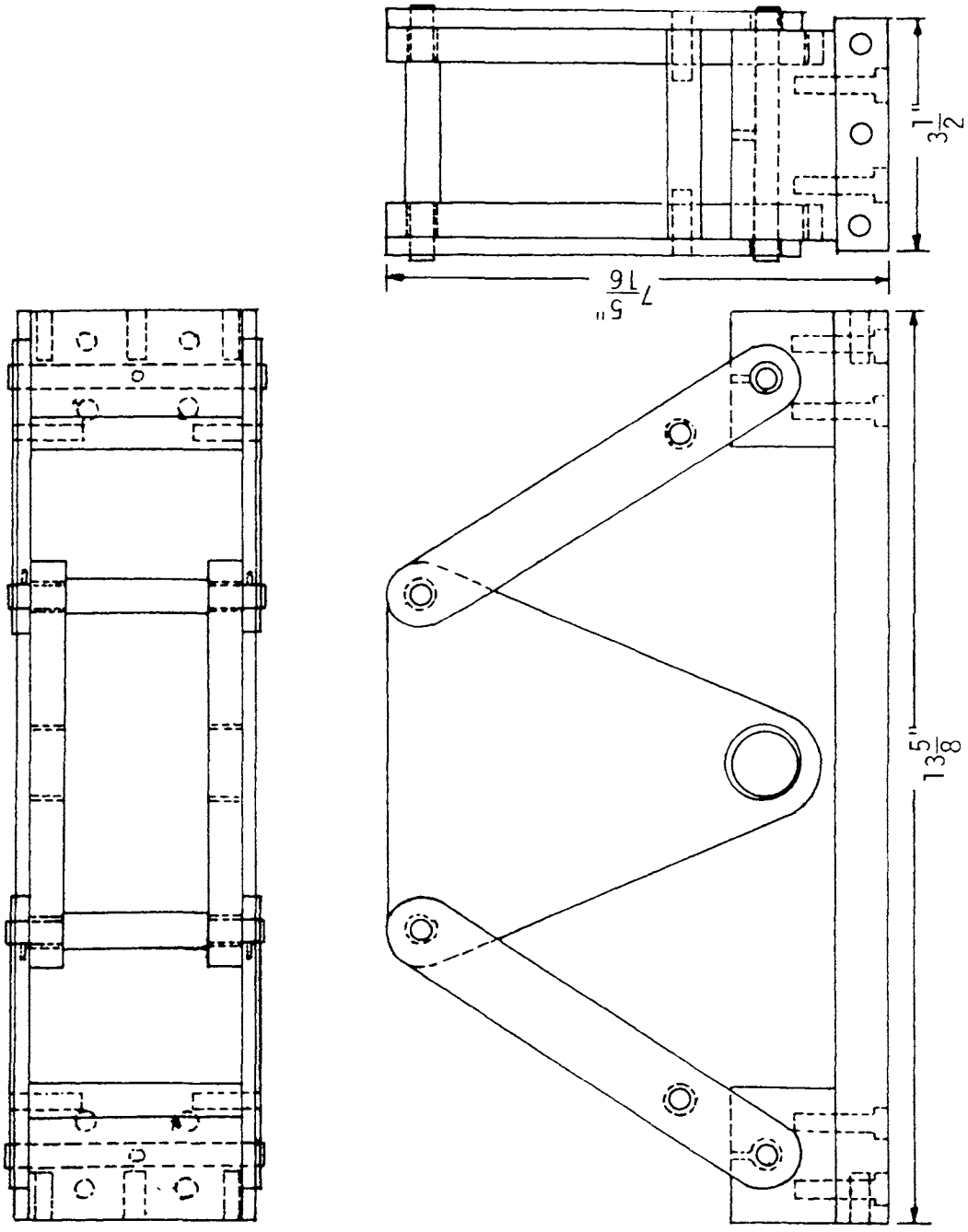

FIGURE C1–GRAVITY LOAD SIMULATOR

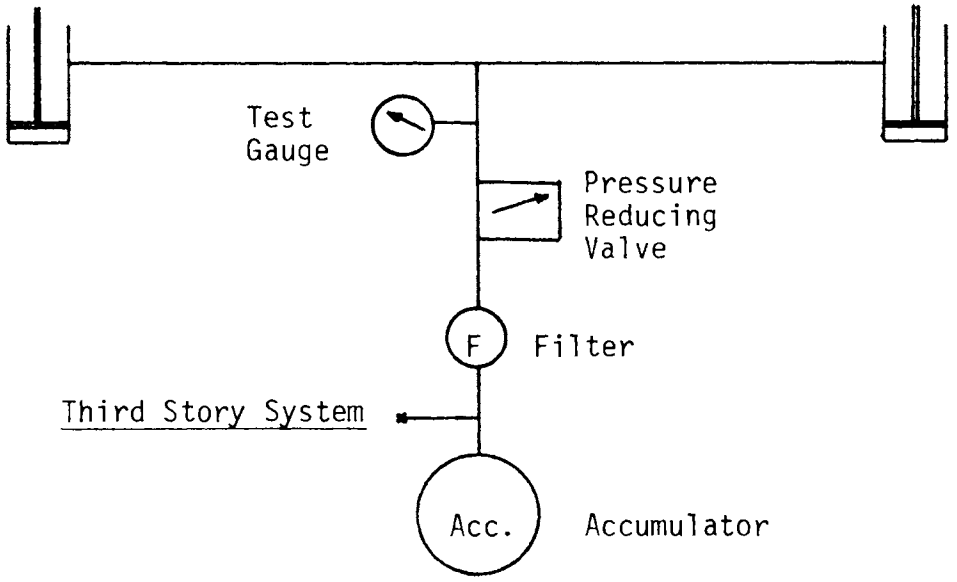

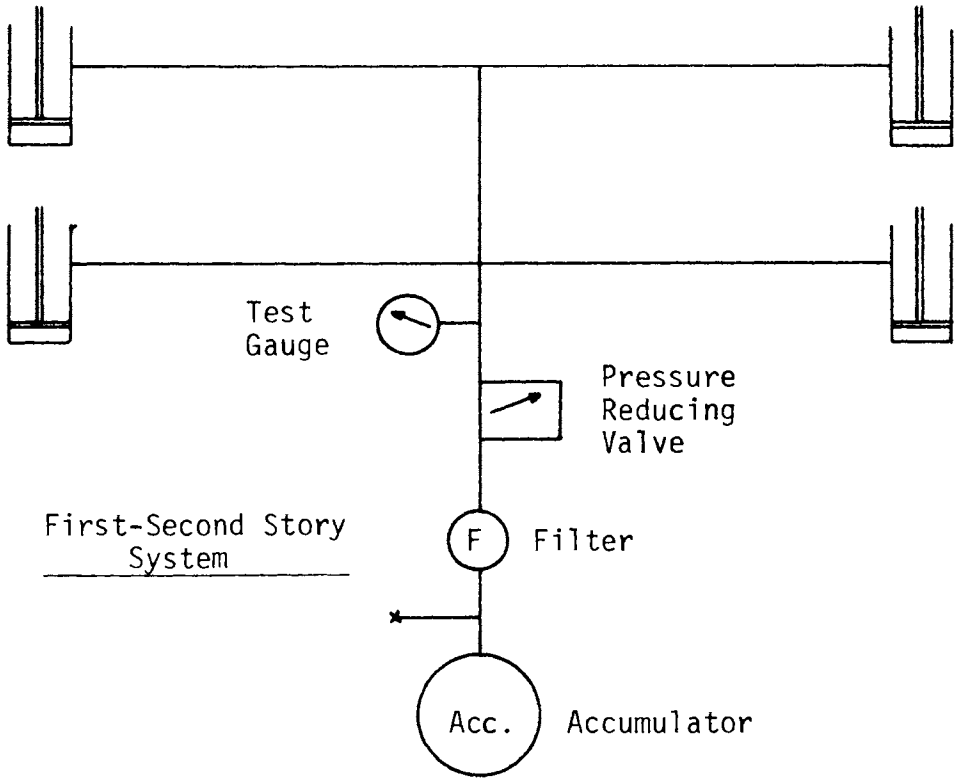

FIGURE C2–SCHEMATIC DIAGRAM OF HYDRAULIC SYSTEM FOR APPLYING VERTICAL LOADS

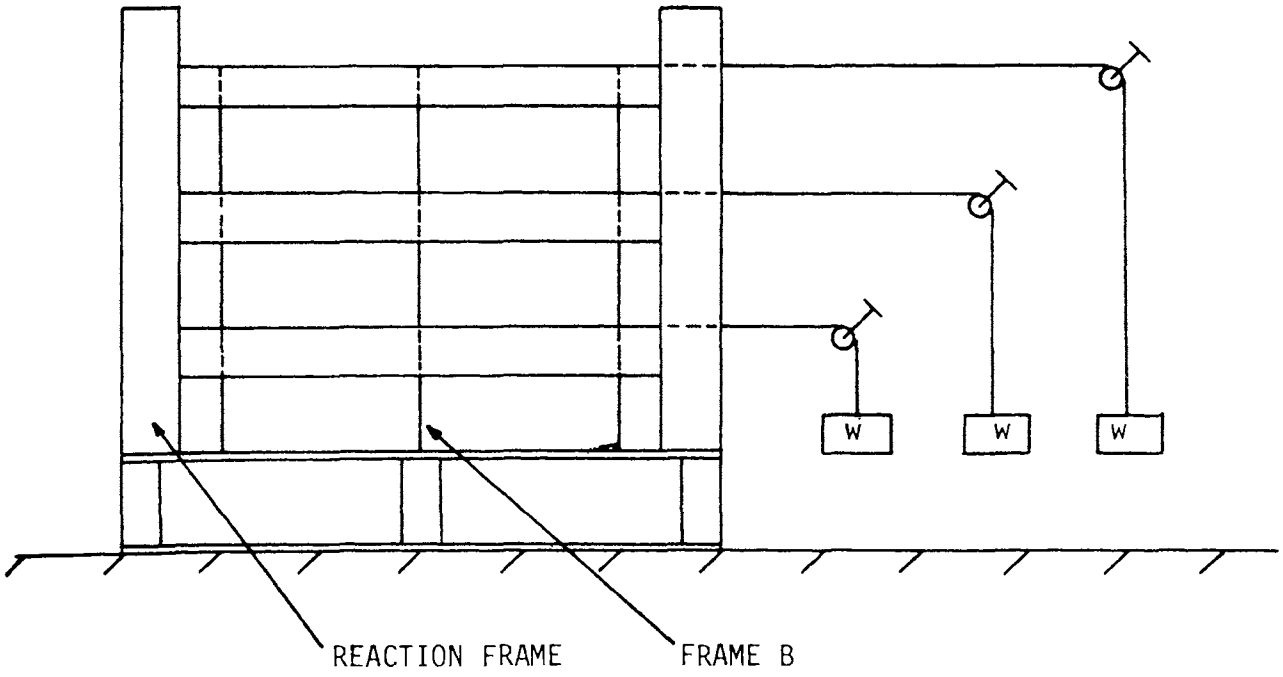

FIGURE C3–HORIZONTAL LOADING SYSTEM TO BE USED FOR FRAME B

TABLE D1 CALIBRATION FACTORS FOR LOAD CELLS

Load Cell	Calibration Factor lb/volt for 3 volt D.C. Excitation	Load Cell	Calibration Factor lb/microinch BLH Type N Strain Indicator
A	232	H1	0.364
B	236	H2	0.364
C	226	H3	0.351
D	240		
E	236		
F	248		
G	235		
H	240		
I	239		
J	240		
K	236		
L	234		

TABLE D2 CALIBRATION FACTORS FOR ROTARY POSITION TRANSDUCERS

Rotary Transducer	Calibration Factor deg/volt for 10 volt D.C. Excitation
R_a	0.71
R_b	0.74
R_c	1.08

E. FRAME A TEST RESULTS

TABLE E1

FRAME A 1/4 POINT LOADS (POUNDS)

Loading	A	B	C	D	E	F	G	H	I	J	K	L
1	79	73	56	60	90	89	84	75	66	82	73	75
2	146	141	118	130	188	183	187	181	165	185	161	168
3	179	180	155	168	234	224	238	234	252	241	211	216
4	228	229	201	218	280	270	287	284	300	290	257	262
5	241	244	208	225	322	309	329	329	338	332	298	304
6	275	277	238	257	363	350	370	371	381	377	340	346
7	308	311	268	289	405	392	414	418	422	421	384	390
8	325	330	285	307	418	404	426	431	436	433	396	402
9	342	347	299	323	441	427	449	456	457	457	417	425
10	355	359	310	334	473	458	483	491	486	491	451	460
11	367	372	322	347	478	463	486	495	491	495	455	462
12	378	384	332	357	491	474	500	510	502	509	470	477
13	367	374	332	357	501	484	508	521	514	522	480	487
14	386	392	340	366	503	486	512	522	515	523	483	491
15	393	400	347	373	513	495	523	534	526	534	491	500
16	397	403	349	376	526	509	534	546	538	547	504	511
17	408	416	361	388	533	516	541	555	544	553	511	518
18	411	418	362	390	541	523	548	561	546	562	516	523
19	431	439	381	410	550	533	559	573	562	572	528	534
20	431	439	381	409	558	539	567	582	568	581	537	544
21	438	446	388	415	572	553	580	595	582	597	551	556
22	443	451	392	420	566	548	573	586	577	590	546	551
23	447	455	396	424	572	554	578	594	582	600	553	557
24	456	463	404	432	575	556	581	597	586	602	556	559
25	454	462	405	433	574	557	580	596	587	605	556	556
26	457	464	405	433	573	554	579	595	584	603	554	558

TABLE E2

FRAME A AVERAGE 1/4 POINT LOADS (POUNDS)

Loading	A–B	C–D	E–F	G–H	I–J	K–L
1	75.5	58	90	80	74.2	74.0
2	143.6	124	186	184	175	164
3	180	162	229	236	247	214
4	229	210	275	285	295	260
5	243	217	314	329	335	301
6	276	248	357	371	379	343
7	310	279	399	416	422	387
8	328	296	411	429	435	399
9	345	311	434	453	457	421
10	357	322	465	487	489	456
11	370	335	470	491	493	459
12	381	345	483	505	506	474
13	381	345	493	515	518	484
14	389	353	495	517	519	487
15	397	360	504	529	532	496
16	400	362	518	540	543	508
17	412	375	525	548	549	515
18	415	376	532	555	554	520
19	435	396	542	566	567	531
20	435	396	549	575	575	541
21	442	402	563	588	590	554
22	447	406	557	580	584	549
23	451	410	563	586	591	555
24	460	418	566	589	594	558
25	458	419	566	588	596	556
26	461	419	564	587	594	556

TABLE E3

FRAME A DISPLACEMENTS (INCHES)

Loading	V1	V2	V3	V4	V5	V6	H1	H2	H3
1	.015	.010	.013	.013	.014	.010	.003	.001	.001
2	.028	.023	.028	.028	.028	.023	.005	.001	.001
3	.035	.030	.036	.037	.036	.031	.006	.001	.001
4	.044	.039	.044	.044	.043	.039	.007	.001	.002
5	.047	.041	.051	.051	.051	.046	.007	.001	.002
6	.054	.047	.059	.059	.060	.055	.008	.001	.002
7	.061	.053	.070	.071	.071	.067	.009	.002	.003
8	.065	.057	.073	.074	.073	.069	.019	.002	.003
9	.069	.060	.079	.081	.079	.077	.011	.003	.005
10	.073	.064	.088	.092	.089	.087	.012	.005	.007
11	.076	.067	.090	.094	.091	.091	.013	.005	.007
12	.081	.069	.093	.097	.095	.095	.014	.006	.007
13	.081	.070	.098	.103	.102	.101	.014	.007	.008
14	.083	.071	.099	.104	.103	.103	.014	.007	.008
15	.086	.074	.103	.109	.108	.107	.015	.007	.007
16	.088	.075	.113	.118	.115	.114	.015	.009	.009
17	.090	.077	.122	.124	.123	.123	.016	.009	.010
18	.094	.080	.126	.130	.127	.127	.016	.010	.010
19	.099	.086	.134	.143	.138	.138	.016	.012	.011
20	.102	.087	.146	.156	.153	.148	.016	.013	.013
21	.104	.088	.166	.177	.171	.161	.016	.019	.015
22	.106	.090	.175	.190	.178	.166	.016	.022	.015
23	.109	.092	.182	.209	.187	.174	.016	.025	.016
24	.112	.094	.194	.242	.198	.178	.016	.028	.017
25	.114	.095	.199	.269	.206	.184	.016	.030	.018
26	.114	.095	.207	.306	.211	.188	.016	.032	.018

TABLE E4

FRAME A STRAINS (MICROINCHES PER INCH)

Gage Number*	Loading Number 1	2	3	4	5	6	7	8	9
1	+120	+225	+280	+360	+385	+445	+490	+525	+550
2	−160	−295	−375	−470	−500	−575	−645	−685	−725
3	−65	−115	−145	−180	−195	−220	−245	−255	−255
4	−35	−70	−90	−115	−110	−130	−150	−170	−180
5	−130	−275	−355	−455	−465	−540	−605	−650	−680
6	+105	+215	+275	+350	+370	+420	+475	+505	+535
7	−120	−250	−310	−380	−425	−490	−555	−580	−615
8	+100	+200	+250	+300	+340	+380	+435	+445	+470
9	−50	−100	−120	−155	−165	−190	−210	−225	−235
10	−40	−80	−100	−135	−130	−150	−175	−185	−195
11	+70	+160	+200	+240	+275	+310	+345	+360	+385
12**	−55	−145	−180	−220	−245	−265	−305	−325	−415
13	+90	+180	+220	+260	+310	+345	+390	+400	+425
14	−150	−340	−400	−475	−550	−635	−725	−755	−795
15	−80	−190	−230	−310	−325	−370	−410	−425	−450
16	−100	−220	−280	−345	−395	−445	−490	−515	−530
17	−140	−310	−400	−480	−550	−625	−710	−740	−775
18	+60	+150	+190	+220	+265	+295	+335	+335	+360
19	−130	−320	−440	−535	−615	−700	−795	−825	−880
20	+80	+180	+250	+290	+335	+380	+430	+440	+470
21	−80	−185	−255	−305	−345	−400	−450	−470	−495
22	−80	−170	−240	−300	−325	−370	−400	−420	−440
23	+80	+180	+250	+290	+340	+380	+430	+440	+450
24	−120	−300	−420	−500	−580	−660	−755	−785	−820
25	+30	+60	+90	+100	+120	+140	+155	+155	+165
26	−140	−320	−440	−520	−590	−680	−775	−800	−860
27	−160	−330	−440	−530	−590	−660	−730	−750	780
28	−130	−290	−410	−500	−550	−625	−700	−725	−765
29	−130	−310	−455	−545	−615	−705	795	−825	−865
30	+10	+65	+95	+110	+135	+145	+165	+165	+165
31	−95	−230	−320	−380	−430	−490	−550	−570	−600
32	−30	−60	−80	−115	−110	−125	−145	−155	−165
33	−130	−280	−390	−480	−530	−600	−670	−690	−730
34	−135	−300	−420	−520	−570	−645	−720	−745	−780
35	−25	−60	−85	−105	−115	−130	−150	−155	−165
36	−90	−210	−290	−350	−390	−445	−505	−525	−550

* See Figure 10 for location of strain gages.

** Erratic gage.

Gage Number	Loading Number 10	11	12	14	15	16	17	18	19
1									
2									
3									
4									
5									
6									
7									
8				Strain indicator for gages 1–20					
9				malfunctioned at loading number 10.					
10									
11									
12									
13									
14									
15									
16									
17									
18									
19									
20									
21	−530	−535	−555	−555	−570	−585	−590	−595	−600
22	−460	−465	−490	−500	−510	−515	−525	−530	−560
23	+495	+490	+515	+510	+525	+540	+550	+560	+565
24	−900	−900	−945	−950	−970	−1000	−1020	−1040	−1065
25	+175	+175	+180	+170	+185	+175	+175	+185	+190
26	−920	−930	−965	−980	−1000	−1020	−1030	−1055	−1080
27	−820	−830	−870	−875	−900	−910	−920	−935	−950
28	−810	−820	−850	−865	−880	−900	−910	−920	−955
29	−930	−935	−975	−985	−1010	−1040	−1050	−1070	−1100
30	+185	+175	+180	+180	+185	+190	+190	+195	+195
31	−630	−640	−670	−680	−685	−700	−705	−720	−730
32	−180	−180	−200	−205	−205	−225	−225	−230	−245
33	−770	−780	−810	−825	−840	−855	−860	−875	−890
34	−820	−835	−870	−885	−900	−920	−930	−945	−980
35	−175	−185	−195	−205	−205	−210	−215	−220	−225
36	−590	−600	−625	−635	−645	−660	−670	−680	−700

Gage Number	Loading Number 20	21	24	26
1				
2				
3				
4				
5				
6				
7				
8				
9				
10				
11				
12				
13				
14				
15				
16				
17				
18				
19				
20				
21	−595	−575	−555	−545
22	−580	−620	−660	−660
23	+570	+580	+560	+540
24	−1075	−1090	−1100	−1085
25	+190	+190	+190	+190
26	−1095	−1110	−1130	−1130
27	−940	−920	−905	−890
28	−970	−1020	−1070	−1080
29	−1115	−1145	−1205	−1215
30	+200	+210	+245	+255
31	−730	−720	−715	−715
32	260	−280	−310	−310
33	885	−880	−880	−880
34	−995	−1035	−1050	−1060
35	−225	−220	−215	−215
36	−710	−730	−755	−760

TABLE E5

FRAME A ROTATIONS (DEGREES)

Loading Number	ROTATIONS R_a*	R_b*	R_c*
1	-0.001	0.001	0.000
2	-0.002	0.002	0.001
3	-0.003	0.003	0.001
4	-0.004	0.005	0.001
5	-0.006	0.006	0.002
6	-0.008	0.007	0.002
7	-0.009	0.009	0.003
8	-0.010	0.010	0.003
9	-0.011	0.010	0.003
10	-0.011	0.012	0.003
11	-0.011	0.012	0.004
12	-0.011	0.012	0.004
13			
14	-0.012	0.013	0.004
15	-0.012	0.013	0.004
16			
17	-0.013	0.014	0.004
18	-0.013	0.015	0.004
19	-0.013	0.015	0.005
20	-0.014	0.017	0.005
21	-0.014	0.019	0.005
22	-0.013	0.021	0.005
23	-0.013	0.024	0.005
24	-0.013	0.026	0.005
25	-0.012	0.026	0.005
26	-0.012	0.026	0.005

* See Figure 10 for location.

** Clockwise defined as positive.

F. FRAME B TEST RESULTS

TABLE F1
FRAME B LOADS (POUNDS)

LOADING	A	B	C	D	E	F	G	H	I	J
1	126	130	120	125	176	180	169	158	167	165
2	294	302	287	298	388	394	382	365	380	374
3	288	295	280	293	395	399	386	370	385	382
4	288	295	282	293	393	399	388	372	380	377
5	288	295	282	293	395	399	388	374	382	381
6	285	295	282	295	393	396	390	374	378	377
7	286	292	282	295	395	394	390	377	370	367
8	287	295	282	295	397	404	388	377	385	381
9	288	295	280	290	393	396	386	374	378	377
10	286	295	280	290	395	392	381	372	368	367
11	281	290	278	290	395	394	381	372	368	367
12	276	286	278	288	404	404	390	381	387	389
13	286	292	284	295	397	399	383	374	380	381
14	290	300	282	293	390	399	383	377	375	377
15	Failure									

LOADING	K	L	APPLIED DEAD WEIGHT ON EACH PULLEY SYSTEM	H1	H2	H3	$\frac{H1+H2+H3}{3}$	Gravity Load Simulator Loss
1	170	170	0	0	0	0		0
2	382	381	0	0	0	0		0
3	389	388	0	0	0	0		0
4	389	388	10	8.4	8.0	9.8		7.8
5	392	391	20	18.6	18.6	19.3		17.8
6	394	393	30	27.3	29.1	28.8		27.4
7	389	388	40	36.8	37.1	38.6		36.5
8	394	393	50	46.6	47.3	49.1		45.7
9	389	388	50	44.5	47.0	48.8		
10	385	384	60	54.6	56.4	58.0		54.4
11	387	386	70	63.6	65.5	67.4		63.5
12	394	393	80	72.8	76.0	77.3		73.5
13	387	386	90	83.0	85.2	87.7		82.4
14	389	388	100	91.7	95.0	98.2		92.0
15			104	95.4	98.8	102.2		96.0

TABLE F2

FRAME B AVERAGE 1/4 POINT LOADS (POUNDS)

LOADING	A-B	C-D	E-F	G-H	I-J	K-L
1	128	122	178	163	166	170
2	298	293	391	373	377	381
3	292	286	397	378	384	388
4	292	287	396	380	378	388
5	292	287	397	381	381	391
6	290	288	394	382	377	393
7	289	288	394	384	368	388
8	291	288	400	382	383	393
9	292	285	395	380	377	388
10	290	285	393	376	367	384
11	285	284	394	376	367	386
12	281	283	404	385	388	393
13	289	290	398	378	380	386
14	295	287	395	380	376	388

TABLE F3

FRAME B DISPLACEMENTS (INCHES)

LOADING	H1	H2	H3	APPLIED DEAD WEIGHT ON EACH PULLEY SYSTEM
1	0	0	0	0
1	0	0	0	0
3	0	0	0	0
4	.021	.016	.012	10
5	.051	.036	.025	20
6	.081	.065	.037	30
7	.108	.087	.048	40
8	.149	.119	.064	50
9	.159	.126	.068	50
10	.193	.155	.084	60
11	.244	.195	.105	70
12	.327	.266	.141	80
12a	.367	.298	.158	86
12b	.380	.310	.165	88
13	.401	.327	.176	90
13a	.428	.352	.187	92
13b	.454	.373	.199	94
13c	.482	.397	.213	96
13b	.499	.412	.221	98
14	.565	.467	.251	100
14a	.592	.490	.264	102
15	FAILURE			104

TABLE F4

FRAME B STRAINS (MICROINCHES PER INCH)

Gage Number	Loading Number 1	2	3	4	5	6	7	8
1	210	474	469	460	431	410	391	365
2	−269	−626	−618	−600	−574	−554	−531	−510
3	−100	−227	−222	−240	−270	−295	−320	−360
4	− 70	−190	−181	−162	−135	−110	− 85	− 50
5	−262	−624	−620	−636	−660	−688	−707	−737
6	200	462	455	478	490	512	533	560
7	−238	−536	−540	−527	−520	−514	−500	−510
8	175	380	389	382	370	361	350	360
9	− 61	−170	−162	−150	−134	−120	−102	− 90
10	−106	−232	−230	−237	−259	−279	−290	−306
11	156	362	368	380	385	390	398	390
12	−220	−525	−527	−530	−549	−556	−564	−560
13	130	280	290	265	221	188	150	120
14	−292	−652	−664	−630	−590	−550	−500	−480
15	−208	−466	−466	−499	−552	−610	−652	−720
16	−191	−450	−450	−410	−364	−312	−268	−208
17	−259	−600	−610	−635	−686	−730	−762	−812
18	101	231	240	274	310	342	378	418
19	−300	−680	−688	−650	−630	−607	−572	−574
20	119	290	297	283	250	235	209	202
21	−200	−458	−460	−430	−381	−341	−308	−260
22	−189	−436	−438	−465	−508	−548	−576	−630
23	130	290	300	315	343	370	380	407
24	−291	−662	−672	−694	−730	−760	−780	−814
25	28	69	70	41	8	− 30	− 62	− 82
26	−292	−659	−465	−630	−582	−540	−494	−488
27	−307	−712	−714	−752	−810	−762	−900	−952
28	−326	−730	−738	−700	−643	−595	−545	−505
29	−289	−655	−670	−708	−752	−800	−835	−875
30	39	88	90	119	158	194	220	250
31	−189	−423	−430	−372	−298	−222	−150	− 78
32	− 70	−160	−160	−209	−272	−342	−402	−488
33	−317	−715	−720	−668	−589	−514	−440	−360
34	−307	−708	−710	−765	−840	−915	−978	−1068
35	− 61	−154	−153	−109	− 40	25	85	160
36	−187	−420	−425	−480	−560	−640	−705	−800

Gage Number	Loading Number 9	10	11	12	13	14
1	380	355	322	281	260	208
2	520	−498	−460	−415	−392	−342
3	340	−370	−400	−449	−498	−600
4	−60	−35	0	51	98	198
5	−750	−818	−920	−862	−908	−986
6	578	598	621	670	710	781
7	−498	−487	−484	−500	−490	−520
8	350	340	340	355	350	373
9	−85	−75	−66	−72	−72	−120
10	300	−310	−318	−307	−317	−270
11	400	400	393	370	350	290
12	570	−568	−565	−544	−528	−474
13	110	60	9	−40	−130	−260
14	−464	−410	−357	−310	−220	−90
15	717	−775	−840	−962	−1059	−1170
16	−200	−137	−63	50	149	252
17	804	−834	−880	−960	−1007	−1100
18	415	440	480	548	592	676
19	570	−529	−510	−597	−597	−620
20	198	160	145	230	234	260
21	245	195	−142	−56	−10	40
22	630	−673	−717	−808	−860	−897
23	400	387	386	385	350	295
24	−800	−790	−800	−810	−787	−738
25	−92	−148	−192	−160	−198	−250
26	−462	−395	−340	−392	−350	−385
27	−943	−982	−1015	−1078	−1110	−1150
28	495	−440	−402	−361	−330	−275
29	−880	−900	−940	−992	−1022	−1050
30	260	278	304	332	360	333
31	48	54	179	326	484	655
32	−502	−590	−702	−872	−1019	−1172
33	400	−362	−340	−344	−350	−312
34	1008	−1030	−1049	−1062	−1054	−1080
35	180	262	370	540	690	849
36	−915	−900	−1015	−1208	−1365	−1530

TABLE F5

FRAME B ROTATIONS (DEGREES)

LOADING	R_a*	R_b*	R_c*
1	–0.003	–0.001	0.003
2	–0.006	–0.001	0.003
3	–0.006	–0.001	0.008
4	–0.004	–0.001	0.009
5	0	–0.001	0.012
6	0.003	–0.001	0.015
7	0.006	0	0.016
8	0.009	0	0.019
9	0.010	0	0.019
10	0.014	0	0.022
11	0.020	0.001	0.026
12	0.026	0.003	0.031
13	0.031	0.004	0.037
14	0.067	0.007	0.049

* See Figure 10 for location.

** Clockwise defined as positive.

REFERENCES

1. Foster, David C., "Fabrication Techniques for Small Scale Steel Models", unpublished Master's thesis, Department of Civil Engineering, Massachusetts Institute of Technology, May, 1966.

2. Oakes, D., "Ultimate Strength Behavior of Steel Wide Flange Beam Column Models," unpublished Master's thesis, Department of Civil Engineering, Massachusetts Institute of Technology, September 1966.

3. Fenves, Steven J., Logcher, Robert D., Mauch, Samual P. and Reinschmidt, Kenneth F., "STRESS: A User's Manual," The MIT Press, Massachusetts Institute of Technology, 1964.

4. Yura, Joseph A., "The Strength of Braced Multi-Story Steel Frames", Fritz Engineering Laboratory Report No. 273.28, Lehigh University, 1965.

BULLETINS

Steel Research for Construction

No. 1 Current Paving Practices on Orthotropic Bridge Decks
Battelle Memorial Institute, October, 1965

No. 2 Strength of Three New Types of Composite Beams
A. A. Toprac, October, 1965

No. 3 Research on and Paving Practices for Wearing Surfaces on Orthotropic Steel Bridge Decks, Supplement to Bulletin 1
Battelle Memorial Institute, August, 1966

No. 4 Protection of Steel Storage Tanks and Pipe Underground
Battelle Memorial Institute, May, 1967

No. 5 Fatigue Strength of Shear Connectors
R. G. Slutter and J. W. Fisher, October, 1967

No. 6 Paving Practices for Wearing Surfaces on Orthotropic Steel Bridge Decks, Supplement to Bulletins 1 and 3
Battelle Memorial Institute, January, 1968

No. 7 Report on Investigation of Orthotropic Plate Bridges
D. Allan Firmage, February, 1968

No. 8 Deformation and Energy Absorption Capacity of Steel Structures in the Inelastic Range
T. V. Galambos, March, 1968

No. 9 The Dynamic Behavior of Steel Frame and Truss Buildings
Dixon Rea, J. G. Bouwkamp and R. W. Clough, April, 1968

No. 10 Structural Behavior of Small-Scale Steel Models
Massachusetts Institute of Technology, April, 1968

Committee of Structural Steel Producers • Committee of Steel Plate Producers

american iron and steel institute

150 East 42nd Street, New York, N. Y. 10017